Structural Studies to Investigate Attractive Interactions between Nucleophiles and Electron-deficient Carbon Atoms.

A thesis submitted as partial fulfilment of the requirements for the degree of Doctor of Philosophy.

By

Jane O'Leary

The Nottingham Trent University
Clifton Lane
Nottingham
NG11 8NS
UK

Declaration

I hereby certify that the work embodied in this thesis is the result of my own investigations except where reference has been made to published literature.

Abstract

This thesis is divided into five chapters. Chapter 1 gives an introduction to x-ray crystallography, detailing the experimental technique, structure solution and refinement. The use of x-ray crystallography to observe interactions in the fields of supramolecular chemistry and crystal engineering are discussed. The remainder of chapter 1 reviews the literature regarding intramolecular interactions between electron-rich and electron-deficient functional groups.

Chapters 2-5 form the results and discussion of the thesis. Chapter 2 details a re-interpretation of 1,5-interactions between dimethylamino or methoxy groups and sp^2 carbon atoms in *peri*-naphthalene compounds **1**. The *peri*-interactions of the methoxy group were found to be rather insensitive to the nature of the *peri*-substituent, hence are not attractive in nature, but are dominated be steric effects. The *peri*-interactions of the dimethylamino group decreases with *peri* group along the series: -CH=CHBr ~ $-CONR_2$, $-CH=C(COPh)_2$, $-CO_2H$ ~ CO_2R, $-COCH_3$, $-CH=C(CN)CO_2CH_3$, -CHO, $-CH=C(CN)_2$, $-CH=C(C(=O)O)_2CMe_2$, this forms the relative order of through-space electron-attracting power for these groups. The nature of the N----C interactions are discussed and an equation (Equation **1**) which can provide an indication as to whether the interactions are attractive or dominated by steric effects is introduced.

[d(MeO----X) + 0.15 – d(Me_2N----X)] Equation **1**

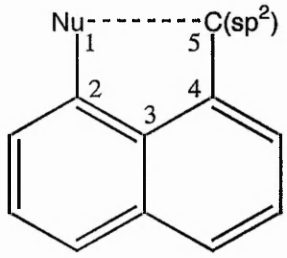

1 Nu = MeO or Me_2N

Chapter 3 is a report on the synthesis and structure of four 8-methylthio-1-alkenylnaphthalene compounds, where the alkene's terminal substituents are electron-withdrawing groups. There is a trend of decreasing S----C separation and out of plane deviations of the *peri*-substituents with increasing electron-attracting power of the alkene's terminal substituents: H, NO_2 < CN, CO_2Me < CN, CN < $-C(C(=O)O)_2CMe_2$. Equation **1** was modified to produce equation **2** in order to assess the nature of the S----C interactions, which appear to be dominated by steric effects.

[d(MeO----X) + 0.21 – d(MeS----X)] Equation **2**

Chapter 4 discusses 1,6-interactions between the dimethylamino group and sp^2 carbon atoms of aldehydes and alkenes in 2,2'-disubstituted biphenyls. All structures show short N----C distances brought about by small inter-ring angles, which are unusual in such *ortho*-disubstituted biphenyls. Where the alkene's terminal substituents are a cyclic diketone **2** or are both cyano groups **3** the compounds have undergone intramolecular cyclisation to form zwitterions.

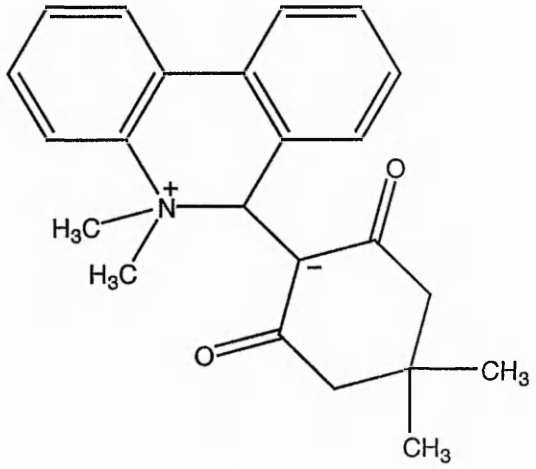

2

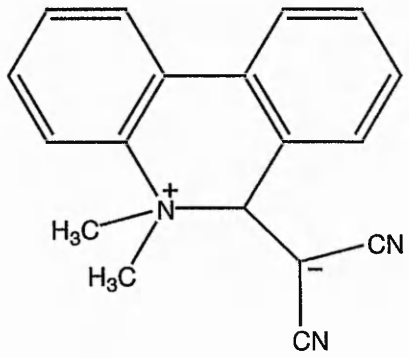

3

Chapter 5 concerns the synthesis and structure of the N-oxides and N,N'-dioxides of 3,3'-dinitro-2,2'-bipyridine and 5,5'-dimethyl-3,3'-dinitro-2,2'-bipyridine. All compounds show short contacts between nitro O atoms and the 2-C atoms of the distant pyridine ring. These interactions are controlled by the orientation of the nitro group with respect to the adjacent pyridine ring. There are also short contacts between oxide O atoms and nitro N atoms in three of the four structures. It is possible that the O----C and O----N interactions are in competition with each other.

Acknowledgements

I would like to thank my supervisor Professor John Wallis whose enthusiasm and dedication have been both inspiring and infectious. I am indebted to him for his never-ending help and advice throughout my Ph.D.

Special thanks also to James (Bob) whose support, encouragement and eternal optimism have been invaluable especially when the 'Chemistry Gods' were not being kind.

Thanks to Nezire and Paul from lab 106 (UKC) for all their help in my first year and to all the members (past and present) of lab 114 (TNTU) for making the past two years so enjoyable. I am also grateful to Mick Wood for many NMR's and help in the lab, and to Dr. Pat Huddleston for his sound chemical advice.

Finally, a thank you to my family and friends for all their help and support throughout my studies.

Contents

Chapter 1 – Introduction

Chapter 1

Introduction

Introduction

1.1 Crystal Structure Analysis

The primary aim of crystal structure analysis by x-ray (or neutron) diffraction is to obtain a detailed picture of the contents of the crystal at the atomic level. This technique provides an unambiguous and complete three-dimensional picture of the molecule whereas other chemical and physical methods of structure determination merely provide relationships from which one can deduce the number and nature of the atoms bonded to each other.

X-ray diffraction can be explained in terms of light microscopy, but with necessary differences.[1] The resolution of a microscope is not high enough for us to "see" atoms, in order to see the details of an object with a microscope those details must be separated by at least half the wavelength of the radiation used to view them. The wavelength of visible light is 4 to 8 x 10^{-5} cm while the separation of atoms in molecules is of the order 10^{-8} cm (1 Å). In order to view these details a smaller wavelength such as that of x-rays, which lie in the nanometre range, must be used.
In a light microscope the radiation (light) is scattered by the object and a lens recombines the scattered waves such that they remain in phase with each other. X-rays, however, are scattered by the electrons and cannot be refocused by any known lens.[2] The recombination is done mathematically to result in an electron-density map with peaks at atomic positions.

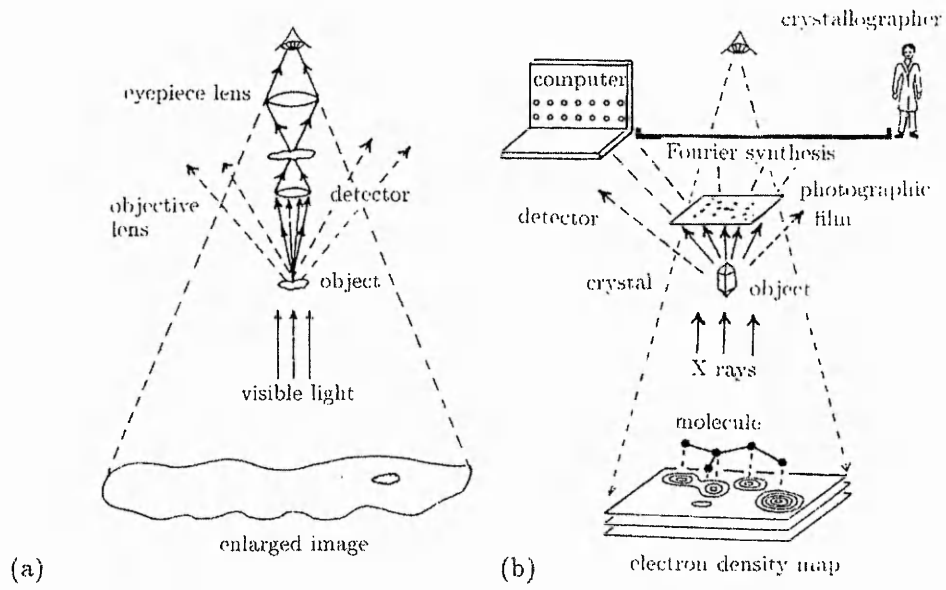

Figure 1 Comparison of the techniques of (a) light microscopy and (b) x-ray diffraction[1]

There is, however, a microscope than can resolve at the atomic level, the atomic force microscope (AFM).[3-5] This consists of a small probe that scans over the surface of a sample and detects interactions between the probe and sample. A variety of forces can be detected; van der Waals, electrostatic, magnetic, capillary and ionic repulsion forces and these are used to produce topographical images of the sample. Many atomic resolution images have been produced by AFM, an example is the amino acid DL-leucine. The surfaces of crystals of this amino acid have been imaged to determine the positions of methyl groups at the end of individual leucine molecules and the results agree with the positions predicted from x-ray diffraction.

AFM is a very useful and valuable technique, and although still relatively new it is developing more and more into a versatile probing instrument. Although this technique can provide some information about molecular structure it does not provide the detailed three-dimensional picture of molecules that is obtained from x-ray (or neutron) diffraction.

1.2 Crystals

The first step towards molecular structure determination is to obtain a suitable crystal, a solid that has, in all three dimensions, a regularly repeating internal arrangement of atoms. Crystals are considered to comprise of a regularly repeating basic structural pattern that may comprise of a single atom / molecule or an assembly of atoms / molecules. One unit of this repeating pattern is termed the unit cell, the size and shape of which determines the crystal lattice. The crystal lattice is the basic network of points, which repeat the way in which the unit cell contents repeat in the crystal.

Johann Friedrich Christian Hessel[6] mathematically derived the symmetry classes of crystals in 1830. He found that combining rotation axes, mirror planes, centres of symmetry and rotatory inversion axes gives rise to seven different types of lattice symmetry or crystal systems. Only three of these seven crystal systems are common for organic crystals; triclinic, monoclinic and orthorhombic and are distinguished by the angles of the unit cell. Within the crystal systems there are various space groups possible, which define the symmetry between the molecules in the unit cell. In total

for all seven crystal systems there are 230 space groups. For the three crystal systems common for organic structures there are 74 space groups, however, only a few of these occur regularly (P1, $P\bar{1}$, P2, $P2_1/c$, C2/c, Cc, $P2_12_12_1$, Pbca), and of these $P2_1/c$ is the most common for organic molecules as it provides effective packing for many different molecules.

In many cases the space group can be determined from the 'systematic absences' in the x-ray data e.g. the space group $P2_1$ will show systematic absences resulting from a two-fold screw axis in which one molecule is translated half a unit cell along one axis then a two-fold rotation is applied to it. The space group $P2_1/c$ will show the same systematic absences as for $P2_1$ in addition to those resulting from a glide plane in which one molecule is reflected in a plane perpendicular to the b axis and then translated by half a unit cell along one axis, in this case the c axis.

Only translational symmetry elements give rise to absences and so there are some space groups which cannot be distinguished from systematic absences alone, e.g. $P2_1$ and $P2_1/m$. The only difference between these two space groups is a mirror plane, which does not give rise to systematic absences. Other features can be used to help distinguish between these two space groups, e.g. the unit cell volume. $P2_1$ defines a unit cell in which there are two symmetry related molecules, while $P2_1/m$ defines a unit cell containing four symmetry related molecules, hence the volume of a unit cell with space group $P2_1/m$ should be twice that of $P2_1$ if the asymmetric unit contains just one unique molecule. Another difference between these two is that $P2_1$ is a non-

centrosymmetric space group, while $P2_1/m$ is a centrosymmetric space group. Most structure solution programs will indicate whether or not the structure is likely to be in a centrosymmetric space group. The distribution of intensities is different for centrosymmetric and non-centrosymmetric crystals, centrosymmetric crystals give a higher number of weak Bragg reflections and so the distribution of intensities is farther from the mean than for a non-centrosymmetric crystal. When the structure factors are normalised to give E values, the different intensity distributions are reflected in the E values, which are 0.798 for a centrosymmetric crystal and 0.886 for a non-centrosymmetric crystal. Thus the E values calculated by structure solution programs can indicate whether or data is from a centrosymmetric or non-centrosymmetric crystal, however they are not conclusive and should not be interpreted as such. Pseudo symmetry can pose a problem. For example when the space group is $P2_1$, but there are two unique molecules that are almost related by a mirror plane, this can be difficult to detect as the space group appears to be $P2_1/m$. If there is any doubt over the space group often the only way is to try and solve the structure in each one. However a solution in the lower symmetry space group may be valid for the higher symmetry space group, and one has to check the refined solution if this is so. Solving a structure by 'direct methods' is not an exact science, so not getting a solution does not necessarily mean that the space group is wrong.

The formation of a crystal depends both on the solubility of the compound and on nucleation and growth. Nucleation is the formation of aggregates on to which further molecules can be adsorbed giving rise to ordered growth and hence crystals. Crystals suitable for modern single-crystal studies are ideally 0.2 – 0.4mm in length in at least

two of the three dimensions. There are many methods used to grow suitable crystals, the most common is that of slow evaporation of an appropriate solvent. This method is particularly effective for small organic molecules. Other methods include vapour diffusion, solvent diffusion (layering) and sublimation.

1.3 Diffraction

The pattern of radiation scattered by any object is called its diffraction pattern.[7-9] In the early 17th century Francesco Maria Grimaldi[9] observed that a fine thread does not cast as sharp a shadow as would be expected, he found that fringes of parallel dark and bright bands are produced at the shadow's edge. This effect he named diffraction, meaning the change in direction of a wave front travelling through a uniform medium. X-rays are diffracted by the electrons of atoms, however it is only when this diffraction is reinforced by the repetition of the unit cell in the crystal that the result is observable. W. L. Bragg[10] showed this in 1913, when he observed that scattered radiation from a crystal behaves as if the diffracted beams were "reflected" from a plane passing through the crystal lattice, these diffracted beams became known as Bragg reflections.

There is a reciprocal relationship between the angular spread of the diffraction pattern and the corresponding repeating dimension of the object causing the diffraction. W. L. Bragg[11] demonstrated this when he compared the diffraction pattern of sodium chloride with that of potassium chloride. The unit cell of potassium chloride is larger

than that of sodium chloride due to the larger size of the potassium ion. The reciprocal relationship between crystal periodicity and diffraction pattern results in the "spots" in the diffraction pattern of potassium chloride to be closer together than those for sodium chloride.

1.4 Data Reduction

For each Bragg reflection, the raw data normally consist of the Miller indices (h,k,l), the integrated intensity I(hkl) and its standard deviation [σ(I)]. However, the parameter required for structure solution is the structure factor amplitude |F(hkl)|, which is a function of the measured intensity of a diffracted beam. The conversion of I(hkl) to |F(hkl)| involves the application of corrections for x-ray background intensity, Lorentz and polarisation factors, absorption effects and radiation damage. This process is known as data reduction.[12]

The Lorentz and polarisation corrections are geometrical corrections made necessary by the nature of the x-ray experiment.[13-16] The Lorentz factor (L) takes into account the different lengths of time that the various Bragg reflections are in the diffracting positions and is calculated as a function of the scattering angle 2θ (Equation 1).

$$L = 1 / \sin 2\theta \qquad \text{Eqn. 1}$$

The polarisation factor (p) corrects for the partial polarisation of the x-ray beam after diffraction and is also calculated as a function of 2θ (Equation 2).

$$p=(1 + \cos^2 2\theta) / 2 \qquad \text{Eqn. 2}$$

The absorption factor (A) accounts for the absorption of each diffracted beam as it travels through the crystal. The extent of this absorption depends on the distance the diffracted beam must travel through the crystal, the nature of the atoms and the wavelength of the incident x-ray beam (Equation 3).[17-25]

$$T = 1 / A = I / I_o = e^{-\mu t} \qquad \text{Eqn. 3}$$

T is the fraction of radiation transmitted, I_o is the intensity of the incident beam, I is the intensity of a Bragg reflection, t is the thickness (in cm) of the crystal and μ is the total linear absorption coefficient for the primary beam (in cm^{-1}). It is a function of x-ray wavelength and atomic number and can be calculated for a compound from published data for its composite atoms.[24] Absorption corrections are only necessary if μt is greater than 0.5, so are not usually required for organic molecules containing atoms between hydrogen and fluorine.

Exposure of a crystal to radiation can result in damage to that crystal, possibly due to the formation of free radicals, loss of solvent of crystallisation or heating of the crystal. This damage causes Bragg reflections to change intensity as a function of time. Radiation damage may be detected by monitoring a set of reference reflections that are measured at regular intervals throughout data collection. If the change in the intensities of these reflections as a function of time can be fit to a simple mathematical function describing a decay curve, this correction can be applied to the experimental data so that the effects of radiation damage on the data are reduced.

1.5 Fourier Synthesis

The diffracted x-ray beams must be recombined in a manner similar to that of the refocusing of light by a lens, but as there is no material capable of this it is achieved by a mathematical calculation called a Fourier synthesis.[26] This mathematical function involves the summation of waves of known frequency, amplitude and phase in order to obtain a new periodic function such as that of the electron density in a crystal.

$$\rho(xyz) = 1/V \sum_h \sum_k \sum_l | F(hkl) | \cos 2\pi (hx + ky + lz - \alpha_{hkl}) \qquad \text{Eqn. 4}$$

V = unit cell volume
$\rho(xyz)$ = electron density at a point x,y,z in the unti cell
F(hkl) = structure factor amplitude (obtained from the intensity of a Bragg reflection)
α_{hkl} = relative phase angle of a Bragg reflection

1.6 The Phase Problem

In order to calculate a correct electron-density map using a Fourier synthesis it is necessary to know both the amplitude and relative phase for each Bragg reflection. The amplitude is a function of the intensity I(hkl) of a Bragg reflection and hence can be obtained from the experimental measurements. The relative phase angle however cannot be directly obtained, as during diffraction experiments all phase information is lost. This problem is termed 'the phase problem' and is overcome by calculating approximated values of α_{hkl} indirectly, or directly by statistical methods.

There are three methods commonly used to derive relative phases; Patterson and heavy atom methods, isomorphous replacement methods and 'direct methods'. The method of choice depends on the nature of the molecule under analysis; Patterson and heavy atom methods are used for molecules containing one or more heavy atom, isomorphous replacement methods for macromolecules and 'direct methods' for small molecules.

1.6.1 Patterson Methods

Patterson methods involve the interpretation of interatomic vectors. The Patterson function (eqn. 5) is a map that indicates all the possible vectors between atoms in a crystal structure and was introduced by A. Lindo Patterson in 1934.[27-29]

$$P(uvw) = 1/V \sum_{h,k,l}\sum\sum |F(hkl)|^2 \cos 2\pi (hu + kv + lw) \qquad \text{Eqn. 5}$$

It is a Fourier synthesis that uses the square of the structure factor amplitude $|F(hkl)|^2$ of each Bragg reflection, but does not require any phase information. Thus the Patterson function can be calculated directly from the x-ray measurement. A peak in the Patterson map corresponds to a vector between two atoms, the heights of the peaks are approximately proportional to the values of Z_iZ_j, where Z_i and Z_j are the atomic numbers of the atoms at each end of the vector. Thus the vectors between atoms with higher atomic numbers, e.g. two identical atoms related by space group symmetry, give rise to the biggest peaks and are most readily identified in the

Patterson map. This feature makes the Patterson method very useful for molecules containing one or more heavy atoms.

Interpretation of the Patterson map gives rise to a trial structure, which in the case of a molecule containing heavy atom(s) consists usually of just the heavy atom(s) and the smaller atom(s) directly bonded to them. The relative phase angles of all the Bragg reflections are calculated for this model, and it is then possible to construct an electron-density map using a Fourier synthesis with the observed structure amplitudes and these phases to locate the remaining smaller atoms from the electron-density peaks.

1.6.2 Isomorphous Replacement Methods

Phases can be estimated by comparing the intensities of isomorphous crystals that differ only in the identity of one atom. This method is used for determining the relative phase angles of macromolecules.[30-37] The intensities of the macromolecule and its heavy atom derivative are measured and the difference used to determine the relative phase angles.

1.6.3 'Direct' Methods

This method involves estimation of the relative phase angles directly from the experimental data.[38-42] There are two imposed conditions that restrict the relative values of the phase angles. The first is that the electron density should never be negative; an electron has a finite probability of being found at a position in the unit cell in which case the electron density is positive, or the probability is zero and hence the electron density is zero, but never negative. The second condition is that the electron-density maps should have high values at and near atomic positions and nearly zero values elsewhere. To combine these, 'direct' methods relies on the concept that the electron density is never negative, and that it consists of isolated sharp peaks at atomic positions.

'Direct' methods use modified structure factors (E(hkl)) so that the maximum information on atomic positions can be obtained. Effects such as the fall off of scattering intensity at higher scattering angles due to atomic size and vibrations are eliminated. E(hkl) is used in Fourier synthesis to generate an E map similar to an electron-density map which is generated using F(hkl), but with sharper and more heightened peaks due to the modified structure factors.

Certain linear combinations of relative phases are uniquely determined by the crystal structure and are independent of the choice of origin. These combinations are called **structure invariants**. They generally involve sets of three reflections $h_1k_1l_1$, $h_2k_2l_2$,

$h_3k_3l_3$ such that $h_1 + h_2 + h_3 = k_1 + k_2 + k_3 = l_1 + l_2 + l_3 = 0$, an example of such a combination are the Bragg reflections 2-13, 42-5 and –6-12. Using this logic it is possible to derive relative phases for large numbers of Bragg reflections.

For a centrosymmetric structure, using a triplet of Bragg reflections each with high E values, the product of the signs of the three relative phase angles has a high probability of being positive (eqn 6). This can be assumed to be the case otherwise the calculated electron-density map may contain negative holes which breaks the first condition required for direct methods which stated that electron density can never be negative.

$$\Sigma_2 \text{ formula} = S(h) \times S(h') \times S(h+h') \approx + \qquad \text{Eqn. 6}$$

This relationship is called the triple product relationship, where S(h) means the sign of the centrosymmetric Bragg reflection, hkl, and is central to direct methods. e.g. if the E values of Bragg reflections 2-13, 42-5 and –6-12 are all large and it is already known that 2-13 and 42-5 have phases of 0° (signs +), then 61-2 probably also has a phase angle of 0°. If 2-13 has a phase angle of 180° (sign -) and 42-5 has a phase angle of 0° (sign +) then 61-2 would probably have a phase angle of 180° (sign -). Statistical methods are used to estimate the probability of the relationship and if that probability is high it is accepted as true.

For non-centrosymmetric structures phase derivation is more difficult as the values are not restricted to 0° and 180°. The phases are usually derived by the tangent formula (eqn 7).

$$\text{Tan}\,[\alpha(h)] \approx \frac{\Sigma_{h'} \left| E(h') E(h-h') \right| \sin[\alpha(h') + \alpha(h-h')]}{\Sigma_{h'} \left| E(h') E(h-h') \right| \cos[\alpha(h') + \alpha(h-h')]} \qquad \text{Eqn. 7}$$

This equation is used to develop additional phases and to refine them. The phases of a few reflections with high E values are given different values. For this method to work a range of phases angles are used, maybe 30, 60, 90, 120, 150 and 180° in order to maximise the chances of determining the remaining phases. If most of the resulting phase angles found by this method are within 45° of the true values then the resulting electron-density map will generally reveal a recognisable portion of the structure.

'Direct' methods select the phase set that is most probably correct from statistics and uses this to calculate an E map. From this map it is possible for the crystallographer to select the peaks corresponding to electron density and to build up a molecular framework to use as an initial trial structure that can be tested and refined. Since the method depends on probabilities, which occasionally are wrong, the method can fail. In this case the results of other phase sets can be examined. Nowadays it is rare to fail to solve a molecular structure with up to ~80 non-hydrogen atoms.

1.7 Structure Refinement

Once approximate three-dimensional atomic coordinates have been determined for most, if not all, of the atoms from electron-density maps the structural model needs to be refined in order to obtain more precise atomic positions. The positions x, y and z, expressed as fractions of the cell dimensions a,b and c, and the atomic displacement parameters U derived for each atom are adjusted so as to improve the agreement between the observed structure amplitudes, $|F(hkl)|_o$ and those calculated from the model $|F(hkl)|_c$. Progress in the refinement procedure is monitored by a value known as the R value, defined by equation 8.

$$R = \sum_{all\ hkl} \left| |F(hkl)|_o - |F(hkl)|_c \right| \Big/ \Sigma\ |F(hkl)|_o \qquad \text{Eqn. 8}$$

The method of least squares refinement is often used to compute the best straight line through a series of points that relate two variables.[43-49] The equation for a line may be calculated such that the sum of the squares of the deviations from that line is a minimum. It is possible to "weight" the points i.e. if one measurement is believed to be more accurate than the other, then this measurement may be given a higher weight than the others. Least-squares relies on the existence of many more experimental observations than parameters to be determined and that experimental errors follow a Gaussian distribution.

For structure refinement, least-squares is used to improve the fit of the data calculated for the model to the observed data by minimising the function D (Equation 9).

However this is not a linear problem and it is not possible to solve for the parameters directly.[50-56]

$$D = \sum_{h,k,l} w_{hkl} (F_o - F_c)^2 \qquad \text{Eqn. 9}$$

This is the equation used in crystallographic least-squares refinement where D is the function to be minimised, w_{hkl} are the weights of the reflections, F_o and F_c are the structure factors of the observed and calculated reflections.

Structure refinement involves many parameters, therefore many successive refinement cycles are usually needed. Each least squares analysis calculates a shift to be applied to each parameter, i.e. x,y,z and μ for each atom. The new model thus generated is subjected to the same procedure to generate a further improved model. This is repeated until there are no further significant changes in individual parameters. The atomic displacement parameter is given a spherical form in the early stages of the refinement, but later on it is allowed to have an ellipsoidal form that is defined by six parameters per atom, since it is a tensor quantity. The refinement is considered complete when changes in individual parameters are no longer significant i.e. when the shifts in atomic parameters from cycle to cycle are negligible with respect to the expected experimental errors.

Two aspects that need to be considered after refinement are extinction corrections and absolute structure determination of chiral molecules.

1.7.1 Extinction

Extinction corrections[57,58] are related to the mosaic spread of the crystal. Most crystals are composed of mosaic blocks that are slightly misorientated with respect to each other to result in a 'non-perfect' crystal, whose internal periodicity is not exact. There are two different types of extinction; primary and secondary extinction. Primary extinction occurs when diffracted beams are re-diffracted before they leave the crystal and results in a reduction in the measured intensity of Bragg reflections from their expected values. Primary extinction is not very significant in a crystal that has a high degree of mosaic spread. In such a crystal the mosaic blocks are all at slightly different orientations, therefore they will diffract at slightly different angles, which allows the diffracted x-rays to leave the crystal without being diffracted a second time. Secondary extinction is observed in a strongly diffracting crystal when the incident x-ray beam loses energy on its passage through the crystal due to diffraction by the first mosaic blocks encountered. The deeper blocks thus receive less incident intensity and therefore reflect less power than would otherwise be the case. The magnitude of secondary extinction depends on the size of the crystal; small crystals suffer less from the effect then large ones. Furthermore, crystals with less well aligned blocks, i.e. those with a high degree of mosaic spread, suffer less than those in which the alignment is nearly parallel, because fewer planes are in position to reflect at a given instant. Extinction is most severe for low-angle, strong reflections and can reduce the overall precision of the data. However, for small crystals of organic molecules extinction is generally not a significant effect and extinction

corrections are not usually required. Nevertheless, if there are a significant number of low angle reflections with F_o less than F_c, it should be considered.

1.7.2 Absolute Structure Determination

For a non-centrosymmetric structure Friedel's law[59], which states that I(hkl) = I(-h-k-l) (where I is the intensity of the reflection), is not obeyed. This is due to anomalous scattering from atoms of different elements and is represented mathematically by adding an imaginary component $i\Delta f''$ to each atomic scattering factor. For a centrosymmetric structure the anomalous scattering effects for reflections hkl and –h-k-l cancel out so that Friedel's law is obeyed, but for non-centrosymmetric structures they do not and $I(hkl) \neq I(-h-k-l)$. This difference means that the diffraction pattern for a particular non-centrosymmetric structure and for its inverse are not identical and so it is possible to determine the absolute structure.

One method used to determine the absolute structure uses the anomalous scattering factor $\Delta f''$, or its sign, as a variable in the least-squares refinement.[60-65] This generates an independent parameter (the Flack parameter) together with its estimated standard deviation, which assesses the confidence of an absolute structure determination. The sign of $\Delta F''$ is larger for atoms of higher atomic mass. The differences in the total intensities of the diffractions from organic crystals arising from

anomalous dispersion are very low, and it can be difficult to assign the correct chirality with total confidence.

It is important to determine the absolute structure for non-centrosymmetric structures, even if the absolute structure is itself either not of particular interest or is believed to be known in advance. Refinement of the wrong enantiomer can induce systematic errors into the structure.

1.8 Twinning

Twinning is a crystal defect, which occurs when two or more crystals of the same material intergrow so that the unit cell of the first is related to the unit cell of the second by a symmetry element. There are two different types of twins; twin lattice symmetry (TLS) twins and twin lattice quasi-symmetry (TLQS) twins. TLQS twins have multiple diffraction patterns and the reflections may be split or give two distinct lattices, while TLS twins show a single diffraction pattern. TLQS twins can usually be detected at data collection, due to split reflections it can be difficult to index the data. TLS twins, however, are more difficult to detect, but often show peculiar systematic absences corresponding to space groups with all reflection planes or all rotation axes e.g. Pmmm. Once the nature of the twinning has been identified it can be possible to solve the structure. By determining the 'twin law' and with the use of a suitable program, structure solution can be achieved.

1.9 Low Temperature Data Collection

Low temperatures can be achieved with either a liquid nitrogen ($T_{min} \approx 100K$) or a liquid helium ($T_{min} \approx 10K$) cryostat, both of which cool the crystal by passing a very cold inert gas stream over it.[66-76] For routine work on molecular crystals temperatures in the range 120-200K are typical. If a reliable low-temperature system is available it is almost always worthwhile considering data collection at low temperature. Reducing the temperature of the crystal can have many advantages and it is essential for compounds melting below 50°C and those that are thermolabile. Air sensitive compounds can usually be stabilised long enough to allow data collection. It is possible to transfer, examine and mount a crystal under a suitably viscous oil, which, upon cooling, forms an impenetrable film around the crystal. At low temperatures molecular thermal motion in the crystal is reduced, allowing the collection of better diffraction data at higher resolution. The reduction in thermal motion also minimises librational effects, i.e. oscillations of a bonded atom along an arc which give rise to apparent, but not real, shortening of bond lengths, since the final structural model is an average over time and space. The use of low temperatures can help to combat disorder. At room temperature pseudo-spherical anions such as BF_4^-, PF_6^-, ClO_4^- and SO_4^{2-} are often hard to model due to extensive thermal motion, however at low temperatures these are less mobile and settle into one or just a few orientations and thus their disorder is much easier to model. Cooling can occasionally have adverse effects on crystals, but this is usually only a problem with poor-quality crystals, generally low temperatures serve to maintain crystal stability and produce better quality diffraction data hence the use of low temperatures is now becoming routine.

1.10 Recent Advances

Since the first x-ray diffraction experiment was performed, by von Laue et al. in 1912, there have been many improvements in the methods used making them more efficient so that much larger, more complicated molecules can be measured. It has now become a routine technique. Recent advances in x-ray measurement include the use of synchrotron radiation sources, area detectors and structure solution from powders.

1.10.1 Sources of X-rays

Sealed x-ray tubes have been in use since 1912 and are still the main laboratory source today. They consist of a source of electrons and a metal anode that emits the x-rays in a permanently sealed unit. The electrons are liberated from a heated filament and accelerated by a high voltage toward the anode, which then emits x-rays. The voltage through which the electrons are accelerated is very high and therefore the power dispensed at the anode is quite large (500-1500W). To keep the anode from melting, it is made hollow and is cooled internally with circulating water, however the heat resistance of the anode determines the maximum power of the tube and hence the intensity of the radiation emitted. They are however, relatively cheap, require almost no maintenance and are highly reliable and stable, with typical lifetimes of 1-2 years in continuous use.

The rotating anode generator has evolved to overcome the problem of overheating.[77,78] The anode is rotated at high speed and the electron beam is directed

onto the edge of the anode so that the heat generated is spread out over a much larger area. This produces more intense radiation than the sealed tubes and gives better diffraction data as the peak-to-background ratio is increased.

More recently synchrotron radiation has been used as the source of x-rays.[79,80] Very high-energy electrons travelling nearly at the speed of light in an electron storage ring are decelerated and emit pulses of very intense x-rays, 100-1000 times the intensity of radiation from a sealed tube. It is possible to obtain good quality data from much smaller crystals than those required for use with rotating anode generators or sealed tubes, and obtain good quality data from very complicated macromolecules. Another advantage of synchrotron radiation is the speed of data collection, it is now possible to record several data sets as a function of time. This can be used to follow the progress of enzyme catalysis, to observe the formation of an enzyme-substrate complex and its transformation into product.[81] The drawback to synchrotron sources is that they are extremely large and expensive installations, normally located at some distant place and much in demand, so that the scheduling of data collection is complicated.

1.10.2 Data Collection

Until a few years ago, the vast majority of single-crystal diffraction data collection for chemical applications was carried out with four-circle (serial) diffractometers. This device has four mechanical circles, each identified by the angle it measures (Figure 2). The circles are used to position the crystal with a particular plane at the right

angle to the beam so that the beam is diffracted in the same horizontal plane as the incident beam and the detector moves only in one plane to intercept the diffracted beam. The mutual orientations of the crystal and detector with respect to the source of radiation are determined experimentally from some initial diffraction data, usually from random search techniques under computer control for a few selected reflections. Once this is achieved automated data collection can begin. The diffractometer systematically measures the intensity of each diffracted beam individually using a point detector and hence data collection can take a long time, a few days for a crystal of a small organic molecule.

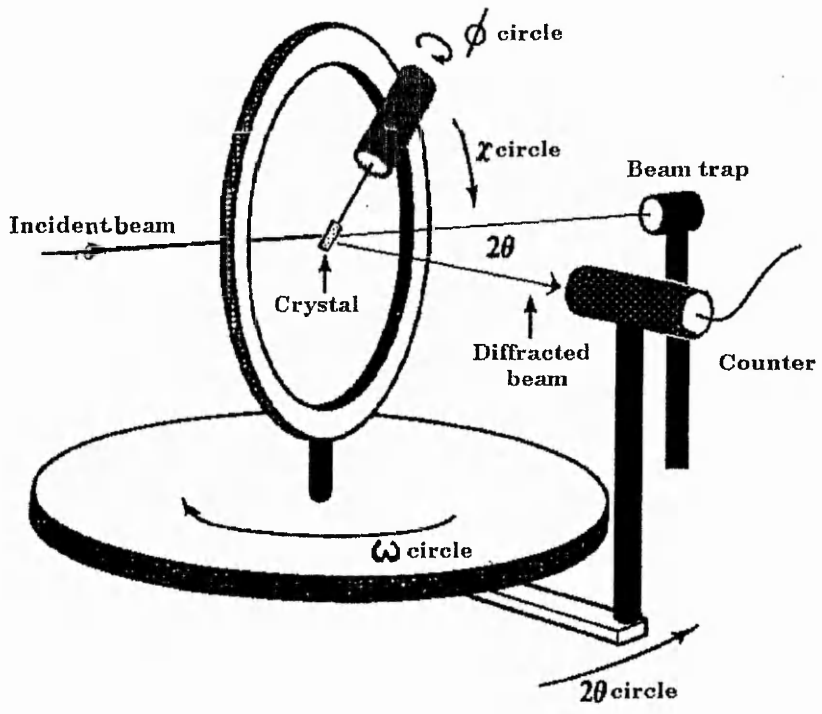

Figure 2 Schematic view of a four-circle (serial) diffractometer.

Area detector diffractometers are rapidly displacing serial diffractometers as the standard devices for data collection.[82-89] The area detector is a large plate-like device that is placed such that its centre is in line with the x-ray beam and the crystal. For any orientation of the crystal a number of diffractions are possible and unlike the serial diffractometer these diffractions need not be in the plane of the incident beam. The main advantage is that a number of diffractions are measured simultaneously and so the time required for data collection is dramatically reduced (several hours for a small organic molecule) whilst still maintaining precision.

1.10.3 Powder Diffraction

Powders usually contain a large number of randomly oriented micro-crystals each of which diffracts to give a continuous ring of Bragg reflections instead of individual spots. The most common use for powder diffraction is to identify the components of the sample[90] by fingerprinting techniques. However, current techniques involve analytical dissection of measured Bragg reflection shapes [91-95] and can be used to derive a data set similar to that for a single crystal, which can be solved and refined to determine the structure.

1.10.4 Neutron Diffraction[96]

Neutrons are diffracted in a similar manner to x-rays, but with one major difference, the electrons of atoms or ions diffract x-rays while neutrons are diffracted by their nuclei. It is this difference that results in the more accurate location of hydrogen atoms with neutron diffraction. Hydrogen, only possessing one electron, does not diffract x-rays very well and can be difficult to locate especially in the presence of atoms with high atomic numbers. Furthermore, when that one electron is involved in a covalent bond the apparent position of a hydrogen atom from x-ray diffraction is positioned towards the atom to which it is bonded. This is particularly important in hydrogen-bonding studies. Neutrons can determine X-H bond distances to a precision of ±0.002Å while the best low temperature x-ray data has errors at least one order of magnitude higher. Neutron diffraction can also be used to distinguish between atoms of similar atomic number and between isotopes.

Neutron diffraction, however, is not a commonly used technique due to its expense and the fact that the only source of neutrons available is a nuclear reactor. Another disadvantage of neutron diffraction is the generally low intensity of the neutrons, which results in the need for larger crystals (1-5mm; *cf.* 0.05-0.5mm for modern CCD x-ray facilities) and the long data collection times.

1.11 Structural Identification

The problem of determining the structure of molecules was addressed at the beginning of the nineteenth century by John Dalton.[97] It was possible to determine the molecular formulae and propose connectivities of simple compounds from chemical analysis, but only predictions could be made as to their structures. Throughout the nineteenth century the interest in molecular structure continued.

The proposal of W. L. Bragg in the early twentieth century that x-ray diffraction could be used to determine molecular structures in crystals[11] meant that the structural predictions from the nineteenth could be verified. The crystal structure of diamond was one of the first to be investigated by x-ray diffraction.[98] It was discovered that each carbon atom is surrounded tetrahedrally by four other carbon atoms, therefore confirming the predictions made by van't Hoff and Le Bel almost forty years previously.[99,100] The C–C distance of 1.544Å was also determined from this experiment and hence it was now possible to absolutely measure the dimensions of covalent molecules.

In 1928 the determination of the structure of hexamethylbenzene, a solid at room temperature, put an end to Kekulé's theory of the structure of benzene, with alternating single and double bonds.[101] It was observed that hexamethylbenzene is hexagonally symmetrical and consists of a flat, regular hexagonal arrangement of carbon atoms with six C,C bonds of equal length. The structure of benzene itself, was determined in 1954 at -3°C, although the data was of poor quality due to disorder

from melting.[102] Later studies confirmed benzene's structure as delocalised with six equivalent C,C bonds.[103]

X-ray diffraction continued to be used as a tool for the structural identification of small organic molecules and later larger, more complicated molecules were measured. The structure of cholesteryl iodide was determined in 1945, which confirmed the predictions made by Bernal on the structure of steroids from earlier x-ray diffraction experiments and refractive indices.[104,105] As the techniques for x-ray diffraction experiments improved so did the size and complexity of the molecules studied, the β-lactam structure of the antibiotic penicillin was confirmed from studies on the salts of benzylpenicillin[106], the structure of vitamin B_{12} was later determined[107] and in 1960 the structure of the first biological macromolecule, the protein myoglobin, was measured.[108]

1.12 Crystallographic Databases

As early as 1906 saw the advent of the first crystallographic database, which by 1919 consisted of information on nearly 10,000 crystalline substances, including 3342 drawings and diagrams of crystals.[109] J.D. Bernal planned the first computerised database in 1965.[110] Today the Cambridge Structural Database (CSD)[111-124] contains information on more than 230,000 carbon-containing crystal structures, which have been determined by x-ray or neutron diffraction. Olga Kennard initiated the database

in the 1970's. The information in the database consists of data extracted from published reports of crystal structure determination and includes atomic coordinates, information on the space group, chemical connectivity and bibliographic details. The database and associated software for geometry calculations, statistical analyses and structural display are invaluable in providing structural information suitable for comparison and indeed to ensure structures are not duplicated in error.

Other databases include the Protein Data Bank (PDB)[125,126], which contains data on structures of biological macromolecules, the Inorganic Crystal Structure Database[127-133], which provides information on all structures containing at least one non-metallic element, but no C,C or C,H bonds and the Powder Diffraction File (PDF)[134-137] containing data of single-phase x-ray diffraction patterns from microcrystalline powders.

1.13 Crystal Packing

A crystal consists of an arrangement of molecules or ions packed in a regular manner such that the total free energy of the system is at a minimum. The packing is determined by the forces between atoms, expressed by the sizes, shapes, charges, dipoles and hydrophobicities of the individual molecules or ions. There are two types of intermolecular forces in crystal structures; electrostatic and van der Waals forces. Electrostatic forces are ion-ion interactions between cations and anions, dipole / dipole interactions, including hydrogen bonds, and dipole / induced dipole

interactions between a polar molecule and a polarisable molecule. Van der Waals forces are those between neutral molecules, i.e. induced dipole / induced dipole (dispersion) forces when a non-polar molecule induces a small, instantaneous dipole in another nearby non-polar molecule.

The packing of ions in crystalline salts occurs so that their charges balance locally as well as throughout the crystal as a whole. In a crystal of sodium chloride the positively charged Na^+ ions are surrounded by six negatively charged Cl^- ions and vice versa so that each individual charge is essentially neutralised by surrounding ions of the opposite charge (Figure 3).[11] Packing of salts also takes into account the relative sizes of the ions, if both cations and anions are similar in size then the crystal will have a sodium chloride-like structure, but if the sizes are very different other arrangements are found.

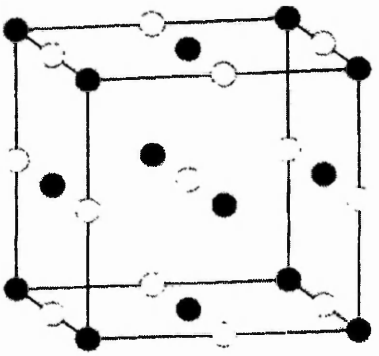

Figure 3 Packing diagram of NaCl [1]

Molecular crystals contain molecules that order through intermolecular interactions in a great variety of ways.[138-140] Polar molecules interact and pack in a head-to-tail

arrangement to minimise the free energy of the system, while non-polar molecules pack through weak low energy interactions through maximising the surface contacts between molecules. If the functional groups are capable of donating or accepting hydrogen bonds, then these interactions will be formed whenever possible and will play an important role in determining the molecular packing arrangement.[141,142] The numbers of hydrogen bond donors and acceptors in a crystal are, ideally, equal, but if this is not the case solvent molecules (e.g. water, methanol) can be incorporated to compensate.[143] Hydrophobic groups in a molecule tend to pack near hydrophobic groups of other molecules in the unit cell, and if a molecule contains both hydrophobic and hydrophilic groups these will pack as far apart as possible.

The strength of these individual interactions are generally very weak[1], e.g. at 25°C the average interaction energy for pairs of molecules with a dipole moment $\mu = 1D$ (such as chloroform) is about 1.4 kJ mol^{-1} when the separation between them is 3 Å. When a polarisable molecule with no permanent dipole moment, such as benzene, interacts with a polar molecule, such as chloroform, the average energy is about 0.8 kJ mol^{-1} and when two non-polar molecules, such as methane, interact at 3 Å the energy of that interaction is about 0.5 kJ mol^{-1}. Hydrogen bonding and electrostatic interactions are much stronger at ~20 kJ mol^{-1} and 250 kJ mol^{-1} respectively. In a crystal a multitude of individual interactions is usually present depending on the nature of the compound.

1.14 Polymorphism

Polymorphism is the existence of two or more crystalline forms of a given compound (dimorphism if there are only two forms) and results from changes in experimental conditions for their preparation. The differences in free energies of different polymorphs can be very small (4-8 kJ mol^{-1}), the polymorph with the lowest free energy is the most stable at a given temperature and pressure hence changes in these parameters can lead to transitions to a more stable polymorph. Polymorphs may differ with respect to physical properties such as melting points or solubilities and their existence often presents serious problems in the pharmaceutical industry since physical properties of crystals are often used as criteria for quality control and thereby the effectivity of a given preparation.[144]

Polymorphs differ with respect to how the molecules are packed in the crystal and the nature and quantity of the individual intermolecular interactions. These interactions are often very weak and it is conceivable that even small changes in temperature or pressure can lead to a phase transformation from one polymorph to another and that most compounds can, under appropriate conditions, crystallize as polymorphs. One molecule that displays polymorphism is 1-(N,N-dimethylamino)-8-nitronaphthalene **1**. Three polymorphs were obtained in the laboratory, which between them contained seven unique molecules in a variety of conformations.[145] Thus the study of polymorphic forms can provide further data on different molecular conformations.

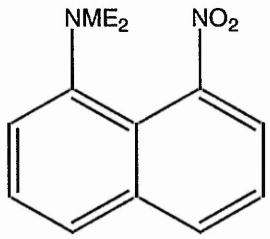

1

1.15 Supramolecular Chemistry

Supramolecular chemistry has been defined as the 'chemistry of molecular assemblies and of the intermolecular bond' by Jean-Marie Lehn who won the Nobel prize for his work in the area in 1987. It can be divided into two broad, partially overlapping areas, supermolecules and supramolecular assemblies. A supermolecule is produced when a molecule (a 'host') binds to another molecule (a 'guest') to produce a 'host-guest' complex. The host is usually a large molecule or aggregate, which has a cavity into which a guest molecule e.g. a monatomic cation, will fit. Supramolecular assemblies are polymolecular species resulting from the spontaneous association of a large number of components.

Supramolecular chemistry concerns non-covalent bonding interactions, which include a range of attractive and repulsive forces, similar to those involved in crystal packing. These include:

(i) electrostatic interactions (ion-ion, ion-dipole, dipole-dipole)

(ii) hydrogen bonding

(iii) π - π stacking interactions

(iv) van der Waals forces

(v) hydrophobic or solvatophobic effects

Supramolecular chemistry relies on the combination of a number of these weak interactions to achieve strong and selective binding.

One of the oldest and most widely known classes of supermolecules is the crown ethers. Their origins are traced back to the 1960's when Charles Pedersen was involved in the preparation of bis(2-(o-hydroxy-phenoxy)ethyl)ether as a multidentate ligand.[146] Whilst attempting to isolate the product he isolated some white crystals in ~4% yield and found that the addition of sodium salts increased the solubility of these crystals in methanol by a very large factor. The crystals were characterised and found to be a macrocycle **1** to which he gave the trivial name 'crown ether' due to its crown-like conformation in the solid phase. Pederson observed from a space filling model that a sodium ion can sit in the cavity of the crown, held together by attractive electrostatic ion-dipole interactions between the cation and the six oxygen donor atoms in the polyether rings. He recognised that the increased solubility of the macrocycle in the presence of sodium salts was due to the crown binding a sodium cation.

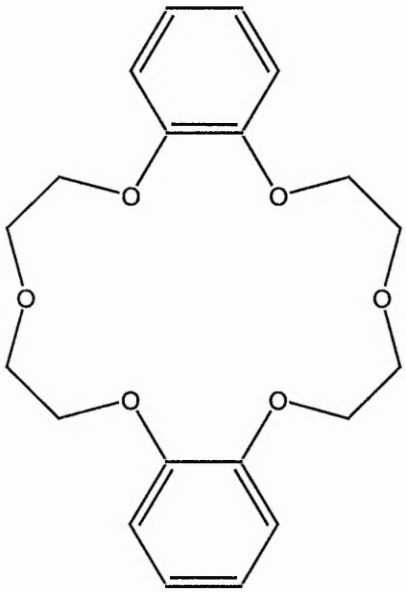

Dibenzo [18] crown-6 (**1**)[146]

Supramolecular assemblies can be obtained upon mixing different appropriately designed components in solution such that the intermolecular forces between them control their orientation, leading to the reversible assembly of such systems. Catenanes and rotaxanes are probably the most widely known of such assemblies, they involve two or more molecular components that are interlinked, but not physically joined by covalent bonds (Figure 4).[147] A catenane consists of two or more rings that are interlocked through non-bonding interactions while rotaxanes consist of a long, fairly linear molecule threaded through a macrocyclic ring. Once formed these systems are generally stable and cannot decompose back to separate components without breaking chemical bonds.

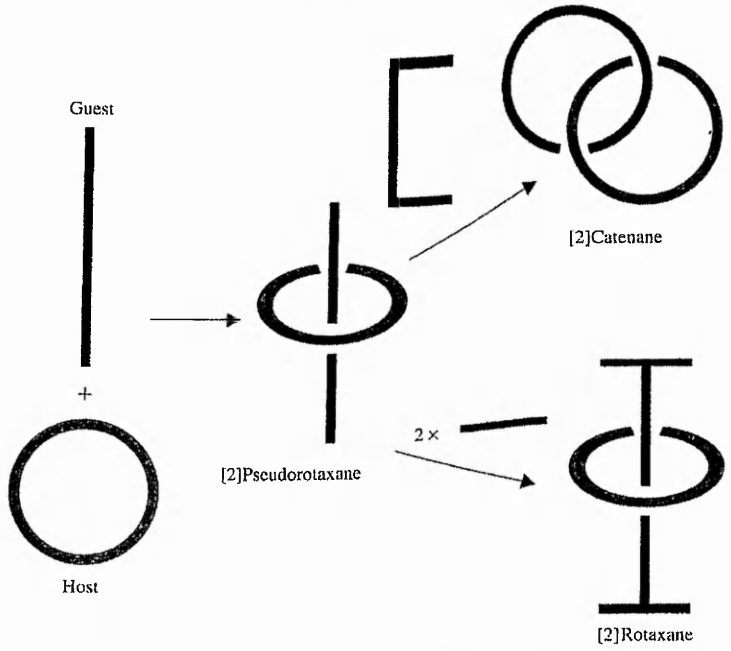

Figure 4 Synthesis of catenanes and rotaxanes via host-guest chemistry[147]

X-ray crystallography is very important in the field of supramolecular chemistry in providing direct information on the intermolecular interactions involved, particularly between host and guest molecules as well as steric fit. A crystallography experiment will clearly show the binding site of a host molecule and provide structural identification for the molecular designer. In the past problems have been encountered obtaining good-quality data for a variety of reasons. The large molecules usually are of awkward shapes and fit together poorly, they often contain solvent molecules, which may diffuse out of the crystal lattice during x-ray experiments, or move around resulting in disordered structures. Larger molecules quite often require collecting of a number of closely related sets of data, often from many crystals.

Modern x-ray diffraction studies, however, have become faster and more efficient with the introduction of area detectors. As these are capable of measuring many

diffractions simultaneously the time required is dramatically reduced and hence solvent diffusion is not such an issue. Experiments are generally carried out at low temperatures (100-150 K), which also serves to prevent solvent diffusion and reduces atomic motion and hence disorder.

When precise information is required for hydrogen bonding studies neutron diffraction must be used, which provides X-H bond distances to a precision of ±0.002 Å, while the errors in the best low temperature x-ray data are at least an order of magnitude higher.

1.16 Crystal Engineering

Crystal engineering has been defined as the understanding of intermolecular interactions in the context of crystal packing and in the utilisation of such understanding in the design of new solids with desired physical and chemical properties. The origins of this field of chemistry data back to the 1960's and the work of Gerhard Schmidt, who introduced the term 'crystal engineering' in the context of solid state reactions.[148] It has developed rapidly, however, especially with the advances made in x-ray crystallography and is now recognised as an important form of supramolecular synthesis. The crystallisation process is, by definition, a self-assembly process in the sense that the component molecules (supramolecular synthons) must find and recognise one another in solution and find their optimum orientation.

The ultimate aim of crystal engineering is to predict the crystal structure of a substance from just its molecular structure. To achieve this one must analyse the synergistic interplay of intermolecular non-covalent interactions. For most organic compounds the intermolecular interactions in their crystals are a complex mosaic of forces of varying strengths, directionalities and distance dependence characteristics, hence prediction is not easy. Computer simulations can be used to predict the possible crystal structures for a given molecule and indicate that which is most energetically favourable, however this is often not the result obtained experimentally either because the computations are approximate or because the crystallisation process is subject to both kinetic and thermodynamic factors. A competition is run by the CCDC (Cambridge Crystallographic Data Centre), which assesses the merits of such programs.[149] Crystal structure prediction is still in its infancy and as yet has been achieved only for relatively simple crystals.

An example of crystal engineering in practice is the 1:1 molecular complex of CBr_4 (**2**) and tetraphenylmethane (**3**) used as synthons to emulate the crystal structure of (4-bromophenyl)methane (**4**) (Scheme 1 and Figure 5).[150] In (**4**) a diamondoid network is formed by linking the tetraphenylmethane units using the tetrahedral supramolecular synthon (**X**). Four bromine atoms are arranged in a tetrahedral fashion similar to that of a CBr_4 molecule. The Br_4 clusters (**X**) are connected to the tetraphenyl moieties through C-Br covalent bonds. These Ph-Br molecular synthons were replaced with the supramolecular synthon (**Y**) involving a Br----phenyl non-covalent interaction. It was thought that these two changes should lead to no major structural change. Thus co-crystallisation of **2** and **3** led exclusively to the formation

of a complex, which is nearly isostructural with **4**, where four molecules of **2** are linked to one CBr_4 molecule in a diamondoid network, this is illustrated in Figure 5. Although formed from very different components, the crystal structures are very similar, hence the predictions proved correct.

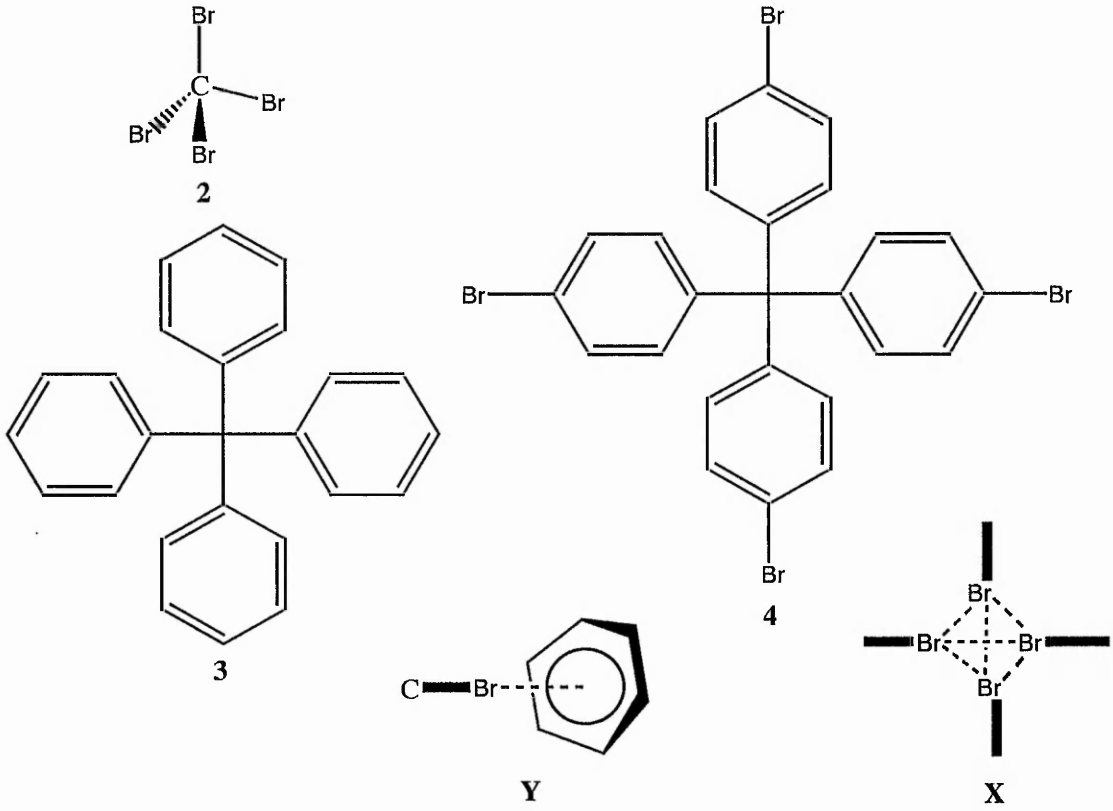

Scheme 1 Supramolecular synthons for the crystal structure of (4-bromophenyl)methane **4**.

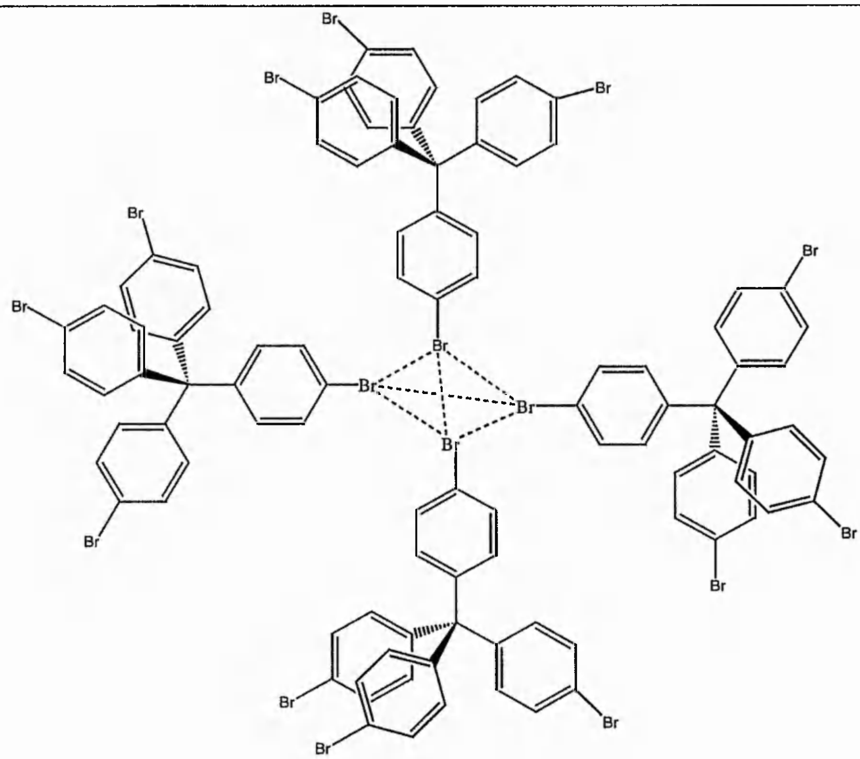

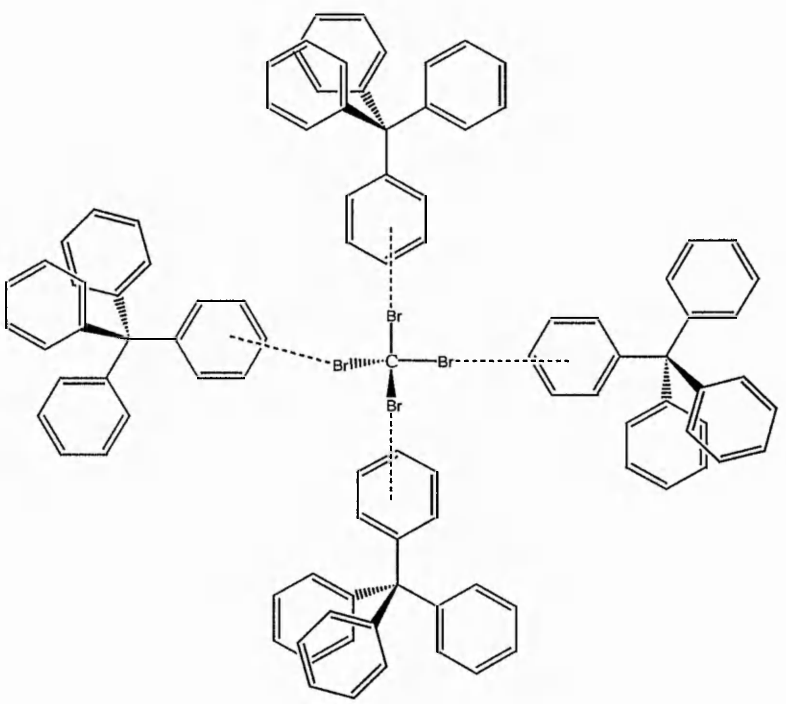

Figure 5 Diamondoid networks formed by **4** and a 1:1 complex of **2** and **3**

With the advances in x-ray crystallography it has been possible to obtain reliable information on intermolecular interactions from good quality data and as more precise, low temperature structure determinations will be available in the future this will lead to a wider variety of such information. Also with more neutron diffraction studies being performed this will lead to precise information about hydrogen bonding interactions.

The Cambridge Crystallographic Database forms an invaluable tool for crystal engineering, it is possible to perform detailed analyses of intermolecular interactions, which can be used to aid structure prediction and for comparison with predicted and calculated structures. The database now contains in excess of 200 000 structures and it is estimated that this will grow to more than half a million by the year 2010. A collaboration between Desiraju and Frank Allen of the Cambridge Crystallographic Data Centre has resulted in the use of an interaction display program, NIPMAT[151] to aid the understanding of the interplay of intermolecular interactions. This program creates a pictorial matrix using the atoms in the molecular skeleton (A_1, A_2, ...A_m, ...A_n) in which the matrix element A_mA_n represents the intermolecular contact A_m---- A_n. This provides a visual plot of all the intermolecular interactions simultaneously, which allows for easier interpretation of the interactions present and will, undoubtedly, be valuable for future structure prediction.

1.17 Interactions Between Functional Groups

X-ray crystallography is an essential technique for the study of through-space interactions between functional groups. Although chemical and spectroscopic techniques can provide evidence of interactions it is only by determining the crystal structure and analysing the molecular geometry that one can observe such interactions. This topic is discussed, in detail, in the remainder of this introduction.

1.17.1 Nucleophilic Addition to a Carbonyl Group

The origins of attractive interactions between functional groups dates back to the early 20th century and degradation studies of opium alkaloids.[152] W.H. Perkin jr. was investigating the nature of cryptopine's functionalities and found the compound was unreactive towards hydroxylamine, semicarbazide and amyl nitrite and ethoxide although it contains a keto group adjacent to an unsubstituted methylene group. On the basis of these results it was suggested that there was an interaction between the amine and carbonyl groups. The two groups are situated across a ten-membered ring, a relationship that was already established to allow for an effective interaction. Sir Robert Robinson formulated the concept of a through-space partial bond between the amino nitrogen and the carbonyl carbon to describe the observed effect.[153]

Spectroscopic studies on these natural products provided further evidence to support the theories, but it was not until 1971 when x-ray crystallographic studies determined

the structures of several related natural products (**5** – **10**) and confirmed the presence of through-space interactions (Table 1).[154-159] The N----C distance for clivorine **8** was determined to be 1.993(3) Å, almost in the range of a covalent bond, while the C=O bond is elongated, 1.258(3) Å. The carbonyl carbon is displaced from the plane of its three substituents by 0.213 Å, approximately half of the analogous distance in a tetrahedral carbon atom. The structure of retusamine **9** shows a cyclooctanone ring that is transformed, by protonation, into a quaternized aminoalcohol, however the C-N bond length is 1.64 Å, significantly longer than expected.

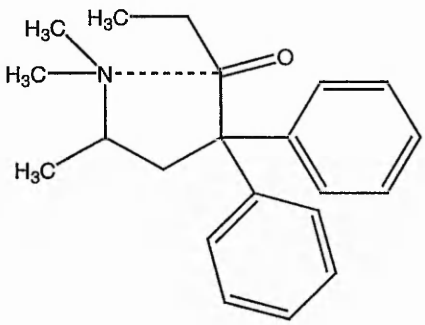

Methadone (**5**)

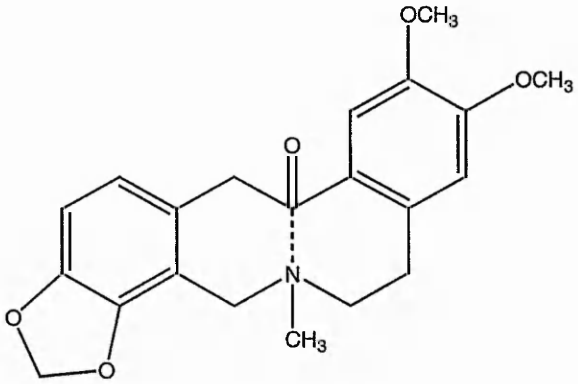

Cryptopine (**6**)

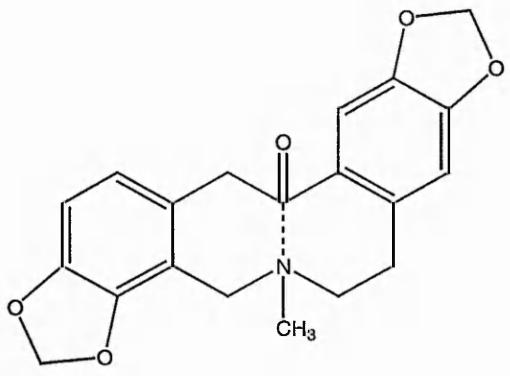

Protopine (**7**)

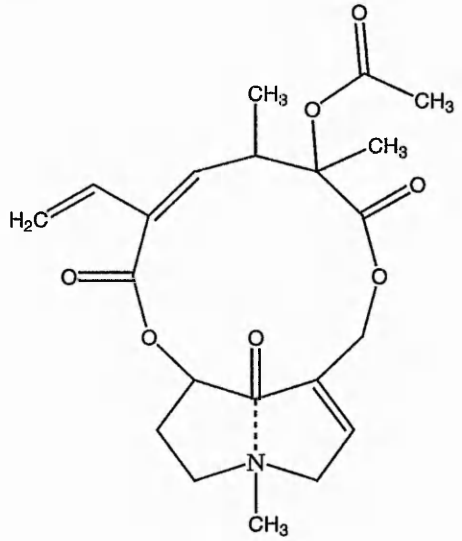

Clivorine (**8**)

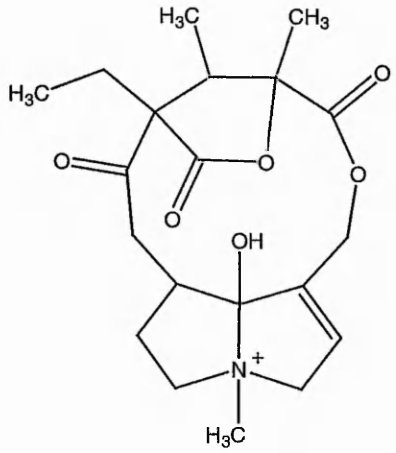

Retusamine (**9**)

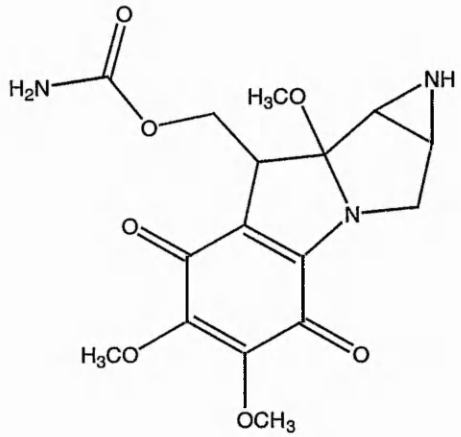

Mitomycin A (**10**)

Table 1 Selected geometries for compounds **5** – **10**

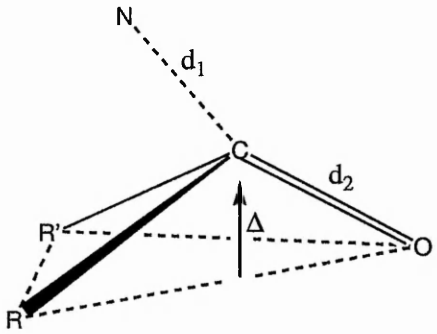

Molecule	d_1 (Å)	d_2 (Å)	Δ (Å)
Methadone **5**	2.910	1.214	0.064
Cryptopine **6**	2.581	1.209	0.102
Protopine **7**	2.555	1.218	0.115
Clivorine **8**	1.993	1.258	0.213
Retusamine **9**	1.64	1.38	0.26
Mitomycin-A **10**	1.490	1.370	0.420

In all cases the N, C and O atoms lie in an approximate local mirror plane and the carbonyl carbon is displaced from the plane of its three substituents towards the approaching nitrogen atom, as illustrated in Table 1. The results in Table 1 show a trend, as the N----C distance decreases the C=O bond lengthens and the displacement of the carbonyl carbon atom from the plane defined by its neighbours increases.

Bent proposed the idea of crystal structures representing early stages of chemical reactions.[160] This led to the proposal, by Bürgi, Dunitz and Schefter, that the data for the six natural products provide points on or close to a reaction coordinate.[161] Thus the data was used to map out the reaction pathway for nucleophilic addition to a carbonyl group. The observed out of plane displacements Δ correlated nicely with the N----C distances, d_1, (Equation 9) to give a smooth curve (Figure 6a).

$$d_1 = -1.101 \log \Delta + 0.867 \text{ Å} \quad \text{Eqn. 9}$$

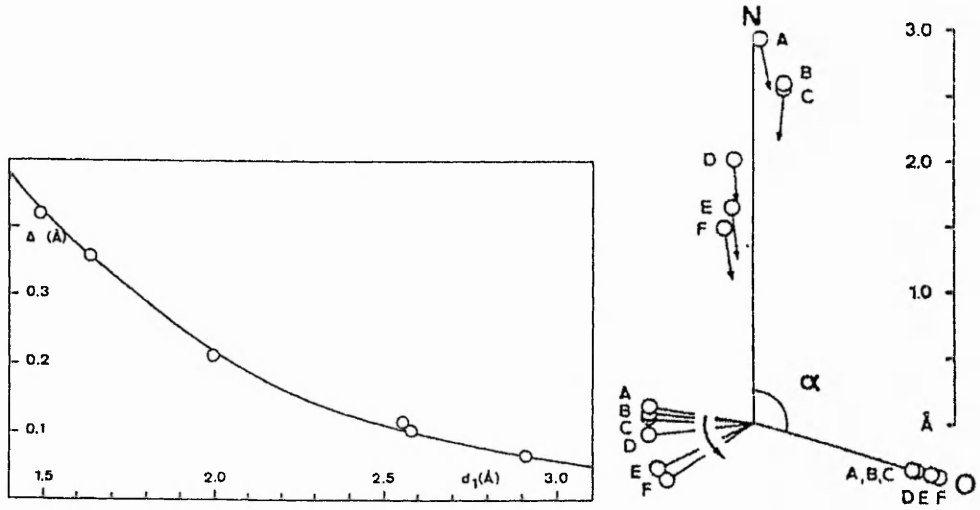

(a) (b)

Figure 6 (a) Correlation plot of Δ vs. d_1 (b) Reaction coordinate projected onto NCO plane[161]

The data from the six crystal structures was projected on to the NCO plane in order to build a picture of the geometric changes that occur during the addition of a nucleophile to a carbonyl group (Figure 6b). It was observed that as the nucleophile approaches the carbonyl carbon at an angle of 100-110°, not perpendicularly as was expected, the plane containing the carbonyl carbon atom and the two alkyl substituents bends away and the C=O bond lengthens.

1.17.2 1,8-Disubstituted Naphthalenes

The 1,8-disubstituted naphthalene framework was used to further investigate the addition of a nucleophile to a carbonyl group.[162] Substituents in the *peri* positions are forced into close contact and so it was expected that any interaction would be easily observed from a distortion of the bond angles.

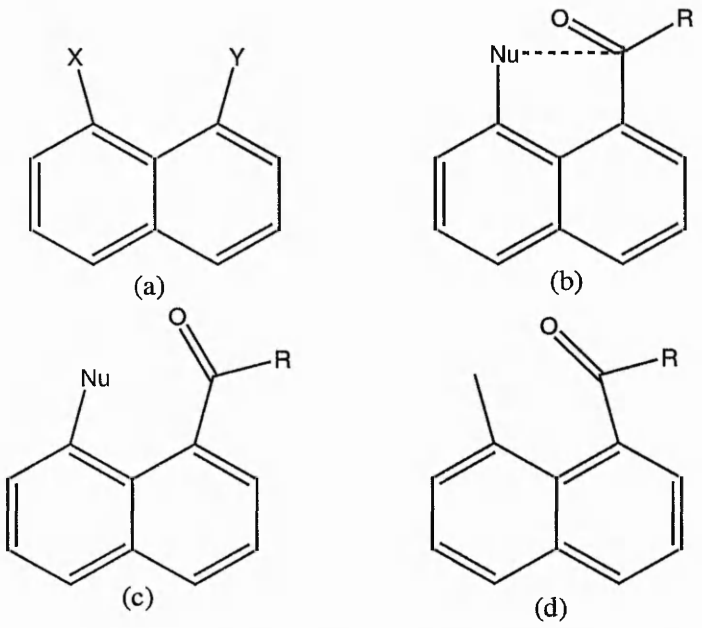

Figure 7 Possible distortion patterns of 1,8-disubstituted naphthalenes.

Most 1,8-disubstituted naphthalenes that have been studied by x-ray analysis show a distortion pattern consistent with a repulsion between the two substituents (Figure 7a). The exocyclic bonds are splayed outwards and in addition the substituents are displaced to opposite sides of the naphthalene plane in order to maximise the distance between the two substituents. Examples of structures displaying this distortion pattern are 1,8-dimethylnaphthalene,[163] 1,8-di-(prop-1-ynyl)naphthalene[164] and 1,8-bis(dimethylamino)naphthalene[165] where the X----Y distances (Figure 7a) are 2.93 Å, 2.86 Å (C----C) and 2.79 Å (N----N) respectively.

Figure 7b shows a theoretical 1,8-disubstituted naphthalene with no distortion and 'normal' bond angles, while Figures 7c and 7d show possible distortion patterns, which may arise from an attractive interaction between the two *peri* substituents. For structure in figure 7b the N----C=O angle would be approximately 90°, for the distortion pattern in Figure 7c this angle would be greater than 90° and for that of Figure 7d the angle would be less than 90°. Thus the 1,8-disubstituted naphthalenes were used to further investigate the approach angle of the nucleophile as it could not be ruled out that the angles observed in the natural products were due to geometric constraints rather than the nucleophilic addition process.

The crystal structure analyses of seven *peri*-disubstituted naphthalene derivatives were determined.[160] All seven showed a similar distortion pattern, Figure 7c, where the bond to the carbonyl carbon is splayed outward and the bond to the nucleophile is splayed inward, towards the carbonyl group. Table 2 shows selected geometries for the structures studied.

Table 2 Geometric details for compounds **11 – 17** (Å, °)

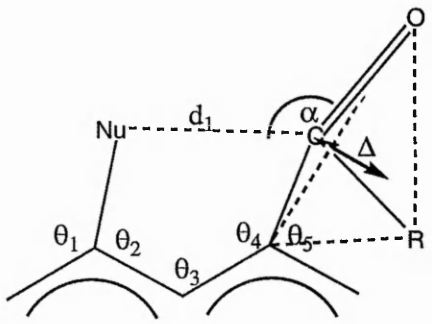

	Nu	R
11	NMe_2	Me
12	NMe_2	OH
13	NMe_2	OMe
14	OMe	Me
15	OMe	OH
16	OMe	NMe_2
17	OH	NMe_2

	d_1	Δ	θ_1	θ_2	θ_3	θ_4	θ_5	α
11	2.557(3)	0.088(3)	123.4(2)	116.6(2)	122.3(2)	123.2(2)	117.2(2)	104.4(2)
12	2.606(5)	0.061(5)	123.0(4)	117.4(3)	122.5(3)	123.9(3)	116.3(3)	102.2(4)
13	2.594(4)	0.062(3)	123.6(3)	117.4(3)	122.4(3)	123.9(3)	116.3(3)	98.6(4)
14	2.606(9)	0.044(10)	124.4(9)	115.9(8)	121.7(8)	125.5(8)	115.3(8)	107.6(9)
15	2.559(4)	0.022(5)	124.7(3)	113.2(3)	124.4(2)	124.3(3)	115.8(3)	93.7(3)
16	2.597(5)	0.039(4)	122.7(4)	114.4(4)	124.3(4)	124.0(3)	115.1(4)	103.3(4)
17	2.620(3)	0.051(3)	122.6(2)	116.5(2)	123.3(2)	123.6(2)	116.2(2)	97.0(2)

The key feature of the distortion pattern is the inward bending of the bond to the nucleophile towards the carbonyl group, which lies nearly perpendicular to the naphthalene plane. It was thought that the outward bending of the bond to the carbonyl group was in order to produce a more favourable Nu----C=O angle and as this would lead to an increase in the Nu----C distance the nucleophile bends inwards to counteract this. For all seven structures this angle is greater than 90° (94– 108°) and reasonably consistent with expectations based on the vector analysis rules proposal by Baldwin.[166] The authors do go on to say, however, that the variability in approach direction due to differences in structure and crystal packing calls for caution in their interpretation.

Another feature common to all seven structures is the small pyramidalisation of the carbonyl carbon towards the approaching nucleophile. This is larger for the dimethylamino derivatives (0.06 – 0.09 Å) than for the methoxy or hydroxy derivatives (0.02 – 0.05 Å) and was interpreted in terms of the relative nucleophilicities of the groups. The pyramidalisation was also observed to follow a trend due to the relative electrophilicities of the carbonyl carbon (COR > CO_2H ~ CO_2R > $CONR_2$) with the exception of the amides, however this anomaly was ascribed to special features of the molecular packing.

For compounds **11-13** the N----C distance only varies a little (2.56 – 2.61 Å) and is always within the sum of the van der Waals radii, ~3.2 Å for N and C atoms. For compounds **14-17** the O----C distances lie in the range 2.56 – 2.62 . It is surprising that the N----C and O----C distance do not vary more considering the expected greater nucleophilicity of the dimethylamino group.

1.17.3 Nucleophilic Addition to a C=C Bond

The 1,8-disubstituted naphthalene framework has also been used to investigate nucleophilic addition to a C=C bond.[167,168] The interactions between a dimethylamino or methoxy group and different electron-deficient alkenes were measured in compounds **18 -21**.

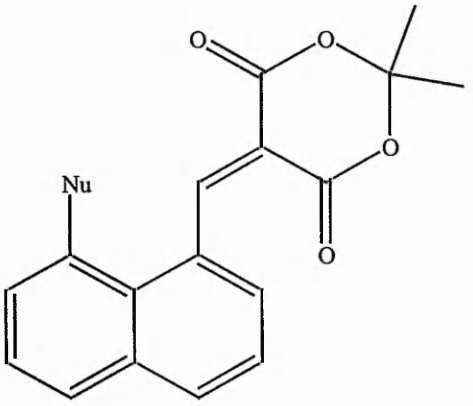

18 Nu = NMe_2
21 Nu = OMe

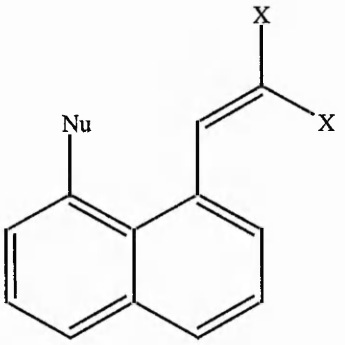

19 Nu = NMe_2, X = CN
20 Nu = NMe_2, X = COPh

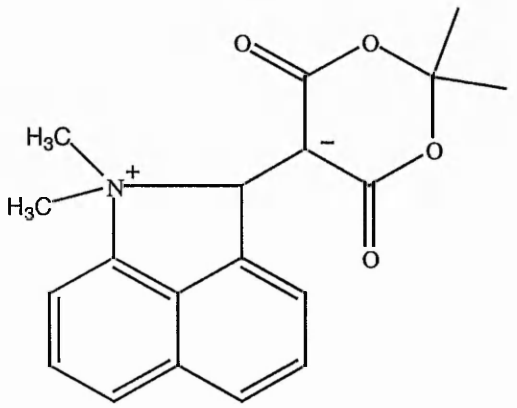

22

The three dimethylamino derivatives were considered to represent different stages in the addition of an amino group to a C=C bond culminating in an almost complete cyclisation where the structure of **18** is best represented as the zwitterion **22** with a N-C bond length of 1.651(3) Å. The dicyano compound **19** shows a close contact, N----C 2.413(2) Å, while the N----C distance in the dibenzoyl compound **20** is longer, 2.679(2) Å.

The data in Table 3 shows that the distortion patterns of **18** and **19** are clearly consistent with an attractive interaction as both exocyclic bonds are splayed inwards. In the dibenzoyl compound **20**, however, the distortion pattern is different, the bond to the nitrogen is splayed inwards while that to the alkene is splayed outwards in a similar pattern to that observed for the carbonyl compounds.

Table 3 Selected molecular geometry for compounds **18-21** (Å, °)

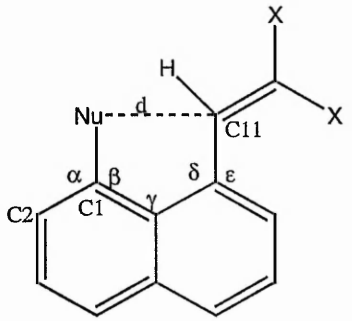

ΔC: deviation of C11 from the plane of its substituents towards the *peri* substituent.

T1 and T2: torsion angles of N-Me bonds with the C1-C2 aryl bond.

	Nu	X	d	α	β	γ	δ	ε	ΔC	T1	T2
18	NMe_2	-C(C(=O)O)2CMe2	1.651 (3)	128.6 (2)	108.8 (2)	113.3 (2)	109.9 (2)	131.4 (2)	0.362 (2)	49.5 (3)	-71.9 (2)
19	NMe_2	CN	2.413 (2)	124.3 (2)	115.9 (1)	120.4 (1)	120.2 (1)	120.3 (1)	0.087 (2)	49.7 (2)	-81.4 (2)
20	NMe_2	COPh	2.679 (2)	122.3 (3)	118.3 (2)	123.5 (2)	122.5 (2)	117.6 (2)	0.015 (2)	26.0 (2)	- 105.0 (2)
21	OMe	-C(C(=O)OC)Me	2.550 (2)	123.6 (2)	115.0 (2)	122.9 (2)	123.2 (2)	117.3 (2)	0.077 (2)	-	-

In the dibenzoyl compound **20** the lone pair of the nitrogen atom was found to be poorly aligned with the α-C of the alkene, the lone pair lies at 30° to the N----C vector, while in the dinitrile **19** this angle is only 13°, a much better alignment and similar to that in the cyclised zwitterionic structure **18**. It was thought that the reason the nitrogen lone pair was not attracted to the alkene in **20** was due to the reduced

conjugation of the carbonyl groups with the C=C bond since neither can be coplanar with the alkene for steric reasons, while in **19** and **18** the nitrile and carbonyl groups are well conjugated with the alkene.

The methoxy derivative **21** shows a longer Nu----C=O distance of 2.550(2) Å, than in the corresponding dimethylamino analogue **18**. The distortion pattern in this compound is such that the alkene is bent outward, and the methoxy group inward *cf.* compound **20**. There is not a sufficient attraction to pull the alkene back towards the nucleophile as there is in the corresponding dimethylamino compound. This, however, is consistent with the lower nucleophilicity of the methoxy group. The MeO----C=C separation in **21** is similar to the MeO----C=O separations discussed in Section 1.17.2, which lie in the range 2.56-2.62 Å. Thus the methoxy group is much less nucleophilic than the dimethylamino group and there is not much variation in the O----sp^2C separations.

All four uncyclised structures show small pyramidalisation at the alkene's α-C, such that the atom is displaced from the plane of its substituents towards the nucleophile, with a trend that parallels the relative electrophilicity of the atom and the Nu----C separations.

1.17.4 Nucleophilic Attack on sp-Carbon and Nitrogen Atoms

In recent years a range of structures exhibiting intramolecular interactions between nucleophiles and sp-carbon and nitrogen atoms have been determined, these include C≡N, N≡N and C≡C bonds.

1.17.4.1 Nucleophilic Attack on a Nitrile Group

The 1,8-disubstituted naphthalene framework has also been used to study interactions of electron-rich atoms with electrophilic sp C atoms of nitrile groups. Compounds **23**[169] and **24**[170] consist of a naphthalene with a nucleophilic group (OMe or NMe_2) in the 1-position and an electrophilic group (C≡N) in the 8-position, thus capable of forming an interaction between the substituents.

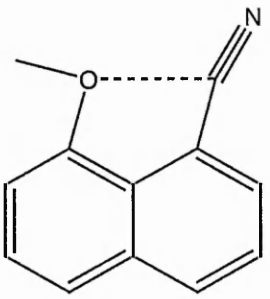

23

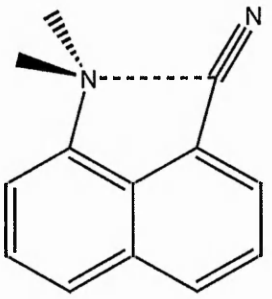

24

Figure 8 Interactions of NMe_2 and OMe groups with a nitrile group

Both structures show short Nu----C distances (O----C 2.594 Å and N----C 2.704 Å) significantly shorter than the sum of the van der Waals radii (~3.2 Å for N,C and

~3.1 Å for O,C). The structures also show the same distortion pattern that was observed in the carbonyl compounds, the bond to nucleophilic group is bent inward towards the nitrile group, which is bent away in the same direction (Figure 8). This distortion pattern results in Nu----C≡N angles of 103.5° in **23** and 106.5° in **24**, thus the approach direction of a nucleophile to a C≡N bond is at an obtuse angle to that bond.

In both structures the C-C≡N groups are bent from linearity (by 6.2° in **23** and 9.1° in **24**) such tht the sp C atom is displaced from the C-C≡N vector towards the approaching nucleophile. This distortion is greater in compound **24** consistent with the greater nucleophilicity of a dimethylamino group than a methoxy group.

Compound **25** also shows a Nu----C≡N interaction.[171] In this system the pyridine N atom provides the nucleophilic centre, which is capable of forming an interaction with the electron-deficient sp C atom of the nitrile group on the other ring.

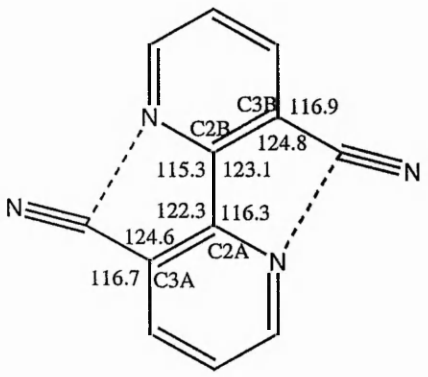

25

Figure 9 Selected bond angles in **25**

The structure of **25** is such that the two rings are at 23.6° to each other. There are close contacts between each pyridine N atom and an adjacent sp C atom (2.69 and 2.74 Å) both significantly shorter than the sum of the van der Waals radii (~3.2 Å). Both C-C≡N groups are bent from linearity (8.4 and 8.7°) such that the sp C atom is displaced from the C-C≡N vector towards the adjacent pyridine atom and the N----C≡N angles are 107.6 and 108.0°.

If the two rings existed in a coplanar arrangement so as to maximise the π overlap the N----C≡angle would be much less (~99°), thus this structure provides evidence that the preferred approach direction of a nucleophile to a C≡N bond is at an obtuse angle (as observed in **23** and **24**), of at least 108°. Indeed the desire to achieve this angle overrides the desire to achieve the closest possible N----C separation. The angles at C2 and C3 (Figure 8) show that the molecule is distorted such that the nitrile group and the pyridine N atoms are bent away from each other, this serves to increase the N----C separation, but also increases the N----C≡N angle to that approaching the preferred angle of attack.

1.17.4.2 Nucleophilic Attack on a Diazonium Group

The crystal structures of four 8-substituted naphthalenoid-1-diazonium cations **26** – **29** (as their tetrafluoroborate salts) were measured, to observe interactions of the $N^{+}\equiv N$ bond with different nucleophilic groups, MeS, Me_2N, NO_2 and $N^{+}\text{-}O^{-}$.[172]

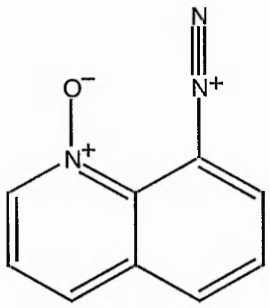

26

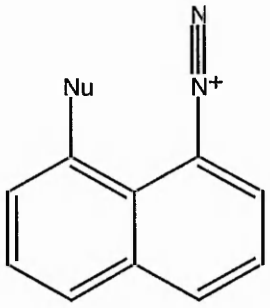

27 Nu = SMe
28 Nu = NMe_2
29 Nu = NO_2

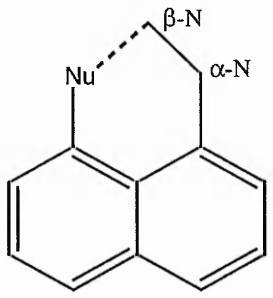

(a)

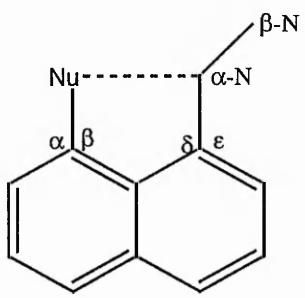

(b)

Figure 10 Geometries resulting from interaction of the nucleophile with the β-N (a) and the α-N (b) atoms.

All four cations were observed to exhibit interactions between an electron rich atom and the diazonium group, with distances (2.443(2) – 2.938(5) Å) well within the sum of the appropriate van der Waals radii. In all cases the interaction is with the α-N atom and results in bending of the C-N≡N group by ~10° such that the α-N atom is displaced towards the nucleophile. This pattern of interactions is that shown in Figure 10b rather than Figure 10a, which would arise from interaction with the β-N atom. This result is in contrast to the reactivity of aromatic diazonium salts. Anions such as

thiolate and cyanide attack at the β-N atom to give 1,2-diazenes[173] while addition to the α-N atom would produce unstable 1,1-diazenes which decompose readily with loss of N_2.[174]

In all four structures the bond to the diazonium group is splayed outwards, resulting in $\delta > \varepsilon$ (Figure 10b), this serves to increase the Nu----N≡N angle similarly to that observed in the 1,8-disubstituted naphthalene carbonyl compounds.[160] In all structures the angle of approach is greater than 90° (93 - 105°). Structure **26** provides the strongest evidence that an obtuse angle is preferred for nucleophilic approach to a N≡N bond. In this structure the nucleophile, which is the N-oxide oxygen atom of a quinoline, does not possess any substituents (in contrast to Me_2N and OMe) that may disfavour outward bending of the bond to the aromatic framework through steric interactions with the *ortho*-H atom. Thus, this molecule provides a fair test of the preferred interaction geometry in this case.

In structures **26** and **28** the outward bending of the bond to the diazonium group is accompanied by inward bending of the bond to the nucleophile, as observed earlier in interactions with carbonyl groups. However, in structures **27** and **29** the nucleophile and the diazonium group are both splayed outward. This was attributed to steric or geometry effects, i.e. due to the larger size of the S atom in the methylthio group and due to the nitro group having to get an oxygen atom into a position to make a 1,6 interaction with the diazonium group.

The results obtained are consistent with the idea that the favoured approach direction of the nucleophile is such as to optimise the overlap between the incoming lone-pair electrons and the anti-bonding π^* orbital of the N≡N bond. Unlike nucleophilic attack on a carbonyl group, this reaction as it proceeds encounters a highly unfavourable activation energy.

1.17.4.3 Nucleophilic Addition to C≡C Bonds

It is possible for alkynes to react with both electrophiles and nucleophiles depending on the alkyne's substituents, electron-deficient alkynes undergo nucleophilic addition reactions such as the addition of aziridine to but-2-yne-1,4-dioate[175], while electron-rich alkynes react with electrophiles e.g. but-3-yne adds one equivalent of bromine.[176] Experimental evidence suggests that both *cis* and *trans* additions of nucleophiles are energetically favourable, e.g. amines add to dimethyl-but-2-yn-1,4-dioate predominantly by *trans* addition in methanol, but by *cis* addition in aprotic solvents.[177] Compounds have been synthesised which attempt to model this behaviour.[178-180]

One of the first alkynes investigated in terms of intramolecular interactions was ethyl 3-(2-nitrophenyl)propynoate **30**.[178] In this compound the triple bond is activated by the carboxylic ester and so is susceptible to nucleophilic attack. An oxygen atom of the ortho-nitro group provides an electron-rich centre to study interactions with the electron-deficient alkyne. There is, indeed, an interaction between the nitro O atom

and the alkynyl C atom attached to the aromatic ring as indicated by the O----C separation of 2.642(2) Å, which is well within the sum of the appropriate van der Waals radii.

A trans bend is observed in the triple bond with angular deviations at both alkynyl carbon atoms of ~7° from linearity and the sp-carbon involved in the interaction deviates from the Ar-C≡C vector towards the electron rich O atom. There is an antiperiplanar relationship between the direction of the approaching electron rich atom and the axis of the orbital of the developing carbanion at the β-C atom of the alkyne.

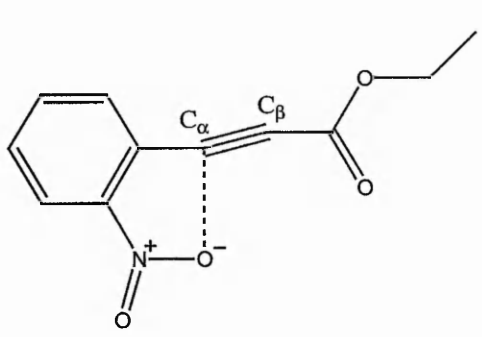

30

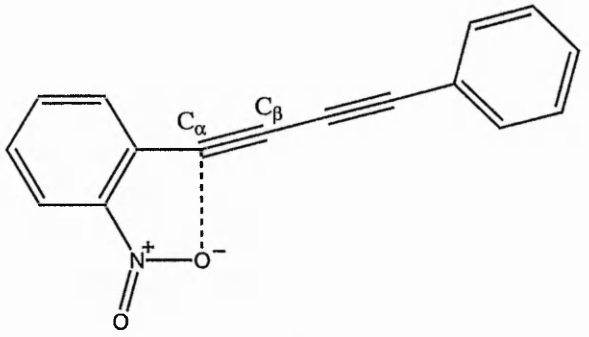

31

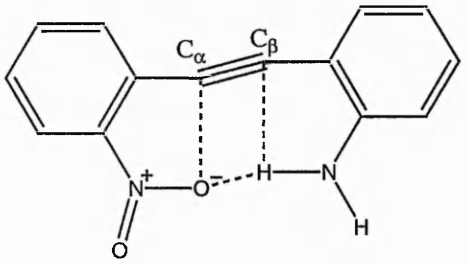

32

Figure 11 Compounds **30** – **32** showing O----C≡C interactions

The dialkyne species **31** shows a similar interaction, 2.636(2) Å, although this structure shows only a bending (by 7.3°) at the sp-C atom involved in the interaction.[179] There is no second bend at the second alkyne C atom as was observed in compound **30**. In this structure the presence of a second C≡C bond results in an alignment of the relevant orbitals such that the developing carbanion centre at the β-C atom can be stabilised by conjugation with the π system of the second triple bond. This is in contrast to compound **30** where the carboxylic ester π orbitals did not lie in the same plane as the developing carbanion centre, possibly due to packing constraints.

Compound **32** incorporates an alkyne bond with the potential to make contacts with both an electron-rich oxygen atom and electron-poor hydrogen atom.[180] This structure was used as a model for an early stage in the addition of a nucleophile and proton to an alkyne. The structure of **32** shows several short contacts, as illustrated in Figure 11. The O----spC separation is 2.672(4) Å, which is slightly longer than the distances observed in **30** and **31**, but still ~0.45 Å within the sum of the van der Waals radii. The same oxygen is also involved in an intramolecular hydrogen bond (2.34(4) Å) with one of the amino hydrogen atoms. There is also a close contact between this amino hydrogen atom and the second sp-C atom, which is not involved in the O----C interaction, (2.43(4) Å). This structure exhibits similar *trans* bending of the alkyne to that observed in compound **30**, the angular deviations being 8.1(3)° at the α-C atom and 6.6(3)° at the β-C atom such that the α-C atom is displaced towards the electron rich O atom.

Ab initio electron density calculation using Bader's 'Theory of Atoms in Molecules'[181] were applied to compound **32**. Using this approach a bond is defined using a critical point in the total electron density distribution. This is a point between two atoms from which if you travel along the interatomic vector, e.g. the x axis, in either direction away from that point the total electron density will increase, however along the y and z axes in either direction the total electron density will rapidly decrease to insignificance. If this rule is not obeyed the distance between two atoms cannot be classified as a bond. The calculations indicated the presence of the O----C≡C interaction observed in the x-ray structure, however no critical point was found between the amino H atom and C_8.

Other studies to investigate interactions with a C≡C bond have been concerned with carbonyl O atoms as the electron rich atom. Two such compounds are **33**[182] and **34**[183]. The two compounds exhibit certain similarities both structural and chemical. They both readily undergo intramolecular addition of a carboxylic acid to the triple bond to give a lactone. Depending on the reaction conditions **33** lactonises to give either the benzopyranone **35** or the isobenzofuranone **36**, while **34** reacts to give just the corresponding furanone. In **34** the presence of the second carboxylic acid group was found to result in a much faster rate of reaction. When the group was absent or located in the 4-position the reaction proceeded much more slowly.

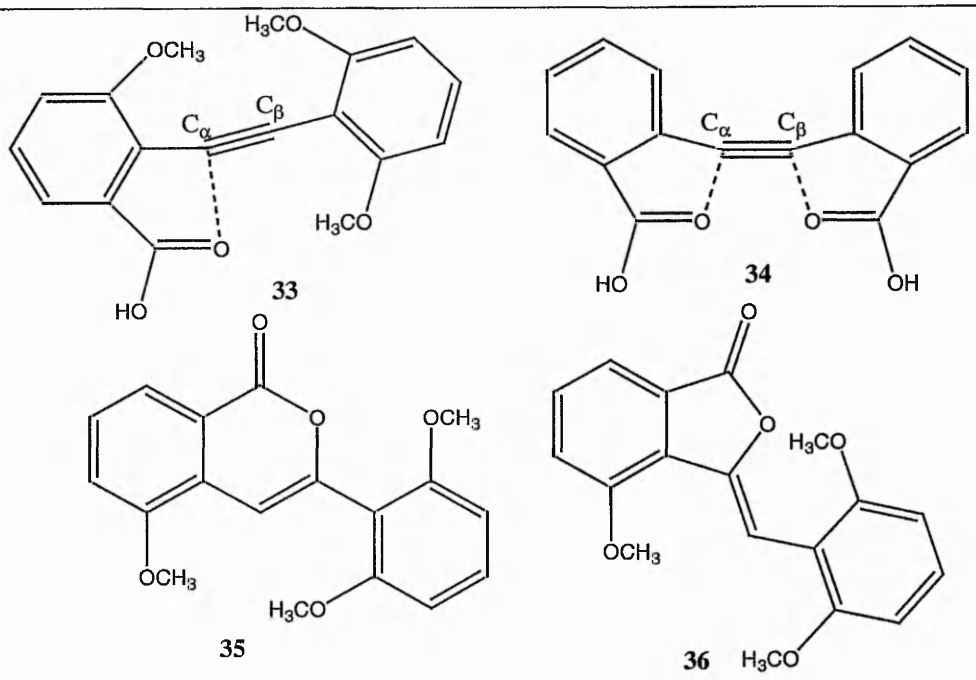

The structures of **33** and **34** show close contacts between the carbonyl O atoms and one of the sp-C atoms (C_7), 2.785(2) and 2.775(2) Å respectively (only half of molecule **34** is crystallographically unique, related to the other half by a twofold axis bisecting the triple bond). In both structures these close contacts result in bending of the triple bond, in **33** this occurs only at one of the sp-C atoms to produce an angle of 171.0(1)° at C_α. The bending in structure **34**, however is interesting in that the alkyne undergoes both *cis* and *trans* bending, *cis* bending occurs in the molecular plane with both sp-C atoms displaced towards the adjacent carbonyl O atoms, while trans bending occurs in the perpendicular plane.

In **34** both carboxylic acid groups are located on the same side of the triple bond, the explanation proposed for this is illustrated in Figure 12. A *trans* conformation is likely to result in repulsion between the carbonyl O atom's lone pair electrons and the developing carbanion centre antiperiplanar to the approaching nucleophile.

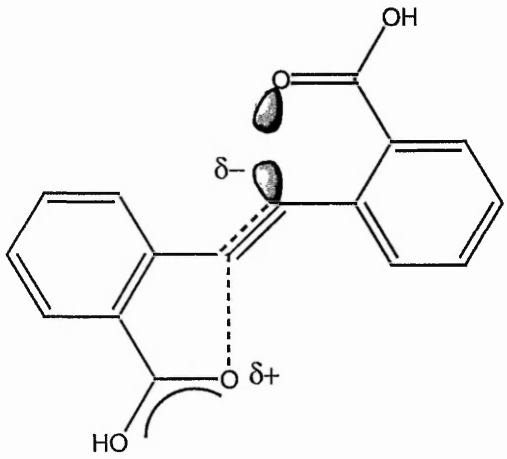

Figure 12 Illustration of the repulsion expected in the *trans* conformation

Both structures show similar Nu----C≡C approach angles, in **33** the O----C_α—C_β angle is 107.8(1) °, while in **34** the corresponding angle is 104.9(1) °. This is achieved through molecular distortions such that the carboxylic acid groups are splayed outwards, away from the molecular plane. These angles agree with the results from computational analyses, which suggest an obtuse angle of approach is preferred.[184-186]

A recent study involving the 1,8-disubstituted naphthalene framework has continued with the study into interactions between nucleophiles and C≡C bonds. Compounds **37** to **41** were used to investigate interactions between the methoxy group and alkynes with terminal substituents of different electron-withdrawing powers.[187]

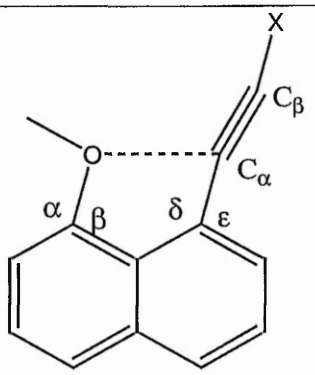

37 X = H
38 X = COMe
39 X = CO_2Me
40 X = CONHPh
41 X = CN

Figure 13 The distortion pattern observed in compounds **37 – 41**

All five structures show close contacts between the methoxy O atom and the α-C atom of the alkyne (2.593(2) – 2.663(2) Å), which are shorter than that of the sum of the van der Waals radii (~3.1Å). Each triple bond shows a *trans* bend with deviations from linearity lying in the range 4.0 – 10.8° such that the α-C atom is displaced from the C-C≡C vector towards the methoxy O atom.

There is a trend between the O----C distance and the orientation and electron-attracting power of the alkyne's terminal group. The longest O----C distances are for the unsubstituted alkyne **37** (2.603(2) Å) and the alkynone **38** (2.641(2) Å). The ketone group in **38** is almost exactly coplanar with the naphthalene ring system and so does not exert a mesomeric electron withdrawing effect on the component of the alkyne's orbital lying in the molecular plane. When the terminal substituent is an amide **40** or a methyl ester **39**, the in-plane π system of the alkyne is partially activated as the carbonyl groups of these structures are rotated out of the molecular plane by 35 - 48°, thus the O----C distances are shorter than for the ketone: 2.598(4) and 2.621(4) Å for the two independent molecules of **40** and 2.606(3) Å for **39**. The

shortest O----C distance is observed in **41** when the terminal substituent is a nitrile, which can activate the alkyne's in plane π orbitals.

Compounds **37 – 41** all show the same distortion pattern consistent with an interaction between *peri*-substituents in naphthalene derivatives where $\alpha > \beta$ and $\delta > \varepsilon$ (Figure 13).[160, 168] In all cases the bond to the methoxy group is splayed inward towards the alkyne group, which is splayed in the same direction, away from the methoxy group. The O----C≡C angles range from 102.1(1) to 108.7(1)° similar to those found in previous studies of interactions with C≡C bonds.[182,183]

1.18 Topics Covered in This Thesis

The remaining four chapters of this thesis detail the further investigation into interactions that have been made. A new analysis of 1,5-*peri*-interactions between N or O atoms and sp^2C atoms is reported in light of the greater amount of data available, and including the structure determination of several new compounds. The first *peri*-interaction between a Me_2N group and a C≡C group has been measured. A study into *peri*-interactions of the MeS group with different electron-deficient alkenes is discussed. A series of 2,2'-disubstituted biphenyl derivatives have been synthesised to investigate 1,6-interactions of the Me_2N group with the CHO group and with different electron-deficient alkenes. Finally interactions in 3,3'-dinitro-2,2'-bipyridine derivatives are discussed.

1.19 References

1. Glusker, J.P. and Trueblood, K.N., *Crystal Structure Ananlysis for Chemists and Biologists*, Wiley-VCH, New York, 1994.
2. Michette, A.G., *Nature*, 1991, **353**, 510.
3. Hansma, P.K., Elings, V.B., Marti, O. and Bracker, C.E., *Science*, 1988, **242**, 209.
4. Radmancher, M., Tillmann, R.W., Fritz, M. and Gaub, H.E., *Science*, 1988, **257**, 1900.
5. Frommer, J., *Angew. Chem., Int. Ed. Engl.*, 1992, **31**, 1298.
6. Hessel, J.F.C., *Krystallometrie oder Krystallonomie und Krystallographie* [Crystallometry, or crystallonomy and crystallography.] In Gehler's *Physikalisches Wörterbuch*, Schweickert, Liepzig, 1830, **5**, 1023.
7. Jenkins, F.A. and White, H.E., *Fundamentals of Optics*, 4th edn., McGraw-Hill, New York, 1976.
8. Greenler, R.G. and Hable, J.W., *Amer. Scientist*, 1989, **77**, 369.
9. Grimaldi, F.M., *Physico-Mathesis de Lumine, Coloribus, et Iride* [Physical insights into light, colours, and the spectrum (rainbow).] Hæredis Victorii Benatii, Bologna, 1665.
10. Bragg, W.L., *Proc. Camb. Phil. Soc.*, 1913, **17**, 43.
11. Bragg, W.L., *Proc. R. Soc. London, Ser. A*, 1913, **89**, 248.
12. Blessing, R.H., *Crystallographic Reviews*, 1987, **1**, 3.
13. Mark, H. and Szilard, L., *Z. Physik*, 1926, **35**, 743.
14. Kirkpatrick, P., *Phys. Rev.*, 1927, **29**, 632.

15. von Laue, M., *Z. Krist.*, 1926, **64**, 115.

16. Azaroff, L.V., *Acta Cryst.*, 1955, **8**, 701.

17. Busing, W.R. and Levy, H.A., *Acta Cryst.*, 1957, **10**, 180.

18. Bond, W.L., *Acta Cryst.*, 1959, **12**, 375.

19. Walker, N. and Stuart, D., *Acta Cryst.*, 1983, **A39**, 158.

20. DeTitta, G.T., *J. Appl. Cryst.*, 1985, **18**, 75.

21. Sears, V.F., *J. Appl. Cryst.*, 1984, **17**, 226.

22. De Meulenær, J. and Tompa, H., *Acta Cryst.*, 1965, **19**, 1014.

23. Chidambaram, R., *Computing in Crystallography*, eds. Diamond, R., Ramaseshan, S. and Venkatesan, K., Indian Academy of Sciences, Bangalore, 1980.

24. Lipson, H., *International Tables for X-ray Crystallography.* Volume II. *Mathematical Tables. Section 5. Physics of Diffraction Method.*, eds. Kasper, J.S. and Lonsdale, K., Kynoch Press, Birmingham, 1959.

25. Koch, B. and MacGillavry, C.H., *International Tables for X-ray Crystallography.* Volume III. *Physical and Chemical Tables. Section 3. Measurements and Interpretation of Intensities*, eds. MacGillavry, C.H. and Rieck, G.D., Kynoch Press, Birmingham, 1962.

26. Fourier, J.B.J., *Théorier Analytique de la Chaleur.* [Analytical theory of heat.] Firmin Didot, Paris, 1822. English translation, Freeman, A., 1872.

27. Patterson, A.L., *Z. Krist.*, 1935, **A90**, 517.

28. Patterson, A.L., *Phys. Rev.*, 1934, **46**, 372.

29. Patterson, A.L., *Z. Acta Cryst.*, 1949, **2**, 339.

30. Blow, D.M. and Rossmann, M.G., *Acta Cryst.*, 1961, **14**, 1195.

31. Crick, F.H.C. and Magdoff, B.S., *Acta Cryst.*, 1956, **9**, 901.

32. Harker, D., *Acta Cryst.*, 1956, **9**, 1.

33. Perutz, M.F., *ActaCryst.*, 1956, **9**, 867.

34. Bijovet, J.M., *Nature* (*London*), 1954, **173**, 888.

35. Kendrew, J.C., Bodo, G., Dinitzis, H.M., Parrish, R.G. and Wyckoff, H., *Nature* (*London*), 1958, **181**, 662.

36. Blow, D.M. and Crick, F.H.C., *Acta Cryst.*, 1959, **12**, 794.

37. Robertson, J.M., *Nature* (*London*), 1939, **143**, 75.

38. Hauptman, H.A., *Physics Today*, 1989, **November**, 24.

39. Woolfson, M.M., *Direct Methods in Crystallogrphy*, Oxford University Press, Oxford, 1961.

40. Ladd, M.F.C. and Palmer, R.A., *Theory and Practice of Direct Methods in Crystallography*, Plenum, New York, London, 1980.

41. Hauptman, H.A. and Karle, J., *Solution of the Phase Problem.* I. *The Centrosymmetric Crystal*, American Crystallographic Association Monograph No.3, New York, 1953.

42. Woolfson, M.M., *Acta Cryst.*, 1987, **A43**, 593.

43. Whittaker, E.T. and Robinson, G., *The Calculus of Observation*, 4th edn., Blackie, Glasgow, 1958.

44. DuMond, J.W.M. and Cohen, E.R., *Rev. Mod, Phys.*, 1953, **25**, 691.

45. Pepinsky, R., Robertson, J.M. and Speakman, J.C., *Computing Mthods and the Phase Problem in X-ray Crystal Analysis*, Pergamon Press, New York, London, Paris, 1961.

46. Stout, G.H. and Jensen, L.H., *X-ray Structure Determination*, Macmillan, London, 1968. 2nd edn. John Wiley, New York, 1989.

47. Prince, E., *Mathematical Techniques in Crystallography and Materials Science*, Springer-Verlag, New York, Heidelberg, Berlin, 1982.

48. Jensen, L.H., *Methods in Enzymology*, 1985, **115**, 227.

49. Hestenes, M.R. and Stiefel, E., *Natl. Bur. Stand.*, 1985, **49**, 409.

50. Rollett, J.S., *Computing Methods in Crystallography*, Pergamon Press, Oxford, 1965.

51. Rollett, J.S., *Computational Crystallography*, ed. Sayre, D., Clarendon Press, Oxford, 1982.

52. Hendrickson, W.A., Refinement of protein structures. *Proceedings of the Daresbury Study Weekend (15-16 November) – Refinement of Protein Structures*, eds. Machin, P.A., Campbell, J.W. and Elder, M., SRC Daresbury Laboratory, Warrington, U.K., 1981.

53. Sussman, J.L., The use of CORELS for the refinement of biological macromolecules. *Proceedings of the Daresbury Study Weekend (15-16 November) – Refinement of Protein Structures*, eds. Machin, P.A., Campbell, J.W. and Elder, M., SRC Daresbury Laboratory, Warrington, U.K., 1981.

54. Hendrickson, W.A. and Konnert, J.H., *Computing in Crystallography*, eds. Diamond, R., Rameseshan, S. and Venkatsesan, K., Indian Academy of Science, Bangalore, 1980.

55. Jack, A. and Levitt, M., *Acta Cryst.*, 1978, **A34**, 931.

56. Jones, P.G., *Chem. Soc. Rev.*, 1984, **13**, 157.

57. James, R.W., *The Optical Principles of the Diffraction of X-rays*, Cornell University Press, Ithaca, New York, 1965.

58. Buerger, M.J., *Crystal-Structure Analysis*, Wiley, New York, 1960.

59. Friedel, G., *Comptes Rendus, Acad. Sci.*, (*Paris*), 1913. **157**, 1533.

60. van der Helm, D., Glusker, J., Johnson, J.P., Minkin, J.A., Burrow, N.E. and Patterson, A.L., *Acta Cryst.*, 1968, **B24**, 578.

61. Johnson, C.K., *Proceedings of the 1969 International Summer School on Crystallographic Computing*, Munksgaard, Copenhagen, 1970.

62. Rogers, D., *Acta Cryst.*, 1981, **A37**, 734.

63. Flack, H., *Acta Cryst.*, 1983, **A39**, 876.

64. Bernardinelli, G. and Flack, H.D., *Acta Cryst.*, 1985, **A41**, 500.

65. Watkin, D.J., *Chem. Britain*, 1989, **25**, 32.

66. Douzou, P., *Cryobiochemsitry: An Introduction*, Academic Press, London, New York, 1977.

67. Rudman, R., *Crystallography in North America*, eds. McLachlan, D., Jr. and Glusker, J.P., American Crystallographic Asociation, New York, 1983.

68. Rudman, R., *Low Temperature X-ray Diffraction: Apparatus and Techniques*, Plenum, New York, 1976.

69. Machin, K.J., Begg, G.S. and Isaacs, N.W., *J. Appl. Cryst.*, 1984, **17**, 358.

70. Hajdu, J., McLaughlin, P.J., Helliwell, J.R., Sheldon, J. and Thompson, A., *J. Appl. Cryst.*, 1984, **18**, 528.

71. Cosier, J. and Glazer, A.M., *J. Appl. Cryst.*, 1986, **19**, 105.

72. Henriksen, K., Larsen, F.K. and Rasmussen, S.E., *J. Appl. Cryst.*, 1986, **19**, 390.

73. Abrahams, S.C., Colin, R.L., Lipscomb, W.N. and Reed, T.B., *Rev. Sci. Instrum.*, 1950, **21**, 396.

74. Kaufman, H.S. and Frankuchen, I., *Rev. Sci. Instrum.*, 1949, **20**, 733.

75. Dulmage, W.J. and Lipscomb, W.N., *Acta Cryst.*, 1951, **4**, 330.

76. Williams, P.S., *Rev. Sci. Instrum.*, 1933, **4**, 334.

77. Müller, A., *Proc. R. Soc.* (*London*), 1929, **A125**, 507.

78. Taylor, A., *J. Sci. Instrum.*, 1949, **26**, 225.

79. Usha, R., Johnson, J.E., Moras, D., Thierry, J.C., Fourme, R. and Kahn, R., *J. Appl. Cryst.*, 1984, **17**, 147.

80. Helliwell, J.R., *Macromolecular Crystallography with Synchrotron Radiation*, Cambridge University Press, Cambridge, 1992.

81. Moffat, K., Szebenyi, D and Bilderback, D., *Science*, 1984, **223**, 1423.

82. Hamlin, R., *Trans. Amer. Cryst. Assn.*, 1982, **18**, 95.

83. Hamlin, R., *Trans. Amer. Cryst. Assn.*, 1982, **18**, 1.

84. Xuong, N.H., Nielsen, C., Hamlin, R. and Anderson, D., *J. Appl. Cryst.*, 1985, **18**, 342.

85. Arndt, U.W., *J. Appl. Cryst.*, 1986, **19**, **145.**

86. Messerschmidt, A. and Pflugrath, J.W., *J. Appl. Cryst.*, 1987, **20**, 306.

87. Blum, M., Metcalf, P., Harrison, S.C. and Wiley, D.C., *J. Appl. Cryst.*, 1987, **20**, 235.

88. Howard, A.J., Gilliland, G.L., Finzel, B.C. and Poulos, T.L., *J. Appl. Cryst.*, 1987, **20**, 383.

89. Kabsch, W., *J. Appl. Cryst.*, 1988, **21**, 916.

90. Hanawalt, J.D., Rinn, H.W. and Frevel, L.K., *Ind. Eng. Chem., Anal. Ed.*, 1938, **10**, 457.

91. Rietveld, H.M., *J. Appl. Cryst.*, 1969, **2**, 65.

92. Will, G., arish, W. and Huang, T.C., *J. Appl. Cryst.*, 1983, **16**, 611.

93. Hill, R.J. and Madsen, I.C., *J. Appl. Cryst.*, 1986, **19**, 10.

94. Thompson, P. and Wood, I.G., *J. Appl. Cryst.*, 1983, **16**, 458.

95. Hill, R.J. and Howard, C.J., *J. Appl. Cryst.*, 1987, **20**, 467.

96. Bacon, G.E., *Neutron Diffraction*, 2nd edn., Oxford university Press, Oxford, 1962.

97. Dalton, J., *A new System of Chemical Philosophy*, Russel, Manchester, 1808.

98. Bragg, W.H. and Bragg, W.L., *Nature* (*London*), 1913, **91**, 557.

99. van't Hoff, J.H., *Arrangements of Atoms in Space* (English translation), Longmans, Green, London, 1898.

100. Le Bel, J.A., *Société chimique de France Bulletin*, 1874, **22**, 337. English translation in: *Classics in the Theory of Chemical Combinations*, Dover, New York, 1963.

101. Lonsdale, K., *Nature* (*London*), 1928, **122**, 810.

102. Cox, E.G. and Smith, J.A.S., *Nature* (*London*), 1954, **173**, 75.

103. Bacon, G.E., Curry, N.A. and Wilson, S.A., *Proc. R. Soc. London, Ser. A*, 1964, **279**, 98.

104. Bernal, J.D. and Crowfoot, D., *Z. Krist.*, 1936, **A39**, 464.

105. Bernal, J.D., Crowfoot, D. and Fankuchen, I., *Philos. Trans. R. Soc. London, A*, 1940, **239**, 135.

106.Crowfoot, D., Bunn, C.W., Rogers-Low, B.W. and Turner-Jones, A., *The Chemistry of Penicillin*, eds. Clarke, H.T., Johnson, J.R. and Robinson, R., Princeton University Press, Princeton, 1949.

107.Hodgkin, D.C., Pickworth, J., Robertson, J.H., Trueblood, K.N., Prosen, R.J. and White, J.G., *Nature* (*London*), 1955, **176**, 325.

108. Kendrew, J.C., Dickerson, R.E., Strandberg, B.E., Hart, R.G. and Davies, D.R., *Nature* (*London*), 1960, **185**, 422.

109. Groth, P., *Chemische Kristallographie*, Engelmann, Leipzig, 1906-1919.

110. Bernal, J.D., *Science in History*, Hawthorn, New York, 1965.

111. Allen, F.H., Bellard, S., Brice, M.D., Cartwright, B.A., Doubleday, A., Higgs, H., Hummelink, T., Hummelink-Peters, B.G., Kennard, O., Motherwell, W.D.S., Rodgers, J.R. and Watson, D.G., *Acta Cryst.*, 1979, **B35**, 2331.

112. Kennard, O., Watson, D.G., Allen, F.H., Motherwell, W., Town, W. and Rodgers, J.R., *Chem. Britain*, 1975, **11**, 213.

113. Wilson, S.R. and Huffman, J.C., *J. Org. Chem.*, 1980, **45**, 560.

114. Allen, F.H., Kennard, O. and Taylor, R., *Acc. Chem. Res.*, 1983, **16**, 146.

115. Bürgi, H.B. and Dunitz, J.D., *Acc. Chem. Res.*, 1983, **16**, 153.

116. Schweizer, W.B., *Crystallographic Computing 3*, eds. Sheldrick, G.M., Kruger, C. and Goddard, R., Clarendon Press, Oxford, 1985.

117. Murray-Rust, P. and Motherwell, W.D.S., *Acta Cryst.*, 1978, **B34**, 2518.

118. Murray-Rust, P. and Bland, R., *Acta Cryst.*, 1978, **B34**, 2527.

119. Taylor, R. and Kennard, O., *Acta Cryst.*, 1983, **B39**, 517.

120. Murray-Rust, P. and Raftery, J., *J. Mol. Graphics*, 1985, **3**, 50.

121.Murray-Rust, P. and Raftery, J., *J. Mol. Graphics*, 1985, **3**, 60.

122.Taylor, R., *J. Mol. Graphics*, 1986, **4**, 123.

123. Murray-Rust, P., *Methods and Applications in Crystallographic Computing*, eds. Hall, S.R. and Ashida, T., Clarendon Press, Oxford, 1984.

124.Murray-Rust, P., *Molecular Structure and Biological Activity*, eds. Grffin, J.F. and Duax, W.L., Elsevier Biomedical, New York, 1982.

125. Bernstein, F.C., Koetzle, T.F., Williams, G.J.B., Meyer, E.F., Jr., Brice, M.D., Rodgers, J.R., Kennard, O., Shimanouchi, T. and Tasumi, M., *J. Mol. Biol.*, 1977, **112**, 535.

126. Abola, E.E., Bernstein, F.C., Bryant, S.H., Koetzle, T.F. and Weng, J., *Crystallographic Databases. Information Content, Software Applications, Scientific Applications*, International Union of Crystallography, Bonn, Cambridge, Chester, 1987.

127. Bergerhoff, G., Hundt, R., Sievers, R. and Brown, I.D., *J. Chem. Inf. Comput. Sci.*, 1983, **23**, 66.

128. Bergeroff, G. and Brown, I.D., *Crystallographic Databases. Information Content, Software Applications, Scientific Applications*, International Union of Crystallography, Bonn, Cambridge, Chester, 1987.

129. Brown, I.D., *Acta Cryst.*, 1985, **A41**, 216.

130. Brown, I.D., *Acta Cryst.*, 1983, **A41**, 399.

131. Brown, I.D., Bradley, S.M. and Altermatt, D., *Molecular Structure: Chemical Reactivity and Biological Activity*, eds. Stezowski, J.J., Huang, J-L. and Shao, M-C., Oxford University Press, Oxford, 1988.

132. Altermatt, D. and Brown, I.D., *Acta Cryst.*, 1985, **B41**, 240.

133. Brown, I.D. and Altermatt, D., *Acta Cryst.*, 1985, **B41**, 244.

134. Jenkins, R. and mith, D.K., *Crystallographic Databases. Information Content, Software Applications, Scientific Applications*, International Union of Crystallography, Bonn, Cambridge, Chester, 1987.

135. Mighell, A.D. and Himes, V.L., *Acta Cryst.*, 1986, **A42**, 101.

136. Parrish, W., *Crystallography in North America*, eds. McLachlan, D., Jr. and Glusker, J.P., American Crystallographic Association, New York, 1983.

137. Hanawalt, J.D., *Crystallography in North America*, eds. McLachlan, D., Jr. and Glusker, J.P., American Crystallographic Association, New York, 1983.

138. van der Waals, J.D., The Continuity of the Gaseous and Liquid States, English translation, Barth, J.A., Leipzig, 1881.

139. London, F., *Z. Phys. Chem.,* 1930, **B**, 222.

140. London, F., *Z. Physik*, 1930, **63**, 245.

141. Etter, M.C., *Acc. Chem. Res.*, 1990, **23**, 120.

142. Jeffrey, G.A., *Patterson and Pattersons. Fifty Years of the Patterson Function*, eds. Glusker, J.P., Patterson, B.K. and Rosi, M., International Union of Crystallography / Oxford University Press, New York, 1987.

143. Desiraju, G.R., *J. Chem. Soc., Chem. Commun.*, 1991, 426.

144. Byrn, S.R., *Solid-state Chemistry of Drugs*, Academic Press, New York, 1982.

145. Dunitz, J.D., Egli, M. and Wallis, J.D., *Helv. Chim. Acta*, 1986, **69**, 225.

146. Pedersen, C.J., *J. Am. Chem. Soc.*, 1967, **89**, 7017.

147. Steed, J.W. and Atwood, J.L., *Supramolecular Chemistry*, John Wiley & Sons, New York and other international cities, 2000.

148.Schmidt, G.M.J., *J. Chem. Soc.*, 1964, 2014.

149. Lommerse, J.P.M., Motherwell, W.D.S., Ammon, H.L., Dunitz, J.D., Gavezzotti, A., Hofmann, D.W.M., Leusen, F.J.J., Mooij, W.T.M., Price, S.L., Schweizer, B., Schmidt, M.U., van Eijck, B.P., Verwer, P. and Williams, D.E., *Acta Cryst.*, 2000, **B56**, 697.

150. Desiraju, G.R., *J. Chem. Soc., Chem. Commun.*, 1997, 1475.

151. Rowland, R.S., *Am. Crystallogr. Assoc. Abstr.*, 1995, **23**, 63.

152. Perkin, W.H., *J. Chem. Soc.*, 1916, **109**, 815.

153. Kermack, W.O. and Robinson, R., *J. Chem. Soc.*, 1922, **121**, 427.

154. Tulinsky, A. and van der Hende, J.H., *J. Am. Chem. Soc.*, 1967, **89**, 2905.

155. Wunderlich, J.A., *Acta Cryst.*, 1967, **B23**, 846.

156. Hall, S.R. and Ahmed, F.R., *Acta Cryst.*, 1968, **B24**, 337.

157. Hall, S.R. and Ahmed, F.R., *Acta Cryst.*,1968, **B24**, 346.

158. Birnbaum, K.B., Klasek, A., Sedmera, P., Snatzke, G., Johnson, L.F. and Santavy, F., *Tetrahedron Lett.*, 1971, 3421.

159. Birnbaum, K.B., *Acta Cryst.*, 1972, **B28**, 2825.

160. Bent, H., *Chem. Rev.*, 1968, **68**, 587.

161. Bürgi, H.B., Dunitz, J.D. and Schefter, E., *J. Am. Chem. Soc.*, 1973, **95**, 2544.

162. Schweizer, W.B., Procter, G., Kaftory, M. and Dunitz, J.D., *Helv. Chim. Acta*, 1978, **61**, 2783.

163. Bright, D., Maxwell, I.E. and de Boer, J., *J. Chem. Soc., Perkin Trans. 2*, 1973, 2101.

164. Jungk, A.E., *Chem. Ber.*, 1972, **105**, 1595.

165. Einspahr, H., Robert, J.B., Marsh, R.E. and Roberts, J.D., *Acta Cryst.*, 1973, **B29**, 1611.

166. Baldwin, J.E., *J. Chem. Soc., Chem. Commun.*, 1976, 738.

167.Bell, P.C. and Wallis, J.D., *J. Chem. Soc., Chem. Commun.*, 1998, 257.

168. O'Leary, J., Bell, P.C., Wallis, J.D. and Schweizer, W.B., *J. Chem. Soc., Perkin Trans. 2*, 2001, 133.

169. Procter, G., Britton, D. and Dunitz, J.D., *Helv. Chim. Acta*, 1981, **64**, 471.

170. Parvez, M. and Schuster, I.I., *Acta Cryst.*, 1990, **C46**, 947.

171. Baxter, P.N.W., Connor, J.A., Povey, D.C. and Wallis, J.D., *J. Chem. Soc., Chem. Commun.*, 1991, 1135.

172. Wallis, J.D., Easton, R.J.C. and Dunitz, J.D., *Helv. Chim. Acta*, 1993, **76**, 1.

173. van Beek, L.K.H., van Beek, J., Boven, J. and Schoot, C.J., *J. Org. Chem.*, 1971, **36**, 2194.

174. Hinsberg, W.D., Schultz, P.G. and Dervan, P.B., *J. Am. Chem. Soc.*, 1982, **104**, 766.

175. Huisgen, R., Giese, B. and Huber, H., *Tetrahedron Lett.*, 1967, 1833.

176. Köstler, R., Kramer, K.-H. and Liedtke, R., *Liebigs Ann. Chem.*, 1973, 1241.

177. Dolfini, J.E., *J. Org. Chem.*, 1965, **30**, 1298.

178. Rice, C.G. and Wallis, J.D., *J. Chem. Soc., Chem. Commun.*, 1993, 572.

179. Bengaard, H., Larsen, S., Sorensen, H., Robinson, K. and Wallis, J.D., *Acta Cryst.*, 1999, **C55**, 106.

180. Pilkington, M., Wallis, J.D., Smith, G.T. and Howard, J.A.K., *J. Chem. Soc., Perkin Trans. 2*, 1996, 1849.

181. Bader, R.F.W., *Atoms in Molecules: A Quantum Theory*, Oxford University Press, Oxford, 1990.

182. Evans, K.L., Fronczek, F.R. and Gandour, R.D., *Acta Cryst.*, 1995, **C51**, 983.

183. Pilkington, M., Tayyip, S. and Wallis, J.D., *J. Chem. Soc., Perkin Trans. 2*, 1994, 2481.

184. Strozier, R.W., Caramella, P. and Houk, K.N., *J. Am Chem. Soc.*, 1979, **101**, 1340.

185. Dykstra, C.E., Arduengo, A.J. and Fukunaga, T., *J. Am. Chem. Soc.*, 1978, **100**, 6007.

186. Eisenstein, O., Procter, G. and Dunitz, J.D., *Helv. Chim. Acta*, 1978, **61**, 2538.

187. Bell, P.C. and Wallis, J.D., unpublished work.

Chapter 2

A Re-Interpretation of 1,5-Interactions Between Methoxy or Dimethylamino Groups and Electron-Poor sp^2 Carbon Atoms in *Peri*-Naphthalenes

A Re-Interpretation of 1,5-Interactions Between Methoxy or Dimethylamino Groups and Electron-Poor sp^2 Carbon Atoms in *Peri*-Naphthalenes

2.1 Introduction

The peri-disubstituted naphthalene framework has played a prominent role in investigating interactions between electron-rich and electron-poor atoms. An investigation by Dunitz et al. provided data for seven *peri*-disubstituted naphthalene derivatives containing a nucleophile (NMe_2, OMe and OH) and a carbonyl-containing group (COMe, CO_2Me, CO_2H and $CONMe_2$).[1] All seven compounds showed similar distortion patterns (Figures 1 and 2a), in which the bond to the carbonyl carbon is splayed outward and the bond to the nucleophile is splayed inward, towards the carbonyl group. This distortion pattern along with partial pyramidalisation of the carbonyl carbon from the plane of its substituents towards the nucleophile and the short Nu----C distances were considered to arise from an attractive interaction between the nucleophile and the carbonyl carbon and thought to represent an early stage in the addition of a nucleophile to a carbonyl group.

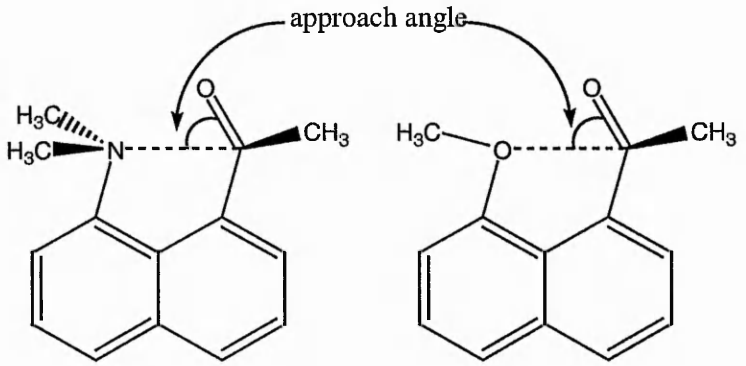

Figure 1 Attractive interaction in *peri*-disubstituted naphthalenes representing the addition of a nucleophile to a carbonyl group.

Since the original study further data have become available, and selected geometric parameters for 16 compounds are given in Tables 1 and 2. All 16 compounds display the same distortion pattern, described above and illustrated in Figure 2a, where the substituents are splayed in the same direction. In nearly all cases the carbonyl group is oriented so that one face of the group is presented to the *peri*-substituent, and the orientation of the nucleophile is such that a lone pair of electrons is directed towards the adjacent carbonyl group. These geometries produce an obtuse angle of attack of the nucleophilic N or O atom on the carbonyl group and have been interpreted as attractive interactions involving overlap of lone pair electron density from the nucleophile with the LUMO of the carbonyl group. If the substituents were distorted in the opposite direction, as illustrated in Figure 2b, the approach angle would be less than 90°, a more unfavourable angle for overlap of the lone pair electron density with the carbonyl's LUMO. Also observed in all structures are small displacements of each carbonyl carbon from the plane of its substituents (0.02 – 0.08 Å) towards the nucleophile.

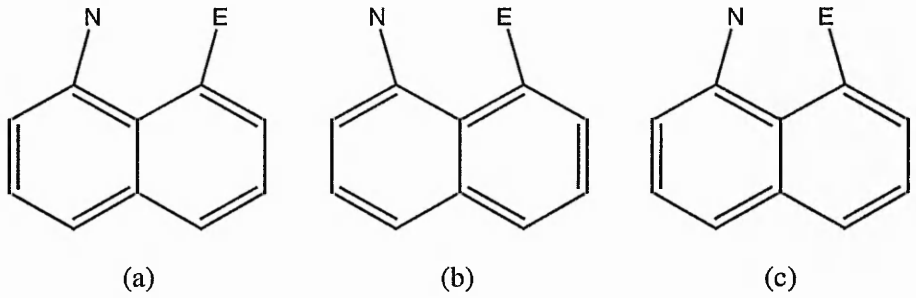

Figure 2 Distortion patterns in *peri*-substituted naphthalenes: (a) with nucleophilic group (N) splayed inward and electrophilic group (E) splayed in the same direction, (b) with N splayed outward and E splayed in the same direction and (c) with these groups attracted towards each other.

It is expected that for the same carbonyl containing group the N----C distance would be shorter than the O----C distance due to the greater nucleophilicity of the dimethylamino group over the methoxy group. Surprisingly this is not the case. Although in the ketone derivatives **2**, **9** and **10** the N----C distance (2.557(3) Å)[1] is *slightly shorter* than the O----C distances (2.606(9) and 2.579(3) Å)[1,2], for the amide derivatives **5**, **6**, **15** and **16** the N----C distances (2.698(3) Å for **5** and 2.764(3) Å for **6**)[3] are *longer* than the corresponding O----C distances (2.597(5) Å for **15** and 2.623(2) Å for **16**)[1,3]. This latter result has been interpreted recently as indicating greater '*peri* bonding' between a methoxy and carboxamide group than between a dimethylamino and carboxamide group and was used to explain the slower rates of racemisation of the *peri*-methoxy carboxamide **16** compared to the *peri*-dimethylamino carboxamide **6**.[3]

A recent study investigating interactions between a dimethylamino group and electron deficient alkenes observed a distortion pattern more consistent with an attractive

interaction, in which for some cases the *peri*-substituents are displaced *towards* each other (Figure 2c).[7] Selected geometric parameters for these compounds, along with data for two methoxy derivatives and data from the Kirby group are given in Tables 3 and 4, structural diagrams are shown in Figure 3.[4]

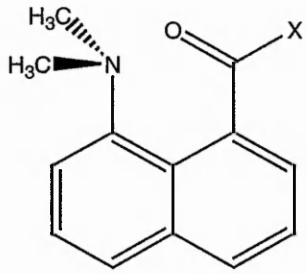

1 X = H
2 X = Me
3 X = OH
4 X = OMe
5 X = NMe_2
6 X = NPr^i_2

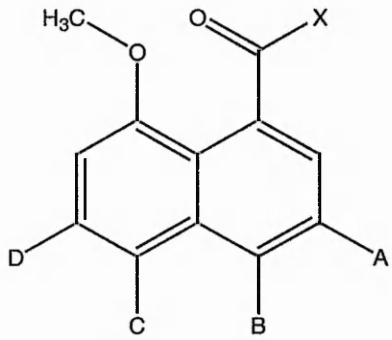

7 X = H, A=D=H, B=OMe, C=OTs
8 X = H, A=B=D=H, C=OTs
9 X = Me, A=B=C=D=H
10 X = Me, A=D=H, B=OMe, C=OTs
11 X = OH, A=B=C=D=H
12 X = OH, A=B=D=H, C=OMe
13 X = OH, A=B=H, C=OMe, D=CO_2H
14 X = OMe, A=B=D=H, C=OMe
15 X = NMe_2, A=B=C=D=H
16 X = NPr^i_2, A=B=C=D=H

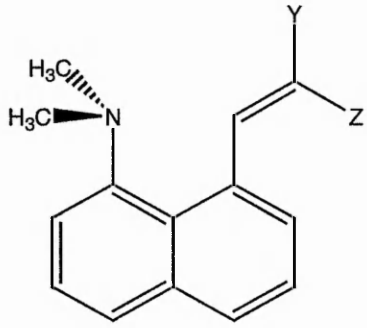

17 Y = Z = -(C(=O)O)$_2$CMe$_2$
18 Y = Z = CN
19 Y = CN, Z = CO_2Et
20 Y = Z = COPh
21 Y = Br, Z = H
22 Y = H, Z = Br

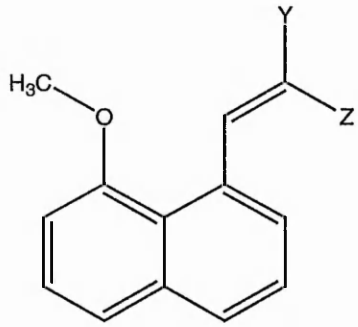

23 Y = Z = -(C(=O)O)$_2$CMe$_2$
24 Y = Z = CN

Figure 3 Structural diagrams for compounds **1-24**

Table 1 Selected geometric data for 1-(dimethylamino)naphthalene-8-carbonyl derivatives

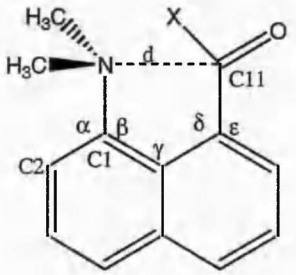

ΔC: deviation of C11 from the plane of its substituents towards the *peri* substituent.

T1 and T2: torsion angles of N-Me bonds with the C1-C2 aryl bond.

	X	d	α	β	γ	δ	ε	ΔC	T1	T2
1[4]	H	2.489(5)	124.3(4)	116.0(3)	120.6(3)	122.2(4)	118.5(4)	0.061(4)	44.5 (5)	-85.2 (5)
2[1]	CH_3	2.557 (3)	123.4 (2)	116.6 (2)	122.3 (2)	123.2 (2)	117.2 (2)	0.088 (3)	44.5 (5)	-81.3 (3)
3[1]	OH	2.606 (5)	123.0 (4)	117.4 (3)	122.5 (3)	123.9 (3)	116.3 (3)	0.061 (5)	53.1 (5)	-77.1 (5)
4[1]	OCH_3	2.594 (4)	123.6 (3)	117.4 (3)	122.4 (3)	123.9 (3)	116.3 (3)	0.062 (3)	48.2 (5)	-80.1 (4)
5[3]	NMe_2	2.698 (3)	122.9 (2)	117.0 (2)	123.7 (2)	124.8 (2)	115.5 (2)	0.055 (3)	34.8 (5)	-93.2 (3)
6[3]	NPr^i_2	2.764 (3)	121.1 (3)	118.4 (2)	125.1 (2)	125.4 (2)	114.1 (2)	0.051 (3)	40.4 (4)	-85.8 (3)

Table 2 Selected geometric data for 1-methoxynaphthalene-8-carbonyl derivatives

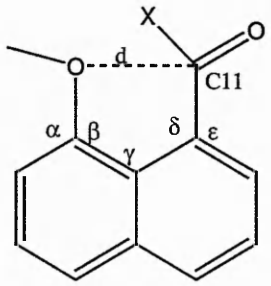

ΔC: deviation of C11 from the plane of its substituents towards the *peri* substituent.

	X	d	α	β	γ	δ	ε	ΔC
7[2]	H	2.628 (4)	123.4 (2)	115.1 (2)	122.5 (2)	126.4 (2)	114.9 (2)	0.089 (4)
8[2]	H	2.644 (4)	123.5 (3)	115.3 (2)	123.9 (3)	124.7 (3)	115.8 (3)	0.072 (4)
9[1]	CH_3	2.606 (9)	124.4 (9)	115.9 (8)	121.7 (8)	125.5 (8)	115.3 (8)	0.044 (10)
10[2]	CH_3	2.579 (3)	124.0 (2)	114.1 (2)	122.0 (2)	125.5 (2)	115.3 (2)	0.070 (3)
11[1]	OH	2.559 (4)	124.7 (3)	113.2 (3)	124.2 (2)	123.4 (3)	115.8 (3)	0.022 (5)
12[5]	OH	2.566 (2)	124.7 (2)	114.1 (2)	123.3 (2)	124.0 (2)	115.0 (2)	0.042 (2)
13[6]	OH	2.526 (3)	124.7 (2)	114.1 (2)	123.3 (2)	122.1 (2)	117.4 (2)	0.036 (2)
14[1]	OCH_3	2.588 (3)	125.6 (3)	114.3 (2)	123.7 (2)	124.4 (2)	115.6 (2)	0.037 (2)
15[1]	NMe_2	2.597 (5)	122.7 (4)	114.4 (4)	124.3 (4)	124.0 (3)	115.1 (4)	0.039 (4)
16[3]	NPr^i_2	2.623 (2)	124.4 (2)	114.8 (2)	123.4 (2)	124.2 (2)	116.0 (2)	0.049 (1)

Table 3 Selected geometric data for 1-(dimethylamino)naphthalene-8-alkenyl derivatives

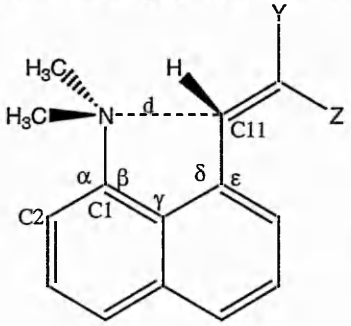

ΔC: deviation of C11 from the plane of its substituents towards the *peri* substituent.

T1 and T2: torsion angles of N-Me bonds with the C1-C2 aryl bond.

	Y,Z	d	α	β	γ	δ	ε	ΔC	T1	T2
17[7]	-(C(=O)O)$_2$CMe$_2$	1.651(3)	128.6(2)	108.8(2)	113.3(2)	109.9(2)	131.4(2)	0.362(2)	49.5 (2)	-71.9 (2)
18[7]	CN,CN	2.413 (2)	124.3 (2)	115.9 (1)	120.4 (1)	120.2 (1)	120.3 (1)	0.087 (2)	49.7 (2)	-81.4 (2)
19[7]	CN, CO_2Et	2.531 (2)	123.3 (2)	116.8 (1)	122.4 (1)	121.6 (1)	118.6 (2)	0.041 (2)	47.9 (2)	-82.9 (2)
20[7]	COPh, COPh	2.679 (2)	122.3 (2)	118.3 (2)	123.5 (2)	122.5 (2)	117.6 (2)	0.015 (2)	26.0 (2)	-105.0 (2)
21[4]	Br,H	2.717 (5)	122.0 (4)	118.8 (4)	124.0 (4)	122.0 (4)	117.8 (4)	-	23.8 (6)	-106.5 (5)
21	Br,H	2.742 (5)	122.0 (4)	118.0 (4)	125.1 (4)	122.5 (4)	118.1 (4)	-	22.7 (6)	-105.9 (5)
21	Br,H	2.758 (2)	123.2 (1)	117.1 (1)	127.0 (1)	121.8 (1)	116.6 (1)	-	14.9 (2)	-110.4 (2)
22[4]	H,Br	2.749 (5)	122.3 (4)	118.5 (3)	124.2 (3)	123.3 (3)	117.2 (3)	-	26.6 (5)	-103.6 (4)

Table 4 Selected geometric data for 1-methoxynaphthalene-8-alkenyl derivatives

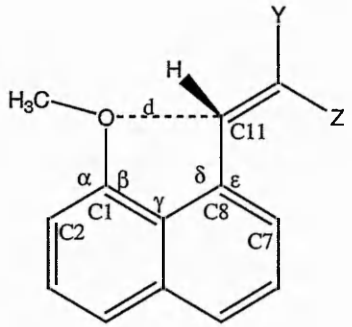

ΔC: deviation of C11 from the plane of its substituents towards the *peri* substituent.

	Y,Z	d	α	β	γ	δ	ε	ΔC
23[8]	-(C(=O)O)$_2$CMe$_2$	2.550 (2)	123.6 (2)	115.0 (2)	122.9 (2)	123.2 (2)	117.2 (2)	0.077 (2)
24[8]	CN,CN	2.611 (1)	124.3 (1)	114.9 (1)	124.1 (1)	123.5 (1)	117.0 (1)	0.029 (1)

In the dimethylamino derivatives **17** – **22** there is a progressive decrease in the N----C=C separation from compound **22** where the alkene's terminal substituents are a hydrogen atom and a bromine atom (N----C: 2.749(5) Å)[4] to compound **17** where the substituents are two lactone carbonyl groups both of which are coplanar with the alkene and for which the structure is best represented as the zwitterion **25** with the formation of a N-C bond of length 1.651(3) Å.[7]

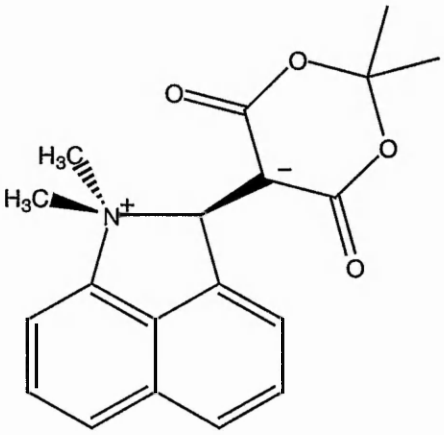

25

The methoxy analogues of **17** and **18**, compounds **23** and **24**, show longer O----C=C separations (2.550(2) and 2.611(1) Å)[8] than the corresponding N----C=C distances (1.651(3) and 2.413(2) Å)[7], consistent with the methoxy group being of lower nucleophilicity than the dimethylamino group, but show the same trend. The distortion patterns of **23** and **24** are that of Figure 2a; there is no indication of the alkene being attracted back towards the methoxy group. The structure of methoxy compound **24** was determined as part of this work. Its molecular structure is shown in Figure 4, with relevant molecular geometry in Table 4. Crystal packing of **24** is shown in Section 2.8 towards the end of this chapter.

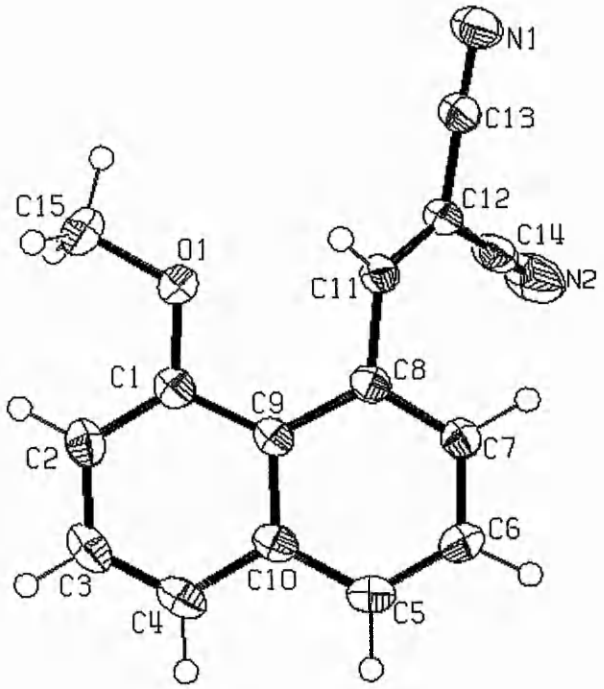

Figure 4 Molecular structure of **24** with anisotropic displacement parameters drawn at the 50% level.[9]

The results from the study of interactions between nucleophiles and electron deficient alkenes prompted a re-examination of the interactions between nucleophiles and sp^2 C atoms, in an attempt to determine whether or not some or all of these are indeed attractive interactions.

2.2 Relative Nucleophilicities of the Dimethylamino and Methoxy Groups

Tables 1-4 contain geometric information on a wide range of 8-(dimethylamino)- and 8-methoxy-naphthalene derivatives, which contain a sp^2C atom in the 1-position and only hydrogen atoms ortho to these substituents. For the dimethylamino derivatives, the N----C distances decrease with *peri* group along the series: -CH=CHBr ~ -$CONR_2$, -CH=$C(COPh)_2$, -CO_2H ~ CO_2R, -$COCH_3$, -CH=$C(CN)CO_2CH_3$, -CHO, -CH=$C(CN)_2$, -CH=$C(C(=O)O)_2CMe_2$ from 2.764 to 1.651 Å. This forms a relative order of through-space electron-accepting power for these groups. The decrease in the N----C distance is accompanied by a decrease in the outward bending of the alkenyl or carbonyl group. For the dicyanoethenyl derivative **18** the *exo* angles, δ and ε, are almost equal (120.2(1) and 120.3(1)°)[7] while for the carboxamides **5** and **6** and the bromoethenyl derivatives **21** and **22** the group is splayed out by 3-5.6°.[3,4]

For the methoxy derivatives there is much less variation in the O----C distances (2.526 – 2.623 Å), which only differ by 0.097 Å, *cf.* the 0.351 Å difference in N----C distance between **18** and **6**, indicating that the O----C distance is not very sensitive at all to the nature of the other *peri* substituent. It is not possible to infer any real trend in the O----C distance with *peri* substituent since the differences in these distances are of the same order as those produced by adoption of different packing arrangements or by different measurement temperatures. For example the three carboxylic acid derivatives **11**, **12** and **13** differ in their O----C distances by 0.04 Å, which is nearly

half the variation for the whole series of methoxy compounds. To determine whether or not a trend exists it would be necessary to measure a greater number of *peri*-methoxy compounds, including polymorphic forms where available, to average out the effects of crystal packing, and to make these measurements at very similar temperatures, ideally at ca. 100K. Recently, Akiba et al. have published the structure of a 1,8-dimethoxyanthracene, which carries a carbocation group in the 9-position **26**.[10] In this structure the ($(MeO)_2C^+$-) group lies perpendicular to the anthracene and has a *peri* interaction to each methoxy group on the ring. The O----C separations are 2.43(1) and 2.45(1) Å, *only ca.* 0.1 Å shorter than any of the MeO----C contacts in Tables 2 and 4. This structure highlights the low nucleophilicity of the methoxy group as even with the very electrophilic carbocation group the O----C separation is still relatively large when compared with the N----C separations in the dimethylamino derivatives.

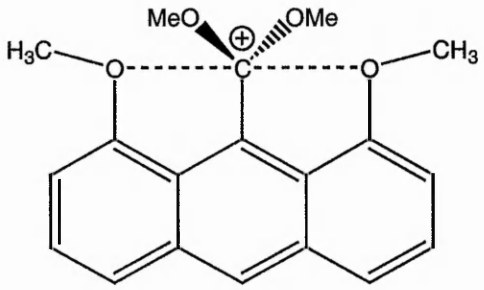

26

Compounds **27**[11] and **28**[12] contain *peri* interactions between methoxy groups and aromatic rings. The O----C distances are 2.606(5) and 2.644(5) Å in the two independent molecules of **27** and 2.659(5) Å in **28**. These values do not lie far

outside the range for the compounds in Tables 2 and 4, further indicating the low sensitivity of the O----C distance to the electronic character of the carbon atom.

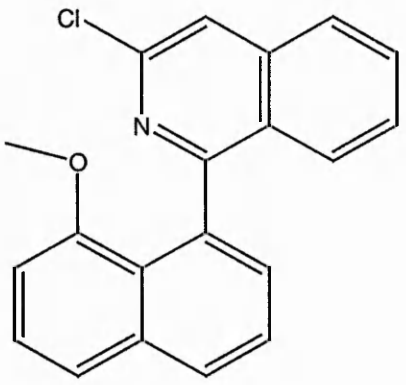

27

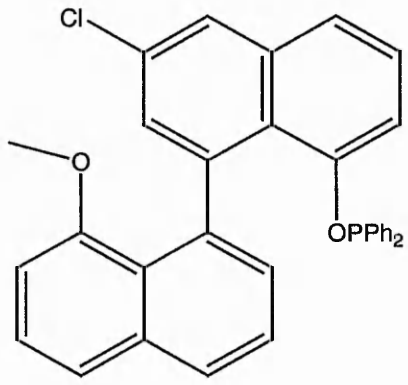

28

In all of the methoxy derivatives there is no significant variation in the bending of the alkenyl or carbonyl group in the naphthalene plane, this bond is bent outwards by an average of ~4°. Thus the sp^2 C atom is showing no indication of being attracted back towards the methoxy O atom. The low variability in both the O----C distance and the *exo* angles at the 8-position suggests that the O----C separations are only weakly influenced by the electronic character of the *peri* substituent, and are controlled mainly by steric effects.

Compounds of type **29**[13] and **30**[13e,14] can be used to estimate the difference in effective sizes of bonded nitrogen and oxygen atoms in the *peri*-naphthalene system. This will be useful in assessing whether or not a separation results from attractive or steric interactions. The average N----N distance in six 1,8-bis(dimethylamino) compounds of type **29** is 2.81 Å, and the average O----O distance in five 1,8-

dimethoxy compounds of type **30** is 2.50 Å. This corresponds to a difference in the effective radii of bonded nitrogen and oxygen atoms of ca. 0.15 Å. Thus if a Me_2N----sp^2C interaction distance is less than the sum of the corresponding MeO----sp^2C interaction distance and the difference in size of the bonded nitrogen and oxygen atoms (~0.15 Å) the Me_2N----sp^2C interaction is likely to have an attractive component. For example applying this proposal to compare the interactions of a dimethylamino group with both an electron-deficient alkene **18** and a carboxamide **5** indicates that the interaction with the electron-deficient alkene in **18** is attractive because (d(MeO----X) + 0.15) – d(Me_2N----X) = 0.348 Å, while the interaction with the carboxamide in **5** is dominated by steric effects because (d(MeO----X) + 0.15) – d(Me_2N----X) = 0.049 Å. This proposal, however, is just a rough guide as the value of 0.15 Å for the difference in the effective radii of the nitrogen and oxygen atoms is only a reasonable estimate based on the nearest possible structural data.

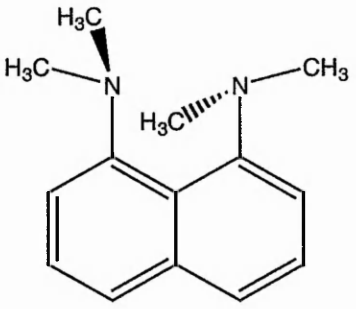

29

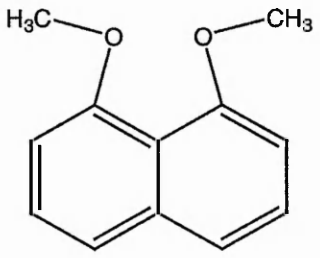

30

2.3 Pyramidalisation of the Carbonyl Carbon

In an investigation by Bürgi, Dunitz and Schefter into interactions between tertiary amino groups and carbonyl groups in a series of alkaloids it was observed that the carbonyl carbon was displaced from the plane of its substituents towards the amino N atom.[15] This displacement was correlated with the N----C distances to give a smooth curve and it was proposed that the data for the alkaloids provide points on or close to a reaction coordinate. The investigation into *peri* interactions of 8-(dimethylamino)- and 8-methoxynaphthalene-1-carbonyl derivatives performed five years later also observed partial pyramidalisation of the carbonyl carbon.[1] This was interpreted as indicating an attractive interaction between the *peri* substituents. Tables 1-4 show the small pyramidalisations of the sp^2 C atoms (0.01 – 0.09 Å) in all of the *peri*-naphthalene compounds studied. For comparison a survey of all aryl ketones in the CSD[16] surprisingly shows a mean pyramidality at the carbonyl carbon of 0.014 Å. Two specific examples are the *peri*-naphthalene benzoyl derivatives **31**[17] and **32**[18] in which each carbonyl carbon is displaced from the plane of its substituents, by 0.029 and 0.042 Å respectively, towards an incipient hydrogen atom of the other *peri* substituent.

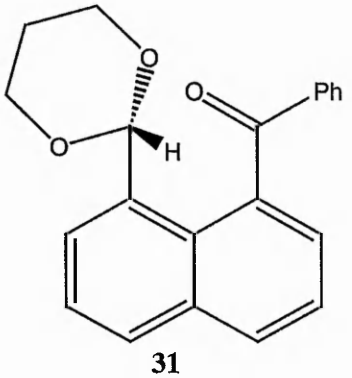

31

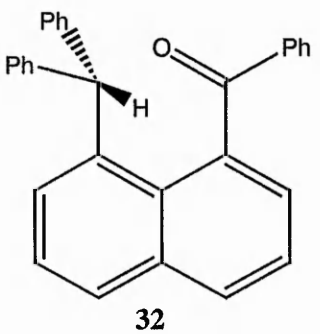

32

In a detailed study by Cieplak[19] it was observed that the original correlation of partial pyramidalisation with N----C distance for the alkaloids overestimated the non-planarity of the carbonyl group at large N----C distances. Since the original study crystal structures of nine more compounds containing *tert*-amine and carbonyl fragments became available and an analogous survey of O----C=O interactions manifested by short intermolecular or intramolecular contacts was performed. Thus a revised plot of partial pyramidalisation with N----C and O----C distance was determined (Figure 5). Cieplak observed that indeed there is a tendency for pyramidalisation to increase with decreasing distance, but that the N----C=O data points with a distance greater than 2.5 Å show a quite similar distribution to the O----C=O interactions and he concluded that there is no essential difference between the two, a proposal in contrast to the earlier conclusions that non-planarity of carbonyls in contact with O and N atoms reflected the difference in nucleophilicity of the two atoms. In a study of aliphatic ketones Cieplak also observed that the carbonyl carbon atoms of such compounds show significant pyramidalisation depending on the conformation of the sp^3 C ligands.[19]

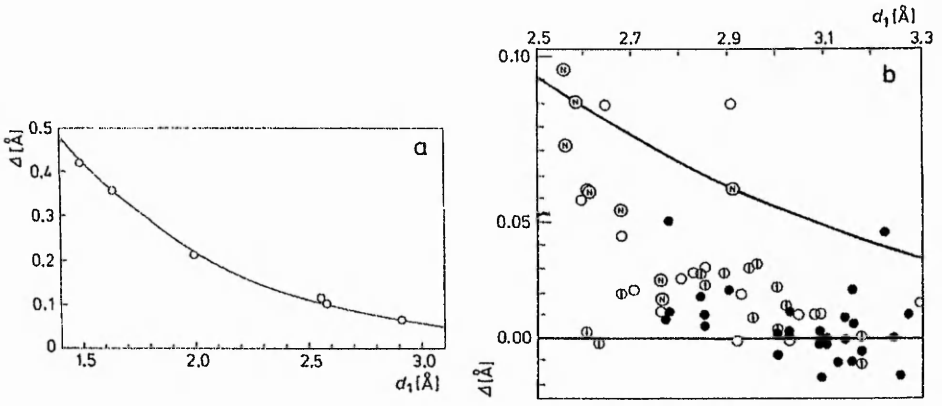

(a) (b)

Figure 5 (a) Initial plot of pyramidalisation Δ vs. N----C=O distance d_1 (b) revised plot of partial pyramidalisation Δ vs. N----C=O and O----C=O distances d_1>2.5 Å. (N = N----C=O interactions, remaining symbols refer to O----C=O interactions). Taken from ref. no. 19.

With all this in mind it is misleading to interpret some of the small pyramidalities of the sp^2 C atoms in *peri*-naphthalenes as indicators of attractive interactions when in fact it may simply be due to the molecular environment.

2.4 Alignment of the Dimethylamino Group's Lone Pair

A further indication of the attractive nature of certain *peri* Me_2N----sp^2C interactions is the orientation of the dimethylamino group's lone pair relative to the *peri* group. This is indicated by the torsion angles the two Me-N bonds make with the naphthalene ring (Tables 1 and 3). It is notable that as the N----C distance increases there is a greater tendency for the axis of the nitrogen atom's lone pair to move out of the plane of the naphthalene ring. In this way the lone pair can gain some conjugation with the π electrons of the aromatic system when there is little to gain by interaction with a *peri* substituent. Thus, for the ethenyl derivatives **20-22**, which have N----C distances in the range 2.679 – 2.758 Å, the lone pair axes make torsional angles of 38.5 – 47.8° with the naphthalene rings, hence the lone pair is not well aligned towards the *peri* group (Figure 6a). For **18**, which has a N----C distance of 2.413 Å, the corresponding torsional angle is 15.8° and the lone pair is directed towards the *peri* group (Figure 6b).

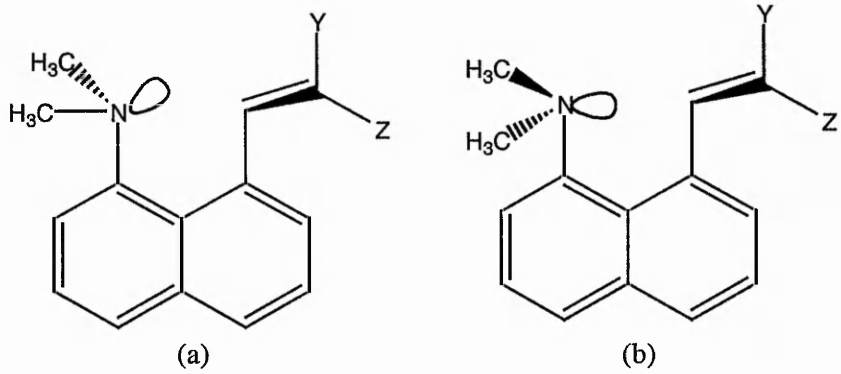

Figure 6 Alignment of the amino N atoms lone pair to the sp^2C atom – (a) not well aligned, (b) well aligned.

2.5 Rates of Racemisation of *Peri*-Substituted Naphthalene-1-Carboxamides

A recent investigation by Clayden et al. focussed on the rates of racemisation of 8-substituted naphth-1-amides.[3] The conformation of the naphthamide is chiral because the amide group lies roughly perpendicular to the aromatic plane, and racemisation is achieved by rotation of the amide group by 180°. Clayden observed that when the substituent in the 8-position was a methoxy group **16** the rate of racemisation was significantly slower than for the dimethylamino analogue **6**, and thus the free energy of activation for the racemisation is greater for the methoxy compound **16** (108.0 kJ mol^{-1}) than for the dimethylamino compound **6** (102.2 kJ mol^{-1}). Clayden also noted that the O----C=O distance (2.62 Å) was shorter than the corresponding N----C=O distance (2.76 Å). He concluded that there was stronger '*peri* bonding' in the methoxy derivative compared with the dimethylamino derivative. However, stronger

'*peri* bonding' is not to be expected from the less nucleophilic methoxy group and so these results must be due to other factors.

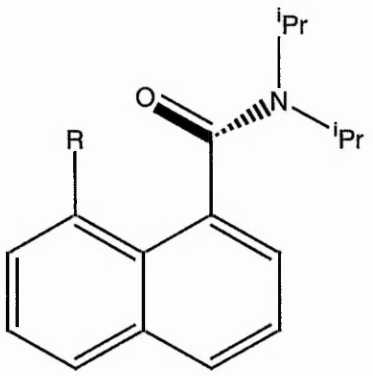

16 R = OMe
6 R = NMe_2

The reason for the O----C distance in **16** being *shorter* than the N----C distance in **6** is likely to be due to steric interactions rather than attractive interactions and to be a result of the smaller size of the methoxy O atom. It has already been proposed that interactions in these *peri*-naphthalene systems can be assessed by comparing the O---C and N---C distances and taking into account the difference in the relative sizes of the bonded O and N atoms (~0.15 Å), hence the *considerably longer* N----C distance indicates the interactions in **16** and **6** are dominated by steric effects.

Racemisation of compounds **16** and **6** involve a transition state in which the carboxamide group is coplanar with the naphthalene ring, but this will involve significant steric pressure from the *peri* substituent. In order to relieve this pressure the substituent must bend outwards, away from the amide group. The methoxy group is limited in the amount to which it can bend by the steric interaction of the methyl

group with the *ortho* hydrogen atom (Figure 7). This effect is not so severe for the dimethylamino group since neither methyl group lies in the aromatic plane.

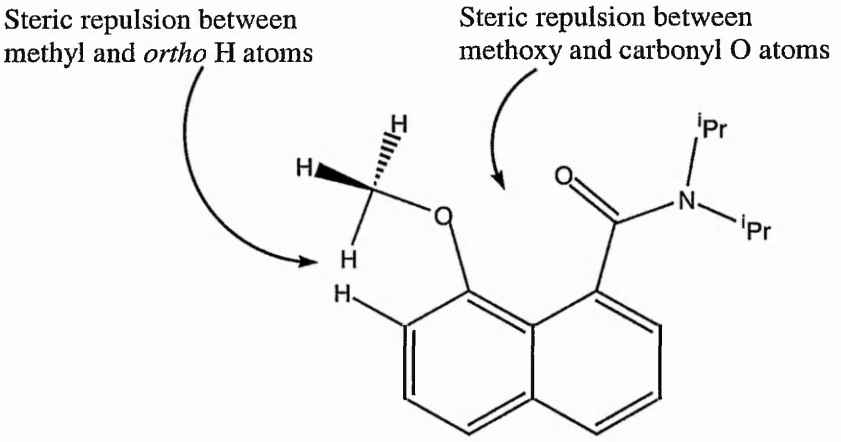

Figure 7 Repulsion of the in-plane methoxy group with the *ortho* hydrogen atom and the in-plane amide group in the transition state of the racemisation of **16**.

The methoxy group may, however, rotate out of the plane of the naphthalene ring to avoid repulsion from the *ortho* hydrogen atom. This requires loss of conjugation of one of the oxygen's lone pairs with the aromatic π-system as the CH_3-O bond moves from its position coplanar with the naphthalene plane to lie perpendicular to the plane. This would contribute to the greater activation energy for the racemisation process (108 kJ mol^{-1} for **16**, cf. 102.2 kJ mol^{-1} for **6**). In the dimethylamino derivative the nitrogen atom's one lone pair does not lie perpendicular to the aromatic plane, but close to this plane and so is involved to a much lesser degree in conjugation with the aromatic π-system. This effect is illustrated in the two conformations of anisole, in which the methoxy group lies coplanar with, or perpendicular to, the aromatic ring. The energy differences between the two conformations have been calculated to be 5.8

and 10 kJ mol^{-1} for the isolated molecule[20,21] and 6.3 and 25.2 kJ mol^{-1} in the liquid phase[22,23], these differences could adequately account for the differences in the activation energies of **16** and **6**.

2.6 Extension to Interactions of N or O with sp C Atoms

The re-interpretation of interactions between N or O atoms with sp^2 C atoms in *peri*-naphthalenes can be extended to interactions between N or O atoms with sp C atoms. Such interactions have been discussed previously in section 1.17.4, but it is now necessary to review the interactions in a similar manner to the interactions with sp^2 C atoms in order to determine their true nature.

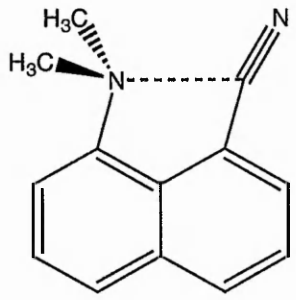

33

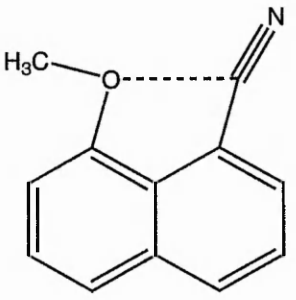

34

The naphtho-1-nitriles **33** and **34**, which have a *peri*-dimethylamino or a *peri*-methoxy group respectively both show short Nu----C≡N distances of 2.704(6) Å in **33**[24] and 2.594(4) Å in **34**.[25] Thus the O----C distance in the methoxy derivative is *shorter* than the N----C distance in the dimethylamino derivative and the small value

of 0.040 Å for the parameter [d(MeO----X) + 0.15 – d(Me_2N----X)] indicates that the interaction is dominated by steric effects. The torsion angles that the Me-N bonds make with the naphthalene ring in **33** are 22.2 and –109.14°. Thus the N atom's lone pair lies at ~43° and is poorly aligned towards the nitrile C atom, similar to that observed in the dibenzoyl derivative **20** and the carboxamides **5** and **6**. This provides further evidence of a poor attractive interaction. Comparison with the series constructed earlier indicates that the (weak) through-space electron-attracting power of the nitrile group is similar to that of a carboxamide group.

The recent study investigating interactions of a methoxy group with electron-deficient alkynes in 1,8-disubstituted naphthalenes **35-39** found O----C distances in the range 2.593(2) – 2.663(2) Å.[26,27] Attempts to synthesise several corresponding dimethylamino analogues were unsuccessful and it was concluded that this group was too reactive for investigating interactions with electron-deficient alkyne groups in *peri* substituted naphthalenes. It is possible, however, to prepare an unactivated alkyne in which the terminal substituent is a triphenylsilyl group **40**.

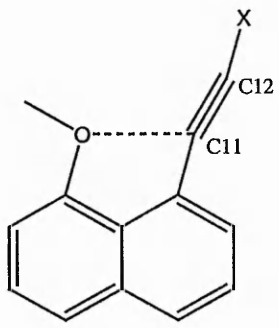

35 X = H
36 X = COMe
37 X = CO_2Me
38 X = CONHPh
39 X = CN

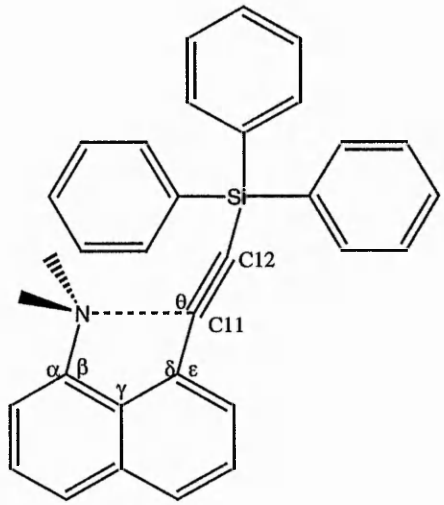

40

Figure 8 Interactions in alkynylnaphthalene derivatives.

The structure of **40** was measured by single crystal x-ray diffraction at 150 K, the results are shown in the molecular structure (Figure 9) and crystal packing (Section 2.8) diagrams and selected molecular geometry is given in Table **5**.

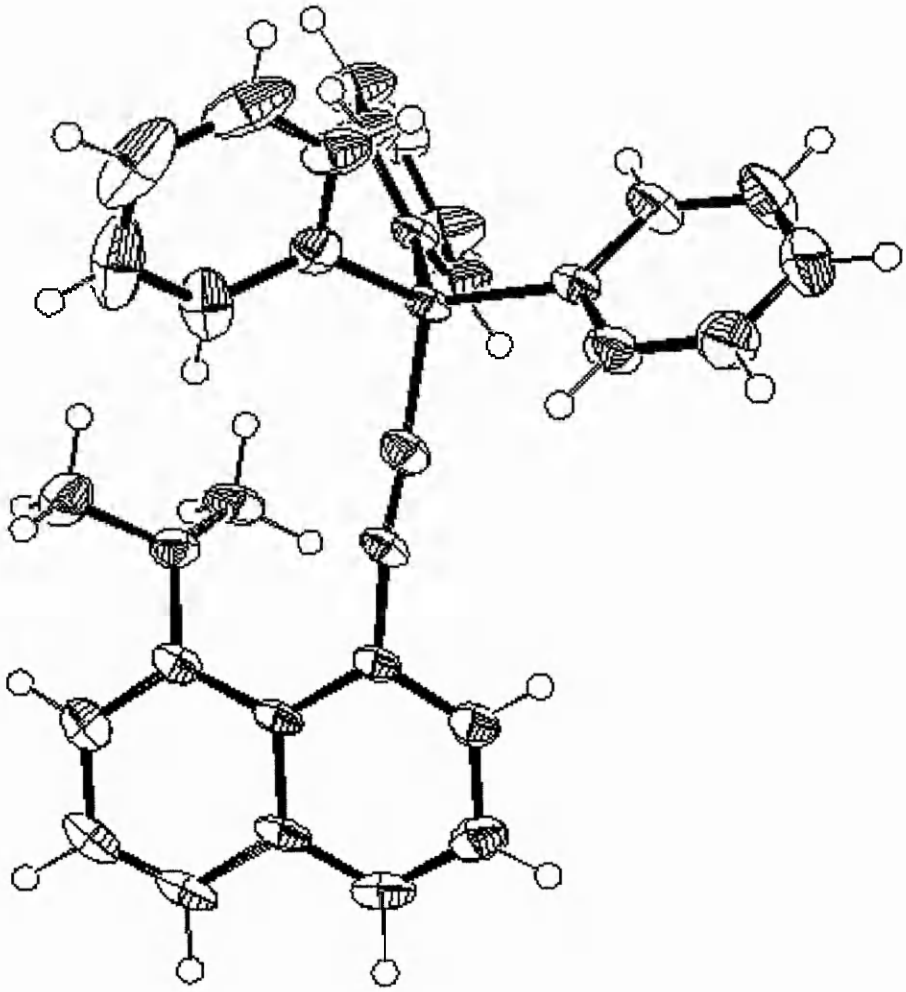

Figure 9 Molecular Structure of **40** with anisotropic displacement parameters drawn at the 50% level.[9]

Table 5 Selected molecular geometry for **40** (Å, °)

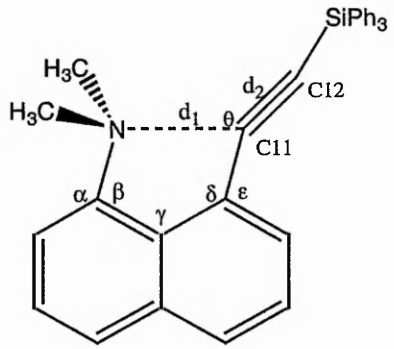

ΔC = Deviation of C_{11} from the plane of the naphthalene ring
ΔN = Deviation of the N atom from the plane of the naphthalene ring

d_1	α	β	γ	δ	ε
2.766(2)	121.9(2)	118.6(2)	125.3(2)	124.5(2)	115.4(2)
d_2	angle at C11	angle at C12	θ	ΔC	ΔN
1.212(3)	171.7(2)	176.4(2)	105.9(1)	0.182(2)	-0.202(2)

The distortion pattern observed in **40** is such that both *peri* substituents are splayed in the same direction cf. the carbonyl compounds discussed previously. The 1,5-N----spC distance is 2.766(2) Å and there is a *trans* bend in the triple bond such that the α-C is displaced towards the dimethylamino group. The C-C≡C-Si torsion angle is 167(2)°. The angles at the C11 and C12 are 171.7(2) and 176.4(2)° respectively, deviations of 8.3 and 3.6° from linearity. The *peri* substituents are slightly displaced from the plane of the naphthalene ring in opposite directions by 0.202(2) and 0.182(2) Å for the dimethylamino N atom and the α-C of the alkyne respectively. This out of plane distortion has been observed in other *peri*-naphthalenes, e.g. in the 1-

(dimethylamino)naphthalene-8-carbonyl derivatives these distortions are in the range 0.11-0.24 Å for the dimethylamino N atom and 0.10-0.29 Å for the carbonyl C atom.

It would be desirable to compare this compound with its methoxy analogue **41**, however such a structure has not been published and the nearest structure to this is **35**, which contains a -C≡C-H group, an unactivated alkyne, as the second *peri* substituent. The O----C distance in **35** is 2.663(2) Å, which is *shorter* than the N----C distance in **40**, and the parameter [d(MeO----X) + 0.15 – d(Me_2N----X)] for this pair of compounds is 0.047 Å. This small value indicates that the interactions between the dimethylamino group and an unactivated alkyne may be mainly steric in nature. This is further supported by the torsion angles of the Me-N bonds with the naphthalene rings, 24.4(3) and –105.9(2)°, which indicate that the lone pair axis makes a torsional angle of ~41° to the aromatic plane. Thus the N atom's lone pair is involved in partial conjugation with the aromatic π-system and is poorly aligned with the alkyne's α-C atom. From this evidence it is concluded that an unactivated alkyne is a very weak through-space electron-acceptor and similar to the nitrile and carboxamide groups. The interaction in **40** is controlled primarily by steric factors.

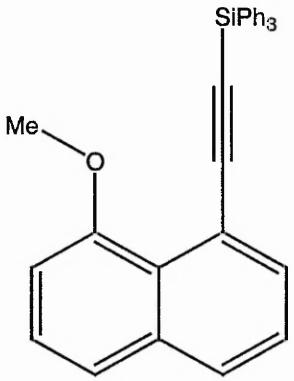

41

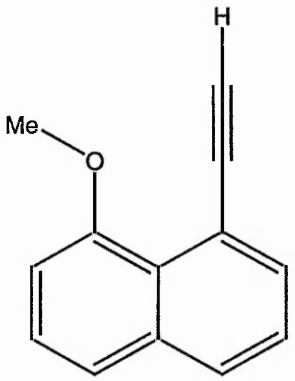

35

2.7 Interactions of N and O Atoms with N-Phenylcarboxamides

In the light of recent results and their interpretations it would be useful to have data for more 8-(dimethylamino) and 8-methoxynaphth-1-amides for comparison with those already available. To this end N-phenylcarboxamides **42** and **43** were synthesised (Schemes 1 and 2) to continue the discussion on the nature of the O----C=O and N----C=O interactions. Of particular importance is that the N-phenylamides would be expected to have less electron donation from the amide N atom into the carbonyl group than a dimethylamino amide, so might be expected to behave more like esters. Thus unlike the interactions of the dimethylamino group with carboxamides discussed previously in compounds **5** and **6**,[3] interactions of this nucleophile with phenylcarboxamides may be expected to consist of an attractive component. This provides an opportunity to test out the guidance d(MeO----X) + 0.15 – d(Me_2N----X) for expressing the nature of the N----C interaction.

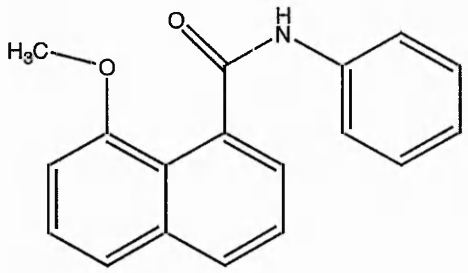

42

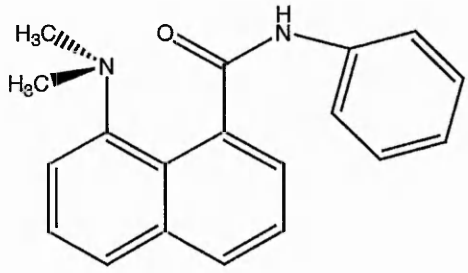

43

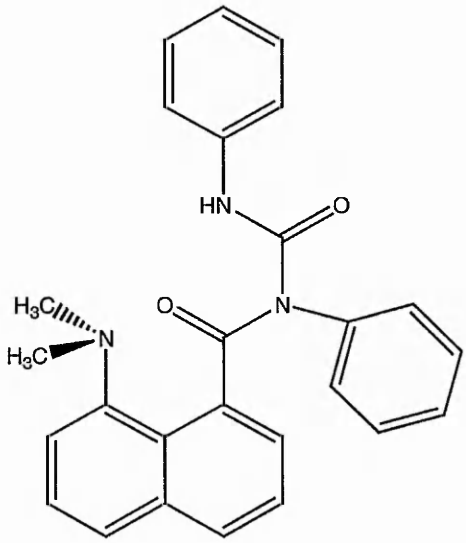

44

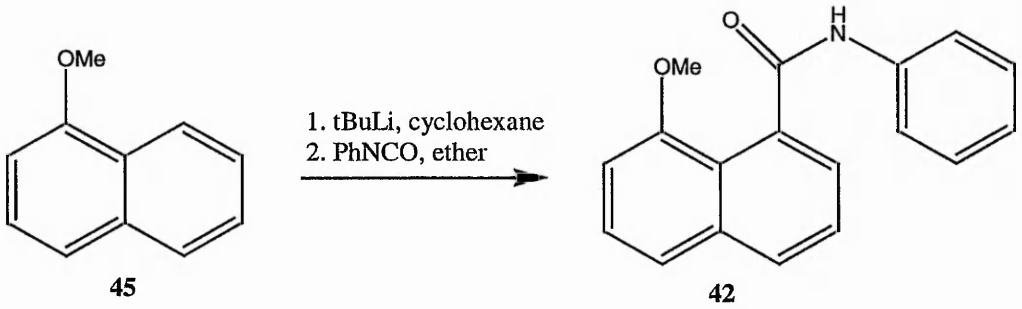

45 **42**

Scheme 1 Preparation of **42**

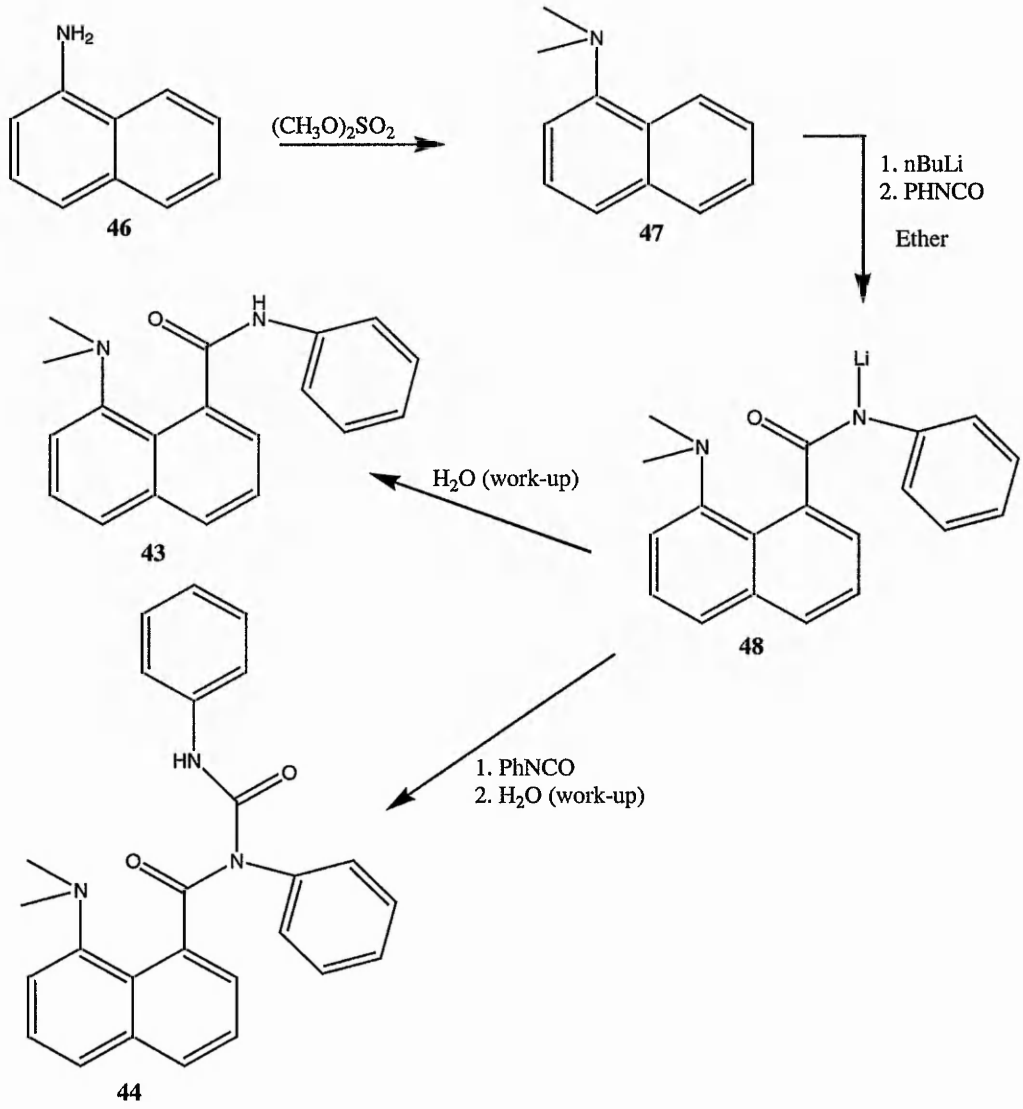

Scheme 2 Preparation of **43** and **44**

Compound **42** was prepared through *peri*-lithiation of 1-methoxynaphthalene **45** with t-butyl lithium at room temperature (Scheme 1), filtration of the lithium salt under nitrogen and reaction with phenyl isocyanate at -78°C to produce **42** in 72% yield. The structure of **42** was supported by a change in the ^{1}H NMR shifts and relative integration of the aromatic protons, δ: 8.28-6.62 for 1-methoxynaphthalene **45** and δ:

7.83-6.82 for **42**. The NH group was found in the aromatic region and its presence detected from the change in the relative integrations and by exchanging the proton for a deuterium atom using a D_2O shake and re-running the NMR experiment. ^{13}C NMR showed a resonance at δ: 170.0 corresponding to the carbonyl carbon atom and showed fourteen signals in the region δ: 155.0 – 106.0 corresponding to the 16 aromatic C atoms, fourteen of which are non-equivalent. The infrared spectrum of **42** shows absorptions at 1654 (C=O) and 3278 (N-H) cm^{-1}. The molecular composition and purity of **42** was confirmed by elemental analysis (observed values are within the recommended 0.3% of the calculated values) and the molecular mass by high resolution mass spectrometry (the difference between the observed and calculated values is within the recommended 5 ppm limit).

Compound **43** was prepared through *peri*-lithiation of 1-(dimethylamino)naphthalene **47** at room temperature (Scheme 2), filtration of the lithium salt **48** under nitrogen and reaction with phenyl isocyanate at -40°C to yield two compounds, which were separated by flash chromatography on silica gel to give **43** in 23% yield and an unexpected 2:1 addition product **44** in 46% yield. The latter is formed by the lithium salt of **43** adding to a further molecule of PhNCO.

The structures of **43** and **44** were supported by ^{1}H and ^{13}C NMR. The shift of the dimethylamino group in the starting amine **47** was δ: 2.73, while in **43** these protons were found at δ: 2.61 and in **44** the two methyl groups were observed to be non-equivalent resulting in two resonances at δ: 2.98 and 2.57. Surprisingly only one resonance was observed for the NMe_2 group in the ^{13}C NMR of **44** at δ: 49.9,

however, the H atoms of the dimethylamino group are much more sensitive to the environment, being on the 'outside' of the group than the C atoms. The NH groups were observed at δ: 7.17 and 11.60 in **43** and **44** respectively, the difference between the two corresponding to the different molecular environments, in **43** the NH is that of an amide while in **44** the NH is of a urea, which later x-ray studies showed was involved in an intramolecular hydrogen bond with a carbonyl O atom. In the ^{13}C NMR the carbonyl carbon shifts occur at δ: 169.8 for **43**, and at δ: 175.5 and 152.3 for the amide and urea C=O groups of **44**. The infrared spectra of **43** and **44** show absorptions at 3268 and 3265 cm^{-1} respectively corresponding to the N-H stretches. The carbonyl stretches are observed at 1648 cm^{-1} (**43**) and at 1705 and 1661 cm^{-1} (**44**). The molecular formulae of **43** and **44** were confirmed by high resolution mass spectrometry.

Crystals of **42-44** were prepared by slow evaporation of solutions in appropriate solvents. The crystals were observed under a polarising microscope, those which showed uniform extinction of light as the crystal was rotated through crossed polar lenses were selected and cut to size (typically 0.3 x 0.3 x 0.2 mm). X-ray diffraction data was collected at the EPSRC X-ray Crystallography Service in Southampton University at 150 K (**42**) and room temperature (**43** and **44**) and processed at the Nottingham Trent University. All three structures were solved using 'direct methods', the SHELXS-97 program[28] and refined using SHELXL-97[29]. The crystal structure of **42** contains two independent molecules in the asymmetric unit of space group $P\bar{1}$. One of these molecules is disordered such that there is 85.1% occupancy in

one orientation and 14.9% occupancy in another orientation. The structure was refined using a BLOC instruction so that the ordered molecule was refined independently of the disordered molecule and an EADP constraint so that the anisotropic displacement parameters for the two occupancies of the disordered molecule were the same. A SAME instruction was also used so that the geometry of the ordered molecule was used to restrain the geometry of the disordered molecule. The final R value is 0.064. The disorder in the second molecule of **42** is illustrated in the ORTEP[9] diagram in Figure 10, which shows the two orientations of the molecule. All further discussion of the structure of **42** will refer only to the ordered molecule. The molecular structure of **42** is illustrated in Figure 11 and selected geometric data given in Table 6. The crystal structures of **43** and **44** both contain one unique molecule in the asymmetric unit of space groups $P2_1/c$ and $P\bar{1}$ respectively. The final R values are 0.046 for **43** and 0.051 for **44**. Results for compounds **43** and **44** are illustrated in the ORTEP[9] diagrams in Figures 12 and 13 and selected geometric data given in Table 6. The crystal packing of compounds **42-44**, including intermolecular contacts, is illustrated in Section 2.8 towards the end of this chapter.

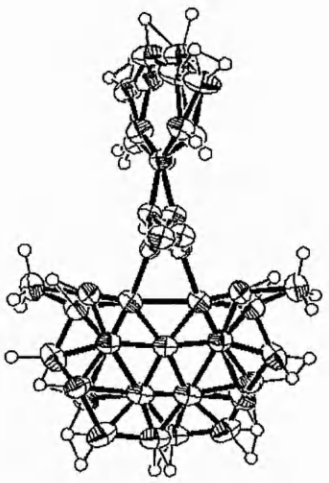

Figure 10 Ortep[9] diagram of the disordered molecule of **42**.

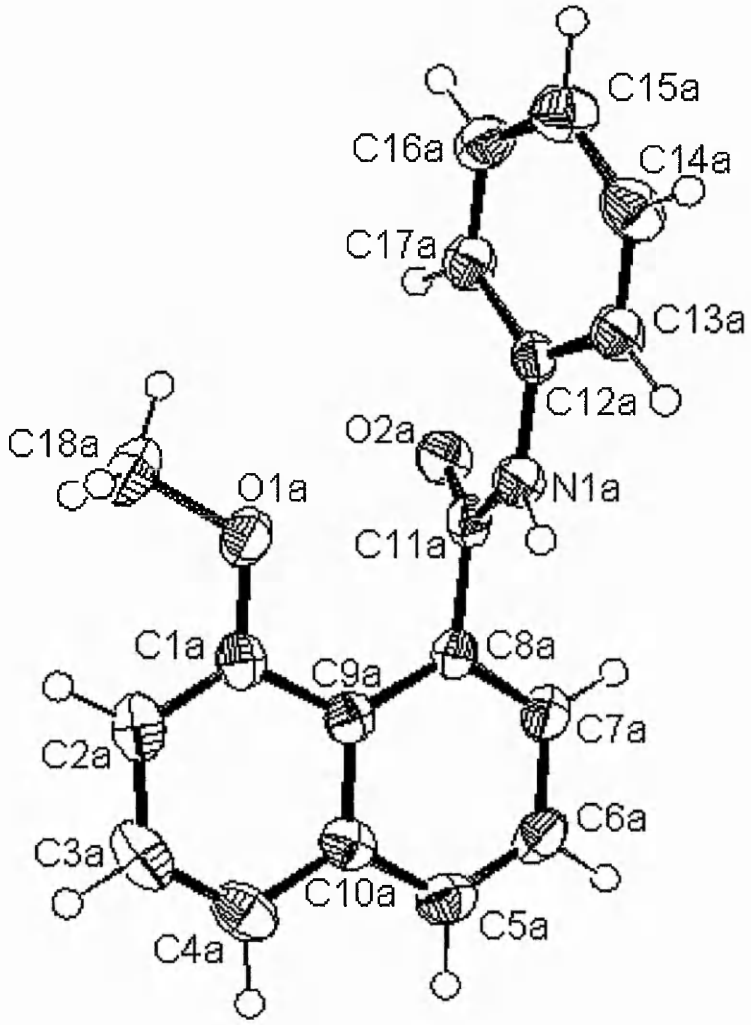

Figure 11 Molecular structure of one molecule of **42** with anisotropic displacement parameters at the 50% level.

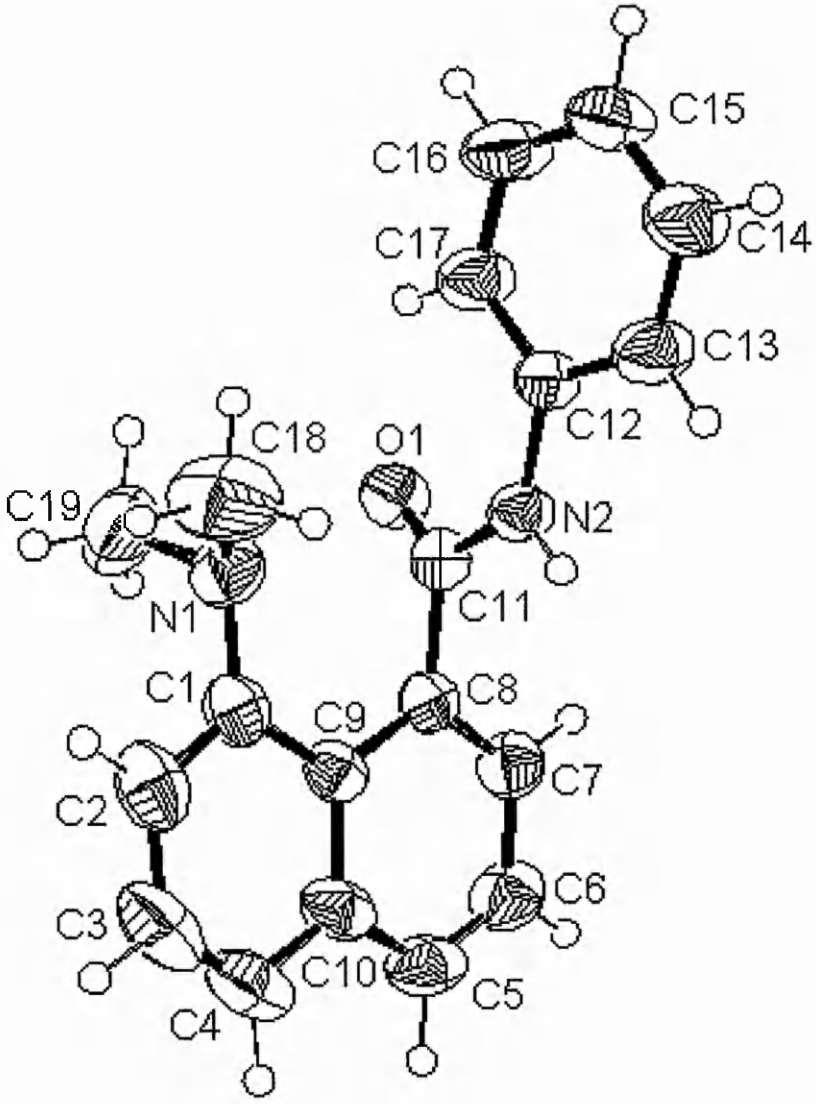

Figure 12 Molecular structure of **43** with anisotropic displacement parameters at the 50% level.

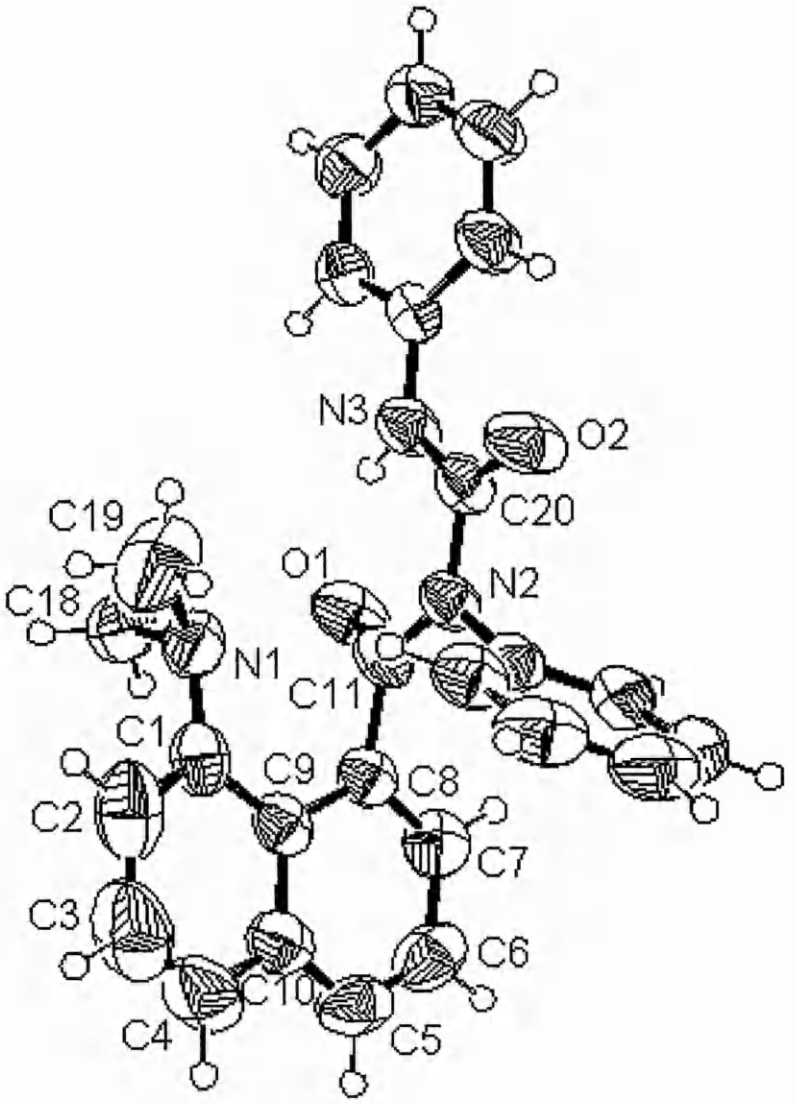

Figure 13 Molecular structure of **44** with anisotropic displacement parameters at the 50% level.

Table 6 Selected geometric data for compounds **42 – 44**

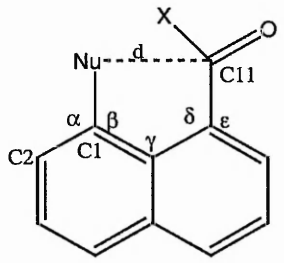

ΔC: deviation of C11 from the plane of its substituents towards the *peri* substituent.

T1 and T2: torsion angles of N-Me and O-Me bonds with the C1-C2 aryl bond.

	d	α	β	γ	δ	ε	ΔC	T1	T2
42	2.577(2)	124.3(1)	114.3(1)	123.8(1)	123.2(1)	116.9(1)	0.029(2)	8.3(3)	-
43	2.619(2)	123.0(1)	117.4(1)	123.4(1)	122.8(1)	116.9(1)	0.053(1)	50.8(2)	-79.3(2)
44	2.647(2)	123.4(2)	117.4(1)	123.0(1)	123.5(1)	116.7(1)	0.047(2)	32.1(3)	-94.3(2)

All three compounds show the distortion pattern characteristic of such compounds, in which both substituents are splayed in the same direction, with the carbonyl containing group splayed outwards. The patterns of angles α - ε are similar for the three compounds and compare well to the carbonyl derivatives discussed previously, they compare closest to the carboxylic acid and ester derivatives.[1,5,6] The O----C distance in **42** is 2.577(2) Å, *shorter* than the N----C distances for both the amide **43** 2.619(2) Å and the urea **44** 2.647(2) Å. The value of the parameter [d(MeO----X) + 0.15 –d(Me_2N----X)] is 0.108 Å for **42** and **43**. This predicts that the Me_2N----sp^2C interactions in **43** involves a small attractive component. There is no methoxy analogue of **44**. However, since the MeO----C separations are very insensitive to the

nature of the sp^2C, **42** can be used to estimate whether or not the interaction in **44** is attractive. The value of the parameter [d(MeO----X) + 0.15 – d(Me_2N----X)] is 0.080 Å for **42** and **44**, thus the Me_2N----sp^2C interaction in this compound also involves a small attractive component. These values lie between those calculated for the carboxylic ester (0.144 Å) and carboxamides (0.049 and 0.009 Å), thus the interactions in **43** and **44** are more attractive in nature than those of the dialkyl carboxamides[1,3] and the phenylcarboxamide group has a through-space electron-attracting strength in between those of a carboxamide and a carboxylic ester group.

Further evidence of an attractive interaction in **43** is from the torsion angles of the Me-N bonds with the naphthalene ring, these are 50.8(2) and –79.3(2)°. This indicates that the N atom's lone pair axis lies at 14.2° to the naphthalene ring and is well aligned towards the carbonyl carbon. In **44** the corresponding torsion angles are 32.1(3) and –94.3(2)°, hence the lone pair lies at 31.1° to the naphthalene ring and the alignment is not so good. (This is accounted for later in the discussion). In **42** the methoxy group lies almost in the plane of the naphthalene ring, the torsion angle of the Me-O bond with the naphthalene ring is 8.3(3)°.

The structure of **44** contains some interesting features. There is a hydrogen bond between the terminal phenylamine group of the acyl urea and the carbonyl group bonded to the naphthalene ring. This completes a planar six-membered ring system, which lies at 79.5(2)° to the naphthalene ring's best plane (Figure 14). The H----O distance is 1.86(2) Å and the angle at H is 77.4°.

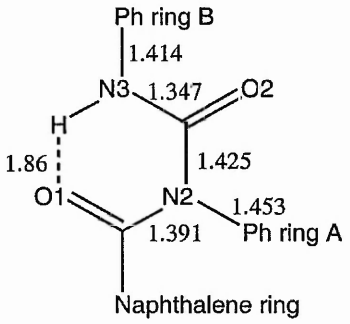

Figure 14 Hydrogen-bonded ring system in **44**

The two phenyl rings lie at 83.4(2)° (ring A) and 13.4(3)° (ring B) to the six-membered urea ring system. Thus the terminal nitrogen, N3, is involved in conjugation with phenyl ring B, but the N atom located between two carbonyl groups, N2, is not conjugated with ring A. A survey of all the structures in the CSD[15] containing the substructure **49** found that the torsion angle C1-C2-N-C3 is commonly 50-70°, the lowest torsion angle found was *ca.* 38°, but the phenyl ring never lies coplanar with the amide ring in structures of this type.

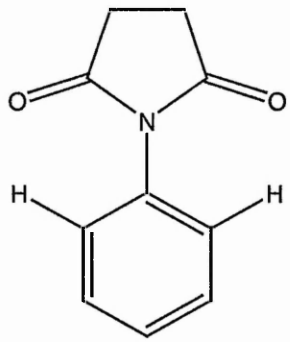

49

For **44** this is also evident in the respective N-C(Ar) bond lengths of 1.414 (N3-C(Ar)) and 1.453 (N2-C(Ar)) Å, thus conjugation of N3 with phenyl ring B has lead to a shorter N3-C bond than that of N2 to phenyl ring A. The former is in accord with **42** and **43** where the angles between the amide group and phenyl ring planes are 25.2(2)° (**42**) and 21.0(2)° (**43**), hence the amide N atom's lone pair can conjugate with the phenyl ring's π-system.

The position of phenyl ring A in **44** is such that it lies on the same side of the naphthalene plane as one of the dimethylamino methyl groups (C19). There is a short contact between an ortho hydrogen (H13) of the phenyl ring and one of the methyl hydrogens of C19, the H----H separation is only *ca.* 2.27 Å, which corresponds to van der Waals contact. This repulsion between the *peri* groups explains the *longer* N----sp^2C distance in **44** compared to that found in **43**, which is in contrast to what is expected. In **43** the carbonyl carbon receives some electron density from the adjacent N atom, hence it is not as electron-deficient as the carbonyl carbon of a ketone. In **44** the corresponding N atom lies between two carbonyl groups, hence the electron density donated is shared between both sp^2C atoms. Thus the sp^2C atom involved in the *peri*-interaction in **44** is expected to be more electron-deficient than that in **43** and undergo a stronger interaction with the dimethylamino N atom. This is reflected in the N2-C11 bond lengths, which are 1.391 Å for **44** and 1.356 Å for **43**. The steric repulsion between phenyl ring A and the dimethylamino methyl group restricts the N----sp^2C separation in **44**. It also restricts the orientation of the dimethylamino group such that the N atom's lone pair cannot be directed towards the *peri* group. In an attempt to ease the repulsion the *peri* groups are also displaced to opposite sides of the

naphthalene plane. The sizes of the displacements are 0.325(2) Å for the dimethylamino N atom and 0.161(2) Å for the carbonyl C atom, which are *larger* than the corresponding distortions in **43** (0.218 (2) and 0.133 (2) for N1 and C11 respectively).

There are other structural features of **42-44** that compare well with the *peri* naphthalenes discussed earlier. All three show small pyramidalisations of the carbonyl carbon towards the *peri* substituent, 0.029(2) Å in **42**, 0.053(1) Å in **43** and 0.047(2) Å in **44**. Although it has already been established that small pyramidalisations in such compounds can be misleading due to influences of such factors as molecular environment, the pyramidalisations in compounds **42-44** do follow the same trend set by the Nu----C distances (Nu = nucleophile). The Nu----C=O angles are 95.6(1)° in **42**, 98.0(1)° in **43** and 98.5(1)° in **44**. These are comparable with the corresponding angles in the ketone, carboxylic acid and carboxamide analogues are 104.4, 102.2 and 96.7 and 98.7° for the dimethylamino derivatives[1,3] and 107.6, 93.7 and 90.0° for the methoxy derivatives[1-3,6], and support the theory that the preferred approach direction of a nucleophile is at an obtuse angle to the carbonyl group.

In conclusion the phenylcarboxamides do undergo *peri* interactions with dimethylamino and methoxy groups approaching those of a carboxylic ester group. A comparison of the values calculated for the parameter [d(MeO----X) + 0.15 – d(Me_2N----X)] for the relevant pair of dimethylamino and methoxy derivatives has shown that the values for the Me_2N----C interactions in **43** and **44** lie in between those

for the carboxylic ester **3** and amides **5** and **6**. Thus the interactions in **43** and **44** appear to consist of a small attractive component. The distortion patterns in **42 – 44**, as indicated by the angles α - ε, have been compared to those of the compounds in Tables 1 and 2 and are most like the carboxylic acid and ester derivatives **3**, **4**, **11-14**. The theoretical N lone pair direction appears to be well aligned towards the carbonyl C atom in **43**, the alignment is similar to that in the corresponding carboxylic ester derivative **3**. In **44** this alignment is not so good but can be accounted for by an extra repulsion between the NMe and N-Ph groups. This effect also contributes to the longer N----C distance in **44**.

2.8 Crystal Packing

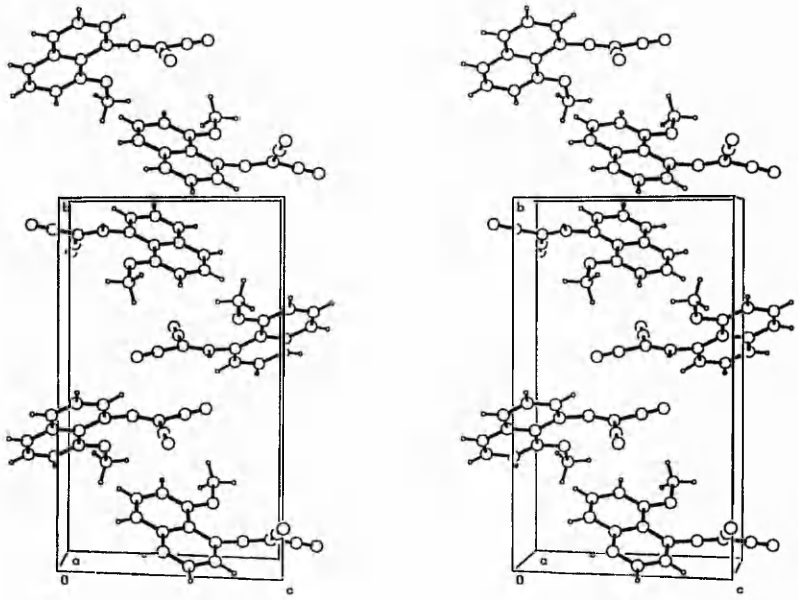

Figure 15 Crystal packing of **24** at 150K.

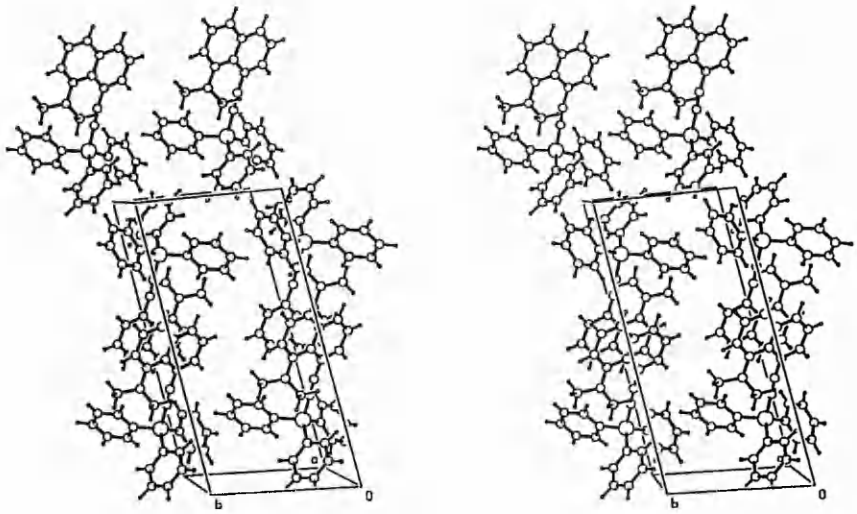

Figure 16 Crystal packing of **40**.

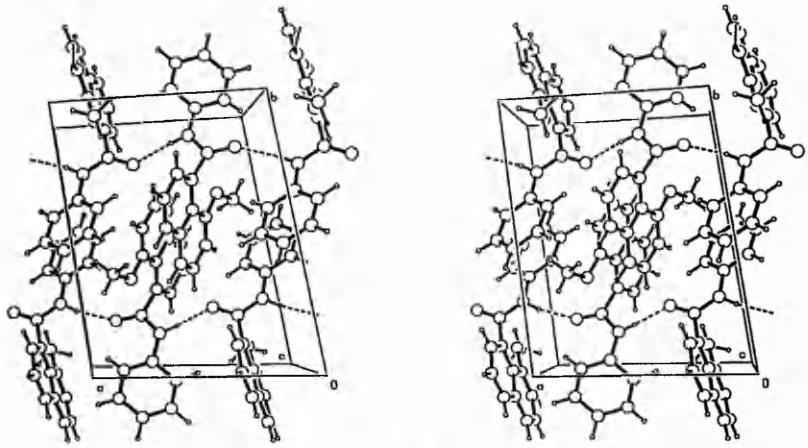

(a)

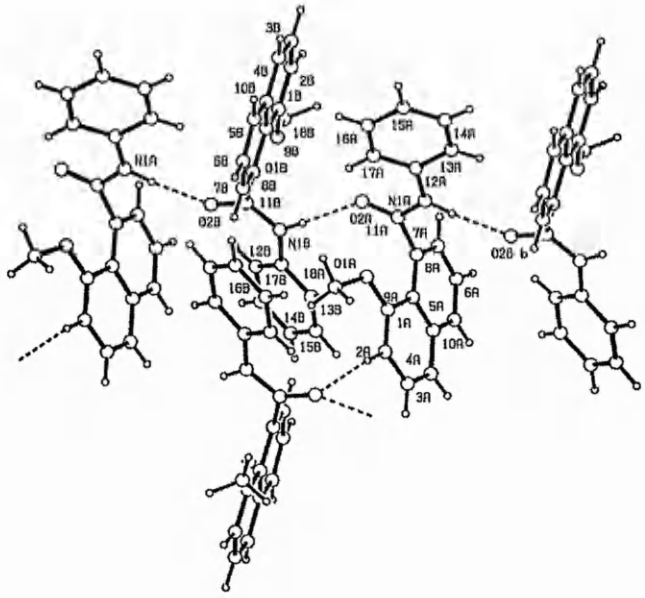

(b)

Figure 17 Crystal packing of **42** at 150 K (a) in the unit cell and (b) intermolecular contacts.

The crystal packing of **42** involves intermolecular hydrogen bonding between the amide N(1)-H and carbonyl O(2) atom (2.03 Å) to create a chain, as shown above. There are also contacts between the carbonyl O(2) atom and an aromatic hydrogen (C(2)-H) (2.42 Å). Due to the disorder in the structure the estimated standard deviations for these contacts were not calculated.

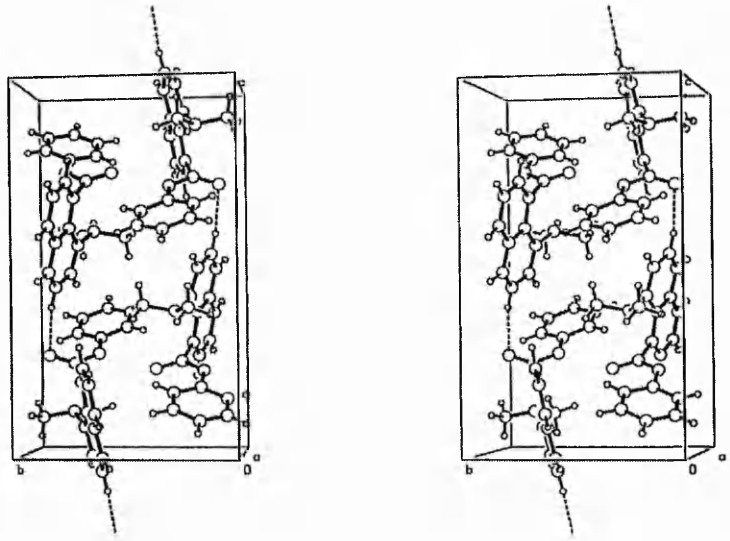

(a)

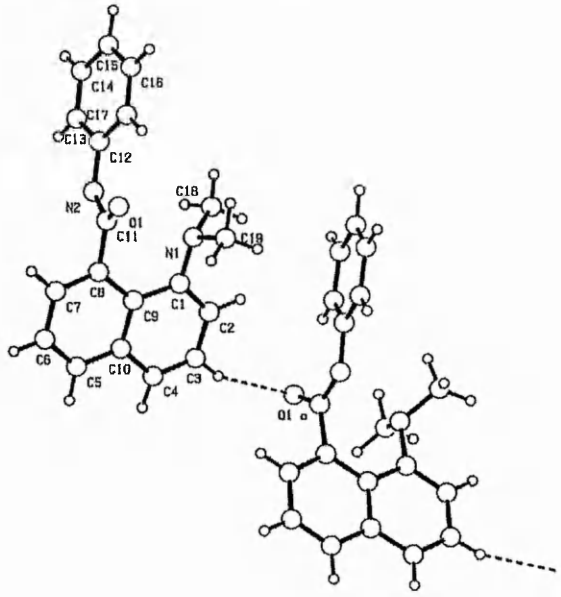

(b)

Figure 18 Crystal packing of **43** at room temperature
(a) in the unit cell and (b) intermolecular contacts.

The crystal packing of **43** involves intermolecular hydrogen bonding between the carbonyl O(1) atom and an aromatic hydrogen (C(3)-H) (2.51(3) Å).

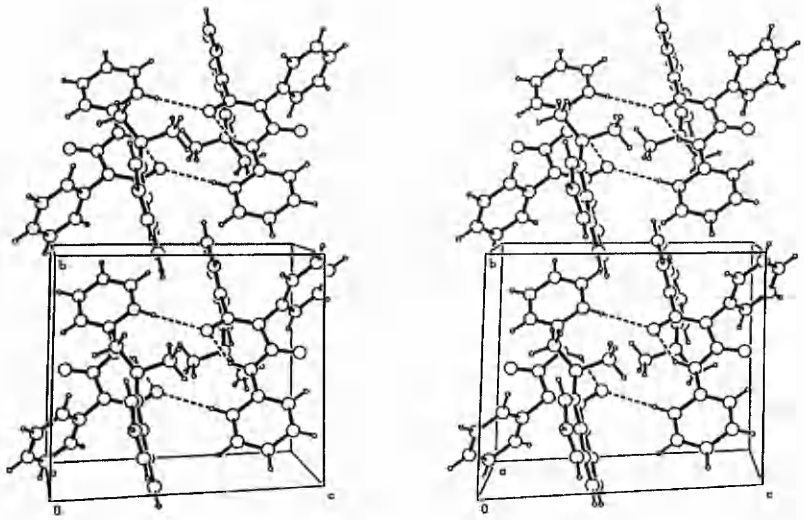

(a)

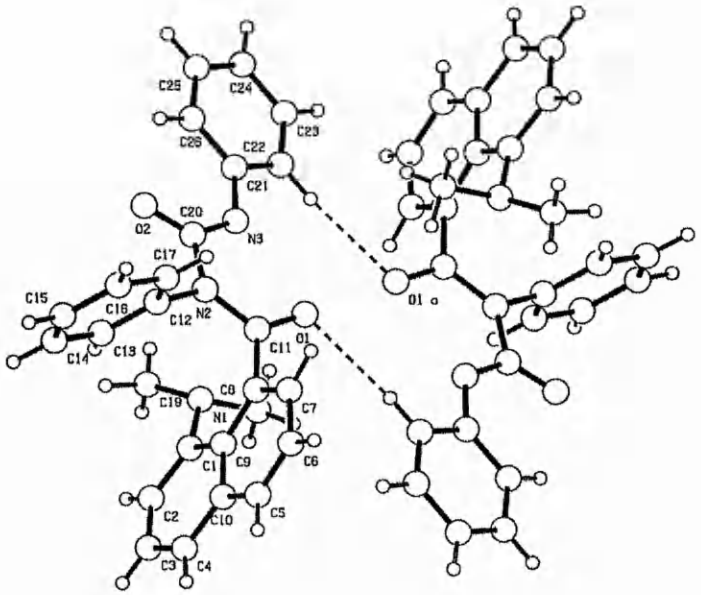

(b)

Figure 19 Crystal packing of **44** at room temperature
(a) in the unit cell and (b) intermolecular contacts.

The crystal packing of **44** involves C(22)-H----O(1) (2.52(2) Å) hydrogen bonding between pairs of molecules.

2.9 Experimental

Preparation of 1-Dimethylaminonaphthalene **47**

Dimethyl sulfate (13.2 ml, 140 mmol) was added to a stirred solution of 1-aminonaphthalene **46** (20 g, 140 mmol) in THF (200 ml) at 0°C. The mixture was stirred at 0°C for 1 h. before the pH was adjusted to pH 11 with 4M NaOH. Dimethyl sulfate (13.2 ml, 140 mmol) was added and the mixture was stirred at room temperature overnight. The pH was adjusted to pH 11 with 4M NaOH before dimethyl sulfate (6.6 ml, 70 mmol) was added and the mixture refluxed for 1 h. The pH was once more adjusted to pH 11 with 4M NaOH and the mixture transferred to a separatory funnel. The organic layer was washed with water and extracted with 2M HCl. The acidic extracts were neutralised with 4M NaOH and extracted with ether. The organic solution was dried ($MgSO_4$), evaporated and the crude oil was purified by distillation to yield **47** as a colourless liquid (13.9 g, 58%), b.p. 138-141°C at 13 mm Hg (lit. b.p. 139-140 °C at 13 mm Hg)[30]; ^{1}H NMR ($CDCl_3$) δ: 8.20 (1H, dd, J = 8.2, 0.8 Hz, Ar-H_1), 7.70 (1H, d, J = 7.6 Hz, Ar-H_1), 7.41-7.22 (4H, m, Ar-H_4), 6.91 (1H, d, J = 7.4 Hz, Ar-H_1), 2.73 (6H, s, N(CH_3)$_2$); ^{13}C NMR ($CDCl_3$) δ: 150.7, 134.7, 128.7, 128.2, 125.6, 125.5, 124.9, 124.0, 122.7, 113.8 (Ar-C_{10}), 45.0 (N(CH_3)$_2$).

Preparation of 8-Dimethylamino-1-acetylnaphthalene **50**[31]

n-Butyllithium (2.6M solution in hexane, 32 ml, 82 mmol) was added to a stirred solution of 1-dimethylaminonaphthalene **47** (3.0 g, 17 mmol) in dry ether (50 ml) at

room temperature under nitrogen. After 48 h. the precipitated lithium salt was filtered under nitrogen and washed with dry hexane. The lithium salt was then suspended in dry ether and cooled to -78°C. A solution of acetic anhydride (1.7 ml, 17 mmol) in dry ether (10 ml) was added dropwise, the mixture was allowed to warm to room temperature over 4 h. The mixture was cooled to -20°C and the reaction was quenched with a solution of methanol (3.3 ml) in ether (1.7 ml). The resulting mixture was diluted with ether (50 ml) and washed with water (3 x 50 ml). The organic solution was dried ($MgSO_4$) and evaporated and the crude residue was purified by flash chromatography on silica gel (hexane:ether, 2:1) to yield the product **50** as a yellow solid (0.72 g, 19%), m.p. 107-108°C (lit. m.p. 107-108°C); ^{1}H NMR ($CDCl_3$) δ: 7.82 (1H, dd, J = 8.2, 0.9 Hz, ArH_1), 7.64 (1H, dd, J = 8.2, 1.0 Hz, ArH_1), 7.51-7.43 (2H, m, ArH_2), 7.32 (1H, dd, J = 7.4, 1.2 Hz, ArH_1), 7.25 (1H, dd, J = 7.0, 1.0 Hz, ArH_1), 2.60 (6H, br s, N(CH_3)$_2$), 2.35 (3H, s, C(=O)CH_3); ^{13}C NMR ($CDCl_3$) δ: 201.8 (*C*=O), 150.1, 140.4, 134.9, 128.8, 128.3, 126.7, 125.9, 124.7, 123.1, 118.2 (ArC_{10}), 31.7 (C*C*H$_3$).(NMe$_2$ group not observed in the ^{13}C NMR spectrum).

Preparation of 1-Triphenylsilyl-2-(8'-dimethylamino-1'-naphthyl)ethyne **40**

LDA was prepared by stirring diisopropylamine (1 g, 9.9 mmol) and n-Butyllithium (1.2M solution in hexane) (8.2 ml, 9.9 mmol) in THF (25 ml) at -40°C under nitrogen. The mixture was cooled to -78°C and 8-dimethylamino-1-acetylnaphthalene **50** (2.0 g, 9.4 mmol) was added. After stirring for 1 h. at -78°C diethylchlorophosphate (1.8 g, 10.3 mmol) was added and the mixture was allowed to warm to room temperature. The solution was transferred, via cannula, to a stirred solution of LDA in THF,

prepared by stirring diisopropylamine (2.0 g, 20.2 mmol) and n-Butyllithium (1.2M solution in hexane) (16.8 ml, 10.3 mmol) in THF (25 ml) at -78°C under nitrogen. After 3 h. at -78°C a solution of triphenylsilyl chloride (3.0 g, 10.3 mol) in dry THF (15 ml) was added and the mixture was allowed to warm to room temperature and stirred overnight. The mixture was poured in to a saturated solution of aqueous NH_4Cl and extracted with ether (3 x 50 ml). The organic solution was dried ($MgSO_4$) and evaporated to yield a crude green residue, which was purified by flash chromatography on silica gel (hexane:ether, 10:1) to yield the product **40** as a green solid (1.3 g, 31%), mp 120-121°C; ν_{max}/cm^{-1} (KBr): 2143, 1378, 703, 509; ^1H NMR ($CDCl_3$) δ: 7.90 (1H, dd, J = 7.3, 1.3 Hz, ArH_1), 7.81-7.77 (6H, m, ArH_6), 7.62 (1H, dd, J = 7.7, 1.7 Hz, ArH_1), 7.48 (1H, dd, J = 7.9, 1.1 Hz, ArH_1), 7.43-7.34 (11H, m, ArH_{11}), 7.12 (1H, dd, J = 7.4, 1.2 Hz, ArH_1), 2.62 (6H, s, N(CH_3)$_2$); ^{13}C NMR ($CDCl_3$) δ: 151.3 (8'-*C*), 135.7 (*ortho* phenyl-*C*), 135.5, 135.5, 134.9, 134.4, 130.1, 129.7 (*para* phenyl-*C*), 127.9 (*meta* phenyl-*C*), 126.2, 124.8, 123.5, 118.4 (1'-*C*), 116.1 (7'-*C*), 112.1 (2-*C*), 92.1)1-*C*), 45.7 (N(CH_3)$_2$); HRMS (ES): Found: 454.1989 $(M+H)^+$, $C_{32}H_{28}SiN$ requires: 454.1991 $(M+H)^+$.

Preparation of N-Phenyl-8-methoxy-1-naphthamide **42**

t-Butyllithium (1.7M solution in pentane, 20 ml, 33 mmol) was added to a stirred solution of 1-methoxynaphthalene **45** (4.75 g, 30 mmol) in dry cyclohexane (60 ml) at room temperature, under nitrogen. After 48 h. the precipitated lithium salt was filtered under nitrogen and washed with dry ether. The lithium salt was suspended in dry ether and cooled to -78°C. Phenyl isocyanate (3.57 g, 30 mmol) was added

dropwise, the mixture was allowed to warm to room temperature and stirred overnight. The resulting brown solution was poured on to aqueous NH_4Cl and the white solid product was collected by vacuum filtration to yield **42** (6.0 g, 72%), m.p. 188-190°C; ν_{max}/cm^{-1} (KBr): 3278, 1654, 1599, 1549, 1441, 1324, 1260, 1120, 1058, 768, 753; ^1H NMR ($CDCl_3$) δ: 7.81 (1H, t, J = 4.8 Hz, Ar-H_1), 7.57 (2H, d, J = 7.7 Hz, Ar-H_2), 7.43-7.37 (5H, m, Ar-H_4 + NH), 7.32 (2H, t, J = 7.8 Hz, ArH_2), 7.11 (1H, t, J = 7.4 Hz, Ar-H_1), 6.83 (1H, dd, J = 6.9, 1.8 Hz, Ar-H_1), 3.79 (3H, s, OCH_3); ^{13}C NMR ($CDCl_3$) δ: 170.0(C=O), 155.1, 138.5, 135.0, 133.3, 129.3, 129.0, 126.6, 125.5, 125.1, 124.0, 121.4, 120.8, 119.8, 106.0 (Ar-C_{16}), 56.1, (OCH$_3$); Found: C, 77.94; H, 5.36; N, 4.92% $C_{18}H_{15}NO_2$ requires: C, 77.96; H, 5.45; N, 5.05%; HRMS (EI): Found: 277.1107, $C_{18}H_{15}NO_2$ requires: 277.1103.

Crystal data for **42**: $C_{18}H_{15}NO_2$, Mr = 277.32, triclinic, a = 9.7709(4), b = 12.8905(5), c = 13.2494(6) Å, α = 70.822(2), β = 68.573(2), γ = 76.360(2)°, V = 1454.45 Å^3, Z = 4, P$\bar{1}$, Dc = 1.27 gcm^{-3}, μ (MoKα) = 0.08 mm^{-1}, 6430 unique reflections, 3576 with $F_o > 4\sigma(F_o)$, R = 0.064. Full data available on the crystallographic information file on the disk provided.

<u>Preparation of N-Phenyl-8-(dimethylamino)-1-naphthamide **43** and N,N'-Diphenyl-N-(8-dimethylamino-1-naphthoyl)urea **44**</u>

n-Butyllithium (1.6M solution in hexane, 26 ml, 41 mmol) was added to a stirred solution of the amine **47** (1.75 g, 10 mmol) in dry ether (35 ml) at room temperature under nitrogen. After 48 h. the precipitated lithium salt was filtered under nitrogen

and washed with dry ether. The lithium salt **48** was then suspended in dry ether and cooled to -40°C. Phenyl isocyanate (1.67 g, 14 mmol) was added dropwise, the mixture was allowed to warm to room temperature and stirred overnight. The resulting yellow solution was poured on to aqueous NH_4Cl and the product extracted with CH_2Cl_2. The organic solution was dried ($MgSO_4$), evaporated and the crude solid material separated on silica gel (hexane:ether, 2:1) to yield **43** (0.68 g, 23%) and **44** (1.92 g, 46%) as white solids.

N-Phenyl-8-(dimethylamino)-1-naphthamide **43**

(0.68 g, 23%, m.p. 193°C; ν_{max}/cm^{-1} (KBr): 3268, 1648, 1595, 1545, 1495, 1438, 1316, 778, 754, 712; ^1H NMR ($CDCl_3$) δ: 7.87 (1H, dd, J = 8.2 Hz, Ar-H_1), 7.66 (1H, dd, J = 8.1, 1.1 Hz, Ar-H_1), 7.57-7.29 (8H, m, Ar-H_8), 7.17 (1H, br.s, N*H*), 7.08 (1H, t, J = 7.3 Hz, Ar-H_1), 2.61 (6H, s, N(CH_3)$_2$); ^{13}C NMR ($CDCl_3$) δ: 169.8 (*C*=O), 150.9, 138.9, 135.3, 129.6, 128.9, 128.9, 126.6, 126.1, 125.4, 124.8, 123.4, 119.3, 119.3, 119.3 (Ar-C_{16}), 46.0 (N(CH_3)$_2$); HRMS (EI): Found: 290.1425, $C_{19}H_{18}N_2O$ requires: 290.1419

Crystal data for **43**: $C_{19}H_{18}N_2O$, Mr = 290.36, monoclinic, a = 9.4294(10), b = 9.8071(10), c = 17.0263(10) Å, β = 91.254(20)°, V = 1574.13 Å^3, Z = 4, $P2_1/c$, Dc = 1.22 gcm^{-3}, μ (MoKα) = 0.08 mm^{-1}, 3200 unique reflections, 2599 with $F_o > 4\sigma(F_o)$, R = 0.046. Full data available on the crystallographic information file on the disk provided.

N.N'-Diphenyl-N-(8-dimethylamino-1-naphthoyl)urea **44**

m.p. 142°C; ν_{max}/cm^{-1} (KBr): 3442, 3265, 1705, 1661, 1495, 1282, 1194, 1159, 789, 765; ^1H NMR ($CDCl_3$) δ: 11.60 (1H, br.s, N*H*), 7.66 (2H, d, J = 3.8 Hz, Ar-H_2), 7.58 (1H, dd, J = 7.5, 2.0 Hz, Ar-H_1) 7.43-7.23 (7H, m, Ar-H_7), 7.12 (1H, t, J = 7.4Hz, Ar-H_1), 6.84 (5H, br.s, N-C_6H_5), 2.98 (3H, s, (NCH_3), 2.57 (3H, s, NCH_3); ^{13}C NMR ($CDCl_3$) δ: 175.5 (*C*=O), 152.3 (*C*=O), 150.6, 138.1, 137.7, 134.4, 129.4, 129.3, 129.0, 129.0, 127.6, 127.4, 126.4, 126.3, 124.5, 124.5, 123.8, 120.1, 120.1, 117.7 (Ar-C_{22}), 49.9 (N(CH_3)$_2$); Found: C, 75.90; H, 5.68; N, 10.12 $C_{26}H_{23}N_3O_2$ requires: C, 76.26; H, 5.66; N, 10.26%; HRMS (EI): Found: 409.1798, $C_{26}H_{23}N_3O_2$ requires: 409.1790.

Crystal data for **44**: $C_{26}H_{23}N_3O_2$, Mr = 409.48, triclinic, a = 9.7199(2), b = 9.9218(2), c = 12.1498(2) Å, α = 86.0784(12), β = 69.6673(13), γ = 79.9094(11)°, V = 1081.67 $Å^3$, Z = 2, Pī, Dc = 1.26 gcm^{-3}, μ (MoKα) = 0.08 mm^{-1}, 4370 unique reflections, 3072 with $F_o > 4\sigma(F_o)$, R = 0.051. Full data available on the crystallographic information file on the disk provided.

2.10 References

1. Schweizer, W.B., Procter, G., Kaftory, M. and Dunitz, J.D., *Helv. Chim. Acta*, 1978, **61**, 2783.
2. Galluci, J.C., Hart, D.J. and Young, G.J., *Acta Cryst.*, 1998, **B54**, 73.
3. Clayden, J., McCarthy, C. and Helliwell, M., *J. Chem. Soc., Chem. Commun.*, 1999, 2059.
4. Hodgson, D.R.W., Kirby, A.J. and Feeder, N., *J. Chem. Soc., Perkin Trans. 1*, 1999, 949.
5. Blackburn, A.C. and Gerkin, R.E., *Acta Cryst.*, 1997, **C53**, 1077.
6. Gerkin, R.E., *Acta Cryst.*, 1997, **C53**, 1987.
7. Bell, P.C. and Wallis, J.D., *J. Chem. Soc., Chem. Commun.*, 1999, 257.
8. O'Leary, J., Bell, P.C., Wallis, J.D. and Schweizer, W.B., *J. Chem. Soc., Perkin Trans. 2*, 2001, 133.
9. Johnson, C.K. and Burnett, M.N., ORTEPIII, Report ORNL-6895, 1996, Oak Ridge National Laboratory, Tennessee, USA.
10. Akiba, K., Yamashita, M., Yamamoto, Y. and Nagase, S., *J. Am. Chem. Soc.*, 1999, **121**, 10644.
11. Ford, A., Sinn, E. and Woodward, S., *J. Chem. Soc., Perkin Trans. 1*, 1997, 927.
12. Fuji, K., Sakurai, M., Tokhai, N., Kuroda, A., Kawabata, T., Fukazwa, Y., Kinoshita, T. and Tada, T., *J. Chem. Soc., Chem. Commun.*, 1996, 1609.
13. a) Opitz, G., Reith, K. and Rimmler, G., *Tetrahedron Lett.*, 1986, **27**, 167.

b) Einspahr, H., Robert, J.B., Marsh, R.E. and Roberts, J.D., *Acta Cryst.*, 1973, **B29**, 1611.

c) Pozharskii, A.F., Tregub, N.G., Vistiribskii, N.V., Romanova, E.Y., Starikova, Z.A. and Yanovsky, A.I., *Izv. Akad. Nauk SSSR, Ser. Khim.*, 1999, 1311.

d) Wozniak, K., Heygong, H., Klinowski, J., Barr, T.L. and ardcastle, S.E., *J. Phys. Chem.*, 1996, **100**, 11408.

e) Staab, H.A., Krieger, C., Hieber, G. and Oberdorf, K., *Angew. Chem., Int. Ed. Engl.*, 1997, **36**, 1884.

f) Barth, T., Krieger, C., Neugebauer, F.A. and Staab, H.A., *Angew. Chem., Int. Ed. Engl.*, 1991, **30**, 1028.

14. a) Bringmann, G., Zagst, R., Schoner, B., Busse, H., Hemmerling, M. and Burschka, C., *Acta Cryst.*, 1991, **C47**, 1703.

b) Cosmo, R., Hambley, T.W. and Sternhell, S., *Acta Cryst.*, 1990, **46**, 557.

c) Bringmann, G., Saeb, W., Peters, K. and Peters, E.M., *Phytochemistry*, 1997, **45**, 1283.

d) Baker, R.W., Liu, S., Sargent, M.V., Skelton, B.W. and White, A.H., *J. Chem. Soc., Chem. Commun.*, 1997, 451.

15. Bürgi, H.B., Dunitz, J.D. and Schefter, E., *J. Am. Chem. Soc.*, 1973, **95**, 2544.

16. Allen, F.H. and Kennard, O., *Chem Des. Autom. News*, 1993, **8**, 1 and 31.

17. McCullough, K.J., Masayama, A., Morgan, K.M., Nojima, M., Okada, Y., Satake, S. and Takeda, S., *J. Chem. Soc., Perkin Trans. 1*, 1998, 2353.

18. Irngartinger, H., Fettel, P.W. and Siemund, V, *Eur. J. Org. Chem.*, 1998, 2079.

19. Cieplak, A.S., *Structure Correlation*, eds. Bürgi, H.B. and Dunitz, J.D., VCH Weinheim, vol. 1, 1994.

20. Krygowski, T.M., Annulewicz, R., Jarmula, A., Bak, T., Rasala, D. and Howard, S., *Tetrahedron*, 1994, **46**, 13155.

21. Vincent, M.A. and Hillier, I.H., *Chem. Phys.*, 1990, **140**, 35.

22. Garg, S.K. and Smyth, C.P., *J. Chem. Phys.*, 1967, **46**, 373.

23. Owen, N.L. and Hestor, R.E., *Spectrochim. Acta*, 1969, **A25**, 343.

24. Parvez, M. and Schuster, I.I., *Acta Cryst.*, 1990, **C46**, 947.

25. Procter, G., Britton, D. and Dunitz, J.D., *Helv. Chim. Acta*, 1981, **64**, 471.

26. Bell, P.C., Drameh, M., Hanly, N. and Wallis, J.D., *Acta Cryst.*, 2000, **C56**, 670.

27. Bell, P.C. and Wallis, J.D., unpublished work.

28. Sheldrick, G.M., SHELXS-97, Program for the Solution of Crystal Structures, 1997, University of Göttingen, Germany.

29. Sheldrick, G.M., SHELXL-97, Program for Crystal Structure Refinement, 1997, University of Göttingen, Germany.

30. Aldrich Chemical Catalogue, 1999/2000, 687.

31. Kirby, A.J. and Percy, J.M., *Tetrahedron*, 1988, **44**, 6903.

Chapter 3

Interactions Between Methylthio Groups and Electron-Deficient Alkenes in *Peri*-Naphthalenes

Interactions Between Methylthio Groups and Electron-Deficient Alkenes in *Peri*-Naphthalenes

3.1 Introduction

Very little is known about *peri* interactions of S atoms with electrophilic groups. In the literature there is just one example of such an interaction, in which the *peri*-naphthalene compound contains a methylthio group in the 1-position and a diazonium group in the 8-position, in the salt **1**.[1] The 1,5 contact between the methylthio group and the diazonium group, the S----N distance, is 2.938(5) Å.

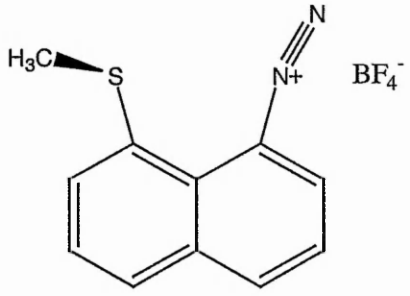

1

The distortion pattern observed for **1** is such that the *peri* groups are splayed away from each other (Figure 1a). This differs from that observed in dimethylamino and methoxy derivatives where the *peri* groups are either bent towards each other (Figure 1b) or more commonly are bent in the same direction (Figure 1c).[2-5] Although this

distortion pattern may appear not to be consistent with an attractive interaction between the *peri* substituents, it may simply be as a result of the larger size of the S-atom, compared to the N and O atoms. Unlike the O-Me bond in the *peri*-methoxy compounds, the S-Me bond does not lie in the aromatic plane, the Me-S-C=C torsion angle is *ca.* 65°. This reduces the steric pressure between the methyl group and the *ortho* H atom as the SMe group is splayed outwards.

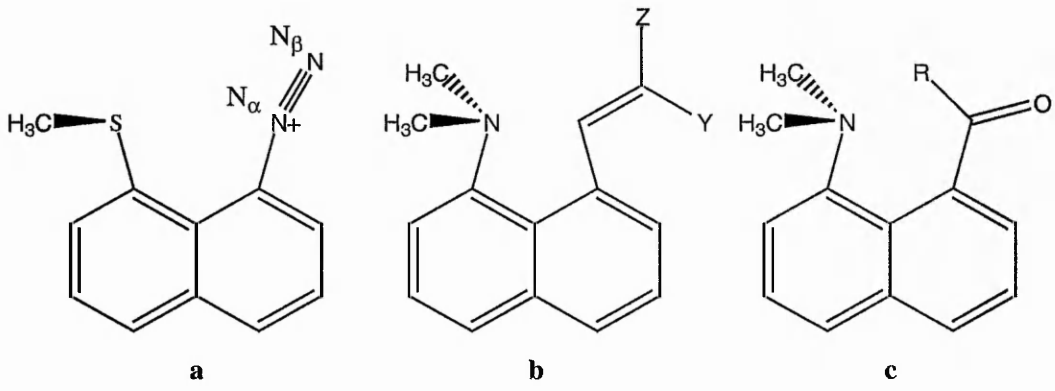

Figure 1 Distortion patterns in *peri*-naphthalenes

One feature of the structure of **1**, which may indicate the presence of an attractive interaction is the bend in the diazonium group, as shown in Figure 1a. The C-N^{+}≡N group is bent from linearity at the α-N atom by 9.9(1)° such that the α-N atom is displaced from the C----β-N line towards the MeS group. This type of bending has also been observed in structures exhibiting interactions between nucleophiles and spC atoms of nitriles[6-8] and alkynes[5,9-13] and has been compared to the partial pyramidalisations observed for sp^2C atoms of carbonyls and alkenes involved in interactions with nucleophiles.[1-3]

3.2 Results and Discussion

It is not possible to gain much information or draw many inferences as to the nature of *peri* interactions of the methylthio group from just one structure. This prompted an investigation into *peri* interactions of the methylthio group with different electron-deficient alkenes. Thus a series of compounds have been synthesised using the *peri* naphthalene framework, with a methylthio group in the 1-position and different electron-deficient alkenes in the 8-position.

The preparation of compounds **9-12** was through a seven step synthesis from 1,8-naphthalic anhydride **2** (Scheme 1). The first step was mercuration of the anhydride **2** with $Hg(OAc)_2$ in aqueous acid to yield the *peri*-mercurated product **3**[14] in 92% as a white solid, which could not be characterised due to its very high insolubility. This mercury compound **3** was treated with I_2 in an aqueous solution of KI to produce 8-iodo-1-naphthalic acid[14] **4** as a white solid in 69% yield. Coupling of **4** with 2-mercaptopropionic acid using activated Cu powder gave the thiolactone[15] **5** in 94% yield, which was then hydrolysed with KOH and treated with MeI in DMSO to give methyl 8-methylthio-1-naphthoate **6** in 74% yield. A possible mechanism for the conversion of **4** to **5** is given in Scheme 2.

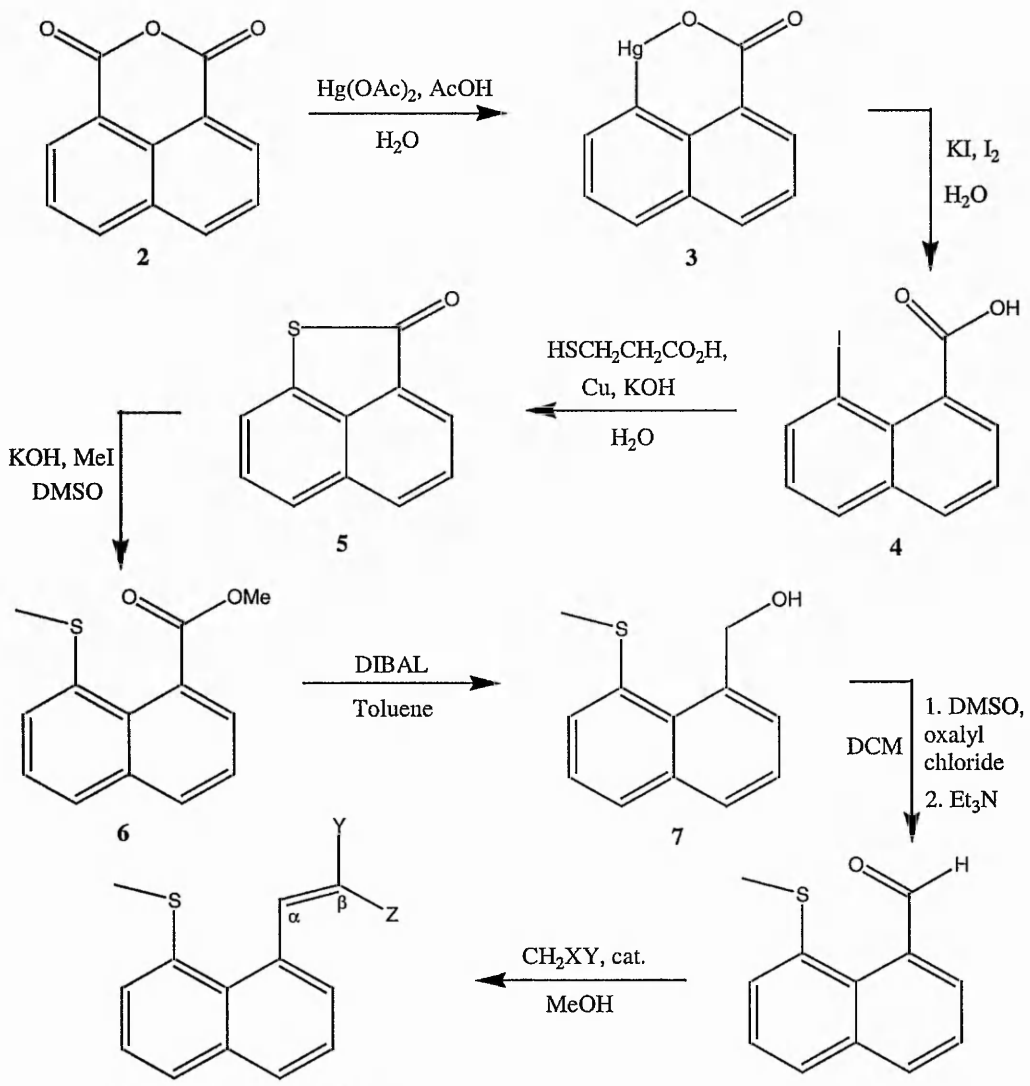

Scheme 1 Synthesis of compounds **9-12**

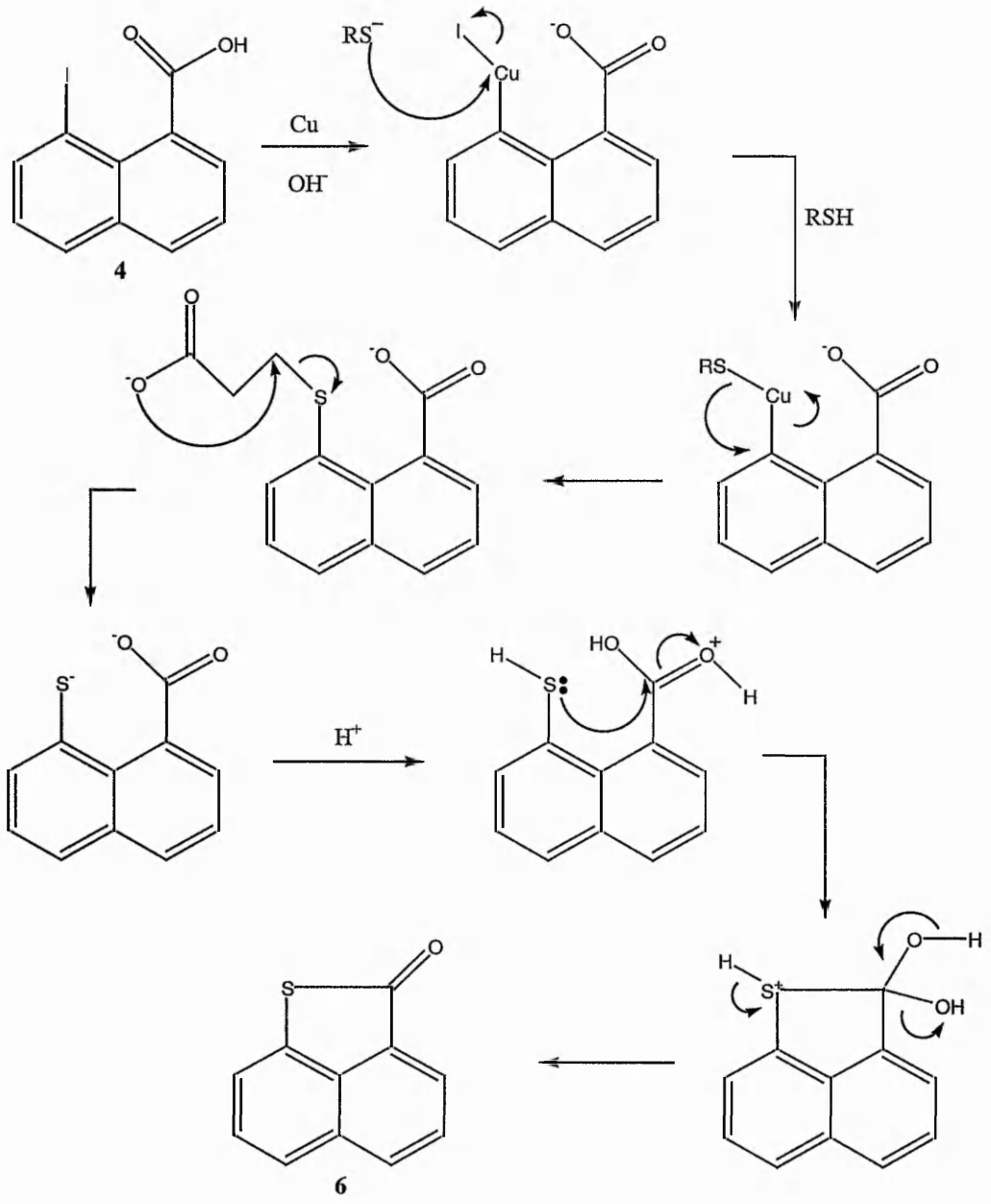

Scheme 2 Mechanism for the conversion of **4** to **5**

It was attempted to reduce the ester **6** to the corresponding aldehyde using one equivalent of DIBAL at -78°C and quenching the reaction with dilute acid at this temperature, however the reaction intermediate proved unstable and all attempts gave the corresponding alcohol **7**. The yield of **7** was subsequently maximised (77%) by using two equivalents of DIBAL. A Swern oxidation was then employed to oxidise this alcohol to the aldehyde **8**, which was obtained in 90% yield. Knoevenagel condensations of 8-methylthio-1-naphthaldehyde **8** with Meldrum's acid, malononitrile, nitromethane and methyl cyanoacetate in methanol using a catalytic amount of ethylenediamine diacetate (Scheme 3) afforded compounds **9-12** in yields ranging from 12-75%.

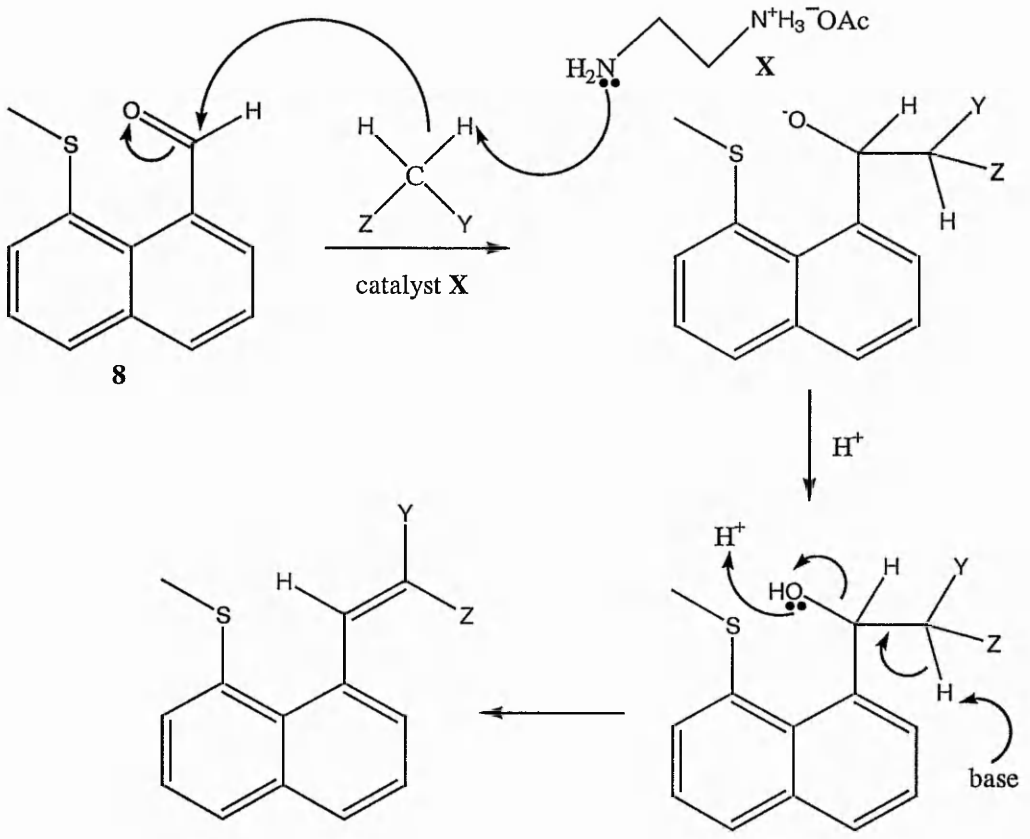

Scheme 3 Mechanism of Knoevenagel condensation of **8**

The structure of **9** was supported by the ^{1}H NMR, the alkenyl proton was observed at δ: 9.58, the CMe_2 group at δ: 1.85 and the MeS group at δ: 2.36. ^{13}C NMR shows the expected carbonyl resonances at δ: 163.0 and δ: 160.6 and the α-C of the alkene was observed at δ: 161.9, (this was confirmed by a C-H correlation NMR experiment). Two signals, at δ: 109.6 and δ: 105.5, correspond to the β-C of the alkene and the 2-C of the dioxane ring, but it was unclear as to which signal was which, therefore a heteronuclear multiple bond correlation (HMBC) NMR experiment was run. This gives cross peaks corresponding to long-range coupling between protons and carbons (Figure 2), hence coupling of the β-C of the alkene with the α-H of the alkene showed that the signal at δ: 109.6 corresponds to the alkene's β-C. The infrared spectrum of **9** shows an absorption at 1728 cm^{-1} corresponding to a carbonyl stretch. The molecular formula of **9** was confirmed by high resolution mass spectrometry.

The ^{1}H NMR of **10** shows a shift at δ: 9.27 corresponding to the alkenyl proton and the MeS group was found at δ: 2.43. In the ^{13}C NMR the expected C≡N resonances were found at δ: 113.8 and δ: 112.5 and the alkenyl carbons were found at δ: 164.9 (α-C) (this was confirmed by a C-H correlation NMR experiment) and δ: 80.9 (β-C). C≡N absorptions were observed at 2228 cm^{-1} in the infrared spectrum and the molecular formula of **10** was confirmed by high resolution mass spectrometry.

The ^{1}H NMR spectrum of **11** shows signals at δ: 9.38 and δ: 7.30 corresponding to the α and β alkenyl protons respectively and the H, H coupling constant of 13.1 Hz indicates a *trans* geometry, which was later confirmed by x-ray studies. In the ^{13}C

NMR the corresponding C atoms were observed at δ: 143.1 and δ: 132.3, these were determined from a C-H correlation NMR experiment. In the infrared spectrum two absorptions were observed at 1489 and 1345 cm^{-1} corresponding to the nitro group. The molecular formula of **11** was confirmed by high resolution mass spectrometry.

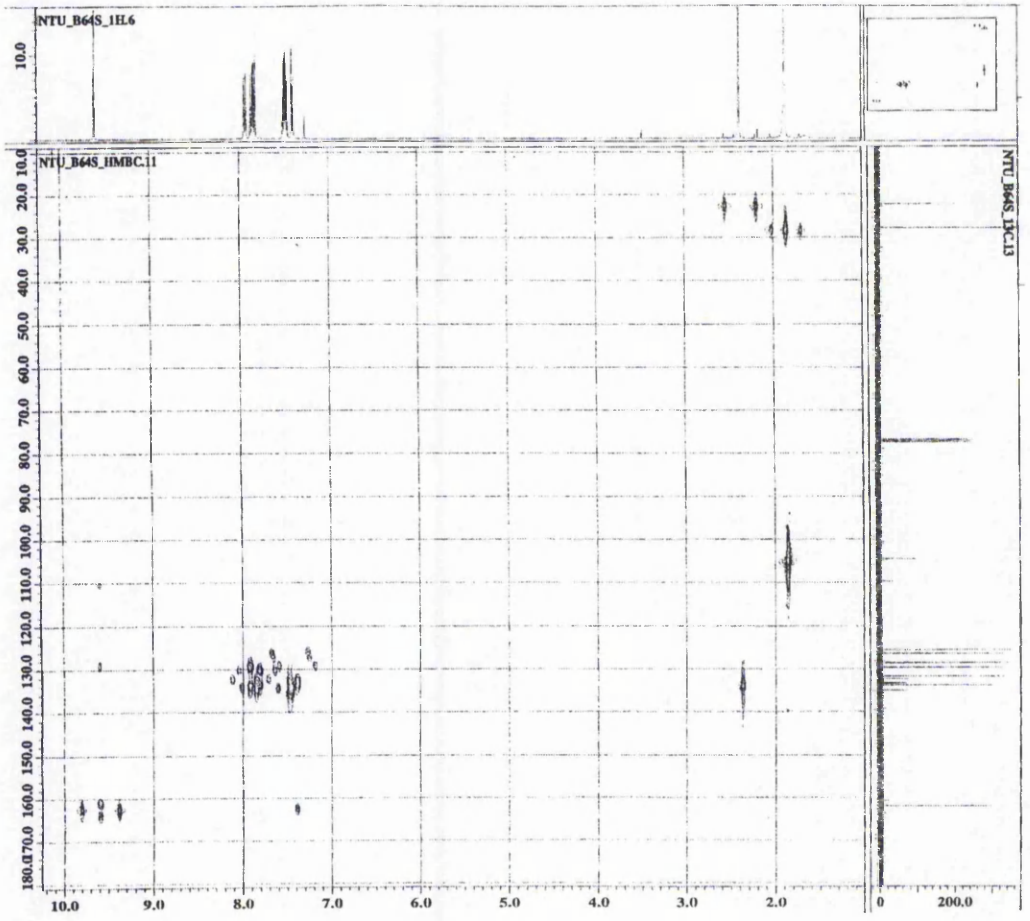

Figure 2 HMBC NMR spectrum of **9**.

The structure of **12** was supported by a signal at δ: 9.55 in the ^{1}H NMR spectrum corresponding to the alkenyl proton and a signal at δ: 3.97 corresponding to the OMe

group. The ^{13}C NMR shows resonances at δ: 163.1 and δ: 115.4 corresponding to the C=O and C≡N carbons respectively. The alkene carbons were observed at δ: 160.5 (α-C) (this was confirmed by a C-H correlation NMR experiment) and δ: 101.2 (β-C). In the infrared spectrum of **12** a C=O absorption was observed at 1728 cm^{-1} and a C≡N absorption at 2222 cm^{-1} and the molecular formula of **12** was confirmed by high resolution mass spectrometry.

Crystals of **9-12** were prepared by slow evaporation of solutions in appropriate solvents. The crystals were observed under a polarising microscope and those which showed uniform extinction of light when rotated through crossed polar lenses were selected and, if necessary, cut to size. X-ray diffraction data was collected at the EPSRC X-ray Crystallography Service in Southampton University at 120 K (**9**, **11** and **12**) and 150 K (**10**) and processed using the SHELXS-97[16] and SHELXL-97[17] programs at the Nottingham Trent University. Results for compounds **9-12** are illustrated in the ORTEP[18] diagrams in Figures 4-7 and the crystal packing diagrams in Section 3.3 towards the end of this chapter. Selected molecular geometric data are given in Table 1.

All four compounds **9-12** show short S----C distances, which are in the range of 2.784(3) – 2.922(1) Å and well within the sum of the van der Waals radii of 3.55 Å for S and C atoms. The closest contact is in compound **9** where the alkene's substituents are lactone ester groups lying coplanar with the alkene, an orientation that allows for full conjugation between the groups. In **10** the S----C distance is 2.850(3) Å, the next

shortest contact and as a result of conjugation of the cylindrical π system of the two nitrile groups with the alkene. The nitro group of **11** lies at an angle of 8.5(8)° to the alkene group, hence the conjugation is only slightly reduced from that of a coplanar arrangement, the S----C distance is 2.895(2) Å. In **12** the alkene group is conjugated with the π system of the nitrile group and the ester carbonyl, which lies at 2.6(5)° to the alkene group. The S----C separation is 2.922(1) Å, which is longer than that in **10**, and to be expected with the smaller electron-withdrawing effect of an ester carbonyl compared to that of a nitrile group.

Compounds **9**, **10** and **12** show a trend of decreasing S----C distance along the series **12→9**, which is the same trend as that observed for the corresponding dimethylamino derivatives. Compound **11** does not fit the trend and will be discussed later. The S----C separations in **9**, **10** and **12** are achieved through distortion of the *peri*-naphthalene framework such that the *peri* bonds bend out of the plane of the naphthalene ring in opposite directions. This is in contrast to that observed in the 8-dimethylamino- and 8-methoxy- 1-carbonyl and 1-alkenyl derivatives where the N----C and O----C separations were achieved through in plane distortions of the *peri* bonds and any out of plane distortions were small. As expected the out of plane distortions in compounds **9**, **10** and **12** follow the same trend as the S----C distances. The largest distortions are observed in compound **12** (0.340(1) and –0.453(2) Å for the S and C11 atoms respectively) where the S----C distance is longest. In this the *peri* groups are bent out of the naphthalene ring plane to increase the distance between the groups, indicating that any (attractive) interaction between the substituents is weak. In compound **9**, however, where the S----C separation is shorter, the out of plane

distortions are much smaller (0.018(4) and –0.074(5) Å for the S and C11 atoms respectively). These distortions are illustrated in the ORTEP[18] diagrams in Figure 3, which show compounds **9**, **10** and **12** oriented such that the viewer looks down the plane of the naphthalene ring.

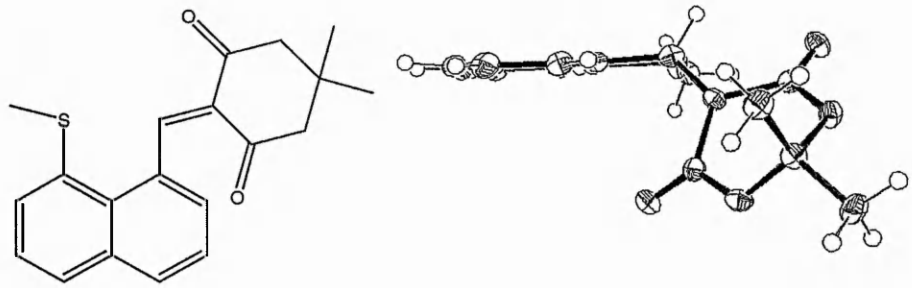

9

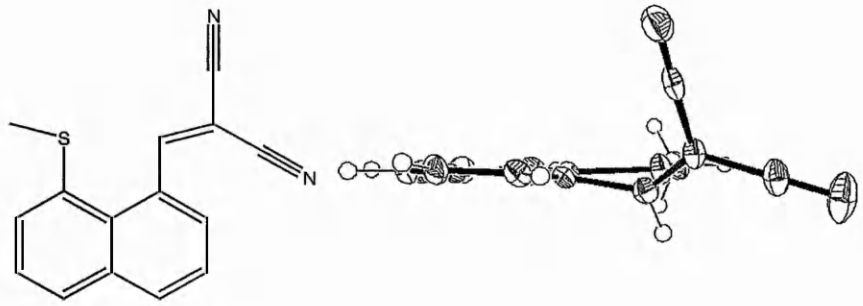

10

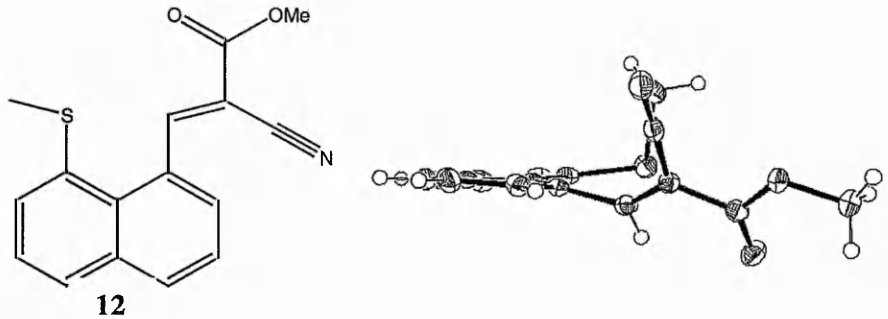

12

Figure 3 Out of plane distortions in compounds **9**, **10** and **12**.

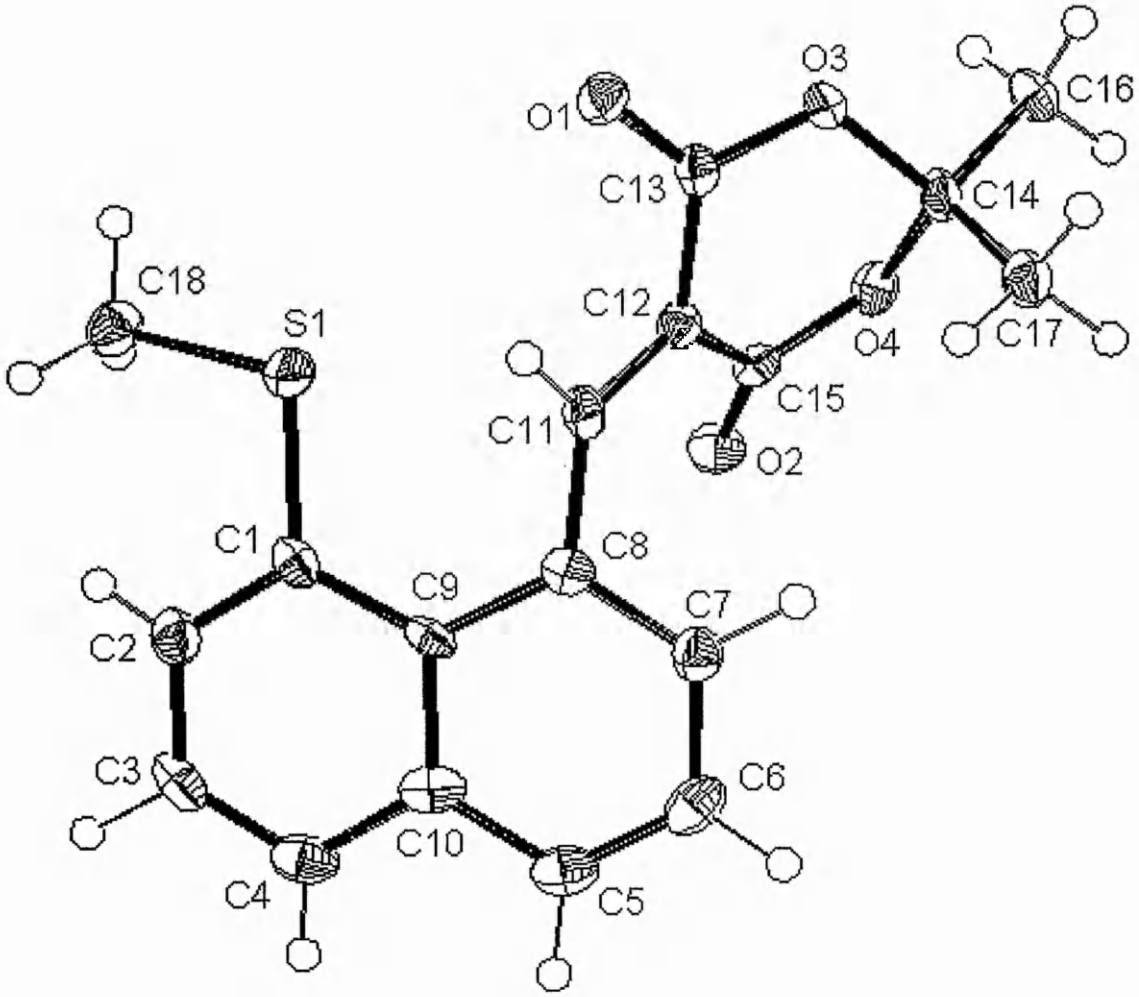

Figure 4 Molecular structure of **9** with anisotropic displacement parameters at the 50% level.

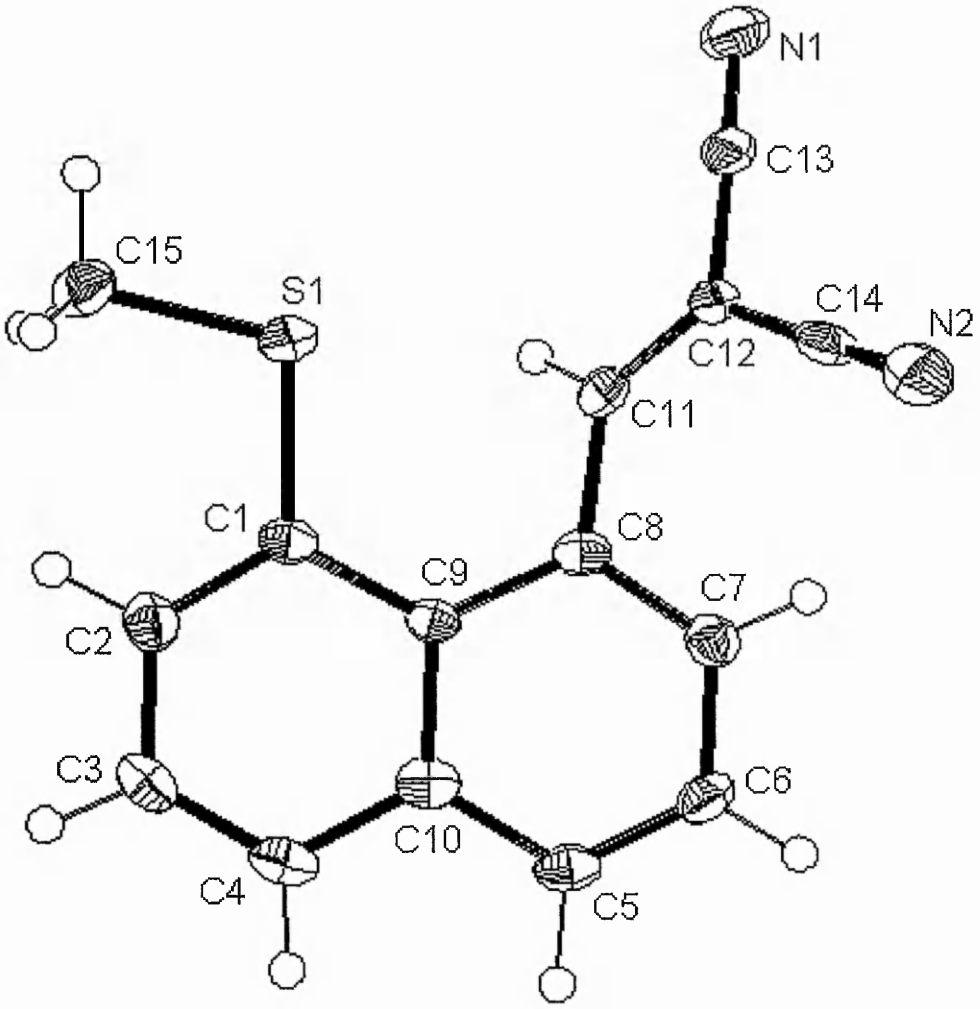

Figure 5 Molecular structure of **10** with anisotropic displacement parameters at the 50% level.

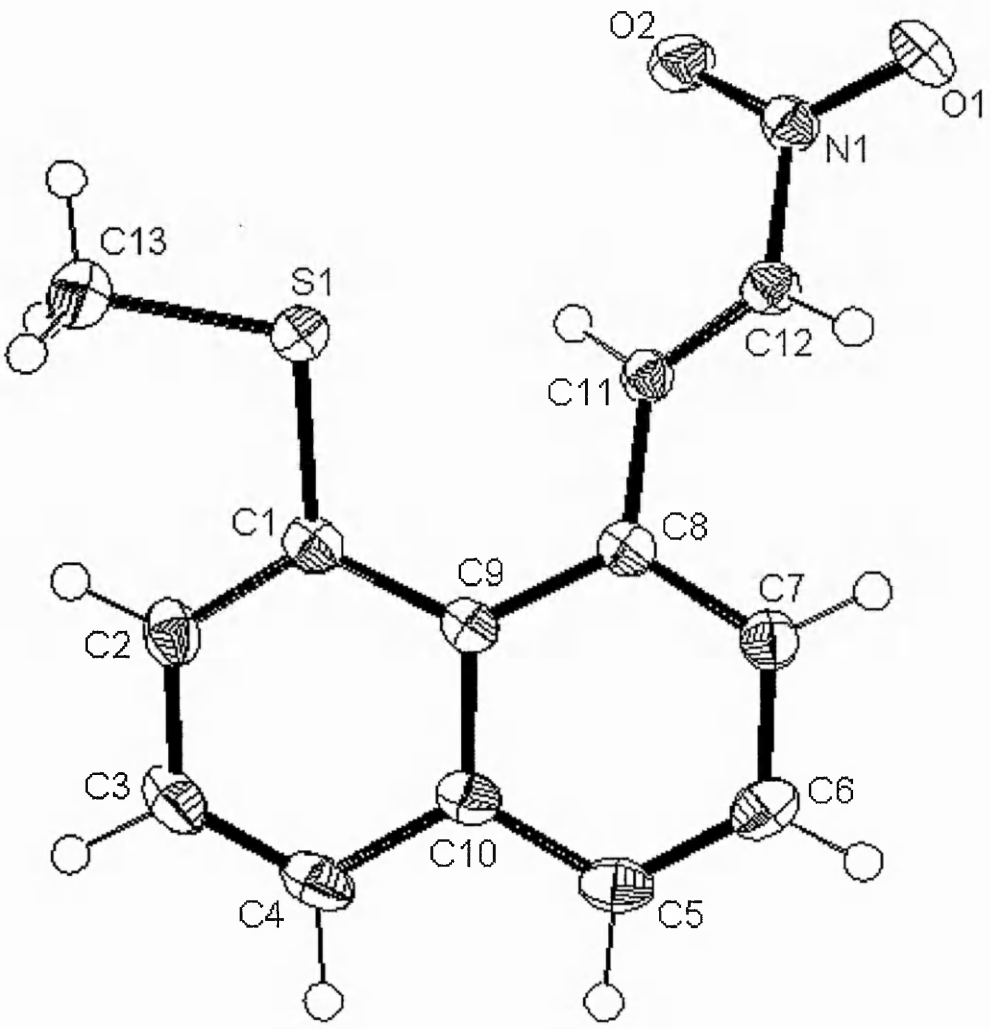

Figure 6 Molecular structure of **11** with anisotropic displacement parameters at the 50% level.

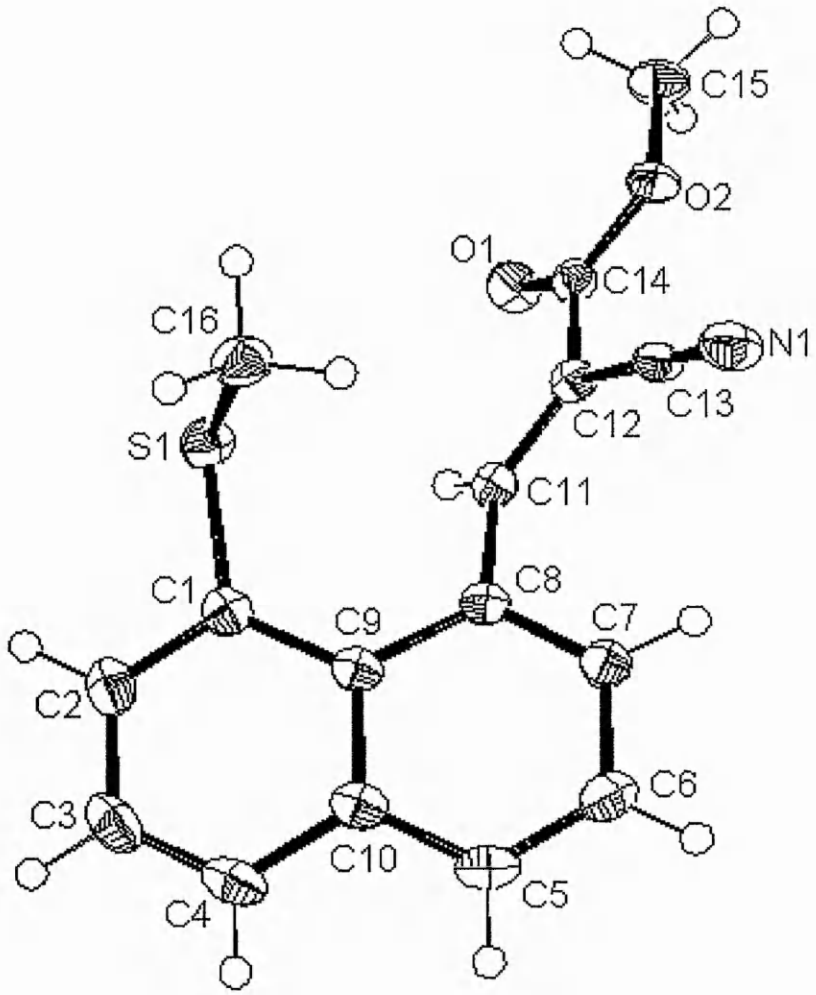

Figure 7 Molecular structure of **12** with anisotropic displacement parameters at the 50% level.

Table 1 Selected molecular geometry for compounds **1**, **9-12** (Å, °)

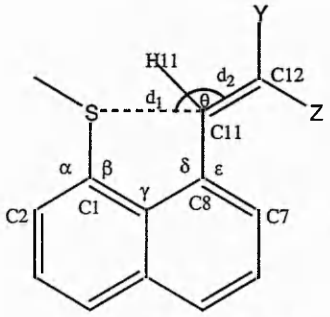

9 Y,Z = -C(C(=O)O)$_2$CMe$_2$
10 Y,Z = CN, CN
11 Y,Z = H, NO_2
12 Y,Z = CN, CO_2Me

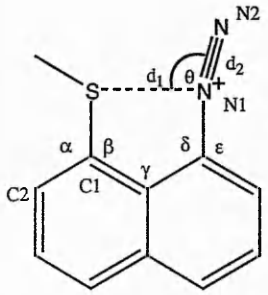

1

T1 = Torsion angle between S-Me bond and C1-C2 bond
T2 = Torsion angle between C11-C12 bond and C7-C8 bond
ΔC / ΔN= Deviation of C11 from the plane of its substituents / deviation of N1 from the line of C8-N1-N2
ΔS = Deviation of S from the naphthalene plane
ΔC '= Deviation of C11or N from the naphthalene plane

	d_1	α	β	γ	δ	ε	ΔC / ΔN
9	2.784(3)	120.9(3)	119.3(2)	125.3(3)	123.4(3)	115.6(3)	0.045(14)
10	2.850(3)	120.9(2)	119.7(2)	125.8(2)	123.5(2)	115.9(2)	0.037(11)
11	2.895(2)	119.6(2)	120.5(1)	125.8(2)	123.0(2)	116.7(2)	0.014(8)
12	2.922(1)	117.0(1)	122.9(1)	124.8(1)	121.7(1)	117.9(1)	0.036(6)
1[1]	2.938(6)	118.9(3)	122.5(3)	127.7(3)	121.7(3)	112.4(3)	9.9(3)
	d_2	ΔS	ΔC'	T1	T2	θ	S----H11
9	1.345(5)	0.018(4)	-0.074(5)	5.9(4)	57.4(4)	114.5(2)	2.63(4)
10	1.338(4)	0.120(3)	-0.257(4)	1.7(3)	48.5(4)	118.2(2)	2.58(2)
11	1.326(3)	0.361(2)	-0.297(3)	5.2(2)	36.4(3)	125.9(1)	2.49(2)
12	1.349(2)	0.340(1)	-0.453(2)	109.1(1)	46.7(2)	115.8(1)	2.71(1)
1[1]	1.079(6)	0.232(6)	-0.196(6)	65.4(3)	-	99.8(3)	-

In compounds **9** and **10** the S-Me bond lies close to the plane of the naphthalene ring as indicated by the torsion angles T1 (Table 1) of 5.9(4) and 1.7(3)°. The exocyclic angles at the Ar-S bond are similar (α and β): 120.9(3) and 119.3(2)° for **9** and 120.9(2) and 119.7(2)° for **10**. It is not possible for the S-Me group to be splayed outwards in order to increase the separation between the *peri* groups due to steric repulsion between the *ortho* hydrogen and the methyl group. Thus to avoid this the group can be displaced out of the plane of the naphthalene ring, as described above, or the group can rotate about the Me-S bond to move the methyl group out of the naphthalene plane. This is observed in compound **12** where the torsion angle T1 is 109.1(1)°. It is possible that in this compound the out of plane distortions, which are the largest of the series, are as large as they can be without causing unfavourable strain of the *peri*-naphthalene framework, but still not enough to achieve the desired S----C separation. Thus rotation of the S-Me group out of the plane of the naphthalene ring allows the group to undergo in-plane displacement towards the *ortho* H atom without encountering steric repulsion. The exocyclic angles α and β of 117.0(1) and 122.9(1)° show that this is indeed what has occurred in this structure.

The pairs of angles at the Ar-sp^2C bond (δ and ε) are very similar for **9** and **10** (123.4(3) and 115.6(3)° (**9**) and 123.5(2) and 115.9(2)° (**10**)) and show that the alkene substituent is splayed outwards by *ca.* 4°. In **12** the alkene is splayed by just 2°, the angles δ and ε are 121.7(1) and 117.9(1)°, thus the outward splaying of the MeS group in this compound has resulted in a smaller in plane distortion of the Ar-sp^2C bond.

As the S----C distance increases in compounds **9**, **10** and **12** the torsion angle of the alkene bond to the naphthalene ring (T2) decreases from 57.4(4)° in **9** to 46.7(2)° in **12**. Thus the alkene lies at a greater angle to the plane of the naphthalene ring as the *peri* substituents are closer to each other. It is possible that when the S----C interaction is not so strong as in **12**, the alkene moves back to lie closer to the plane of the naphthalene ring so that it can conjugate with the aromatic π system, although it is restricted in how close it can get due to steric repulsion between the alkene's terminal substituent which lies *cis* to the naphthalene ring and close to an *ortho* hydrogen.

Compound **11** exhibits the same distortion pattern as observed in **9** and **10**. The S and C11 atoms are displaced out of the plane of the naphthalene ring by 0.361(2) and 0.297(3) Å, and the S-Me group lies approximately in the naphthalene plane, the torsion angle T1 is 5.2(2)°. The in-plane distortions are very slightly different to those in **9** and **10**. The MeS group is displaced towards the *ortho* H atom by *ca.* 0.5°, rather than away from it by *ca.* 0.5°, and the alkenyl group is displaced outward by *ca.* 3° rather than *ca.* 4°.

The feature that separates **11** from the other three compounds is the fact that it only has one terminal alkene substituent whereas the others have two. This allows the alkene group in **11** to lie much closer to the plane of the naphthalene ring, the torsion angle T2 is only 36.4(3)° while in **9**, **10** and **12** steric repulsion from the *ortho* hydrogen as described above forces a larger torsion angle (46.7 – 57.4°) in these structures. This has been observed previously in the 8-methoxy-1-naphthaldehyde derivatives **13** and **14** (shown below).[19] In these structures the carbonyl bond makes a

torsion angle with the naphthalene ring of only 30.8° in **13** and 38.5° in **14**, thus the methoxy O atom is not directed at a face of the carbonyl group. In alkene **11** this results in a short contact between the S atom and the alkene's α-H atom of 2.49(2) Å, which may have some hydrogen bonding character, since the nitro group exerts an electron-withdrawing effect on the alkene. Compound **15**, the dimethylamino analogue of **11** has a significantly larger torsion angle between the C=C bond and the naphthalene ring of 50.5°[20], however this is smaller than the corresponding angles for the other dimethylamino compounds in this series, which lie in the range 54.4-65.5°.[3,4] In **15** the N----C separation is 2.642 Å, which is the longest in the series with the exception of the derivative in which the alkene's terminal substituent are benzoyl groups and the N----C separation is 2.679 Å. **15** and **11** both show a reduced interaction compared to other compounds in their respective series.

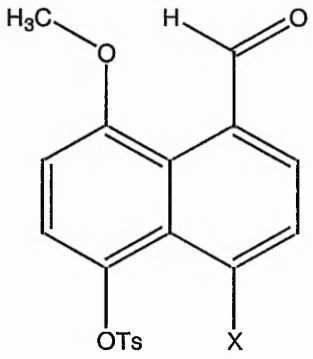

13 X = OMe
14 X = H

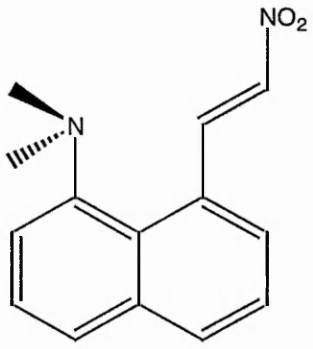

15

All four compounds **9**-**12** show partial pyramidalisation of the alkene's α-carbon (ΔC), the three compounds **9**, **10** and **12** show a trend of increasing ΔC (0.036(6) –

0.045(14) Å) along with decreasing S----C distance, while once again **11** does not fit the trend, the alkene's α-C atom is displaced from the plane of its substituents by just 0.014(8) Å. However, it has already been established (Section 2.3) that such pyramidalisations are not necessarily a feature of attractive interactions and care should be taken in their interpretation. Another common feature in these structures is an obtuse S----C=C angle (α), compounds **9**, **10** and **12** have similar α angles of 114.5(2), 118.2(2) and 115.8(1)°, while that for **11** is much larger 125.9(1)° and a likely result of the much smaller torsion angle T2.

It might be expected that for compounds **9-12** the S----C separation may correlate well with certain physical properties related to the electron-withdrawing power of the terminal alkene substituents. Two such properties are the pKa of the methylene compound (H_2CXY) used in the knoevenagel condensations and the infrared absorption of the alkene bond, the results are shown in Figures 8 and 9.

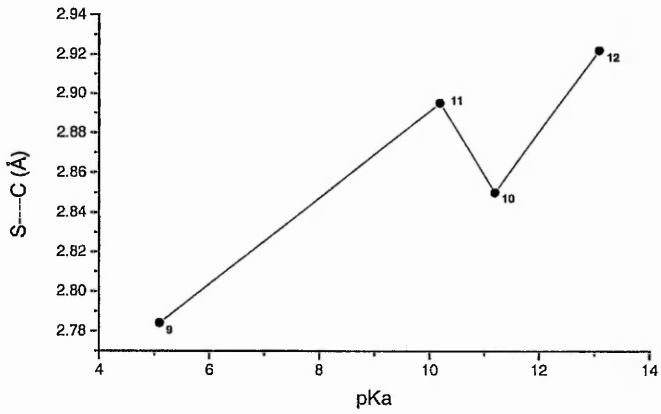

Figure 8 Variation of S----C distance with pKa of the corresponding methylene compound for **9-12**

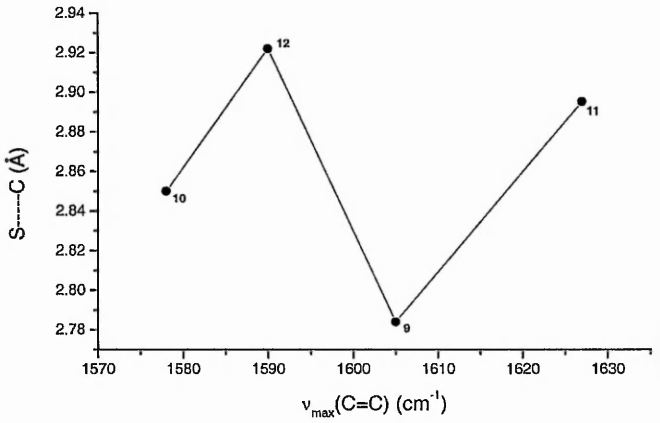

Figure 9 Variation of N----C distance with ν_{max} (C=C) for **9-12**

It might be expected that the S----C separation would decrease with decreasing pKa of the methylene compound, this indeed is the general trend, however the nitro alkene does not fit the pattern. The pKa of nitromethane is 10.2, which is slightly more acidic than malononitrile (pKa = 11.2), however the S----C distance in **11** is greater than that of **10** (2.895(2) Å *cf.* 2.850(3) Å). This appears to be another example of how **11** does not fit the general trends found for compounds **9**, **10** and **12**. Figure 9 shows that there is no apparent correlation between the infrared absorption of the alkene bond and the S----C separation. One might expect that as the S----C separation decreases the alkene bond would weaken due to electron donation from the sulfur atom's lone pair to the antibonding orbital of the C=C bond. This, however, is not observed. Thus it must be concluded that the interactions in **9-12** are not of sufficient strength to overcome the substituent effects on the alkene bond.

Compound **12** differs from **9** and **10** in the orientation of the SMe group to the alkene. In **9** and **10** the S----C vector representing an interaction between the functional groups lies roughly in the Me-S-C plane. In **12** this vector lies roughly perpendicular

to the Me-S-C plane. Nyburg has determined from intermolecular S----S contacts[21] that the bonded S atom is not spherical, but rather is larger perpendicular to the C-S bond than along its extension (the effective radii were determined to be 2.03 and 1.60 Å). This could be due to larger spatial distribution of the p lone pair. Thus in the series **9**, **10**, **12** as the SMe group leaves the plane of the naphthalene ring in **12**, it presents a larger region of the S atom to the alkene. This will act further to increase the S----C=C separation.

The question as to whether or not these S----C interactions are attractive in nature remains. It is helpful to compare the S---C distances with the corresponding O----C and N----C distances in the methoxy and dimethylamino analogues (Table 2). The dimethylamino is the most nucleophilic group, the short N----C distance of 2.413(2) Å in the dicyanoalkene[3] and the N-C bond of length 1.651(3) Å in the Meldrum's acid derivative[3] reflect this. Sulfur is considered to be of greater nucleophilicity than oxygen, but this is not apparent from comparing the S----C and O----C separations, e.g. the differences in S----C and O----C separations between the Meldrum's acid derivative[4] and the dicyanoalkene[4] are 0.066 and 0.061 Å for each series respectively, while that for the dimethylamino analogues is 0.762 Å. The difference in S----C separations between the dicyano alkene and the alkene substituted by a cyano group and a methyl ester group is 0.07 Å, while that for the dimethylamino analogues is 0.12 Å, the structure of the corresponding methoxy derivative has been not measured. This would suggest that the sensitivity of the MeS group towards the nature of the alkene is much lower than that of the Me_2N group, and closer to that of the MeO group, which

has already been established as quite insensitive. However, it is not possible to reach final conclusions based on so few directly comparable structures.

Table 2 N----C, O----C and S----C distances in alkenyl *peri*-naphthalenes

	Alkene's terminal substituents		
Nucleophilic group	$-C(C(=O)O)_2CMe_2$	CN, CN	CN, CO_2Me
Me_2N	1.651(3)[3]	2.413(2)[3]	2.531(2)[3]
MeO	2.550(2)[4]	2.611(1)[4]	-
MeS	2.784(3)	2.850(3)	2.922(1)

The nature of N----sp^2C interactions in certain carbonyl derivatives was concluded to be mainly steric from comparing N---C and O----C distances in comparable structures and taking into account the effective radii of bonded N and O atoms in *peri*-naphthalenes (Section 2.2). Compound **16** can be used to estimate the effective radii of a bonded sulfur atom, the S----S separation is 2.93 Å (an average of the two independent molecules of **16** in the unit cell), thus the effective bonded radius of S is estimated to be 1.46 Å.[22] The effective bonded radius of the O atom in *peri* naphthalenes has already been estimated as 1.25 Å, hence the difference in the effective radii of bonded sulfur and oxygen atoms is *ca.* 0.21 Å. The values of the parameter [d(MeO----X) + 0.21 – d(MeS----X)] (equation 1) for the Meldrum's acid and dicyano derivatives is –0.024 and -0.029 Å. These values are extremely small,

which suggests there is not much difference in the nature of the interactions of the methoxy and methylthio groups with sp^2C atoms.

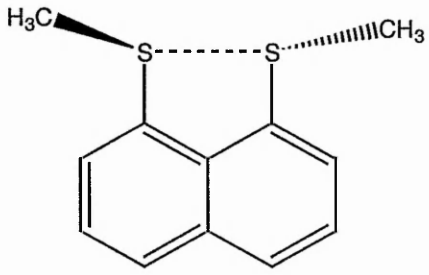

16

The effective bonded radius estimated using **16** is only a rough guide and by no means conclusive as the S----S separation is based on just one structure. It has already been mentioned that the S atom is not spherical, hence the S----S separation may be a function of the orientation of the SMe group. The torsion angles of the S-Me bond with the naphthalene ring in the two independent molecules of **16** are 33.74 and 17.84°, hence are not directly comparable with any of the four structures **9-12** (the corresponding torsion angles in **9-12** are 1.7-5.9 and 109.1°). Thus the difference in the effective radii of bonded sulfur and oxygen atoms may, therefore, be misleading, however, if anything it is an overestimate of the S----S contact distance for a hypothetical conformation of **16**, in which the methyl groups lie in the plane of the aromatic ring. Considering the application of equation 1, a smaller S----S separation would suggest an even less attractive interaction. In **12**, where the S-Me torsion angle with the aromatic ring is larger (109.1°) and the sulfur's p lone pair is involved in the peri-interaction, the effective radius of the sulfur atom will also be larger, hence a structure of type **16**, but with larger torsion angles would be useful to

estimate the radius.

Future work to obtain more data on the interactions of the p lone pair would help to determine the nature of these interactions, this may be achieved by the presence of a larger substituent on the S atom, e.g. the ^{t}Bu group which would be forced to lie out of the plane of the naphthalene ring to avoid steric repulsion from the *ortho* hydrogen. Other future work may involve analysis of the experimental charge density, determined from accurate low temperature x-ray diffraction data, using Bader's 'Theory of Atoms in Molecules'.[23] This characterises bonding interactions by saddle points in the total electron density, hence the presence or absence of attractive S----C=C interactions in compounds **9 – 12** may be determined from the presence or absence of saddle points between the two groups.

3.3 Crystal Packing

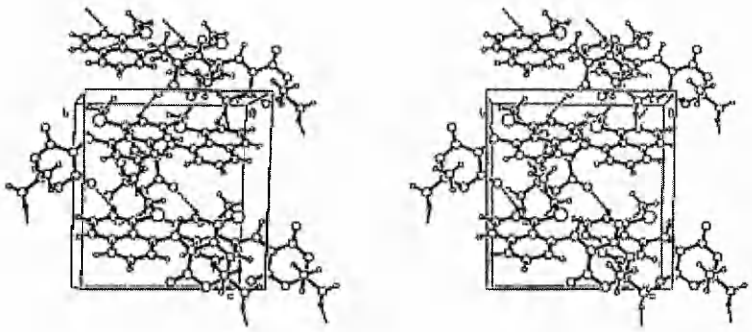

(a)

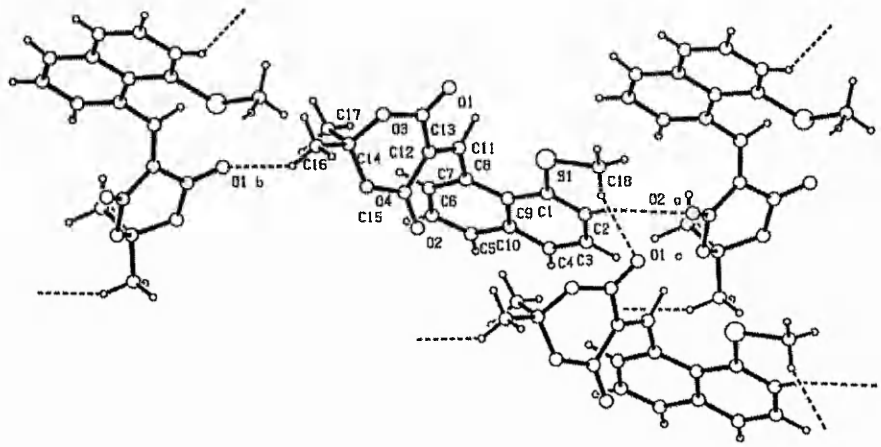

(b)

Figure 10 Crystal packing of **9** at 120 K (a) in the unit cell and (b) intermolecular contacts.

The crystal packing of **9** involves several intermolecular hydrogen bonds. There are short contacts between a methyl hydrogen (C(18)-H) and a carbonyl O(1) atom (2.33(3) Å). An aromatic hydrogen (C(2)-H) is involved in a hydrogen bond to a carbonyl O(2) atom of another molecule (2.59(4) Å) and there is also a contact between a hydrogen atom of the meldrum's acid ring methyl group (C(16)-H) and a carbonyl O(1) atom (2.55(4) Å).

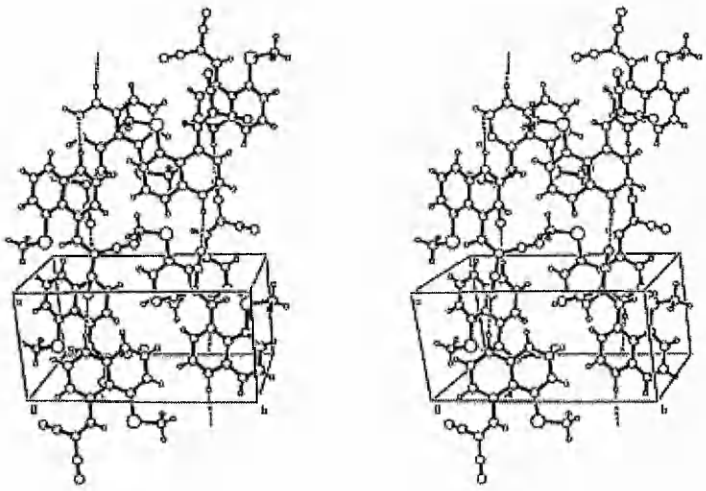

(a)

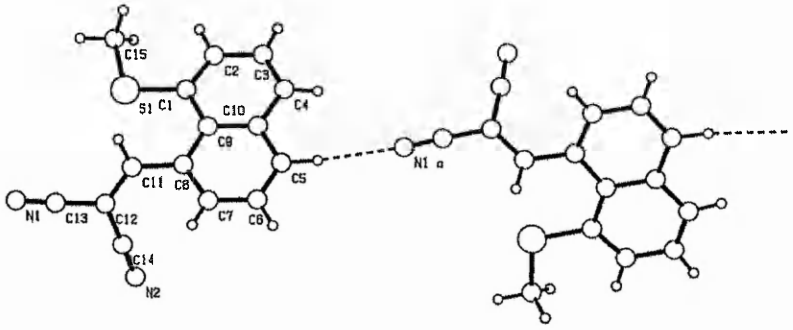

(b)

Figure 11 Crystal packing of **10** at 150 K (a) in the unit cell and (b) intermolecular contacts.

There is one intermolecular contact in the crystal packing of **10**, as shown above, between an aromatic hydrogen (C(5)-H) and a nitrile N(1) atom (2.49(3) Å).

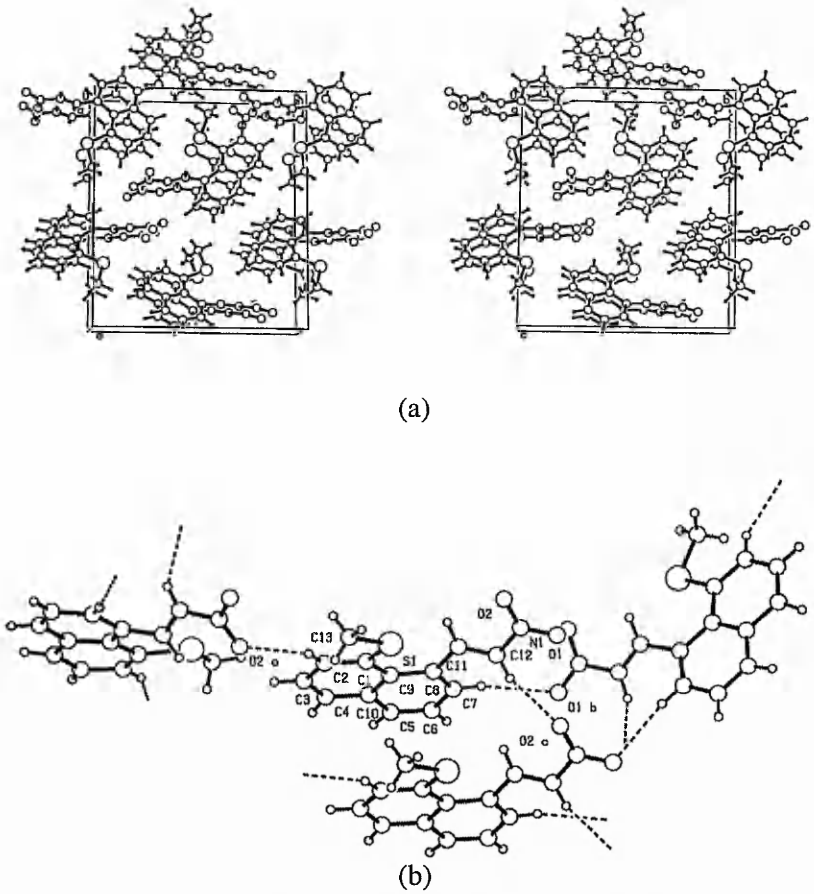

Figure 12 Crystal packing of **11** at 120 K (a) in the unit cell and (b) intermolecular contacts.

In the crystal packing of **11** each molecule makes contacts with three others. An alkenyl hydrogen (C(12)-H) is hydrogen bonded to a nitro O(2) atom (2.43(2) Å) and there are two aromatic C-H-----nitro O contacts between C(7)-H and O(1) and between C(2)-H and O(2) (2.56(2) and 2.50(2) Å).

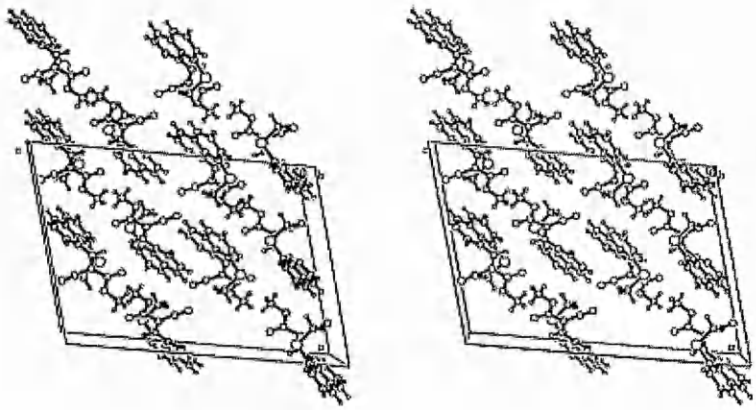

Figure 13 Crystal packing of **12** at 120 K.

There are no intermolecular contacts in the crystal packing of **12**.

3.4 Experimental

Preparation of 8-Carboxynaphth-1-yl mercury (II)[14] 3

A suspension of naphthalic anhydride **2** (10 g, 50 mmol) in 0.5M NaOH (350 ml) was heated until the solid dissolved. The excess base was neutralised with glacial acetic acid (5 ml). To this was added a solution of $Hg(OAc)_2$ (16.25 g, 51 mmol) in a mixture of glacial acetic acid (3 ml) and water (50 ml), which was prepared by heating. The mixture was refluxed for 30 min. before glacial acetic acid (9 ml) was added and the mixture refluxed for 48 h. The mixture was allowed to cool to room temperature and filtered at the pump. The wet, solid material was washed with water and dried *in vacuo* at 105°C to constant weight to yield the off-white solid product **3** which was insoluble in all solvents tested (17.2 g, 92%).

Preparation of 8-Iodo-1-naphthalic acid[14] 4

A mixture of the mercury compound **3** (19 g, 51 mmol) and KI (34.7 g, 209 mmol) in water (190 ml) was stirred at room temperature. To this was added I_2 (13.4 g, 53 mmol) and the mixture was refluxed overnight. The mixture was allowed to cool to room temperature and filtered. A solution of sodium thiosulfate (9.6 g, 38 mmol) in water (38 ml) was added and the solution was acidified with 2M HCl. The resulting precipitate was collected by vacuum filtration, dried and purified by dissolving in hot acetone and treating with activated charcoal to yield the product **4** as a white solid

(10.5 g, 69%), m.p. 150-155°C (lit. m.p. 163.5-164.5 °C); ^{1}H NMR (CD_3OD) δ: 8.23 (1H, dd, J = 7.4, 1.2 Hz, Ar-H_1), 7.91 (2H, d, J = 8.2 Hz, Ar-H_2), 7.72 (1H, d, J = 6.9 Hz, Ar-H_1), 7.48 (1H, t, J = 7.2 Hz, Ar-H_1), 7.18 (1H, t, J = 7.9 Hz, Ar-H_1), 5.04 (1H, br.s, CO_2H); ^{13}C NMR (CD_3OD) δ: 173.5 (CO_2H), 142.9, 136.6, 132.8, 132.1, 130.6, 129.6, 128.3, 126.2, 93.3 (Ar-C_{10}, one peak is doubly degenerate).

Preparation of 2H-Naphtho[1,8-bc]thiophen-2-one[15] **5**

8-Iodo-1-naphthalic acid **4** (27.4 g, 92 mmol) and activated Cu (0.93 g, 14.5 mmol) were added to a stirred solution of 3-mercaptopropionic acid (24 ml, 277 mmol) and KOH (27.1 g, 48 mmol) in water (130 ml), under nitrogen, at room temperature. After 5 h at reflux a solution of KOH (27.1 g, 48 mmol) in water (130 ml) was added and the mixture was refluxed for a further 3 h. Water (80 ml) was added and the mixture was filtered. The filtrate was acidified with 2M HCl and the solid material was collected at the pump. The wet solid was dried *in vacuo* to yield the product **5** as a yellow/green solid (16.0 g, 94%), m.p. 134-140 °C (lit. m.p. 145-146 °C); ^{1}H NMR ($CDCl_3$ + DMSO-d_6) δ: 8.22 (1H, d, J = 8.2 Hz, Ar-H_1), 8.15 (1H, d, J = 7.2 Hz, Ar-H_1), 7.90-7.85 (1H, m, Ar-H_1), 7.81 (1H, t, J = 7.7 Hz, Ar-H_1), 7.67-7.61 (2H, m, Ar-H_2); ^{13}C NMR ($CDCl_3$ + DMSO-d_6) δ: 206.8 (C=O), 133.7, 133.6, 133.2, 131.9 131.3, 128.6, 128.2, 125.5, 125.3, 122.8 (Ar-C_{10}).

Preparation of Methyl 8-Methylthio-1-naphthoate **6**

Powdered KOH (0.5 g, 9 mmol) was stirred in DMSO (2 ml) and after 5 min. the thiolactone **5** (0.14 g.0.75 mmol) was added followed by MeI (0.2 ml, 3 mmol). The resulting dark green mixture gradually lightened to a yellow colour and the reaction was complete after 40 min. The mixture was poured on to water (20 ml) and extracted with CH_2Cl_2. The organic extracts were washed with water and brine, dried ($MgSO_4$) and evaporated to yield a yellow oil, which was purified by flash chromatography on silica gel (cyclohexane:ether, 3:1) to yield the product **6** as a colourless oil (0.13 g, 74%); ν_{max}/cm^{-1} (liquid film): 2922, 2848, 1724, 1498, 1431, 1276, 1200, 1147, 1064, 1019, 963, 826, 769; ^1H NMR ($CDCl_3$) δ: 7.88 (1H, dd, J = 8.2, 1.2 Hz, Ar-H_1), 7.77-7.73 (2H, m, Ar-H_2), 7.60 (1H, d, J = 6.9 Hz, Ar-H_1), 7.48-7.41 (2H, m, Ar-H_2), 3.96 (3H, s, OCH_3), 2.41 (3H, s, SCH_3); ^{13}C NMR ($CDCl_3$) δ: 171.8 (*C*=O), 134.6, 134.6, 132.7, 131.6, 131.3, 130.5, 128.3, 127.7, 126.3, 124.9 (Ar-C_{10}), 52.7 (O*C*H_3), 21.5 (S*C*H_3); HRMS (ES): Found: 250.0909 $(M+NH_4)^+$, $C_{13}H_{12}O_2S$ requires: 250.0902 $(M+NH_4)^+$.

Preparation of 1-Hydroxymethyl-8-methylthionaphthalene **7**

Diisobutyl aluminium hydride (1.5M solution in toluene, 62 ml, 92 mmol) was added at -78°C to a stirred solution of methyl 8-methylthionaphthoate **6** (9.75 g, 42 mmol) in dry toluene (100 ml), under nitrogen. The mixture was stirred at this temperature for

1 h, allowed to warm to room temperature and stirred for 30 min. The mixture was quenched at -78°C with 1M HCl (62 ml) and warmed to room temperature. The mixture was transferred to a separatory funnel and washed with 1M HCl. The organic solution was dried ($MgSO_4$) and evaporated. The crude oil was purified by flash chromatography on silica gel (cyclohexane:ether, 3:1) to yield a yellow solid, which was recrystallised from hexane to yield the product **7** as a white solid (6.6g, 77%), m.p. 52-55°C; ν_{max}/cm^{-1} (KBr): 3330, 2918, 1654, 1566, 1498, 1425, 1358, 1318, 1206, 1169, 1092, 1056, 995, 803, 760; ^1H NMR ($CDCl_3$) δ: 7.73 (1H, d, J = 7.9 Hz, Ar-H_1), 7.65 (1H, dd, J = 7.9, 1.5 Hz, Ar-H_1), 7.50 (1H, dd, J = 6.9, 1.5 Hz, Ar-H_1), 7.44 (1H, dd, J = 7.5, 1.5 Hz, Ar-H_1), 7.38-7.31 (2H, m, Ar-H_2), 5.21 (2H, br. s, CH_2OH), 3.45 (1H, br. s, O*H*), 2.51 (3H, s, SCH_3); 137.2, 135.7, 133.9, 131.1, 130.3, 130.1, 128.1, 127.7, 125.7, 125.1 (Ar-C_{10}), 65.9 (CH_2OH), 19.4 (SCH_3); HRMS (ES): Found: 222.0945 $(M+NH_4)^+$, $C_{12}H_{12}OS$ requires: 222.0953 $(M+NH_4)^+$.

Preparation of 8-Methylthio-1-naphthaldehyde **8**

A solution of dry DMSO (2.75 g, 35.5 mmol) in CH_2Cl_2 (10 ml) was added at -78°C to a stirred solution of oxalyl chloride (1.55 ml, 17.8 mmol) in CH_2Cl_2 (100 ml) under nitrogen. After 2 min. a solution of the alcohol **7** (3.3 g, 16 mmol) in CH_2Cl_2 (15 ml) was added. After 20 min. Et_3N (11.5 ml) was added and the mixture was stirred for a further 5 min. The mixture was transferred to a separatory funnel and the aqueous phase was extracted with CH_2Cl_2. The combined organic extracts were sequentially washed with 2M HCl, saturated $NaHCO_3$ and brine, dried ($MgSO_4$) and evaporated to

yield the product as a brown oil that solidified on standing (2.94 g, 90%), m.p. 40-43 °C (lit. m.p. 43-44 °C)[14]; ^{1}H NMR ($CDCl_3$) δ: 11.10 (1H, s, C*H*O), 7.86 (1H, dd, J = 8.2, 1.2 Hz, Ar-H_1), 7.72-7.64 (3H, m, Ar-H_3), 7.45-7.33 (2H, m, Ar-H_2), 2.34 (3H, s, SCH_3); ^{13}C NMR ($CDCl_3$) δ: 191.9 (*C*=O), 136.8, 134.2, 133.3, 132.8, 131.6, 131.1, 128.1, 128.0, 126.0, 125.1 (Ar-C_{10}), 20.3 (S*C*H$_3$).

Preparation of 2,2-Dimethyl-5-(8-methylthionaphthyl-1-methylidene)-1,3-dioxane-4,6-dione **9**

Meldrum's acid (0.54 g, 3.75 mmol) and ethylenediamine diacetate (0.05 g, 0.3 mmol) were added to a stirred solution of the aldehyde **8** (0.5 g, 2.5 mmol) in dry methanol (7 ml) under nitrogen. After stirring for 1 h. at room temperature a precipitate was obtained, which was collected by vacuum filtration and washed with methanol to yield the product **9** as a yellow solid (0.34 g). The filtrate was evaporated and the residue was purified by flash chromatography on silica gel (cyclohexane:ether, 1:1) to yield further product **9** as a yellow solid (0.16 g), total yield (0.50 g, 61%), m.p. 136-138°C; ν_{max}/cm^{-1} (KBr): 1734, 1605, 1559, 1396, 1352, 1280, 1193, 1020, 926, 823, 762; λ_{max}(MeOH)/nm: 225.1, 306.3, 324.0; ^{1}H NMR ($CDCl_3$) δ: 9.58 (1H, s, =C*H*), 7.90 (1H, d, J = 8.2 Hz, Ar-H_1), 7.87-7.81 (2H, m, Ar-H_2), 7.49-7.37 (3H, m, Ar-H_3), 2.36 (3H, s, SCH_3), 1.85 (6H, s, C(CH_3)$_2$); ^{13}C NMR ($CDCl_3$) δ: 163.0 (*C*=O), 161.9 (=*C*H)[§], 160.6 (*C*=O), 135.0, 133.8, 133.4, 133.2, 132.3, 131.7, 129.6, 128.5, 126.4, 125.5 (Ar-C_{10}) 109.6 (=*C*(CO)$_2$)*, 105.5

($C(CH_3)_2$)*, 27.8 (SCH_3), 22.1 ($C(CH_3)_2$); HRMS (EI): Found: 328.0777, $C_{18}H_{16}O_4S$ requires: 328.0769. (* Confirmed by HMBC, §Confirmed by C-H correlation).

Crystal data for **9**: $C_{18}H_{16}O_4S$, Mr = 328.38, monoclinic, a = 10.6181(5), b = 11.5922(5), c = 13.0123(6) Å, β = 105.599(2)°, V = 1542.65 Å^3, Z = 4, C2/c, D_c = 1.41 gcm^{-3}, μ (MoKα) = 0.23 mm^{-1}, 2679 unique reflections, 2468 with $F_o > 4\sigma(F_o)$, R = 0.039. Full data available on the crystallographic information file on the disk provided.

Preparation of 1,1-Dicyano-2-(8-methylthionaphth-1-yl)ethene **10**

Malononitrile (0.25 g, 3.75 mmol) and ethylenediamine diacetate (0.05 g, 0.3 mmol) were added to a stirred solution of the aldehyde **8** (0.5 g, 2.5 mmol) in dry methanol (7 ml) under nitrogen. The mixture was stirred at room temperature overnight. The resulting precipitate was collected by vacuum filtration and washed with methanol to yield the product as a yellow solid (0.06 g). The filtrate was evaporated and the residue purified by flash chromatography on silica gel (cyclohexane:ether, 5:1) to yield the product **10** as a yellow solid (0.4 g), total yield (0.46 g, 75%), m.p. 114-116°C; ν_{max}/cm^{-1} (KBr): 3027, 2228, 1578, 1493, 1431, 1348, 1206, 914, 833, 798, 764; λ_{max}(MeOH)/nm: 221.7, 298.1; ^{1}H NMR ($CDCl_3$) δ: 9.27 (1H, s, 2-*H*), 8.02 (1H, d, J = 7.9 Hz, Ar-H_1), 7.88-7.80 (2H, m, Ar-H_2), 7.67-7.49 (3H, m, Ar-H_3), 2.43 (3H, s, SCH_3); ^{13}C NMR δ: 164.9 (2-*C*)*, 135.2, 133.8, 133.6, 132.1, 130.2, 129.7, 129.4, 127.0, 125.7 (Ar-C_{10}, one peak is doubly degenerate), 113.8 (*C*N), 112.5 (*C*N), 80.9

(1-*C*), 21.5 (S*C*H$_3$); HRMS (EI): Found: 250.0564, $C_{15}H_{10}N_2S$ requires: 250.0565. (* Confirmed by C-H correlation).

Crystal data for **10**: $C_{15}H_{10}N_2S$, Mr = 250.32, monoclinic, a = 7.5941(4), b = 13.6436(9), c = 12.2968(8) Å, β = 107.972(3)°, V = 1211.92 Å^3, Z = 4, $P2_1/c$, D_c = 1.37 gcm^{-3}, μ (MoKα) = 0.25 mm^{-1}, 2916 unique reflections, 1583 with $F_o > 4\sigma(F_o)$, R = 0.061. Full data available on the crystallographic information file on the disk provided.

Preparation of *E*-2-(8-Methylthionaphth-1-yl)-1-nitroethene **11**

Nitromethane (0.08 ml, 1.5 mmol) and ethylenediamine diacetate (0.018 g, 0.09 mmol) were added to a stirred solution of the aldehyde **8** (0.2 g, 1.0 mmol) in dry methanol (3 ml) under nitrogen. After stirring for several hours at room temperature tlc (cyclohexane:ether,5:1) showed just starting materials were present so piperidine (2 drops) was added and the mixture was stirred overnight. The methanol was evaporated and the residue purified by flash chromatography on silica gel (cyclohexane:ether, 5:1) to yield the product **11** as an orange solid (0.03 g, 12%, m.p. 73-78°C; ν_{max}/cm^{-1} (KBr): 1627, 1489, 1345, 962, 823, 763, 737; λ_{max}(MeOH)/nm: 223.2, 296.1; ^{1}H NMR ($CDCl_3$) δ: 9.38 (1H, d, J = 13.1 Hz, 2-*H*), 7.92 (1H, dd, J = 7.4, 2.2 Hz, Ar-*H*$_1$), 7.76 (1H, dd, J = 8.2, 1.2 Hz, Ar-*H*$_1$), 7.64 (1H, dd, J = 7.4, 1.2 Hz, Ar-*H*$_1$), 7.50-7.42 (3H, m, Ar-*H*$_3$), 7.30 (1H, d, J = 13.1 Hz, 1-*H*), 2.46 (3H, s, S*C*H$_3$); ^{13}C NMR ($CDCl_3$) δ: 143.1 (2-*C*)*, 135.2, 135.1 (Ar-*C*$_2$), 132.3 (1-*C*)*, 131.7,

130.2, 129.3, 129.0, 128.1, 126.5, 125.5 (Ar-C_8' one peak is doubly degenerate), 20.3 (SCH_3); HRMS (ES): Found: 246.0591 $(M+H)^+$, $C_{13}H_{11}NO_2S$ requires: 246.0589 $(M+H)^+$. (* Confirmed by C-H correlation).

Crystal data for **11**: $C_{13}H_{11}NO_2S$, Mr = 245.30, orthorhombic, a = 4.7575(2), b = 14.4311(7), c = 16.5082(10) Å, V = 1133.39 $Å^3$, Z = 8, $P2_12_12_1$, D_c = 1.44 gcm^{-3}, μ (MoKα) = 0.27 mm^{-1}, 2540 unique reflections, 2201 with $F_o > 4\sigma(F_o)$, R = 0.038. Full data available on the crystallographic information file on the disk provided.

Preparation of Ethyl *E*-2-Cyano-3-(8-methylthionaphth-1-yl)-1-propenoate **12**

Methyl cyanoacetate (0.15 g, 1.5 mmol) and ethylenediamine diacetate (0.018 g, 0.09 mmol) were added to a stirred solution of the aldehyde **8** (0.2 g, 1.0 mmol) in dry methanol (3 ml) under nitrogen. After stirring for 1 h. at room temperature a precipitate was obtained, which was collected by vacuum filtration and washed with methanol to yield the product **12** as a yellow solid (0.14 g, 51%), m.p. 106-108°C; ν_{max}/cm^{-1} (KBr): 2944, 2222, 1728, 1590, 1429, 1274, 1239, 1088, 830, 757; λ_{max}(MeOH)/nm: 223.2, 294.8; ^1H NMR ($CDCl_3$) δ: 9.55 (1H, s, 3-*H*), 7.96 (1H, d, J = 8.2 Hz, Ar-H_1), 7.81 (1H, dd, J = 8.2, 1.0 Hz, Ar-H_1), 7.75-7.69 (2H, m, Ar-H_2), 7.56-7.45 (2H, m, Ar-H_2), 3.97 (3H, s, OCH_3), 2.41 (3H, s, SCH_3); ^{13}C NMR ($CDCl_3$) δ: 163.1 (*C*=O), 160.5 (3-*C*)*, 135.1, 134.3, 132.8, 132.4, 132.2, 130.8, 129.7, 128.9,

126.5, 125.6 (Ar-C_{10}), 115.4 (*C*N), 101.2 (2-*C*), 53.2 (O*C*H_3), 21.2 (S*C*H_3); HRMS (ES): Found: 284.0743 $(M+H)^+$, $C_{16}H_{13}NO_2S$ requires: 284.0745 $(M+H)^+$. (* Confirmed by C-H correlation).

Crystal data for **12**: $C_{16}H_{13}NO_2S$, Mr = 283.35, monoclinic, a = 16.2151(2), b = 7.9116(1), c = 22.0688(4) Å, β = 105.0853(7)°, V = 2733.58 $Å^3$, Z = 8, C2/c, D_c = 1.38 gcm^{-3}, μ (MoKα) = 0.24 mm^{-1}, 3040 unique reflections, 2456 with $F_o > 4\sigma(F_o)$, R = 0.037. Full data available on the crystallographic information file on the disk provided.

3.5 References

1. Wallis, J.D., Easton, R.J.C. and Dunitz, J.D., *Helv. Chim. Acta*, 1993, **76**, 1.
2. Schweizer, W.B., Procter, G., Kaftory, M. and Dunitz, J.D., *Helv. Chim. Acta*, 1978, **61**, 2783.
3. Bell, P.C. and Wallis, J.D., *J. Chem. Soc., Chem. Commun.*, 1998, 257.
4. O'Leary, J., Bell, P.C., Wallis, J.D. and Schweizer, W.B., *J. Chem. Soc., Perkin Trans. 2*, 2001, 133.
5. Bell, P.C., Drameh, M., Hanly, N. and Wallis, J.D., *Acta Cryst.*, 2000, **C56**, 670.
6. Procter, G., Britton, D. and Dunitz, J.D., *Helv. Chim. Acta*, 1981, **64**, 471.
7. Parvez, M. and Schuster, I.I., *Acta Cryst.*, 1990, **C46**, 947.
8. Baxter, P.N.W., Connor, J.A., Povey, D.C. and Wallis, J.D., *J. Chem. Soc., Chem. Commun.*, 1991, 1135.
9. Rice, C.G. and Wallis, J.D., *J. Chem. Soc., Chem. Commun.*, 1993, 572.
10. Bengaard, H., Larsen, S., Sorensen, H., Robinson, K. and Wallis, J.D., *Acta Cryst.*, 1999, **C55**, 106.
11. Pilkington, M., Wallis, J.D., Smith, G.T. and Howard, J.A.K., *J. Chem. Soc., Perkin Trans. 2*, 1996, 1849.
12. Evans, K.L., Fronczek, F.R. and Gandour, R.D., *Acta Cryst.*, 1995, **C51**, 983.
13. Pilkington, M., Tayyip, S. and Wallis, J.D., *J. Chem. Soc., Perkin Trans. 2*, 1994, 2481.
14. Bailey, R.J., Card, P.J. and Shechter, H., *J. Am. Chem. Soc.*, 1983, **105**, 6096.
15. Rabai, J., *Synthesis*, 1989, 523.

16. Sheldrick, G.M., SHELXS-97, Program for the Solution of Crystal Structures, 1997, University of Göttingen, Germany.

17. Sheldrick, G.M., SHELXL-97, Program for Crystal Structure Refinement, 1997, University of Göttingen, Germany.

18. Johnson, C.K. and Burnett, M.N., ORTEPIII, Report ORNL-6895, 1996, Oak Ridge National Laboratory, Tennessee, USA.

19. Galluci, J.C., Hart, D.J. and Young, G.J., *Acta Cryst.*, 1998, **B54**, 73.

20. Wallis, J.D., Unpublished work.

21. Nyburg, S.C. and Faerman, C.H., *Acta Cryst.*, 1985, **B41**, 274.

22. Glass, R.S., Andruski, S.W., Broeker, J.L., Firouzabadi, H., Steffen, L.K. and Wilson, G.S., *J. Am. Chem. Soc.*, 1989, **111**, 4036.

23. Bader, R.F.W., *Atoms in Molecules, A Quantum Theory*, Oxford University Press, Oxford, 1990.

Chapter 4

1,6-Interactions Between the Dimethylamino Group and sp^2 Carbon Atoms in 2,2'-Disubstituted-Biphenyls

1,6-Interactions Between the Dimethylamino Group and Alkenyl Carbon Atoms in 2,2'Disubstituted-Biphenyls

4.1 Introduction

To date investigations into interactions between nucleophiles and electrophiles have focussed mainly on the *peri* naphthalene framework, which is capable of forming 1,5 interactions between the substituents (Figure 1).[1-4] In this system, however, the substituents are constrained to some degree by the bonding geometry of the ring system. The *peri* naphthalene framework can be distorted somewhat to change the separation between the substituents. Small displacements of the *peri* groups out of the plane of the naphthalene ring have been observed. In plane displacements, as shown in Figure 1, have also been found. These displacements have been used to characterise the nature of the interactions between the groups. These results may, however, be affected by the groups being constrained to be near to each other, or by effects of interaction with *ortho* substituents.

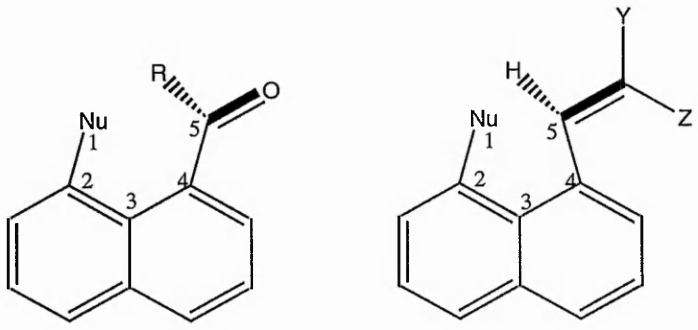

Figure 1 1,5-Interactions in *peri*-naphthalenes

This prompted a study into interactions between the dimethylamino group and electron-deficient sp^2C atoms attached to the biphenyl system. When these groups are located in *ortho* positions on opposite rings they are capable of forming 1,6-N----C interactions, but are not compelled by their molecular framework to be near to one another at all. 1,6-Steric interactions in 2,2',6-trisubstituted and 2,2',6,6'-tetrasubstituted biphenyls are well known since they lead to optical activity where the substituents on one ring are different (Figure 2).[5,6] In such compounds rotation about the Ar-Ar bond is prevented or greatly slowed, hence isomers, called atropisomers, can be separated.

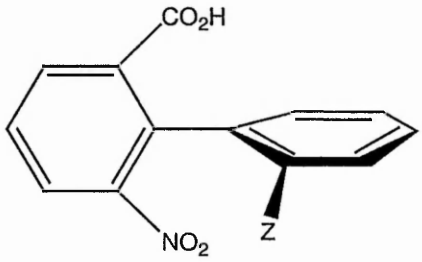

$Z = OCH_3$ $T_{1/2} = 91$ min.
$Z = NO_2$ $T_{1/2} = 125$ min.
$Z = CH_3$ $T_{1/2} = 179$ min.

Figure 2 1,6-Steric interactions in some 2,2',6-trisubstituted biphenyls ($T_{1/2}$ = half-life of racemisation at 118°C)

4.2 Results and Discussion

Compounds **1**-**6** were synthesised to investigate interactions of the dimethylamino group with the carbonyl group of an aldehyde or with different electron-deficient alkenes. In the biphenyl system the groups have more freedom to 'choose' their mutual arrangement. Thus, this system is likely to be a more reasonable model than

the *peri*-naphthalene framework for intermolecular interactions between dialkylamino groups and sp^2C atoms.

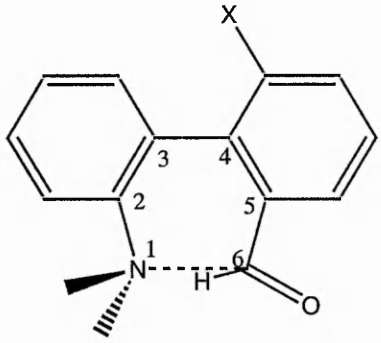

1 X = CHO
2 X = H

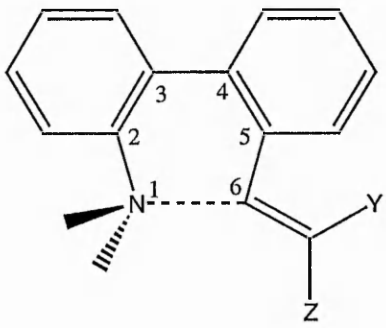

3 Y = Z = -$(C(=O)CH_2)_2CMe_2$
4 Y = Z = CN
5 Y = CN, Z = CO_2Me
6 Y = H, Z = NO_2

1 and **2** were prepared by Stille and Suzuki coupling methodologies (Schemes 1 and 2). The stannyl derivative **9** was prepared through lithiation[7] of the bromoaniline derivative **8** at -78°C and reaction of the aryllithium with chlorotrimethylstannane[8]. The crude material was contaminated with the starting aniline and N,N-dimethylaniline; all three compounds display very similar chromatographic behaviour and have high boiling points, which are too close together to attempt purification by vacuum distillation. Thus the crude material was used in the subsequent Stille coupling with 2-bromoisophthalaldehyde **11**[9], which was prepared in 27% yield through oxidation of the parent dimethyl compound **10** with chromium trioxide. Compound **1** was obtained in 17% yield.

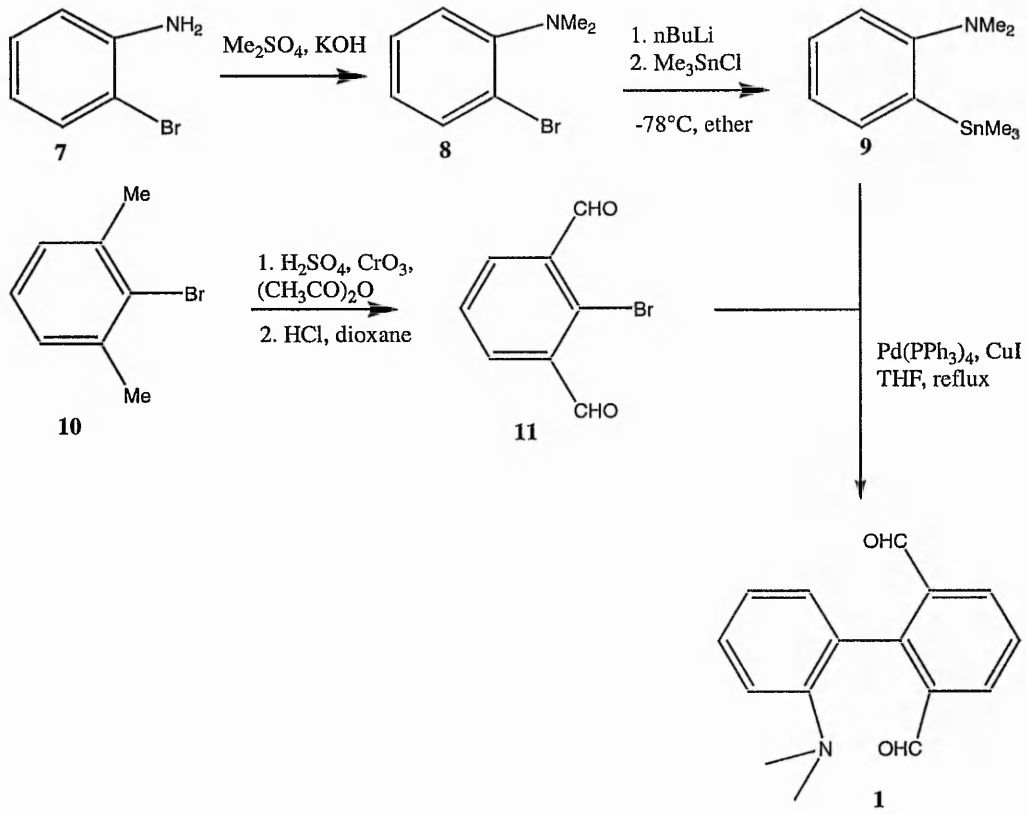

Scheme 1 Preparation of **1**

Suzuki coupling was employed to prepare **2** (Scheme 2) in 85% yield from 2-(N,N-dimethylamino)phenylboronic acid **12**[7] and 2-bromobenzaldehyde. The boronic acid **12** was obtained through lithiation of the bromoaniline derivative **8** at -78°C and reaction of the aryllithium with triisopropyl borate also at -78°C. Early attempts to prepare the boronic acid met with problems in the work-up procedure. The presence of both an acidic $B(OH)_2$ group and a basic NMe_2 group warranted careful monitoring of the pH in order to isolate the product. Only one procedure for the preparation of this boronic acid exists in the current literature[7] and indeed there are no examples of

ortho-disubstituted biphenyls where just one group is a dimethylamino group, which indicates it is not a straightforward preparation. However, the procedure was successful and reproducible, although the boronic acid obtained was shown to be crude by NMR and was used without purification in the subsequent Suzuki coupling.

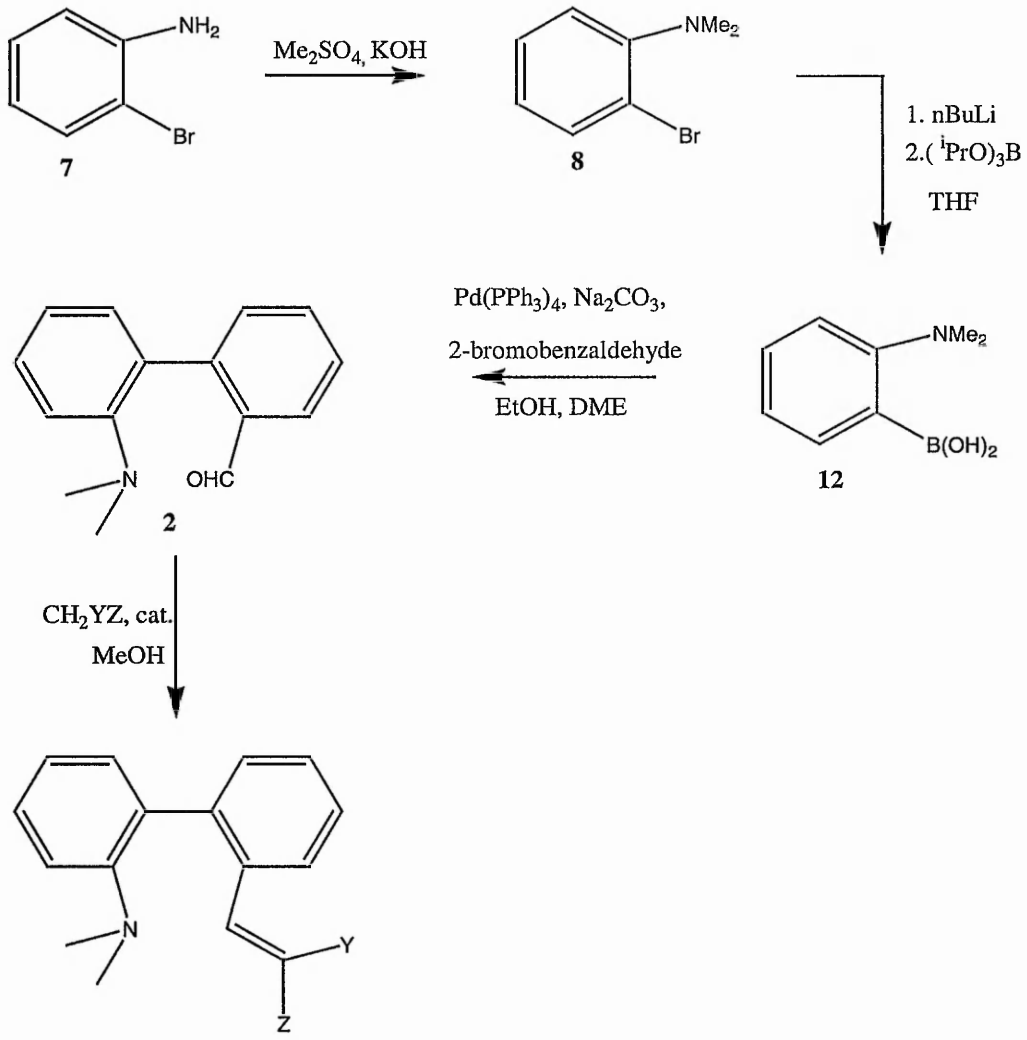

3 Y = Z = -(C(=O)CH_2)$_2$$CMe_2$
4 Y = Z = CN
5 Y = CN, Z = CO_2Me
6 Y = H, Z = NO_2

Scheme 2 Preparation of **2-6**

The structures of **1** and **2** were supported by ^{1}H NMR spectra. Signals at δ: 9.75 and δ: 9.74 corresponding to the aldehyde protons in **1** were observed, the corresponding resonance for **2** was found at δ: 9.57. The Me_2N group was observed at δ: 2.45 for **1** and δ: 2.38 for **2**. The ^{13}C NMR for **1** showed resonances at 191.2 (C=O) and 42.5 (Me_2N) and for **2** 190.7 (C=O) and 42.2 (Me_2N). In the infrared spectra the carbonyl absorptions were observed at 1681 and 1688 cm^{-1} for **1** and **2** respectively. The molecular formulae of **1** and **2** were confirmed by high resolution mass spectrometry and the difference between the observed and calculated molecular weights were within the recommended limit of 5 ppm.

Compounds **3-6** were prepared (Scheme 2) in yields of 31-65% through Knoevenagel condensations of the aldehyde **2** with dimedone, malononitrile, methyl cyanoacete and nitromethane in methanol at room temperature in the presence of a catalytic amount of ethylenediamine diacetate.

Compound **3** exists as the cyclic zwitterion **13**, this was confirmed by x-ray analysis. Compound **4** exists as the cyclic zwitterion **14** in the solid state and in solution in very polar solvents, e.g. DMSO, but in solution in less polar solvents, e.g. $CHCl_3$, as the uncyclised compound. This was first indicated by the compound's behaviour during solubility tests. On dissolving the white solid in a variety of solvents a deeply orange-coloured solution was obtained corresponding to the uncyclised form **4** as shown by the NMR in $CDCl_3$. However, in solution in DMSO the NMR shows the cyclic zwitterion **14**. Compounds **5** and **6** both exist as uncyclised structures.

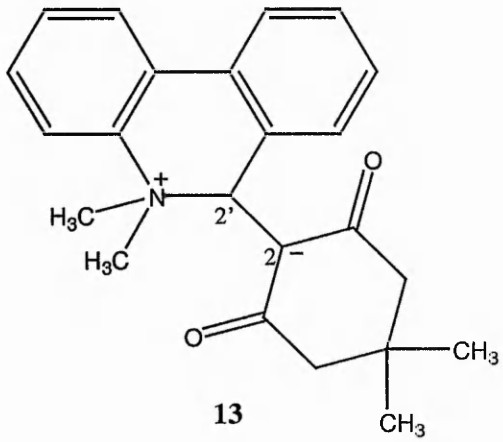

13

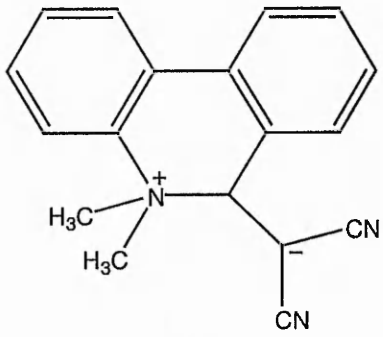

14

In the ^{1}H NMR spectrum of **13** the 2'-H atom, i.e. the former alkenyl proton was found at δ: 6.47. This proton is shifted upfield compared to the corresponding alkenyl protons in compounds **4-6**, which were observed at δ: 7.57, 8.09 and 7.86, the second alkenyl proton in **6** is hidden in a multiplet at δ: 7.18-7.05. The shift of this proton in **13** being more upfield is consistent with saturation of the alkene in **3** through addition of the amino N atom to form the zwitterion **7**. The ^{13}C NMR spectrum of **13** shows resonances at δ: 101.0 and 75.1 corresponding to the C atoms of the former double bond, the former being the carbanionic C atom (the resonance at δ: 75.1 was confirmed by a C-H correlation NMR experiment to correspond to the peak at δ: 6.47 in the ^{1}H NMR). In **4**, **5** and **6** the alkenyl carbons were found at δ: 162.2* and 79.4, δ: 157.5* and 100.2 and δ: 139.9* and 135.8* (* Confirmed by a C-H correlation NMR experiment). In **13** the Me_2N group was found at δ: 3.36 in the ^{1}H NMR and at δ: 51.1 in the ^{13}C NMR, this group is shifted downfield from that observed for **4-6**. The Me_2N group was found at δ: 2.45, 2.39 and 2.42 in the ^{1}H NMR spectra of **4**, **5** and **6** respectively and at δ: 42.3, 42.3 and 42.6 in the corresponding ^{13}C NMR

spectra. This difference is consistent with the formation of an ammonium group in **13**.

The carbonyl carbons of **13** were found at δ: 194.3 and 192.5 in the ^{13}C NMR spectrum. In the ^{13}C NMR spectrum of **4** the nitrile groups give rise to resonances at δ: 114.3 and 112.9. The nitrile group of **5** was observed at δ: 115.8 and a resonance at δ: 163.5 was observed to correspond to the ester carbonyl carbon.

The infrared spectra of **13**, **4-6** all showed the absorptions expected from the functional groups present. The carbonyl groups of **13** were observed at 1598 cm^{-1}. For **4** an absorption at 2170 cm^{-1} corresponding to the nitrile groups was observed. In the infrared spectrum of **5** absorptions at 1725 cm^{-1} (C=O) and 2221 cm^{-1} (C≡N) were observed. It was not possible to assign the ester C-O absorption due to the presence of several strong absorptions in the 1100-1300 cm^{-1} region. The nitro group of **6** gave rise to absorptions at 1335 and 1500 cm^{-1} corresponding to the symmetric and antisymmetric N-O absorptions.

The molecular formulae of **13**, **4-6** were confirmed by high resolution mass spectrometry, in all cases the difference between the observed and calculated molecular weights were within the recommended limit of 5 ppm.

Crystals of **1**, **2**, **13**, **14**, **5** and **6** were grown by slow evaporation of solutions in appropriate solvents. The crystals were analysed under a polarising light microscope and those that showed uniform extinction of light when rotated through crossed polar

lenses were selected for single crystal x-ray analysis. If necessary the crystals were cut to size, typically 0.1-0.2 mm^3. X-ray diffraction data was collected at the EPSRC X-ray Crystallography Service in Southampton University at 150 K (**1** and **2**) and 120 K (**13**, **14**, **5** and **6**) and processed at the Nottingham Trent University using the SHELXS-97[10] and SHELXL-97[11] programs. Results for compounds **1** and **2** are shown in the ORTEP[12] diagrams in Figures 3 and 4. Results for compounds **13**, **14**, **5** and **6** are shown in the ORTEP[12] diagrams in Figures 5-8. Selected molecular geometric data for all compounds are given in Tables 1 and 2 and crystal packing diagrams are in Section 4.3 towards the end of this chapter.

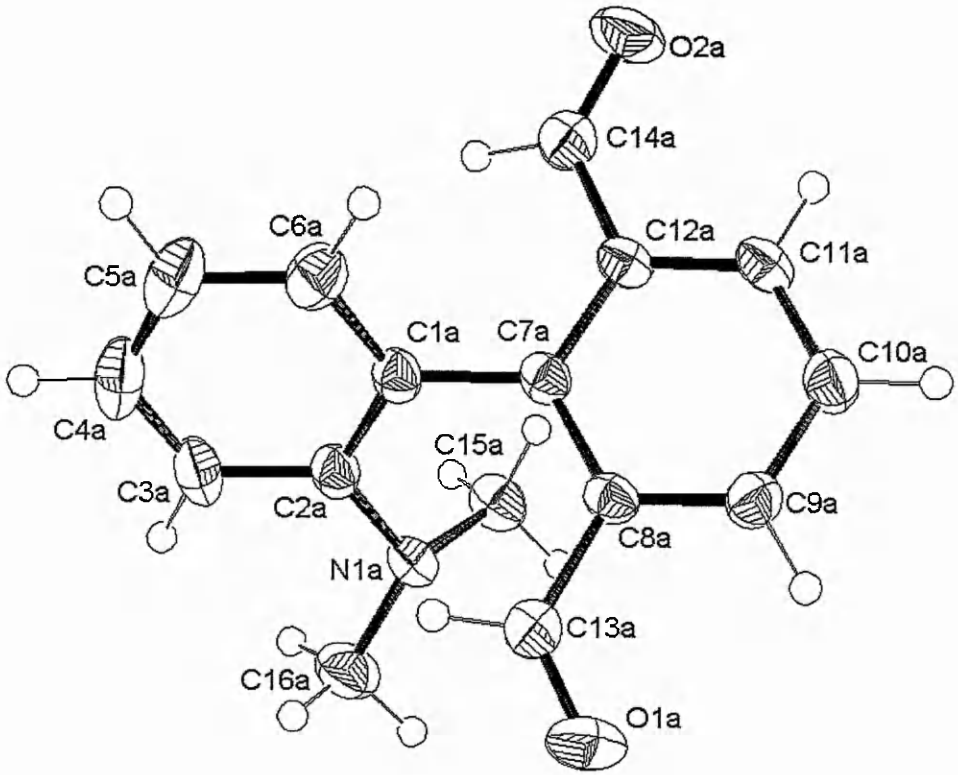

Figure 3 Molecular structure of **1** with anisotropic displacement parameters at the 50% level.

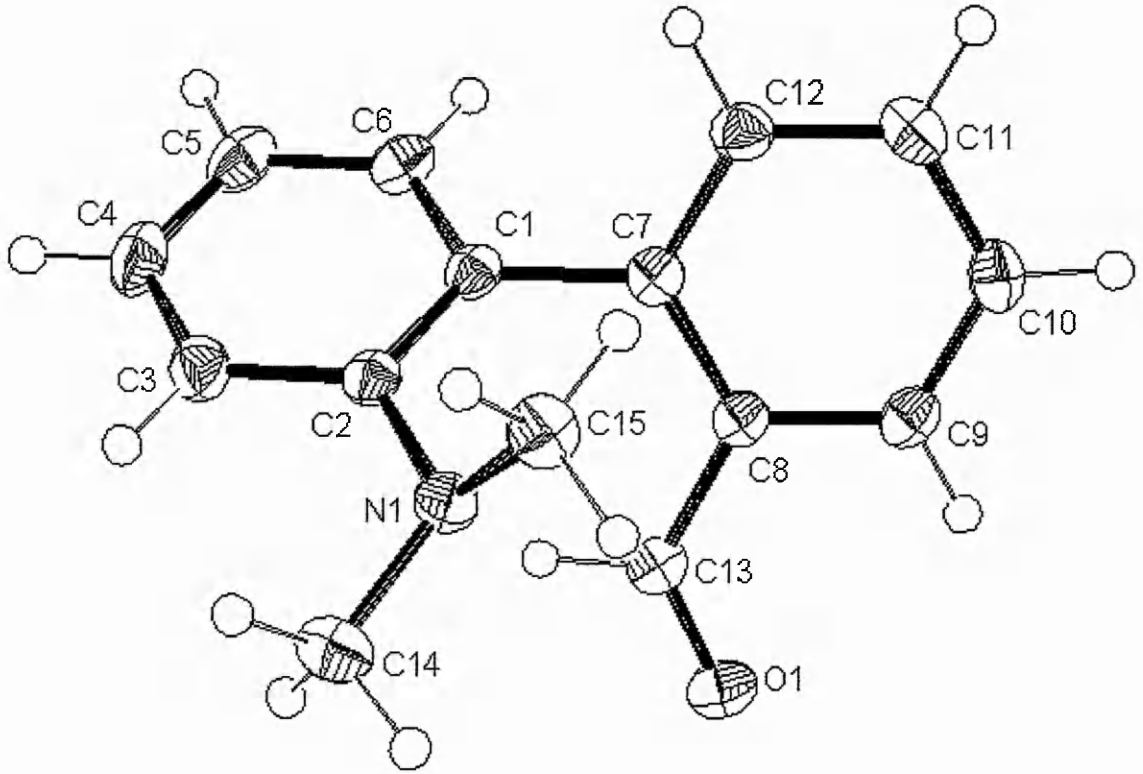

Figure 4 Molecular structure of **2** with anisotropic displacement parameters at the 50% level.

Table 1 Selected geometric data for compounds **1** and **2** (°, Å)

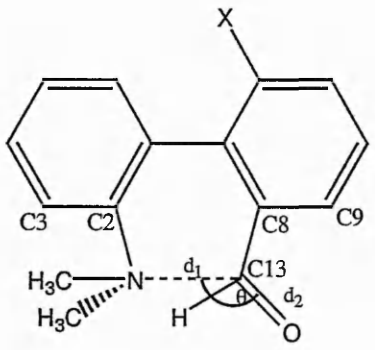

1 X = CHO
2 X = H

T1 and T2 = Torsion angles of N-Me bonds with the C3-C2 aryl bond.
T3 = Torsion angle of C=O bond with the C8-C9 aryl bond.
ΔC = deviation of C13 from the plane of its substituents.
ΔC ' = deviation of C13 from the best plane of the adjacent phenyl ring.
ΔN = deviation of N from the best plane of the adjacent phenyl ring.
+ve values for ΔC, ΔC ' and ΔN indicates deviation towards the other substituent.

	d_1	Inter-ring angle	d_2	T1	T2	T3	ΔC	ΔN	ΔC'	θ
1	2.929(3)	58.1(1)	1.193(3)	118.9(3)	-13.3(3)	10.3(4)	+0.006(12)	-0.004(3)	-0.071(4)	123.8(2)
	3.029(3)	62.4(1)	1.199(3)	116.0(3)	-15.1(3)	7.7(4)	+0.008(13)	-0.012(4)	-0.064(4)	128.1(2)
2	2.989(2)	68.9(1)	1.209(1)	116.5(1)	-14.9(2)	6.2(2)	+0.017(5)	+0.041(2)	-0.067(2)	126.5(1)

Compounds **1** and **2** both show Me_2N----C=O contacts, the N----C separations are 2.929(3) and 3.029(3) Å for the two independent molecules of **1** in the asymmetric unit and 2.989(2) Å for **2**. These N----C=O contact distances are much longer than in the related naphthalene compound **15** (2.489(5) Å)[13], however in **15** the groups are forced to be close to each other, while in **1** and **2** they are not. The interactions in **1** and **2** are of similar lengths to the 1,5-Me_2N / ketone carbonyl interactions in methadone **16** of 2.911 and 2.912 Å[14,15], where the two groups are also not forced to be near one another. The N atoms have pyramidal geometry, and are oriented with one N-Me bond lying close to the adjacent phenyl ring plane. The aldehyde group lies close to the plane of its own phenyl ring.

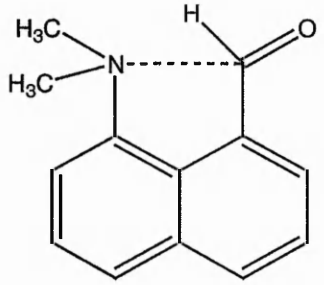

15

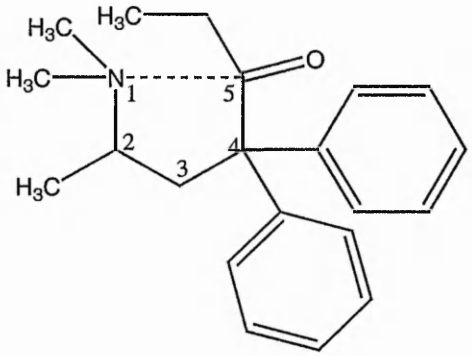

16

In **1** and **2** the phenyl rings lie at 58.1-62.4° to each other in order to bring the two substituents close enough for an interaction to occur. A survey of the CSD[16] showed that, in general, biphenyls with one *ortho* substituent per phenyl ring tend to have their phenyl rings close to perpendicular. Exceptions occur when the substituents are small, as for fluoride[17,18] or alkoxy[19], or can hydrogen bond, as in diols[20,21], a hydroxy ether[22] and the 2,2'-diamine[23], where the interplanar angles are *ca.* 40-55°.

There are no directly comparable biphenyl structures with 1,6-amino / carbonyl interactions in the Cambridge Structural Database. Compound **17**, however, shows a short contact between a methoxy O atom and a carbonyl C atom of a carboxylic acid, the O----C separation is 3.023(5) Å.[24] The conformation of **17** is such that the phenyl rings lie at 54.4(1)° to each other and the methoxy group lies close to the best plane of the adjacent phenyl ring, so that the unconjugated lone pair is not well aligned with the MeO----C=O vector. It has already been suggested that 1,5-MeO----sp^2C interactions in *peri*-naphthalenes are remarkably insensitive to the nature of the sp^2C-containing functional group and interactions are not attractive in nature, but are dominated by steric effects (Section 2.2). Thus 1,6-MeO----sp^2 interactions in 2,2'-disubstituted biphenyls are not likely to be attractive interactions.

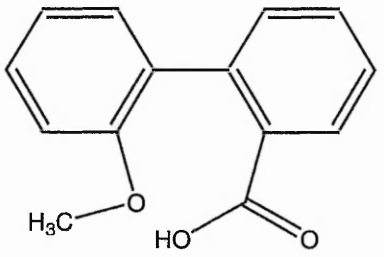

17

In **1** and **2** the theoretical directions of the amino N atom lone pairs lie at *ca.* 19-25° to the N----C(=O) vectors, thus the lone pair is reasonably aligned for effective overlap with the LUMO of the carbonyl carbon. The N----C=O angles lie in the range 123.8(2)-128.2(2)°.

The presence of a second aldehyde group in **1** has little effect on the molecular conformation, the three structures of **1** and **2** are very similar. The only significant differences between the geometries of the two compounds are concerned with the dimethylamino group. In **2** this group is displaced out of the best plane of the adjacent phenyl ring by 0.042 Å towards the carbonyl group, while in the two molecules of **1** the dimethylamino N atoms are not significantly displaced out of the planes of their phenyl rings. The Ar-N bond lengths also differ, in **1** these bond lengths are 1.402(3) and 1.410(3) Å, while in **2** this is slightly longer at 1.422(2) Å. These differences may be due to the through-bond electron-attracting power of the second carbonyl group, although there are no other significant bond-length differences between the two compounds.

Compounds **3-6**, involving dimethylamino groups and alkenyl groups, fall into two groups; **5** and **6** where the N----C separations (2.941(2)-2.975(4) Å) are similar to those found in **1** and **2**, and **3** and **4** where the amino N atom has attacked the α-C atom of the alkene in a Michael-type addition to form the cyclic zwitterions **13** and **14** with N-C bond lengths in the range 1.586(1)-1.600(3) Å). The inter-ring angles range from 23.7(1) to 27.9(1)° in the cyclised structures, **13** and **14**, but from 57.1(1) to 60.1(1)° in the uncyclised structures, **5** and **6**, which are comparable to those in **1** and **2** (58.1(1)-62.4(1)°).

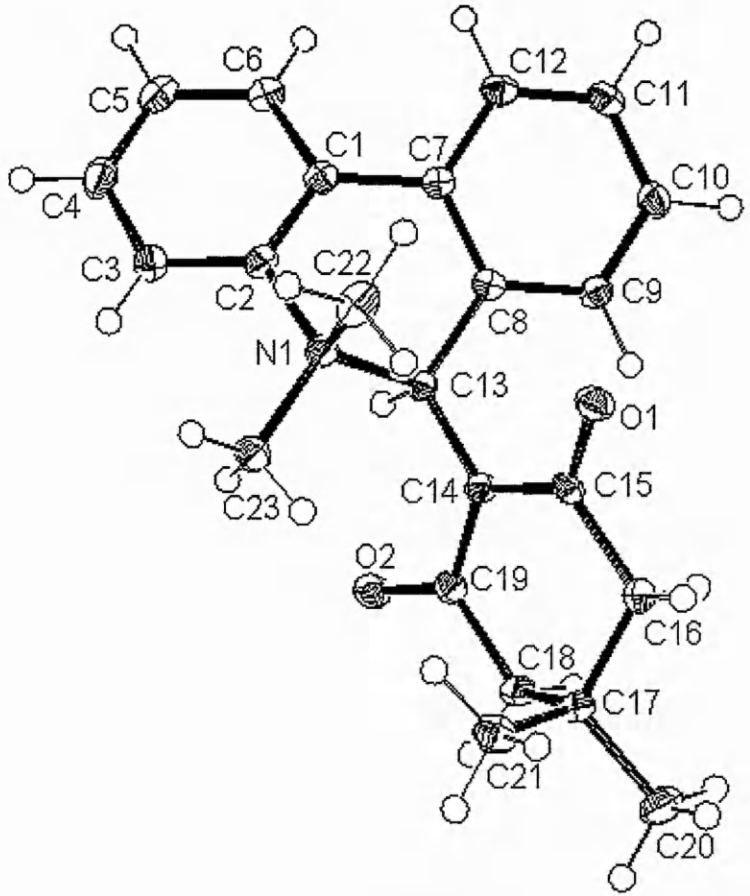

Figure 5 Molecular structure of **13** with anisotropic displacement parameters at the 50% level.

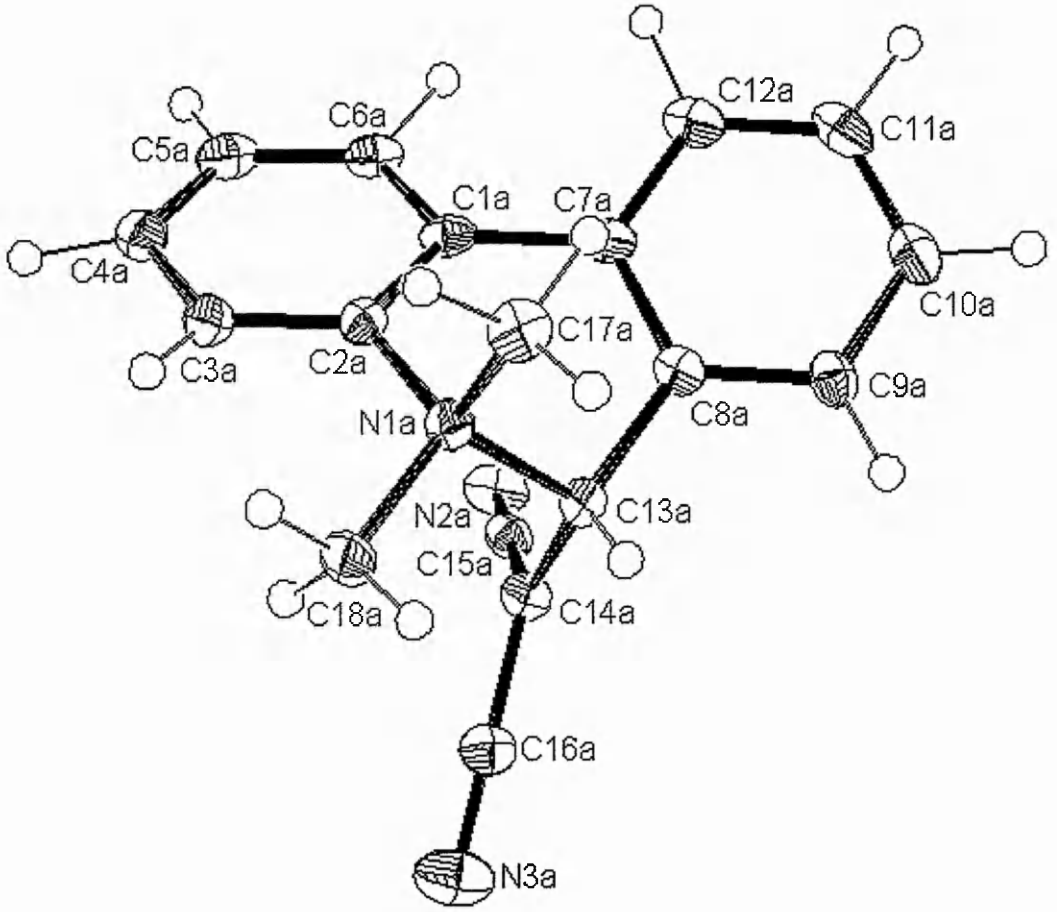

Figure 6 Molecular structure of one molecule of **14** with anisotropic displacement parameters at the 50% level.

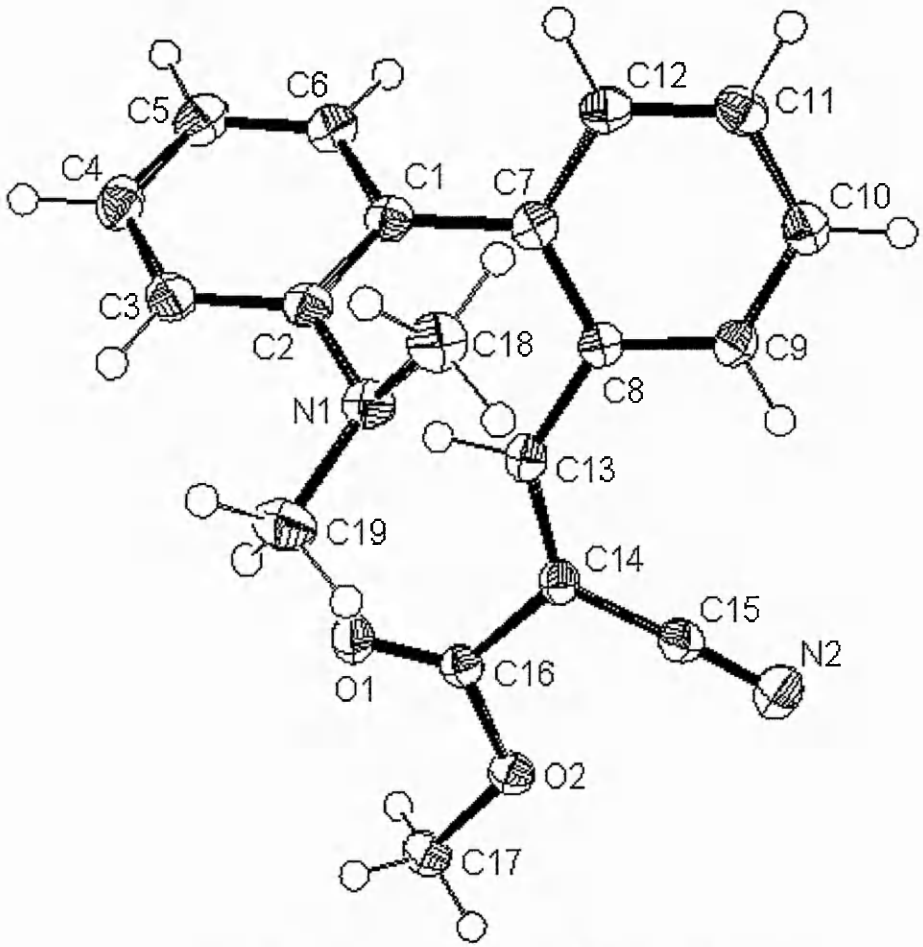

Figure 7 Molecular structure of **5** with anisotropic displacement parameters at the 50% level.

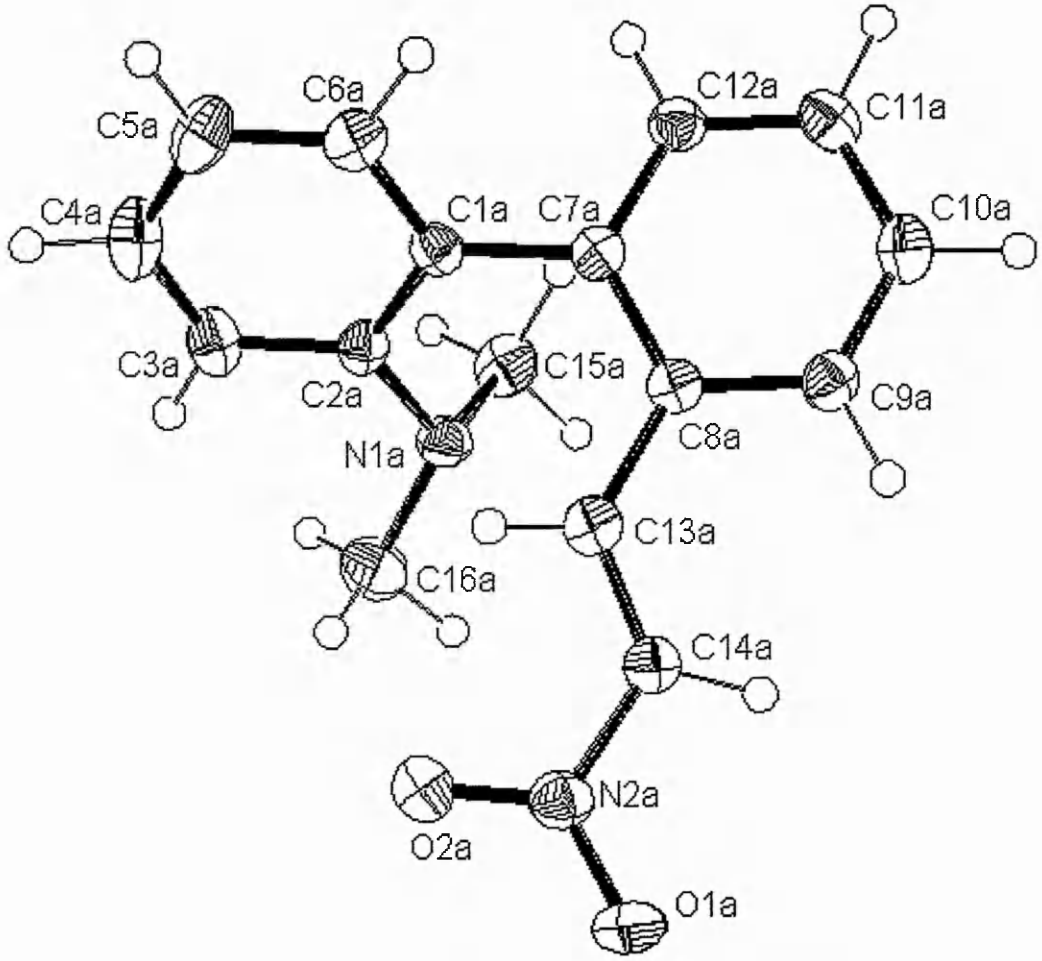

Figure 8 Molecular structure of one molecule of **6** with anisotropic displacement parameters at the 50% level.

Table 1 Selected molecular geometric data for compounds **13**, **14**, **5** and **6** (Å, °)

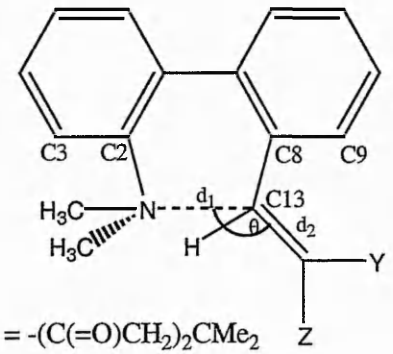

13 Y = Z = -(C(=O)CH_2)$_2$$CMe_2$
14 Y = Z = CN
5 Y = CN, Z = CO_2Me
6 Y = H, Z = NO_2

T1 and T2 = Torsion angles of N-Me bonds with the C3-C2 aryl bond.
T3 = Torsion angle of C=C bond with the C8-C9 aryl bond.
ΔC = deviation of C13 from the plane of its substituents.
ΔC ' = deviation of C13 from the best plane of the adjacent phenyl ring.
ΔN = deviation of N from the best plane of the adjacent phenyl ring.
Positive values for ΔC, ΔC ' and ΔN indicates deviation towards the other substituent.

	d_1	Inter-ring angle	d_2	T1	T2	T3	ΔC	ΔN	ΔC'	θ
13	1.586(1)	23.7(1)	1.504(1)	100.8(1)	-17.8(1)	21.4(2)	+0.393(5)	-0.082(2)	+0.010(2)	113.7(1)
	1.600(3)	27.9(1)	1.486(4)	104.0(3)	-16.3(3)	100.6(3)	+0.31(1)	+0.097(4)	+0.032(4)	112.9(2)
14	1.597(4)	26.6(1)	1.476(4)	104.1(3)	-17.3(3)	96.5(3)	+0.37(1)	+0.029(4)	+0.056(4)	113.5(2)
5	2.941(2)	57.91(5)	1.349(2)	112.0(1)	-19.0(2)	15.6(2)	+0.023(5)	-0.020(2)	-0.086(2)	117.1(1)
6	2.943(4)	57.1(1)	1.326(4)	103.3(3)	-25.5(4)	13.3(4)	0.00(1)	-0.082(4)	-0.043(4)	120.4(2)
	2.975(4)	60.1(1)	1.319(4)	105.8(3)	-23.9(4)	14.9(4)	+0.01(1)	-0.059(4)	+0.008(4)	120.3(2)

Compounds **13**, **14**, **5** and **6** show a trend of decreasing N----C(=C) separation along the series **6**→**13**, that is accompanied by a lengthening of the alkene bond from 1.319(4) Å in **6** to 1.504(1) Å in **13**, and a decrease in the inter-ring angles from 60.1(1)° in **6** to 23.7(1)° in **13**. The N----C=C angle also decreases from 120.3(2)° in **6** to 113.7(1)° in **13** and 112.9(2) and 113.5(2)° in **14**.

In Section 3.2 the relationship between S----C separation and pKa of the methylene compound in 1-methylthionaphthalene-8-alkenyl derivatives was discussed. Figure 9 shows the results of such a correlation for this series of compounds.

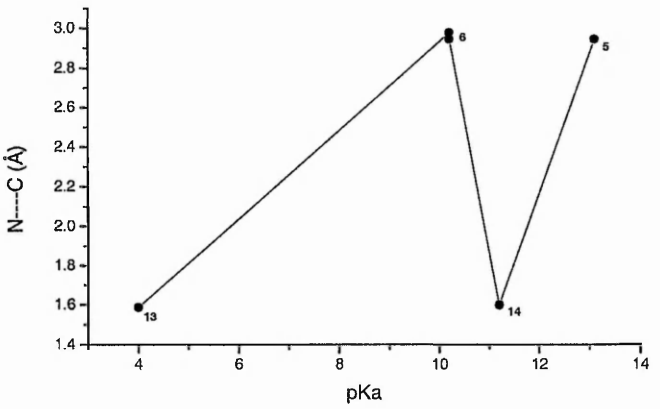

Figure 9 Variation of N----C distance with pKa of the corresponding methylene compound for **13**, **14**, **5** and **6**

One would not expect a straight line for this correlation, as the compounds fall into two groups; cyclised structures with N-C bonds whose lengths are much shorter (1.586(1) - 1.600(3) Å) than in the uncyclised structures with N----C separations (2.943(4) – 2.975(4) Å). A general trend of decreasing N----C separation with decreasing pKa would be expected, however this is not observed. In this series of

compounds the nitro derivative **6** appears to be significantly out of step with the others. Nitromethane has a pKa of 10.2 and so one would expect compound **6** to exist as a cyclic zwitterion, but this is not the case. It was also the nitro derivative that did not fit the trend for the methylthionaphthalene series in Section 3.2.

It is not possible to correlate the N----C separation with the infrared absorption of the alkene bond for this series as compounds **13** and **14** have undergone cyclisation and no longer contain an alkene bond. The infrared spectra of compounds **5** and **6** show absorptions at 1605 and 1630 cm^{-1} respectively corresponding to the C=C bond. As would be expected for the shorter N----C separation of **5** (2.941(2) Å) the alkene bond shows a lower infrared absorption than for compound **6** whose average N----C separation is 2.959(4) Å. It is not possible however, to conclude whether or not the absorption of the alkene bonds is related to the N----C separation in this series of compounds based on just these two uncyclised structures. In order to determine whether a relationship exists between the two parameters one would require a greater number of structures.

There are other molecular features common to all four structures that do not follow any trend. There are deviations of the amino N atoms and the alkenyl α-C atoms from the best planes of their adjacent phenyl rings. These deviations are in the range 0.020-0.097 Å (ΔN) and 0.008-0.086 Å (ΔC'), but are not in the same sense for each compound. In **5** and **6** the groups are displaced away from each other, while in **4** these displacements are towards each other and in **3** the N atom is displaced away from the alkene group while the alkene C13 atom is displaced towards the N atom. In

3 and **4** cyclisation has lead to the formation of a 6-membered ring, a cyclohexadiene ring, which is not flat. A rotation between the aryl rings (*ca.* 25°) has led to this ring adopting a half-chair conformation in which the non-aromatic ring atoms are displaced to opposite sides of the best plane through the ring. Substituents on these two atoms (N1 and C13) can adopt pseudo axial or pseudo equatorial orientations. In **3** the cyclic dimedone substituent adopts the pseudo equatorial position (T3 = 21.4(2)°), and in **4** the $C(CN)_2$ substituent is in the pseudo axial position (T3 = 100.6(3) and 96.5(3)°). This is presumably for crystal packing reasons. Compound **3**, which retains the cyclic structure in solution, would be expected to equilibriate between the conformations with the dimedone residue pseudo equatorial or pseudo axial. In compounds **5** and **6** the torsion angles the alkene bond makes with the aryl C8-C9 bond are 15.6(2), 13.3(4) and 14.9(4)°, thus the alkene π electrons can conjugate with the aromatic π system.

Another feature of compounds **13** and **14** is the geometry about the C13-C14 bond, i.e. that which was the C=C bond. Both structures are oriented such that the torsion angles about this bond are close to 90°. This orientation places the p orbital of the negatively charged C13 atom parallel with the newly formed N^+-C bond where it can overlap with this bond's antibonding orbital. This may be because the cyclisation reaction is not complete and that this overlap is simply a small degree of π-bond character still remaining in the former alkene bond. This would account for the long N^+-C bonds observed in both **13** and **14** (1.586-1.600 Å), which are much longer than the N-Me bonds (1.500-1.509 Å). Alternatively on cyclisation the orientation about the C13-C14 bond may be as a result of a stereoelectronic effect; a favourable overlap

of the anionic p orbital with the N^+-C antibonding orbital in an anomeric-type interaction. This would also account for the long N^+-C bonds in **13** and **14**.

A survey of the CSD[15] found three structures of $[CH(CN)_2]^-$ where the anion is associated with Li^+ or Na^+ cations **18**-**20**.[25] In compound **14** the anion is $[RC(CN)_2]^-$, but it is not associated with a cation, the positively charged ammonium group is not available to coordinate with the anion. Hence it might be expected that the bond lengths in **18**-**20** differ to those in **14**. There are no striking differences between the structures, the bond lengths are generally shorter in **18**-**20**, but this may be due to libration as these structures were measured at higher temperatures (193 K for **18** and **20** and 213 K for **19**) than compound **3** (120 K).

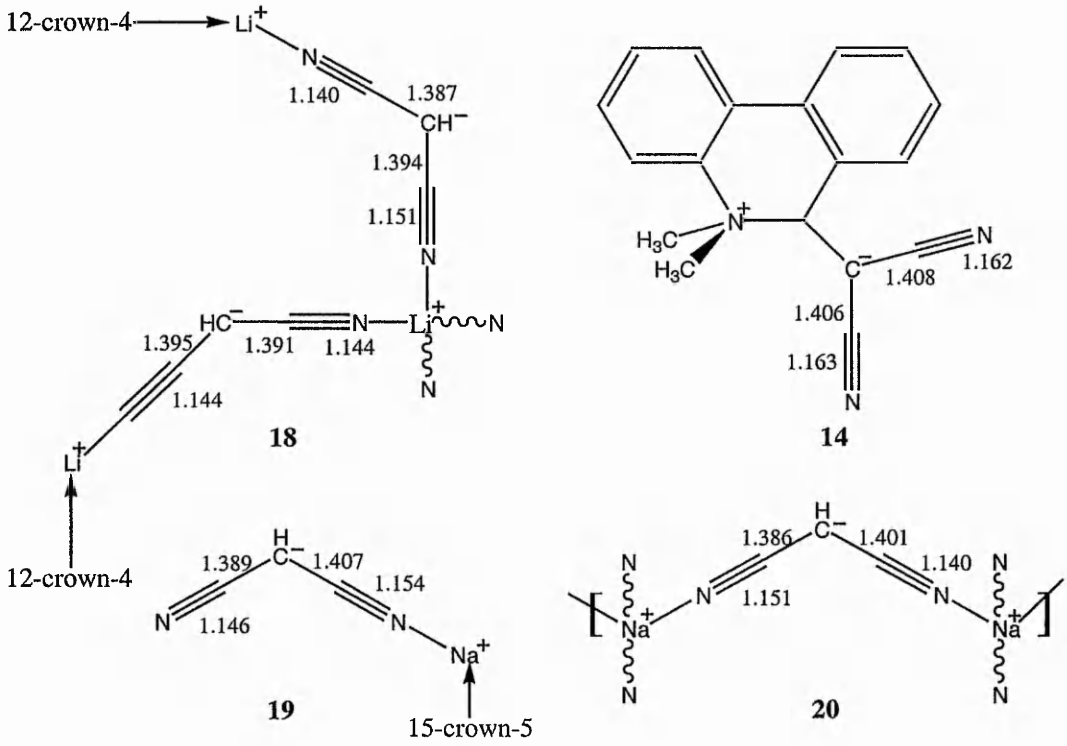

Figure 10 Bond lengths in structures containing the $[RC(CN)_2]^-$ fragment.

The C^--C≡N bond lengths in **14** differ from the C-C≡N bond lengths in compound **5**; 1.407 (C^--C) and 1.162 (C≡N) *cf.* 1.434 (C-C) and 1.147 (C≡N). The shorter C-C bond and longer C≡N bond are consistent with the nitrile groups in **14** being substituents of a carbanionic carbon atom, while in **5** the nitrile group is an alkenyl substituent.

There are no analogous structures for the dimedone anion to compare with compound **13**. The bond lengths of the anionic dimedone ring of **13** are shown below. The bond lengths show that the ring is more or less symmetrical and there is no evidence that the structure is approaching that of an enolate. The bond lengths (for **21** and **23** these are the average of four independent molecules) of four lithium enolates found in the CSD are shown below (Figure 11).[26-28] The enolates **21**-**23** all have longer C-O^- bonds than the C=O bonds in **3**, and shorter C=C bonds than the C-C(=O) bonds in **3**.

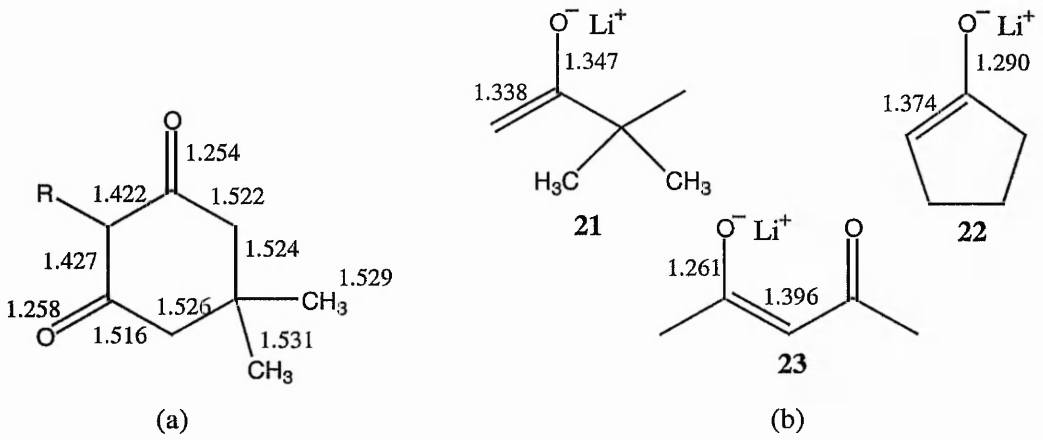

Figure 11 (a) Bond lengths in the dimedone fragment of **3** (b) Bond lengths in the lithium enolates **21**-**23**.

In **5** and **6** the theoretical directions of the amino N atom lone pairs lie at 21.4–24.8° to the N----C(=C) vectors. Thus, as in **1** and **2**, the lone pair is reasonably aligned for effective overlap with the LUMO of the alkenyl α-C atom.

There is much evidence to suggest that the interactions in compounds **1-6** are attractive in nature. The most compelling evidence is the cyclisation that has occurred in **3** and **4** to give **13** and **14**, however in all structures the phenyl rings are oriented such that the inter-ring angle is much less than 90° and the substituents are brought into close contact rather than adopting a near *trans* arrangement in which the substituents would avoid each other completely. In **13** and **14** there is clearly a strong covalent interaction with **13** showing the stronger bond (1.586(1) Å), just shorter than in **14** (1.597(4) and 1.600(3) Å) and not ring opening in solution. The N^+-C bond is shorter in **13** than in the peri-naphthalene **24** (1.651(3) Å)[2], the structures although not directly comparable (cyclic diketone *cf.* cyclic diester) would be expected to exert similar through-space electron-attracting powers. The *peri*-naphthalene analogue of **4**, compound **25**, has not cyclised, the N----C separation is 2.413(2) Å.[2] These results are accountable as there is less strain in the fused six-membered rings formed in **3** and **4** than the five-membered ring formed in **24**, indeed this strain has prevented cyclisation in **25**.

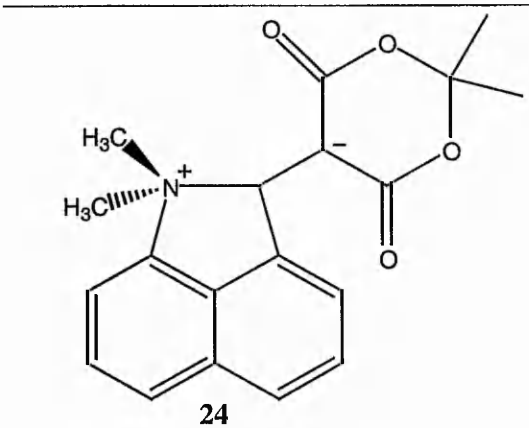

24

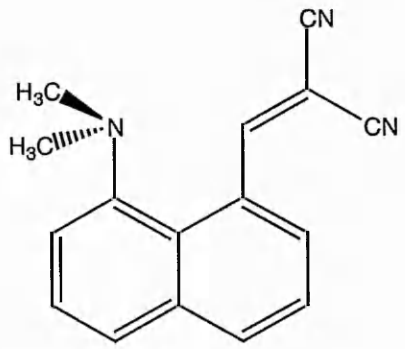

25

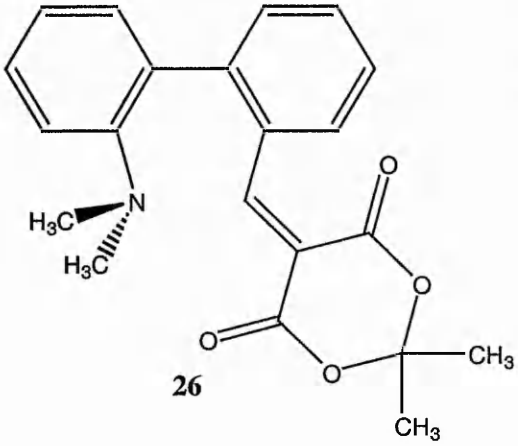

26

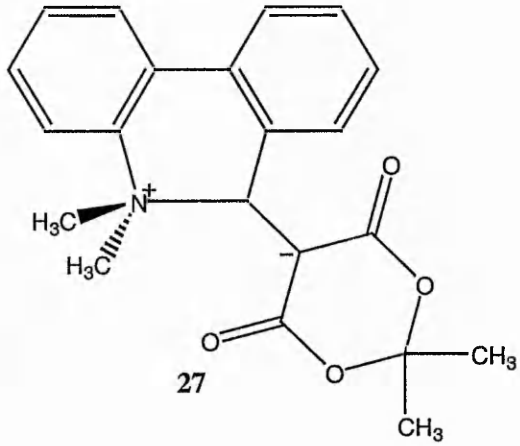

27

The meldrum's acid biphenyl derivative **26** has been synthesised, however it was not possible to grow suitable crystals for x-ray measurement. The compound exists as a white solid, similar in appearance to **13** and **14** and the ^{1}H and ^{13}C NMR spectra suggest it exists as the cyclic zwitterion **27**. The 'alkenyl' proton appears at δ: 6.22 *cf.* δ: 6.47 for **13**, the 'alkenyl' C atoms appear at δ:79.2 and 68.1 *cf.* 101.0 and 75.1 for **13**.

In the uncyclised structures **1**, **2**, **5** and **6** the N----sp^2C separations are all well within the sum of the van der Waals radii for N and C atoms (~3.2 Å) and the amino N lone

pairs are all well aligned with the alkenyl α-C atom. The partial pyramidalisation in **5** (0.023(5) Å) indicates that, like in **13** and **14**, there is also a covalent interaction present, although much weaker than in **13** and **14**. In **6**, however, there is no pyramidalisation at the C13 atom, it has remained planar, the average N----C separation for the two independent molecules of **6** is longer than that of **5** (2.959(4) *cf.* 2.941(2) Å). Thus, the interaction in **6** may be a "closed shell interaction", i.e. one where no orbital overlap takes place, but a polarisation of the alkene bond in response to the nearby N lone pair. In the aldehydes **1** and **2** the N----C separations are 2.979(3) (an average for the two independent molecules of **1**) and 2.989(2) Å, hence longer than in **13** and **14**. There are very small deviations of C13 from the plane of its substituents (0.007(12) and 0.017(5) Å), however when one considers the estimated standard deviations these deviations are negligible, hence the interactions in **1** and **2** appear to be similar to that in **6** and non-covalent in nature. There does not appear to be a trend of decreasing N----C separation with increasing electron-attracting power of the electrophilic substituent, the compounds have either undergone cyclisation to form zwitterions or have not and the N----C separations are all *ca.* 2.9 Å in the open structures, and *ca.* 1.6 Å in the closed structures. The difference in N----C separations in the open structures is only 0.08 Å, hence much smaller than in the 1,5 interactions in the *peri*-naphthalenes and of the same order as crystal packing effects, indeed for the nitro derivative **6** the difference in N----C separations for the two independent molecules is 0.032 Å, this is almost half the total difference in N----C separations. In contrast the *peri*-naphthalene compounds do show a trend in the N----C separations, the difference in N----C separation for the open structures is *ca.* 0.25 Å. Thus the *peri*-naphthalene system provides a more sensitive measurement of through-space

electron-attracting power, however the 2,2'-disubstituted biphenyl system provides a better model for intermolecular interactions as the substituents are not forced to be close to one another.

These conclusions are based on the interpretation of the structural data available, they are not final, but merely reasonable deductions. The use of partial pyramidalisations as an indicator of an attractive interaction has previously been discussed (Section 2.3) and warrants care. However, in this series of compounds there are several structural features that are used to characterise the nature of the interactions, and the partial pyramidalisations is just one of them. Further detailed investigation by accurate electron density measurement may provide further insight into the nature of these interactions. Bader's 'Theory of Atoms in Molecules'[29] has been used to characterise interactions previously[30] and a more accurate measurement of compound **2** is in progress at the university of Edinburgh. Also x-ray structures of more compounds in this series would provide more data with which to characterise the interactions and observe possible trends.

4.3 Crystal Packing

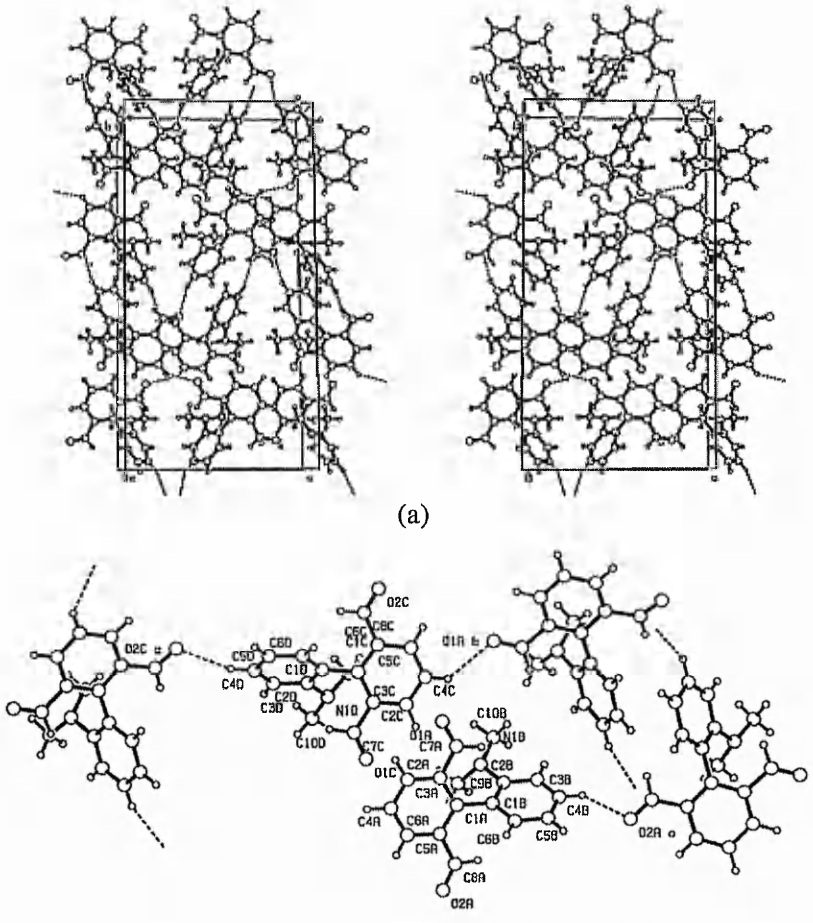

Figure 12 Crystal packing of **1** at 150 K (a) in the unit cell and (b) intermolecular contacts.

In the crystal packing of **1** there are three unique intermolecular contacts for the two unique molecules. One molecule has two hydrogen bonds between aromatic hydrogen atoms and carbonyl oxygen atoms, these are C(4D)-H----O(2C) (2.41(3) Å) and C(4C)-H----O(1A) (2.47(2) Å). The other molecule also shows an aromatic C-H----carbonyl O contact between C(4B)-H and O(2A) (2.54(3) Å).

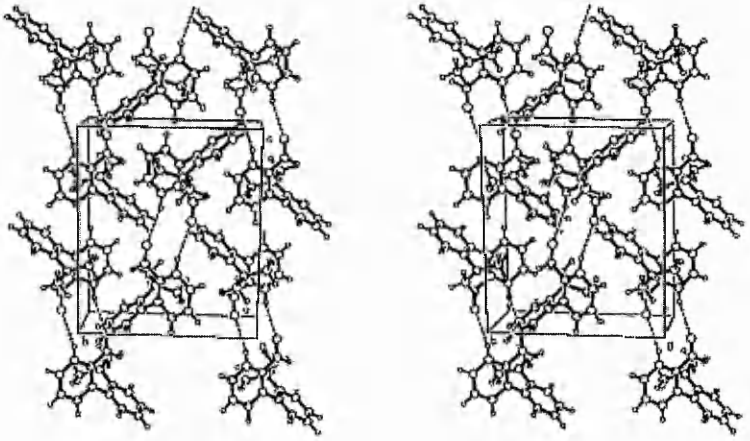

(a)

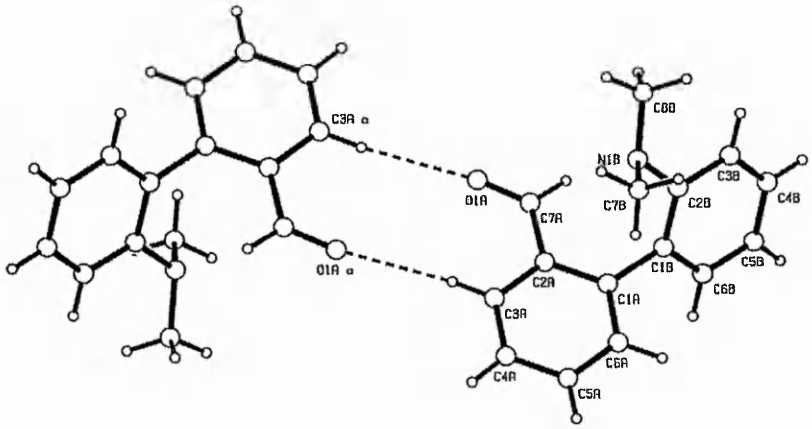

(b)

Figure 13 Crystal packing of **2** at 150 K (a) in the unit cell and (b) intermolecular contacts.

The crystal packing of **2** is such that pairs of molecules are held together with pairs of contacts between aromatic hydrogen atoms (C(3)-H) and carbonyl oxygen atoms (O(1A) (2.56(2) Å).

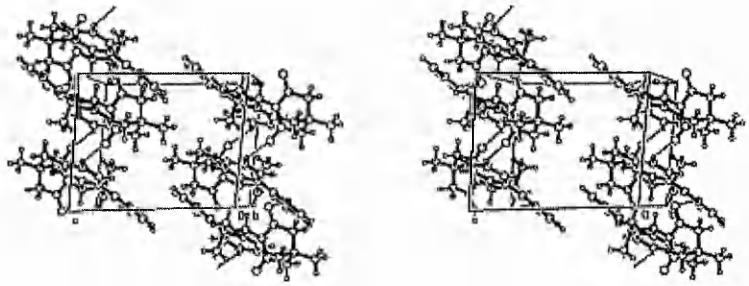

(a)

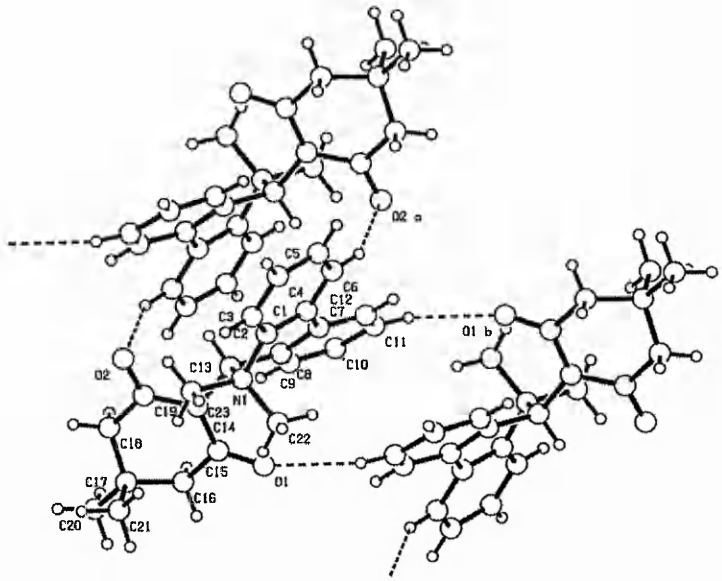

(b)

Figure 14 Crystal packing of **13** at 120 K (a) in the unit cell and (b) intermolecular contacts.

Each molecule of **13** is involved in two intermolecular hydrogen bonds, as both hydrogen donor and acceptor, to each of two molecules. From one molecule there are contacts from the aromatic hydrogen C(6)-H and carbonyl oxygen O(2) atoms to the O(2) and C(6)-H atoms of a second molecule (2.57(2) Å) and from the aromatic hydrogen C(11)-H and carbonyl oxygen O(1) to the O(1) and C(11)-H of a third molecule (2.54(2) Å).

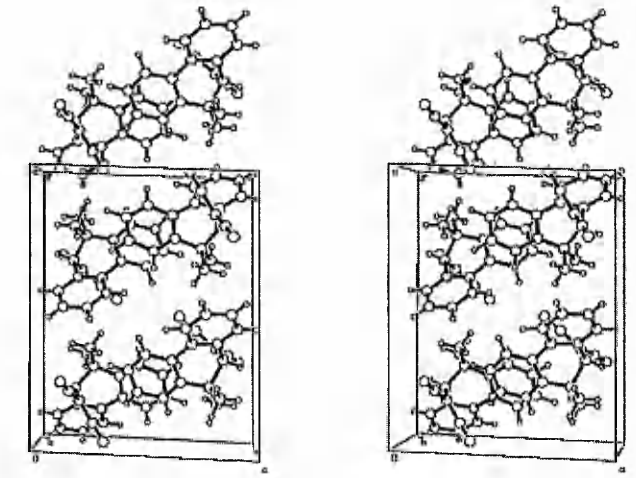

(a)

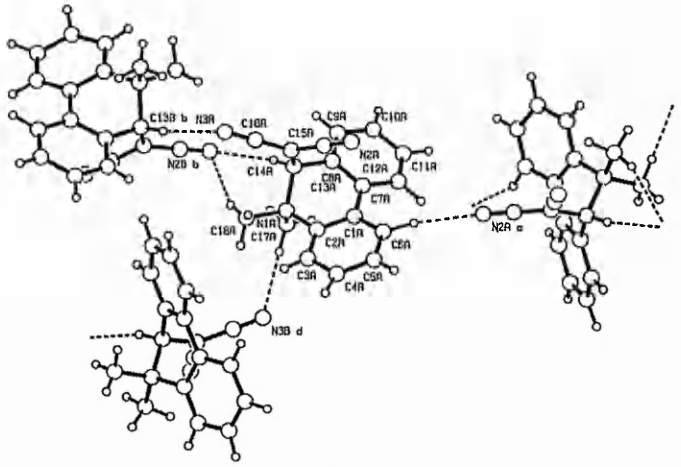

(b)

Figure 15 Crystal packing of **14** at 120 K (a) in the unit cell and (b) intermolecular contacts.

In the crystal packing of **14** there are two independent molecules (labelled A and B). There are contacts between the dimethylamino hydrogen atoms (C(18A)-H and C(17A)-H) of molecule A and nitrile nitrogen atoms (N(2B) and N(3B)) of two molecules of B (2.63(3) and 2.38(3) Å). There is a hydrogen bond between the former alkene hydrogen (C(13A)-H) (molecule A) and a nitrile nitrogen (N(2B) (molecule B) (2.53(2) Å) and another between C(13B)-H (molecule B) and N(3A) (molecule A) (2.37(2) Å). There is also a contact between an aromatic hydrogen (C(6A)-H) (molecule A) and a nitrile (N(2A)) (molecule A) (2.46(5) Å).

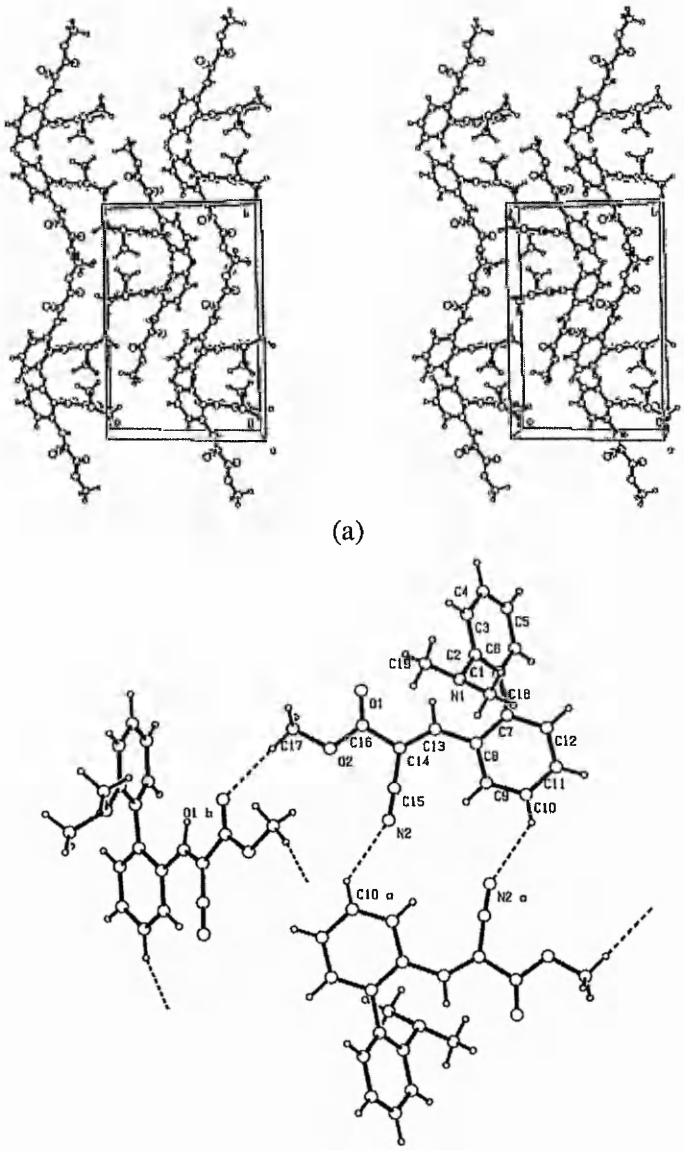

Figure 16 Crystal packing of **5** at 120 K (a) in the unit cell and (b) intermolecular contacts.

There are three unique intermolecular contacts in the crystal packing of **5**. These are between the ester methyl hydrogen (C(17)-H) and the carbonyl oxygen (O(1)) (2.45(2) Å), and a pair of C-H----N≡C contacts involving the aromatic C(10)-H hydrogen atom and the N(2) nitrogen atom (2.56(2) Å).

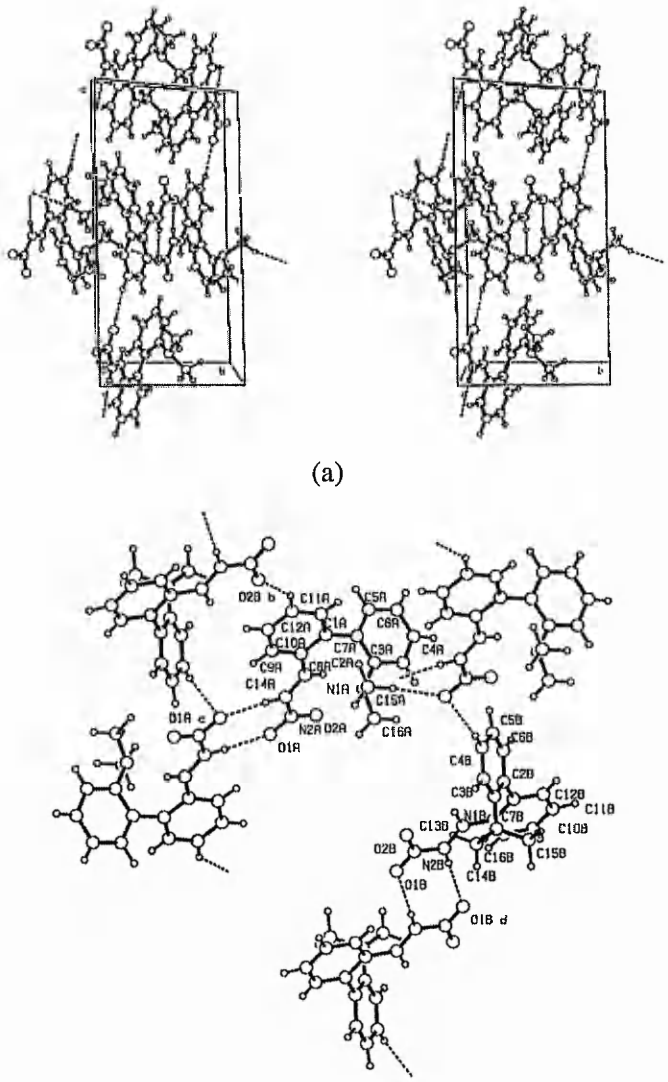

Figure 17 Crystal packing of **6** at 120 K (a) in the unit cell and (b) intermolecular contacts.

In the crystal packing of **6** there are several intermolecular contacts, which all involve the nitro group oxygen atoms. For molecule A there are contacts to an alkenyl hydrogen (C(14A)-H (2.44 (4) Å) and a methyl hydrogen (C(15A)-H) (2.58 (4) Å) from O1A. For molecule B there are contacts to an alkenyl hydrogen (C(14B)-H) (2.58 (3) Å) and an aromatic hydrogen (C(4B)-H) (2.60 (3) Å) from O1B and O1A respectively.

4.4 Experimental

Preparation of N,N-Dimethyl-2-bromoaniline **8**[31]

Dimethyl sulfate (5.5 ml, 58 mmol) was added to a stirring suspension of 2-bromoaniline **7** (10 g, 58 mmol) in water (10 ml). After 30 min the pH was adjusted by the addition of aqueous KOH (25%) until the mixture was alkaline. Dimethyl sulfate (5.5 ml, 58 mmol) was added and the mixture was stirred for a further 30 min before the pH was again adjusted with KOH. A final equivalent of dimethyl sulfate (5.5 ml, 58 mmol) was added and the mixture was stirred for 2-3 h. while regularly adjusting the pH by the addition of KOH. The alkaline mixture was transferred to a separatory funnel and extracted with ether. The organic extracts were extracted with 2M HCl, neutralised with KOH and extracted with ether. The organic solution was dried ($MgSO_4$) and evaporated to yield an oil (6.9g, 59%); ^{1}H NMR ($CDCl_3$) δ: 7.52 (1H, dd, J = 7.9, 1.5 Hz, 3-*H*), 7.20 (1H, dt, J = 7.7, 1.5 Hz, 5-*H*), 7.03 (1H, dd, J = 7.9, 1.6 Hz, 6-*H*), 6.82 (1H, dt, J = 7.6, 1.6 Hz, 4-*H*), 2.75 (6H, s, $N(CH_3)_2$); ^{13}C NMR ($CDCl_3$) δ: 151.7 (1-*C*), 133.8 (3-*C*), 128.0 (5-*C*), 123.8 (4-*C*), 120.4 (3-*C*), 119.1 (2-*C*) (Ar-C_6), 44.1 ($N(CH_3)_2$).

Preparation of 2-Trimethylstannyl- N,N-dimethylaniline **9**[7,8]

n-Butyllithium (1.6M solution in hexane, 3.4 ml, 5.5 mmol) was added dropwise to a stirred solution of amine **8** (1 g, 5 mmol) in dry ether (20 ml) at -78°C, under nitrogen. After 75 min. at -78°C chlorotrimethylstannane (1M solution in THF, 5.5

ml, 5.5 mmol) was added dropwise, the mixture was allowed to warm to room temperature and stirred overnight. Water (30 ml) was added to the mixture and the phases were separated. The aqueous phase was extracted with ether, the combined organic phases dried ($MgSO_4$) and evaporated to yield an orange oil (~1g) shown to be ~60% pure by NMR; ^{1}H NMR ($CDCl_3$) δ: 7.46 (1H, dd, J = 7.2, 1.7 Hz, 3-*H*), 7.33 (1H, dt, J = 7.5, 1.6 Hz, 5-*H*), 7.22 (1H, dd, J = 7.9, 0.7 Hz, 6-*H*), 7.14 (1H, dt, J = 7.2, 1.2 Hz, 4-*H*), 2.62 (6H, s, $N(CH_3)_2$), 0.25 (9H, s, $Sn(CH_3)_3$); ^{13}C NMR ($CDCl_3$) δ: 160.7 (1-*C*), 142.2 (2-*C*), 136.5 (3-*C*), 129.6 (5-*C*), 125.0, 120.4 (4-,6-*C*), 46.8 ($N(CH_3)_2$), -7.49 ($Sn(CH_3)_3$).

Preparation of 2-Bromoisophthalaldehyde[9] **11**

Conc. H_2SO_4 (13.5 ml) was added dropwise to a solution of 2-bromo-1,3-dimethyl benzene **10** (5 g, 27 mmol) in acetic anhydride (50 ml) at 0°C. To this mixture a solution of CrO_3 (16 g, 160 mmol) in acetic anhydride (50 ml) was slowly added over ~3 h. at 0°C. After the addition was complete the mixture was stirred at 15°C for 3 h. then poured on to crushed ice (~400 g) and left standing overnight. The green solid was collected by vacuum filtration and refluxed in a mixture of dioxane (40 ml) and conc. HCl (10 ml) for 5 h. The resulting brown solution was allowed to cool and concentrated *in vacuo*. Water (20 ml) was added and the brown solid was collected by vacuum filtration. The crude material was purified by eluting with CH_2Cl_2 through a plug of silica gel to yield the product **11** as a yellow solid (1.53 g, 27%); ^{1}H NMR ($CDCl_3$) δ: 10.53 (2H, s, 2 x C*H*O), 8.15 (2H, d, J = 7.7 Hz, 4-,6-*H*), 7.57 (1H, t, J =

7.7 Hz, 5-*H*); ^{13}C NMR ($CDCl_3$) δ: 190.6 (2 x *C*=O), 135.2 (4-,6-*C*), 134.4 (2-*C*), 130.7 (1-,3-*C*), 128.2 (5-*C*).

Preparation of 2-(N,N-dimethylamino)biphenyl-2',6'-dicarboxaldehyde **1**

2-Trimethylstannyl-N,N-dimethylaniline **9** (0.66 g, 2.35 mmol) and 2-bromoisophthalaldehyde **11** (0.5 g, 2.35 mmol) were loaded into an oven-dried flask, which had been cooled to room temperature under a nitrogen purge. Dry THF (25 ml) was added followed by $Pd(PPh_3)_4$ (0.14 g, 0.12 mmol) and CuI (0.032 g, 0.17 mmol). The reaction mixture was refluxed under nitrogen for 24 h. Tlc (2:1, cyclohexane:ether) showed the presence of starting materials, therefore more $Pd(PPh_3)_4$ (0.14 g) and CuI (0.032 g) were added and the mixture was further refluxed for 48 h. The THF was evaporated, ethyl acetate (50 ml) was added to the residue and the mixture was filtered through celite. The filtrate was washed with water (3 x 30 ml) and brine (30 ml), dried (Na_2SO_4) and evaporated to yield a brown oil. The crude material was purified by flash chromatography on silica gel (cyclohexane:ether, 2:1) to yield the product **1** as a yellow oil which solidified on standing (0.1 g, 17%), m.p. 98-101°C; ν_{max}/cm^{-1} (KBr): 2858, 1681, 1491, 1456, 1386, 1234, 945, 921, 799, 769; ^{1}H NMR ($CDCl_3$): 9.75 (1H, s, C*H*O), 9.74 (1H, s, C*H*O), 8.24 (2H, d, J = 7.7 Hz 3'-,5'-*H*), 7.62 (1H, t, J = 7.7 Hz, 4'-*H*), 7.45 (1H, t, J = 7.3, 2.6 Hz, Ar-H_1), 7.17-7.13 (3H, m, Ar-H_3), 2.45 (6H, s, N(CH_3)$_2$); ^{13}C NMR ($CDCl_3$): 191.2 (2 x *C*=O), 152.3, 146.2, 133.9, 134.0, 132.6 (4'-*C*), 130.7, 128.0, 124.9, 122.3, 118.6 (Ar-C_{12}), 42.5 (N(CH_3)$_2$); HRMS (ES): Found: 254.1178 $(M+H)^+$, $C_{16}H_{15}NO_2$ requires: 254.1181 $(M+H)^+$.

Crystal data for **1**: $C_{16}H_{15}NO_2$, Mr = 253.30, orthorhombic, a = 14.161(3), b = 27.913(6), c = 6.7018(13) Å, V = 2648.9 $Å^3$, Z = 8, $Pca2_1$, Dc = 1.27 gcm^{-3}, μ (MoKα) = 0.08 mm^{-1}, 3238 unique reflections, 2378 with $F_o > 4\sigma(F_o)$, R = 0.046. Full data available on the crystallographic information file on the disk provided.

Preparation of 2-(N,N-Dimethylamino)phenylboronic acid[7] **12**

n-Butyllithium (1.2M solution in hexane, 21ml, 25mmol) was added dropwise at -78°C to a stirred solution of N,N-dimethyl-2-bromoaniline **8** (4 g, 20 mmol) in dry THF (20 ml) under nitrogen. After 75 min. at -78°C the aryllithium solution was slowly transferred via cannula to a stirred solution of triisopropyl borate (11.5 ml, 50 mmol) in THF (20 ml) also at -78°C under nitrogen. When the addition was complete the mixture was stirred at -78°C for 1 h. then warmed to room temperature and stirred overnight. The reaction was quenched at room temperature with 1M HCl (200 ml) and stirred for 15 min. The pH was adjusted to pH 7 with 4M NaOH and the mixture was transferred to a separatory funnel. The mixture was extracted with ether, the combined organics were dried ($MgSO_4$) and evaporated to yield a brown oil. Tlc (cyclohexane:ether, 2:1) showed the presence of N,N-dimethyl-2-bromoaniline **8** and N,N-dimethylaniline. The brown oil was dissolved in ether and extracted with 2M NaOH. The aqueous extracts were adjusted to pH 7 with 4M HCl and extracted with ether. The organic solution was dried ($MgSO_4$) and evaporated to yield the product **12** as a tan oil (~2.2 g), shown to be crude by NMR; ^{1}H NMR ($CDCl_3$) δ: 7.91-7.17 (4H, br. m, Ar-*H*$_4$), 3.21 (2H, br.s, O*H*), 2.73 (6H, br.s, N(C*H*$_3$)$_2$); ^{13}C NMR ($CDCl_3$) δ: 159.8, 135.7, 132.0, 125.8, 120.3, 116.2 (Ar-*C*$_6$), 46.3 (N(*C*H$_3$)$_2$).

2-(N,N-Dimethylamino)biphenyl-2'-carboxaldehyde **2**

Crude 2-(N,N-dimethylamino)phenylboronic acid **12** (1.8 g) was dissolved in ethanol (5 ml) and loaded into a dry flask containing $Pd(PPh_3)_4$ (0.7 g, 0.61 mmol) and 2-bromobenzaldehyde (2.68 g, 14.5 mmol) in DME (100 ml) under nitrogen. A solution of Na_2CO_3 (6.42 g, 60.6 mmol) in degassed water (30 ml) was added to the reaction flask and the mixture was heated under reflux for 48 h. The solution was allowed to cool to room temperature and diluted with ether (200 ml). The phases were separated, the organic layer was extracted with 1M NaOH (50 ml) and 1M HCl (4 x 150 ml). The combined aqueous phases were made alkaline (pH 14) with 6M NaOH and extracted with ether (3 x 150 ml). The organic solution was dried ($MgSO_4$) and evaporated to yield the crude product which was purified by flash chromatography on silica gel, eluting first with $CHCl_3$ followed by EtOAc to yield the product **2** as a pale yellow oil which solidified on standing (1.23 g, 85%), m.p. 75-78°; ν_{max}/cm^{-1} (KBr): 2832, 1688, 1594, 1492, 1450, 1247, 1193, 945, 770; ^1H NMR ($CDCl_3$): 9.57 (1H, s, C*H*O), 7.92 (1H, d, J = 7.7 Hz, Ar-H_1), 7.65 (1H, t, J = 7.6 Hz, Ar-H_1), 7.47-7.31 (4H, m, Ar-H_4), 7.14 (1H, t, J = 7.4 Hz, Ar-H_1), 7.06 (1H, d, J = 7.2 Hz, Ar-H_1), 2.38 (6H, s, $N(CH_3)_2$); ^{13}C NMR ($CDCl_3$): 190.7 (*C*=O), 151.4, 142.7, 133.8, 133.1, 131.1, 131.1, 130.0, 129.5, 127.5, 126.7, 123.0, 118.1 (Ar-C_{12}), 42.2 ($N(CH_3)_2$); HRMS (ES): Found: 226.1229 $(M+H)^+$, $C_{15}H_{15}NO$ requires: 226.1232 $(M+H)^+$.

Crystal data for **2**: $C_{15}H_{15}NO$, Mr = 225.29, monoclinic, a = 8.1685(2), b = 11.0420(3), c = 13.7448(4) Å, β = 101.889(1)°, V = 1213.1 $Å^3$, Z = 4, $P2_1/n$, Dc = 1.23 gcm^{-3}, μ (MoKα) = 0.08 mm^{-1}, 2783 unique reflections, 2211 with $F_o > 4\sigma(F_o)$,

R = 0.051. Full data available on the crystallographic information file on the disk provided.

Preparation of 2-(1',2'-Dihydo-1',1'-dimethylbenzo(c)-quinolinium-2'-yl)-5,5-dimethyl-1,3-dioxocyclohexan-2-ide **13**

A solution of the aldehyde **2** (0.4 g, 1.8 mmol) in dry methanol (6 ml) was stirred under nitrogen at room temperature. Dimedone (0.8 g, 5.6 mmol) was added, followed by ethylenediamine diacetate (0.03 g, 0.2 mmol). After 2 h. tlc (ethyl acetate) showed complete consumption of the aldehyde. The methanol was evaporated and the residue was triturated with ether. The product **13** was collected by vacuum filtration as a cream-coloured solid (0.19g, 31%), m.p. 122-128°C; ν_{max}/cm^{-1} (KBr): 2923, 1598, 1511, 1400, 1140, 765, 752; λ_{max}(MeOH)/nm: 208.4, 280.4; ^{1}H NMR ($CDCl_3$) δ: 7.96 (1H, dd, J = 7.9, 1.3 Hz, Ar-H_1), 7.83 (1H, d, J = 8.7 Hz, Ar-H_1), 7.62-7.28 (6H, m, Ar-H_6), 6.47 (1H, s, 2'-*H*) 3.36 (6H, s, 1'-1'-CH_3), 2.38 (2H, s, 4-*H*), 2.28 (2H, s, 6-*H*), 1.10 (6H, s, 5-,5-CH_3); ^{13}C NMR ($CDCl_3$) δ: 194.3 (*C*=O), 192.5 (*C*=O), 143.0, 131.1, 130.4, 129.8, 129.5, 129.3, 129.3, 129.1, 128.6, 126.6, 122.8, 117.4 (Ar-C_{12}), 101.0 (2-*C*), 75.1 (2'-*C*)*, 51.6 (4-*C*), 51.1 (1'-,1'-*C*H_3), 50.2 (6-*C*), 31.3 (*C*(CH_3)$_2$), 28.9 ((*C*H_3)$_2$C). HRMS (ES): Found: 348.1966 $(M+H)^+$, $C_{23}H_{25}NO_2$ requires: 348.1964 $(M+H)^+$. (* Confirmed by C-H correlation).

Crystal data for **13**: $C_{23}H_{25}NO_2$, Mr = 347.45, triclinic, a = 9.3343(2), b = 10.2514(2), c = 11.3449(2) Å, α = 114.4419(8), β = 91.7559(8), γ = 105.0489(8)°, V = 942.56 Å^3, Z = 2, P$\bar{1}$, Dc = 1.29 gcm^{-3}, μ (MoKα) = 0.08 mm^{-1}, 4243 unique reflections, 3328

with $F_o > 4\sigma(F_o)$, R = 0.042. Full data available on the crystallographic information file on the disk provided.

Preparation of (1',2'-Dihydro-1',1'-dimethylbenzo(c)quinolinium-2'-yl)-dicyanomethide **14** / 1,1-dicyano-2-(2'-(dimethylamino)biphen-2''-yl)ethene **4**

To a stirred solution of the aldehyde **2** (0.4 g, 1.8 mmol) in dry methanol (6 ml) under nitrogen at room temperature was added malononitrile (0.37 g, 5.6 mmol), followed by ethylenediamine diacetate (0.03 g, 0.2 mmol). After 1 h. the white solid product **14** had precipitated out of solution and was collected by vacuum filtration (0.3 g, 62%), m.p. 92-94°C (melts to give an orange liquid); ν_{max}/cm^{-1} (KBr): 2917, 2848, 2170, 1486, 1470, 1446, 1403, 1357, 1265, 1237, 1188, 1150, 999, 922, 773, 730, 687; λ_{max}(MeOH)/nm: 210.6, 270.0, 299.2; ^{1}H NMR ($CDCl_3$) δ: 8.18 (1H, d, J = 7.9 Hz, Ar-H_1), 7.68 (1H, t, J = 7.4 Hz, Ar-H_1), 7.57 (1H, s, 2-*H*), 7.52-7.47 (2H, m, Ar-H_2), 7.39 (1H, t, J = 7.6 Hz, Ar-H_1), 7.25-7.06 (3H, m, Ar-H_3), 2.45 (6H, s, $N(CH_3)_2$); ^{13}C NMR ($CDCl_3$) δ: 162.2 (2'-*C*)*, 151.1, 143.4, 134.2, 131.7, 131.0, 130.7, 130.2, 128.6, 128.1, 127.8, 122.7, 118.4 (Ar-C_{12}), 114.3 (*C*N), 112.9 (*C*N), 79.4 (1-*C*), 42.3 ($N(CH_3)_2$)); HRMS (ES): Found: 274.1336 $(M+H)^+$, $C_{18}H_{15}N_3$ requires: 274.1344 $(M+H)^+$. (* Confirmed by C-H correlation).

This compound exists in two different forms; in solution in moderately polar solvents, e.g. $CHCl_3$, it is uncyclised with structure **4**, but in the solid state it exists as the cyclised zwitterion **14**. The results of ^{1}H and ^{13}C NMR as a solution in DMSO-d_6 are shown below. The proton resonances are broad as are two of the signals in the ^{13}C spectrum and it was not possible to observe all of the required carbon signals, this suggests that the compound is possibly opening and closing in solution, but the large

shift upfield of the alkenyl proton suggests that on average over time the structure is closer to the zwitterion.

^{1}H NMR (DMSO-d_6) δ: 7.78 (1H, d, J = 7.2 Hz, Ar-H_1), 7.72 (1H, d, J = 6.9 Hz, Ar-H_1), 7.63-7.40 (6H, m, Ar-H_6), 6.57 (1H, s, 2-*H*), 2.92 (6H, s, N(CH_3)$_2$); ^{13}C NMR (DMSO-d_6) δ: 144.0, 134.2, 131.1, 130.4, 129.7, 129.5, 128.8, 128.5, 127.5, 127.2, 126.7, 120.6, 120.3 (Ar-C_{12}), 118.4 (br.), 43.3 (br.), 46.3 (N(CH_3)$_2$

Crystal data for **14**: $C_{18}H_{15}N_3$, Mr = 273.33, monoclinic, a = 11.4599(4), b = 8.2053(3), c = 14.7752(7) Å, β = 92.1424(13)°, V = 1388.37 Å^3, Z = 2, $P2_1$, Dc = 1.31 gcm^{-3}, μ (MoKα) = 0.08 mm^{-1}, 5665 unique reflections, 4753 with $F_o > 4\sigma(F_o)$, R = 0.052. Full data available on the crystallographic information file on the disk provided.

Preparation of Methyl *E*-2-Cyano-3-(2-dimethylaminobiphen-2'-yl)-1-propenoate **5**

A solution of the aldehyde **2** (0.4 g, 1.8 mmol) in dry methanol (6 ml) was stirred under nitrogen at room temperature. Methyl cyanoacetate (0.32 ml, 3.6 mmol) was added, followed by ethylenediamine diacetate (0.03 g, 0.2 mmol). After 2 h. the yellow solid product **5** had precipitated out of solution and was collected by vacuum filtration (0.32g, 59%), m.p. 104-106°C; ν_{max}/cm^{-1} (KBr): 2926, 2854, 2221, 1725, 1605, 1590, 1442, 1264, 1246, 1200, 1118, 1097, 975, 941, 768, 736, 668; λ_{max}(MeOH)/nm: 208.1, 232.7, 301.2, 306.2; ^{1}H NMR ($CDCl_3$) δ: 8.29 (1H, d, J = 8.2 Hz, Ar-H_1), 8.09 (1H, s, 3-*H*), 7.62 (1H, t, J = 7.5 Hz, Ar-H_1), 7.48-7.44 (2H, m, Ar-H_2) 7.35 (1H, dd, J = 7.4, 1.5 Hz, Ar-H_1), 7.18 (1H, d, J = 7.4 Hz, Ar-H_1), 7.09-7.02

(2H, m, Ar-H_2), 3.84 (3H, s, OCH_3), 2.39 (6H, s, N(CH_3)$_2$); ^{13}C NMR ($CDCl_3$) δ: 163.5 (1-*C*), 157.5 (3-*C*)*, 151.4, 143.9, 133.1, 131.8, 131.6, 130.5, 129.7, 129.4, 128.5, 127.5, 122.2, 118.1 (Ar-C_{12}), 115.8 (*C*N), 100.2 (2-*C*), 53.0 (O*C*H$_3$), 42.3 (N(*C*H$_3$)$_2$). HRMS (EI): Found: 307.1438 (M+H), $C_{19}H_{18}N_2O_2$ requires: 307.1447 (M+H). (* Confirmed by C-H correlation).

Crystal data for **5**: $C_{19}H_{18}N_2O_2$, Mr = 306.36, monoclinic, a = 8.2446(2), b = 17.2928(4), c = 11.6833(2) Å, β = 107.1770(17)°, V = 1591.42(6) Å^3, Z = 4, C2/c, Dc = 1.377 gcm^{-3}, μ (MoKα) = 0.24 mm^{-1}, 3040 unique reflections, 2456 with $F_o > 4\sigma(F_o)$, R = 0.037. Full data available on the crystallographic information file on the disk provided.

Preparation of E-2-(2'-(Dimethylamino)biphen-2''-yl)-1-nitroethene **6**

A solution of the aldehyde **2** (0.4 g, 1.8 mmol) in dry methanol (6 ml) was stirred under nitrogen at room temperature. Nitromethane (0.15 ml, 2.7 mmol) was added, followed by ethylenediamine diacetate (0.03 g, 0.2 mmol) and the mixture was left to stir overnight. The yellow solid product **6** precipitated out of solution and was collected by vacuum filtration (0.31 g, 65%), m.p. 107-111°C; ν_{max}/cm^{-1} (KBr): 3103, 2829, 1630, 1594, 1500, 1480, 1455, 1335, 967, 940, 844, 751, 733; λ_{max}(MeOH)/nm: 209.0, 232.0, 306.4; ^{1}H NMR ($CDCl_3$) δ: 7.86 (1H, d, J = 13.6 Hz, 2-*H*), 7.63 (1H, d, J = 7.9 Hz, Ar-H_1), 7.58-7.34 (6H, m, Ar-H_6), 7.18-7.05 (2H, m, Ar-H_1, 1-*H*), 2.42 (6H, s, N(CH_3)$_2$); ^{13}C NMR ($CDCl_3$) δ: 151.3, 143.8 (ArC_2), 139.9 (2-*C*), 135.8 (1-*C*), 132.1, 131.9, 131.1, 129.5, 128.2, 127.5, 126.8, 122.1, 118.4 (Ar-C_{10} one peak is

doubly degenerate), 42.6 ($N(CH_3)_2$); HRMS (ES): Found: 269.1289 $(M+H)^+$, $C_{16}H_{16}N_2O_2$ requires: 269.1290 $(M+H)^+$.

Crystal data for **6**: $C_{16}H_{16}N_2O_2$, Mr = 268.31, triclinic, a = 8.8510(2), b = 9.8816(3), c = 18.2164(7) Å, α = 92.1632(14) β = 96.4141(15), γ = 116.416(2)°, V = 1411.10 $Å^3$, Z = 4, $P\bar{1}$, Dc = 1.26 gcm^{-3}, μ (MoKα) = 0.08 mm^{-1}, 6275 unique reflections, 3632 with $F_o > 4\sigma(F_o)$, R = 0.076. Full data available on the crystallographic information file on the disk provided.

Preparation of 5-(1',2'-Dihydo-1',1'-dimethylbenzo(c)-quinolinium-2'-yl)-2,2-dimethyl-4,6-dioxo-1,3-dioxan-5-ide **27**

A solution of the aldehyde **2** (0.4 g, 1.8 mmol) in dry methanol (6 ml) was stirred under nitrogen at room temperature. Meldrum's acid (0.8 g, 5.6 mmol) was added, followed by ethylenediamine diacetate (0.03 g, 0.2 mmol). After several hours tlc (2:1, cyclohexane:ether) showed just starting materials present in the mixture, hence piperidine (2 drops) was added and the mixture was refluxed for 3 h. The methanol was evaporated and the residue was triturated with t-butanol. The product **27** was collected by vacuum filtration as a white solid (0.13 g, 21%), m.p. 198-206°C (melts to give a brown liquid); ν_{max}/cm^{-1} (KBr): 3070, 3022, 1619, 1455, 1436, 1390, 1367, 1299, 1276, 1256, 1200, 1159, 1098, 994, 932, 797, 759, 726; λ_{max}(MeOH)/nm: 211.7, 256.0; ^1H NMR ($CDCl_3$) δ: 7.93 (1H, d, J = 7.9 Hz, Ar-H_1), 7.82 (1H, d, J = 6.9 Hz, Ar-H_1), 7.62-7.45 (6H, m, Ar-H_6), 6.22 (1H, s, 2'-*H*), 3.41 (6H, s, 1'-1'-CH_3),

1.77 (6H, s, 2-,2-CH_3); ^{13}C NMR ($CDCl_3$) δ: 169.1 (*C*=O), 165.5 (*C*=O), 143.1, 130.6, 130.5, 130.0, 129.8, 129.5, 129.4, 129.4, 129.0, 126.9, 123.4, 117.9 (Ar-C_{12}), 102.0 (2-*C*), 79.2 (2'-*C*), 68.1 (5-*C*), 50.0 (1'-1'-CH_3), 26.4 (2-,2-CH_3); HRMS (ES): Found: 352.1538 $(M+H)^+$, $C_{21}H_{21}NO_4$ requires: 352.1549 $(M+H)^+$.

4.5 References

1. Schweizer, W.B., Procter, G., Kaftory, M. and Dunitz, J.D., *Helv. Chim. Acta*, 1978, **61**, 2783.
2. Bell, P.C. and Wallis, J.D., *J. Chem. Soc., Chem. Commun.*, 1998, 257.
3. O'Leary, J., Bell, P.C., Wallis, J.D. and Schweizer, W.B., *J. Chem. Soc., Perkin Trans. 2*, 2001, 133.
4. Wallis, J.D., Easton, R.J.C. and Dunitz, J.D., *Helv. Chim. Acta*, 1993, **76**, 1.
5. Hall, M., *Prog. Stereochem.*, 1969, **4**, 1.
6. Norman, R.O.C., *Principles of Organic Synthesis*, Methuen & Co. Ltd., London, 1968.
7. Old, D.W., Wolfe, J.P. and Buchwald, S.L., *J. Am. Chem. Soc.*, 1998, **120**, 9722.
8. Kroth, H.-J., Schumann, H., Kuivila, H.G., Schaeffer Jr., C.D. and Zuckerman, J.J., *J. Am. Chem. Soc.*, 1975, **97**, 1754.
9. Wille, E.E., Stephenson, D.S., Capriel, P. and Binsch, G., *J. Am. Chem. Soc.*, 1982, **104**, 405.
10. Sheldrick, G.M., SHELXS-97, Program for the Solution of Crystal Structures, 1997, University of Göttingen, Germany.
11. Sheldrick, G.M., SHELXL-97, Program for Crystal Structure Refinement, 1997, University of Göttingen, Germany.
12. Johnson, C.K. and Burnett, M.N., ORTEPIII, Report ORNL-6895, 1996, Oak Ridge National Laboratory, Tennessee, USA.

13. Hodgson, D.R.W., Kirby, A.J. and Feeder, N., *J. Chem. Soc., Perkin Trans. 1*, 1999, 949.

14. Bürgi, H.-B., Dunitz, J.D. and Shefter, E., *Cryst. Struct. Commun.*, 1973, **2**, 667.

15. Bye, E., *Acta Chem. Scand., Ser B*, 1974, **28**, 5.

16. Allen, F.H. and Kennard, O., *Chem. Des. Autom. News*, 1993, **8**, 31.

17. Jones, J.B. and Brown, D.S., *Acta Cryst.*, 1982, **B38**, 317.

18. Neronova, N.N., *Zh. Strukt. Khim.*, 1968, **9**, 147.

19. Ferreira, M.A., Costa, M.D.D., Mendes, I.M.C., Drumond, M.G., Piloveloso, D. and Fernandes, N.G., *Acta Cryst.*, 1998, **C54**, 837.

20. Sartori, G., Maggi, R., Bigi, F., Arienti, A., Casnati, G., Bocelli, G. and Mori, G., *Tetrahedron*, 1992, **48**, 9483.

21. Byrne, J.J., Chavant, P.Y., Averbuch-Pouchot, M.-T. and Vallée, Y., *Acta Cryst.*, 1998, **C54**, 1154.

22. Lin, W.O., da Costa, J.B.N., Alt, H.G. and Rogers, R.D., *Z. Naturforsch., Teil B*, 1989, **44**, 1331.

23. Ottersen, T., *Acta Chem. Scand., Ser. A*, 1977, **31**, 480.

24. Krygowski, T.M., Anulewicz, R., Daniluk, T. and Drapala, T., *Struct. Chem.*, 1989, **1**, 371.

25. Hiller, W., Frey, S., Strahle, J., Boche, G., Zarges, W., Harms, K., Marsch, W., Wollert, R. and Dehnicke, K., *Chem. Ber.*, 1992, **125**, 87.

26. Amstutz, R., Schweizer, W.B., Seebach, D. and Dunitz, J.D., *Helv. Chim. Acta*, 1981, **64**, 2617.

27. Schroder, F.A. and Weber, H.P., *Acta Cryst.*, 1975, **B31**, 1745.

28. Onuma, S. and Shibata, S., *Rep. Fac. Sci., Shizuoka Univ.*, 1978, **12**, 45.

29. Bader, R.F.W., *Atoms in Molecules: A Quantum Theory*, Oxford University Press, Oxford, 1990.

30. Pilkington, M., Wallis, J.D., Smith, G.T. and Howard, J.A.K., *J. Chem. Soc., Perkin Trans. 2*, 1996, 1849.

31. Gilman, H., *J. Am. Chem. Soc.*, 1940, **62**, 344.

Chapter 5

Interactions in 3,3'-Dinitro-2,2'-bipyridine Derivatives

Interactions in 3,3'-Dinitro-2,2'-bipyridine Derivatives

5.1 Introduction

Earlier work in the group had produced three x-ray structures of 3,3'-dinitro-2,2'-bipyridine[1] **1**, its N-oxide **2** and N,N'-dioxide **3**, which appeared to have 1,5 interactions between nitro oxygen atoms and carbon atoms in the 2-position of the opposite pyridine rings. The O----C separations were in the range 2.630(3) – 2.980(3) Å. There were, however, some uncertainties about the structures of the N-oxide **2** and N,N'-dioxide **3**, which were measured at room temperature. In the N-oxide **2** the nitro N,O bonds were of unequal lengths (1.254(3) and 1.232(3) Å, and 1.259(3) and 1.233(3) Å) the difference being 0.022 and 0.026 Å for the two nitro groups. This was thought to be as a result of thermal motion in the crystal, or possibly some disorder with respect to the orientations of the nitro groups. If there was a real structural difference in the N,O bond lengths, then this effect should still be clear when the thermal motion was reduced by a measurement at low temperature. The N,N'-dioxide **3** appeared to have a systematic error in all the thermal vibrational amplitudes, which led to them being elongated in the same sense (Figure 1). The elongation of the ellipsoids could be due to some deficiency in the particular crystal used, a not very secure mounting of the crystal, or maybe inherent in the crystal.

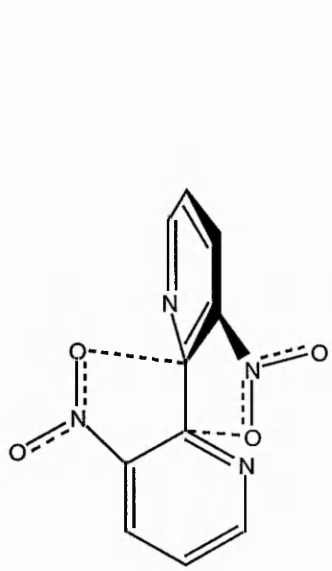

1

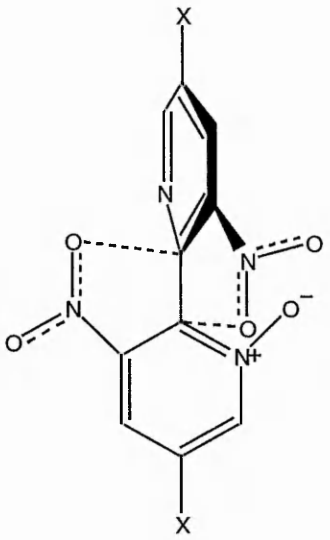

2 R = H
4 R = CH_3

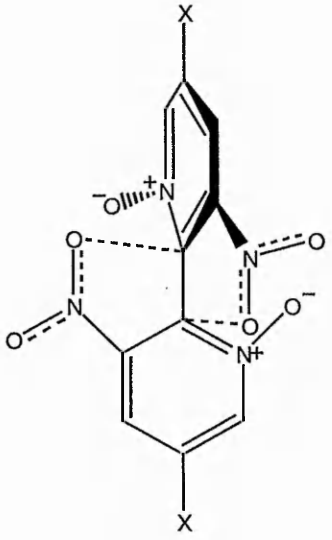

3 R = H
5 R = CH_3

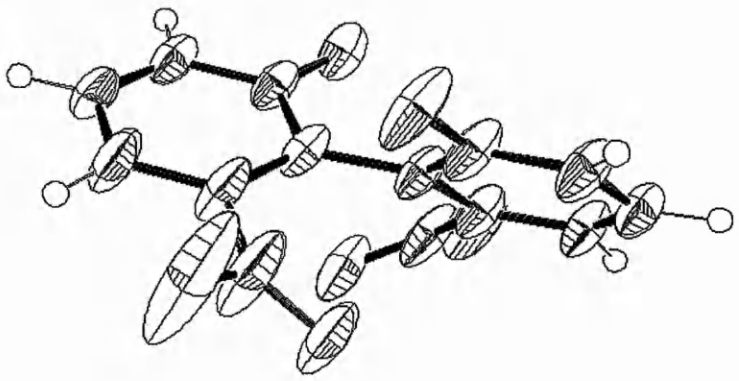

Figure 1 Ortep[2] diagram of **3** showing elongation of the thermal ellipsoids.

5.2 Results and Discussion

It was decided that more crystals of **2** and **3** should be grown and their x-ray structures measured at low temperature in order to obtain data from more ordered and less mobile molecules. It was also hoped that the problem with the room temperature structure of the N,N-dioxide **3** would not occur in a low temperature structure. To obtain more data two new compounds were synthesised, **4** and **5,** which should show similar interactions since they differ by only a remote methyl group from the initial N-oxide and N,N'-dioxide.

Compounds **2** and **3** were synthesised in two steps from 2-chloro-3-nitropyridine **6** (Scheme 1). The first step concerned coupling of the pyridine **6** using the Ullman method of activated Cu powder in DMF under nitrogen to yield the crude product as a solid, which was purified by recrystallisation from ethanol to give 3,3'-dinitro-2,2'-bipyridine[3] **1** as a yellow solid in 73% yield. The second step was oxidation of **1** with 3-chloroperbenzoic acid in chloroform at 34-50°C to give a mixture of the N-oxide and N,N'-dioxide, which were separated on basic alumina using gradient elution (chloroform/methanol, methanol 0-10%) to yield 3,3'-dinitro-2,2'-bipyridine-1-oxide **2** (36%) and 3,3'-dinitro-2,2'-bipyridine-1,1'-dioxide **3** (54%) as yellow solids.

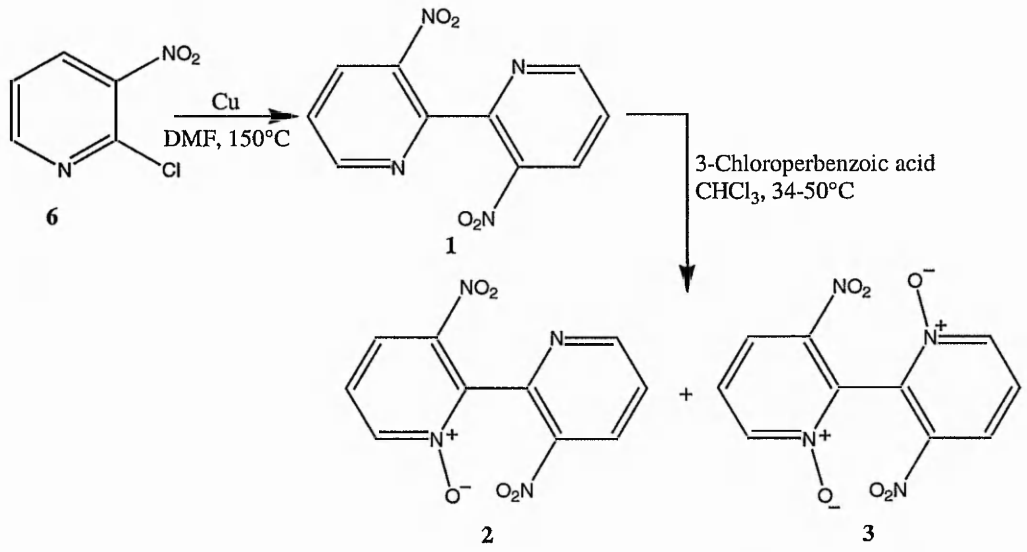

Scheme 1 Preparation of compounds **2** and **3**

The structures of **2** and **3** were supported by their ^{1}H and ^{13}C NMR spectra. There were changes in the shifts of the H and C atoms compared to the parent bipyridine **1**, and the unsymmetrical nature of **2** leads to twice as many resonances as for **1** and **3**. For example the 6,6'-H atoms were observed at δ: 8.87 for **1**, but at δ: 8.82 for **3**, while the 6,6'-C atoms were observed at δ: 152.9 for **1**, but at δ: 144.0 for **3**. It was possible to assign most of the ^{1}H and ^{13}C resonances for **2** and **3** using C-H correlation NMR experiments and by comparing the spectra with those of **4** and **5**. In the infrared spectra of **2** and **3** the antisymmetric nitro N,O bond stretch was observed at 1526 cm^{-1} for **2** and 1536 cm^{-1} for **3**, the corresponding symmetric stretch, however, was not observed. The molecular formulae of **2** and **3** were confirmed by high resolution mass spectrometry.

Compounds **4** and **5** were synthesised in four steps from 2-amino-5-picoline **7**. The first step was nitration of the picoline **7** using a 1:1 mixture of conc. H_2SO_4 and conc. HNO_3 at 0°C, followed by the addition of more conc. HNO_3 at 30°C. The reaction was quenched by slow addition of the reaction mixture to boiling water and then by pouring this mixture on to ice. The precipitated product was collected and purified by recrystallisation from water to yield 2-hydroxy-3-nitro-5-methylpyridine **8** in 37% yield as an orange solid. **8** was refluxed in $POCl_3$ for 6 h. before the excess $POCl_3$ was removed by vacuum distillation and the crude product poured on to ice. The precipitated 2-chloro-3-nitro-5-methylpyridine **9** was isolated as a brown solid in 36% yield. **9** was self-coupled using the Ullmann method with activated copper powder in DMF under nitrogen. The reaction was complete after 6 h., the mixture was poured in to water and the solid material was collected by filtration. On washing with conc. NH_3, water and CH_2Cl_2 the 3,3'-dinitro-5,5'-dimethyl-2,2'-bipyridine **10** product was obtained in 25% yield as a brown solid. The final step was oxidation of **10** with 3-chloroperbenzoic acid in chloroform at 50°C, to give a mixture of the N-oxide and the N,N'-dioxide which were separated on basic alumina using gradient elution (chloroform/methanol, methanol 0-10%) to yield 5,5'-dimethyl-3,3'-dinitro-2,2'-bipyridine-1-oxide **4** in 10% yield and 5,5'-dimethyl-3,3'-dinitro-2,2'-bipyridine-1,1'-dioxide **5** in 17% yield as yellow solids.

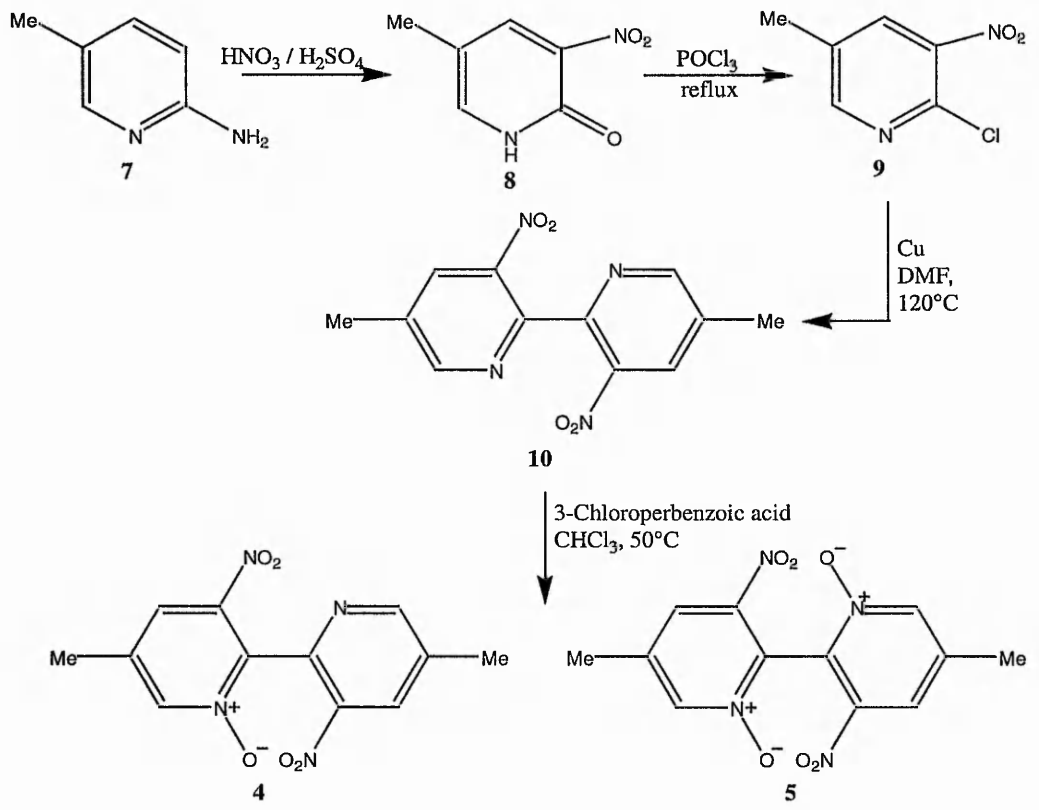

Scheme 2 Preparation of compounds **4** and **5**

The structures of **4** and **5** were supported by ^{1}H and ^{13}C NMR spectra. The methyl groups were observed at δ: 1.86 and δ: 1.79 (**4**) and δ: 1.95 (**5**) in the ^{1}H NMR and δ: 16.4 and 16.2 (**4**) and δ: 18.3 (**5**) in the ^{13}C NMR. In the parent compound **10** these shifts were δ: 2.54 and δ: 17.3. It was possible to assign most of the ^{1}H and ^{13}C resonances for **4** and **5** using C-H correlation NMR experiments and by comparing the spectra with those of compound **2** and **3**. In the infrared spectra of the nitro N,O bond stretches were observed at 1354 cm^{-1} (sym.) and 1542 cm^{-1} (anti.) for **4** and at 1378 cm^{-1} (sym.) and 1549 cm^{-1} (anti.) for **5**. The molecular formulae for **4** and **5** were confirmed by high resolution mass spectrometry.

Crystals of **2-5** were prepared by slow evaporation of solutions in appropriate solvents. The crystals were observed under a polarising light microscope and those which showed uniform extinction of light when rotated through crossed polar lenses were selected and, if necessary, cut to size. X-ray diffraction data was collected at the EPSRC X-ray Crystallography Service in Southampton University at 150 K (**2** and **3**) and 120 K (**4** and **5**) and processed at the Nottingham Trent University using the SHELXS-97[4] and SHELXL-97[5] programs. The results for **2-5** are shown in the ORTEP[2] diagrams in Figures 2-5 and the crystal packing diagrams in Section 5.3 towards the end of this chapter. Selected molecular geometric data are given in Table 1. The low temperature structure of **2** shows almost symmetrical nitro groups, the N,O bond lengths are 1.225(2) and 1.218(2) Å, and 1.229(2) and 1.223(2) Å. Thus the inequality in the N,O bond lengths at room temperature was as a result of thermal motion and is not a problem at 150 K. The low temperature structure of **3**, however, shows the same systematic error as that in the room temperature structure. The structure was refined to an R factor of 5.7% using a triclinic cell of dimensions 6.1226 x 7.4847 x 13.5200 $Å^3$, α = 102.8525, β = 90.226, γ = 111.154, but the ellipsoids were systematically elongated. However, extra spots are present in the diffraction pattern of **3** and a very large cell of dimensions 20.3578 x 22.7139 x 22.7139 $Å^3$ α = 89.5742, β = 87.1617, γ = 74.5216 can be used to index them. This cell would contain over 30 molecules and solution would be an extremely difficult laborious process. No full understanding of this problem has been obtained, but it is possible that some sort of superstructure exists. However, despite this problem the overall molecular conformation must be approximately correct to refine to an R factor of *ca.* 6% using the main diffraction spots.

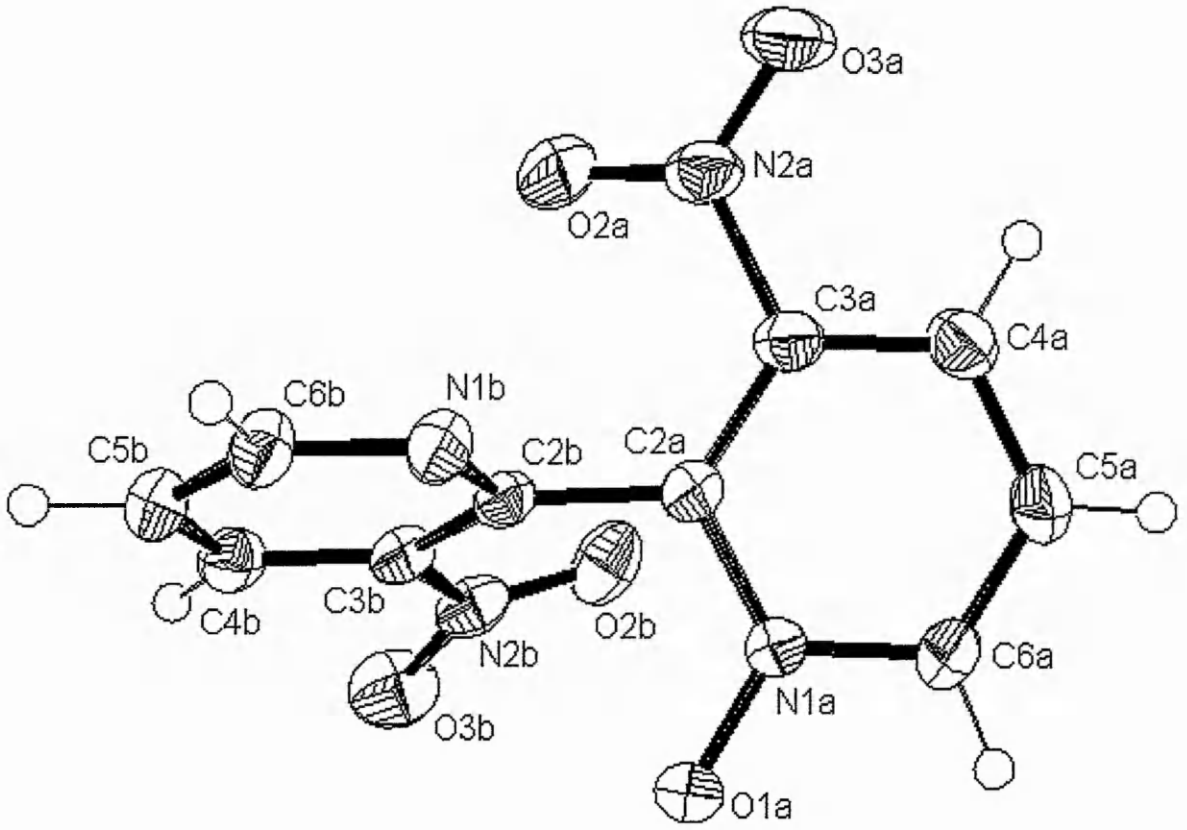

Figure 2 Molecular structure of **2** with anisotropic displacement parameters at the 50% level.

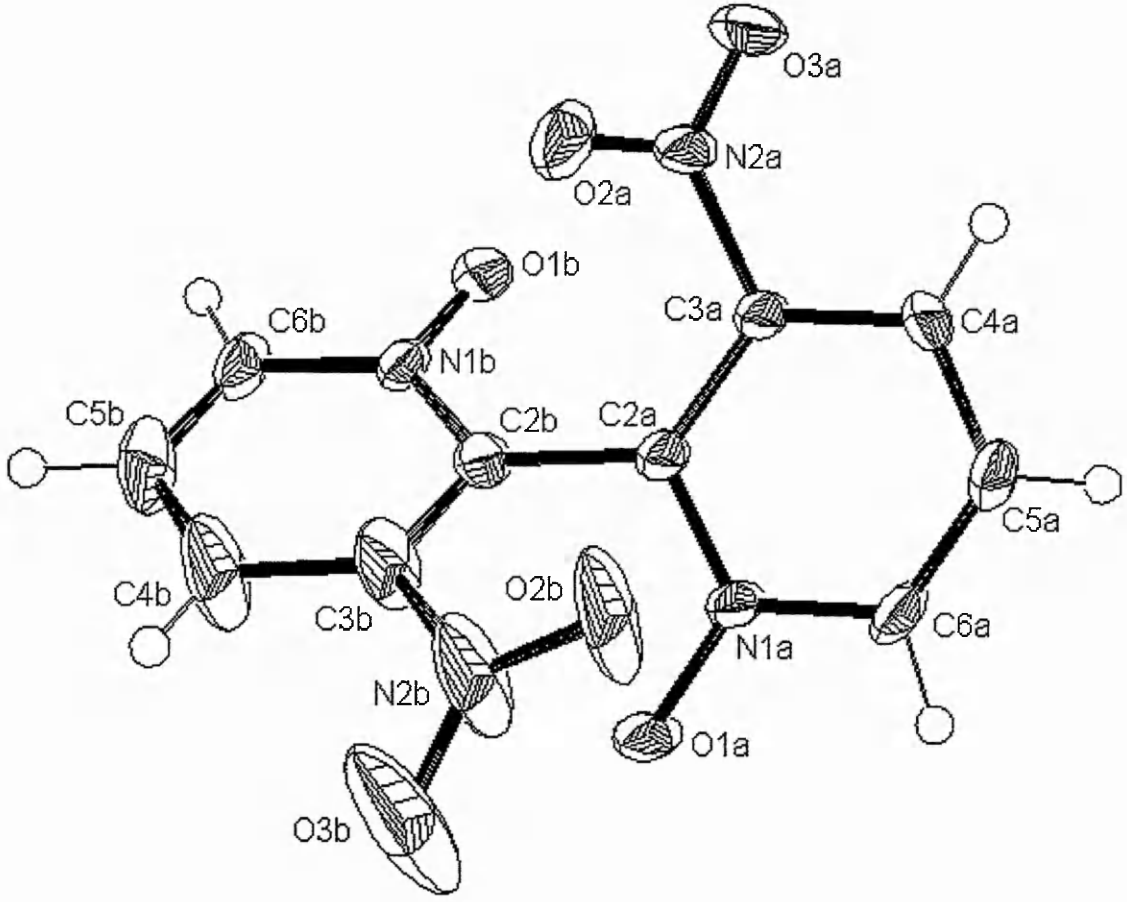

Figure 3 Molecular structure of **3** with anisotropic displacement parameters at the 50% level.

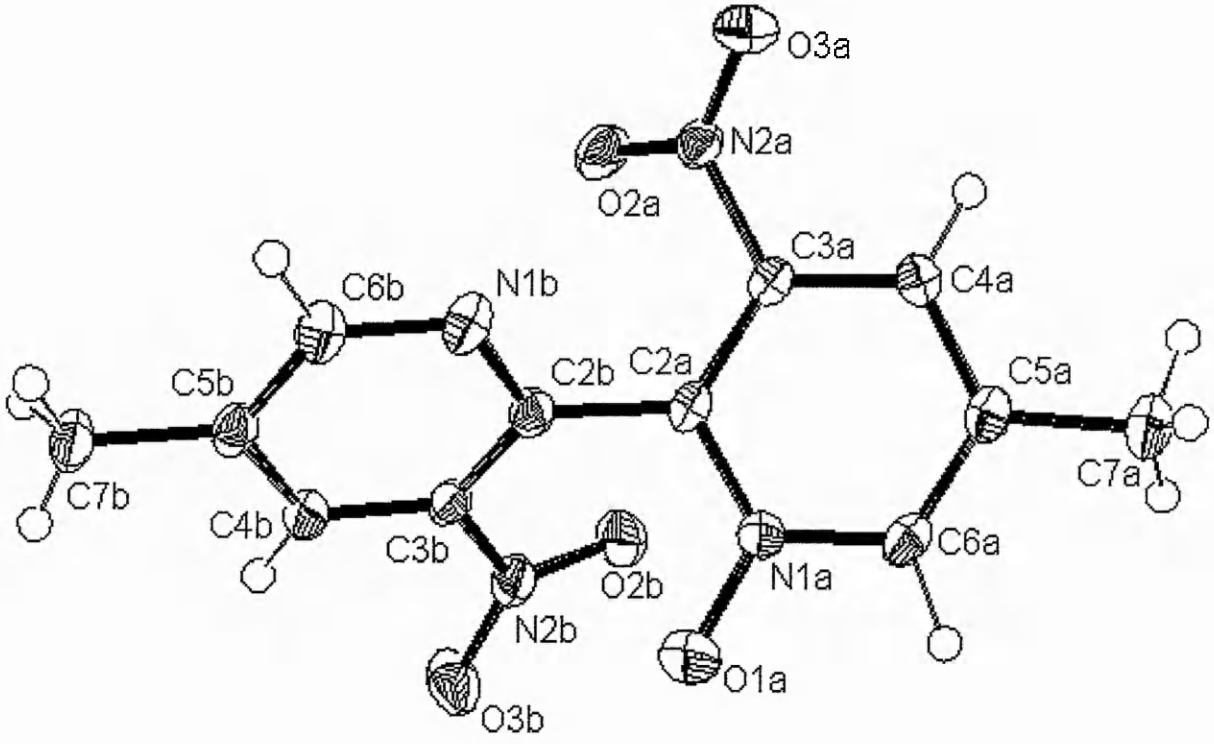

Figure 4 Molecular structure of **4** with anisotropic displacement parameters at the 50% level.

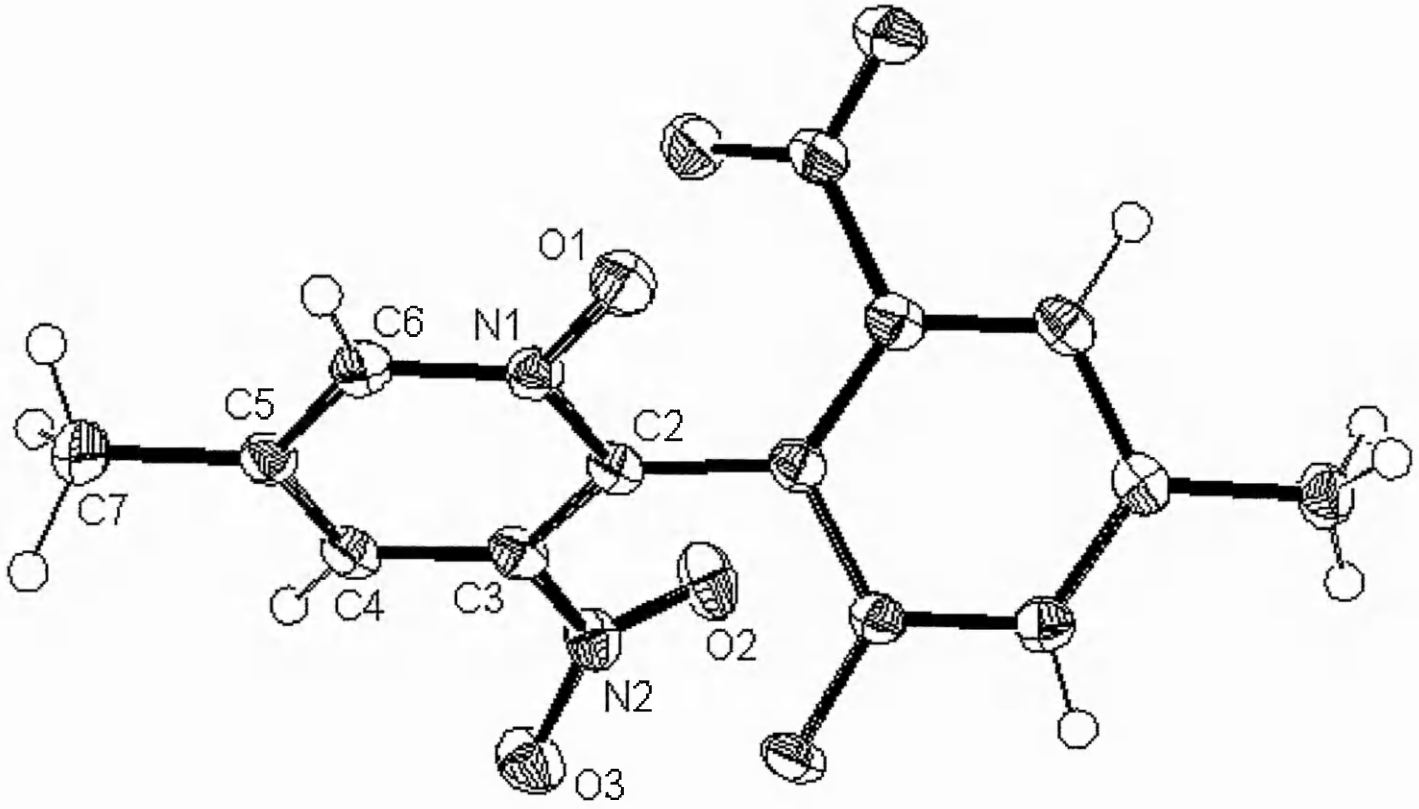

Figure 5 Molecular structure of **5** with anisotropic displacement parameters at the 50% level.

Table 1 Selected geometric data for compounds **1 – 5** (Å, °)

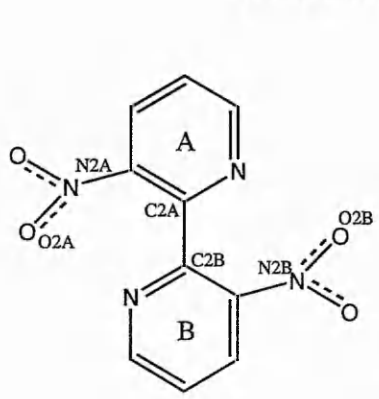

1

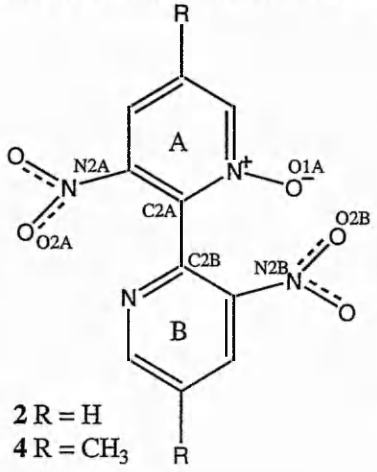

2 R = H
4 R = CH_3

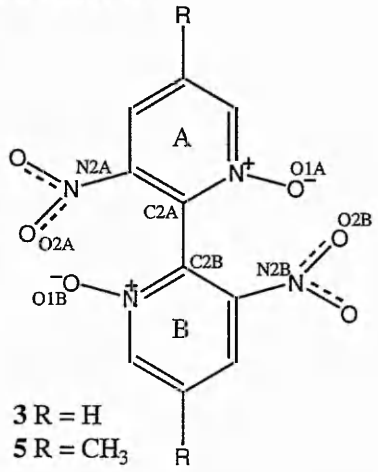

3 R = H
5 R = CH_3

	O2A----C2B	O2B----C2A	O1A----N2B	O1B----N2A	angle ring (A) / ring (B)	angle ring (A) / NO_2 (A)	angle ring (B) / NO_2 (B)
1[1]	2.916(2)	2.980(2)	-	-	42.9(1)	42.8(1)	52.0(1)
2	2.644(2)	2.623(2)	3.140(2)	-	72.22(5)	18.2(2)	19.8(2)
3	2.772(3)	2.762(4)	2.772(6)	2.804(3)	55.8(1)	35.3(3)	33.3(3)
4	2.839(2)	2.726(2)	2.874(3)	-	55.9(1)	40.9(1)	22.8(2)
5	2.789(3)	*	2.737(3)	*	52.84(5)	36.9(2)	*

* Only half of **5** is crystallographically unique

All five bipyridine compounds **1-5** show short contacts between nitro O atoms and the 2-C atom of the distant pyridine ring in the range 2.623(2) – 2.980(2) Å. The shortest O----C contacts occur in the monoxide **2** (Figure 6), 2.623(2) Å between O2B and C2A and 2.644(2) Å between O2A and C2B. There is not much difference between the two contacts, hence the presence of an oxide in the 1-position of the pyridine ring serves to decrease both O---C separations *cf.* O---C separations of 2.916(2) and 2.980(2) Å in the parent dinitrobipyridine **10**. The O----C separation is controlled only by the orientation of the nitro group with respect to the adjacent pyridine ring and would be a minimum if the nitro group was coplanar with its pyridine ring. In **2** the nitro groups are close to the plane of the pyridine rings, the angles between the two groups are 18.2(2) and 19.8(2)° and the pyridine rings lie at 72.22(5)° to each other.

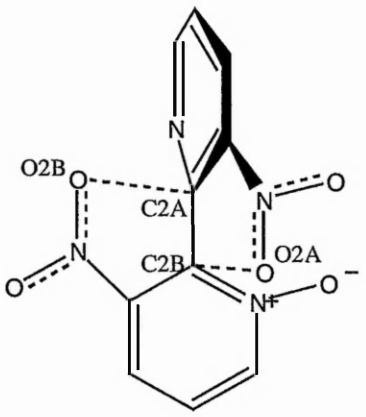

Figure 6 O----C contacts in the monoxide **2**

In the dioxide **3** the O----C separations are 2.772(3) and 2.762(4) Å, which are significantly longer than those in **2**. The nitro groups lie at 35.3(3) and 33.3(3)° to their attached pyridine rings and the pyridine rings lie at 55.8(1)° to each other. In

this structure there are also close contacts between the electron-rich oxide O1 atoms and the electron-deficient nitro N2 atoms, the O----N separations are 2.772(6) and 2.804(3) Å. In **2** the corresponding O----N separation is 3.140(2) Å, which is at van der Waals separation. These short O----N contacts in **3** are achieved by rotation of the nitro groups out of the pyridine ring planes and the relatively small inter-ring angle.

The dimethyl analogue of **3**, compound **5**, shows similar O----C contacts to those of **3**, the separations are 2.789(3) Å. The nitro groups lie at 36.9(2)° to the attached pyridine rings and the pyridine rings lie at 52.84(5)° to each other. In **5** there are O----N contacts of length 2.737(3) Å, which are similar to those found in **3**. The structure of **4** might be expected to be similar to that of **2** and show similar O----C contacts since the only difference between the two is the presence of methyl groups in the 5-position of each pyridine ring, however, this is not the case. The two O----C separations in **4** are significantly longer, and different from each other, at 2.726(2) and 2.839(2) Å. They are brought about by angles of 22.8(2) and 40.9(1)° respectively between the nitro groups and their attached pyridine rings. The inter-ring angle is 55.9(1)°. It seems that one nitro group lies close to the plane of the adjacent pyridine ring and one of its O atoms is involved in the shorter contact with the 2-C atom of the distant pyridine ring while the other nitro group is rotated more out of the aromatic plane and the O----C separation is much longer. There is a close contact between the oxide O1 atom and the nitro N2 atom of 2.874(3) Å, surprisingly this close contact involves the same nitro group that is involved in the shorter O----C interaction. It might have been expected that the nitro group that is rotated out of the aromatic plane

may be involved in a close contact to the oxide O1 atom, similar to those observed in compounds **3** and **5**, however this is not the case.

A survey of *ortho*-nitrobiphenyls in the CSD[6] was performed. There are several compounds that show short 1,5 NO_2----sp^2C contacts (Figure 7) similar to the 2,2'-dinitrobipyridine derivatives **1-5**. There is a notable difference between compounds with no further *ortho* substituents (of which there are six examples, the O----C distances are in the range 2.9-3.1 Å and the inter-ring angles are 44-63°)[7] and those where the second ring carries one *ortho* NO_2 or CO_2H group (of which there are four examples, the O----C distances are in the range 2.6-2.8 Å and the inter-ring angles are 56-96°)[7d,8]. The second *ortho* substituent favours a closer NO_2----C contact between the two halves of the molecule accompanied by a small increase in the inter-ring angle.

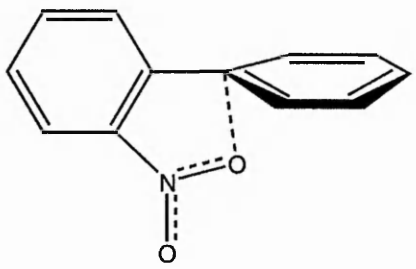

11 O----C 2.88 Å

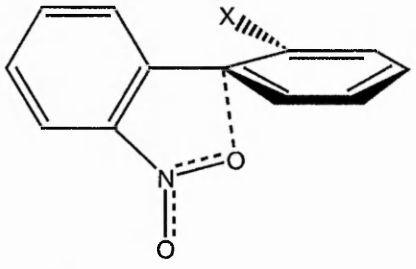

12 X = NO_2 O----C 2.81 Å
13 X = CO_2H O----C 2.73 Å

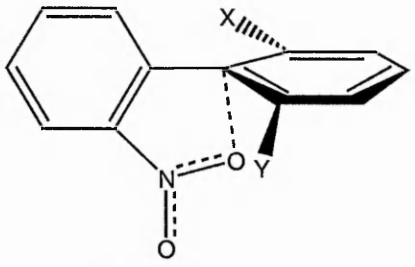

14 X = NO_2 Y = CO_2H O----C 2.66 Å

Figure 7 NO_2----sp^2C interactions in some 2-nitrobiphenyl derivatives.

A possible explanation is that the second substituent delocalises charge away from the 2'-C making it more attractive to an electron rich O atom, this is illustrated below (Figure 8). The increase in inter-ring angle would not have been expected on steric grounds alone, as one would expect the steric interactions in 2-nitrobiphenyl and 2,2'-dinitrobiphenyl to be similar.

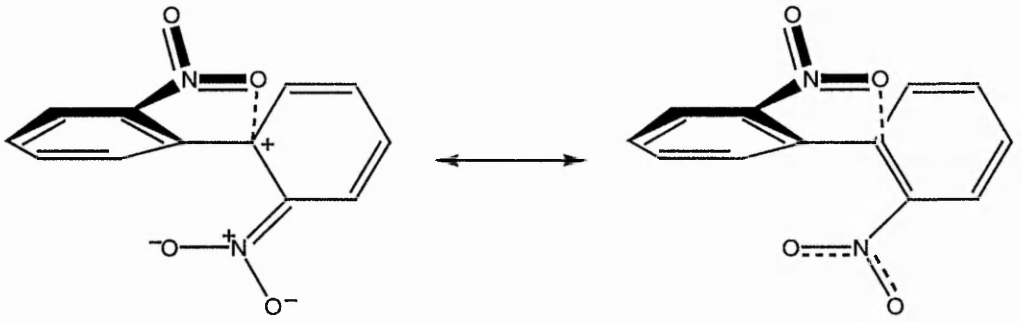

Figure 8 Charge delocalisation due to NO_2----sp^2C interactions in biphenyls.

For compounds with one or two further NO_2 and/or CO_2H groups the shorter NO_2----sp^2C contact is retained (2.6-2.8 Å)[8a,9], but with the inter-ring angle nearer to 90°. In these compounds there is at least one steric interaction between two functional groups, which favours the near perpendicular arrangement.

In summary, of the 2-nitrobiphenyl derivatives in the CSD, those without another *ortho* NO_2 or CO_2H substituent always show a longer O----C contact by *ca.* 0.2 Å than those with two or more such groups.

It seems, at first glance, that compounds **1**, **2**, **3** and **5** show a trend of increasing O----C separation from the monoxide **2** to the dioxides **3** and **5** to the parent

dinitrobipyridine **1**. The trend of increasing O----C separation is accompanied by rotation of the nitro groups out of the adjacent pyridine ring planes (18.2(2)-52.0(1)°) and by a decreasing inter-ring angle (72.22(5)-42.9(1)°). Compound **4** does not fit this trend, as one would predict the interactions in **4** to be similar to those in **2**, but this is not the case. The presence of a second interaction, between the oxide O1 atoms and the nitro N2 atoms disrupts this trend. It appears that in the monoxide **2** the O----C interaction dominates and the geometry is such that the O----N distance is at van der Waals separation. In the dioxides **3** and **5** and the monoxide **4** both O----C and O----N contacts are present and are possibly in competition with each other.

In conclusion this family of structures **1-5** all show 1,5 interactions between one nitro O atom per nitro group and the 2-C of the opposite pyridine ring. The interactions are more significant as the angle between the aromatic rings increases, and the angle between the nitro group and the adjacent aromatic ring decreases. The shortest contacts (2.623(2) and 2.644(2) Å for **2**) are similar to those in compounds **15-18** below where the O----C separations are 2.642(2) Å for **15**[10], 2.636(2) Å for **16**[11], 2.611(1) Å for **17**[12] and 2.606(5) and 2.644(5) Å for the two independent molecules of **18**[13].

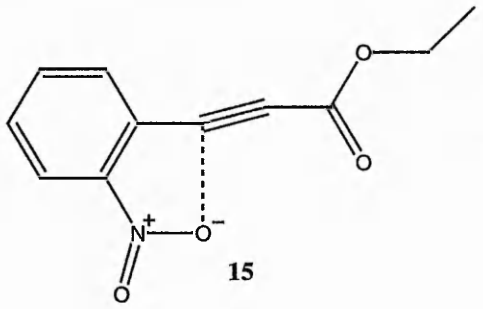

15

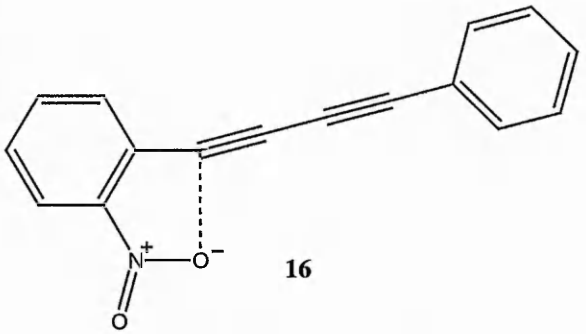

16

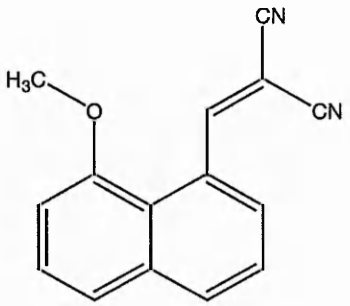

17

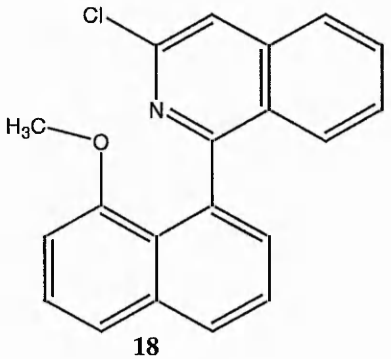

18

The dinitrobipyridine **1** compares more closely to the *ortho*-nitrobiphenyl derivatives with no additional *ortho* substituent, than with the 2,2'dinitrobiphenyls. However, the lack of any *ortho* substituent on the ring N atoms accounts for the interplanar angle of only 42.9(1)°. The addition of one or two oxide substituents, providing steric repulsion increases this angle (52.8-72.2°). The distinct difference between the conformations of the 2-nitrobiphenyls and those of 2,2'-dinitro and 2-nitro-2'-carboxyl biphenyls suggests that there is an element of cooperativity between the pair of interactions.

5.3 Crystal Packing

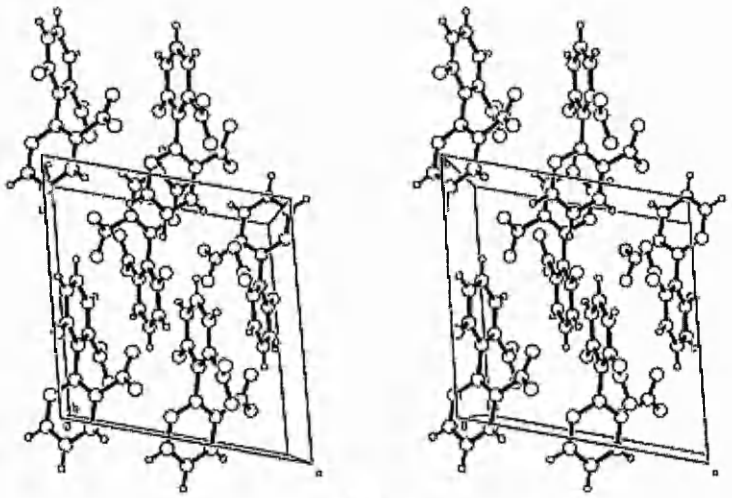

(a)

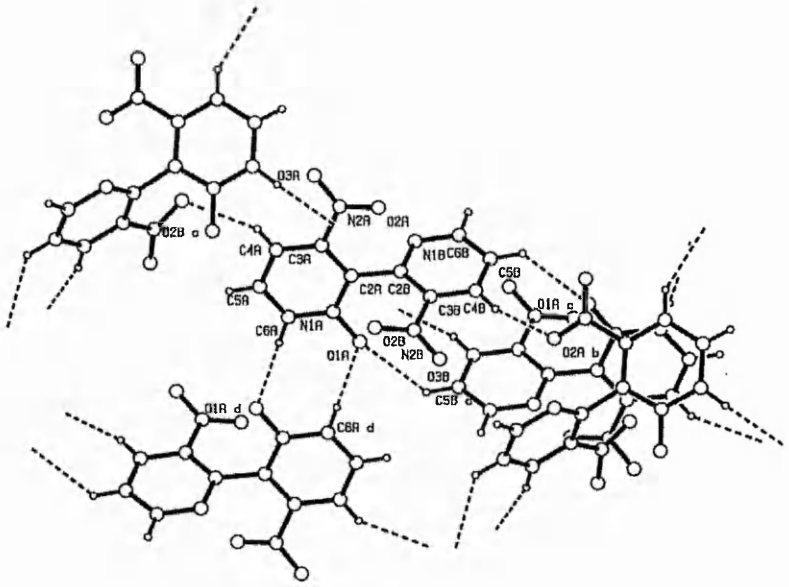

(b)

Figure 9 Crystal packing of **2** at 150 K (a) in the unit cell and (b) intermolecular contacts

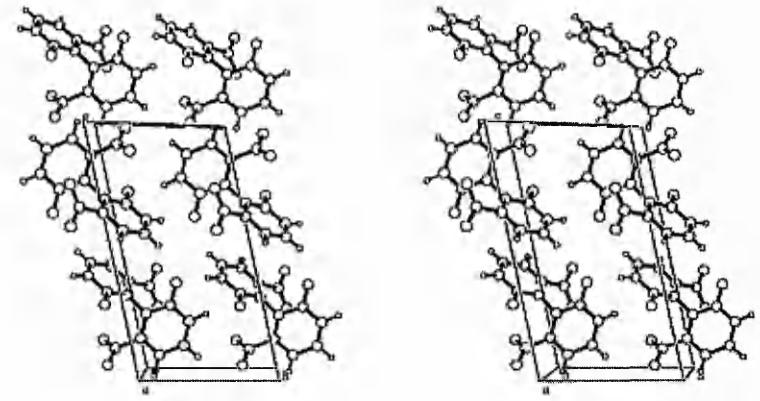

(a)

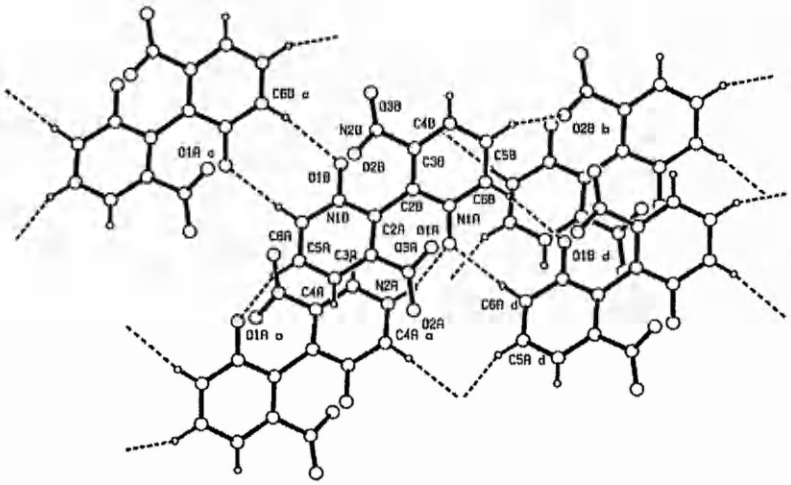

(b)

Figure 10 Crystal packing of **3** at 150 K (a) in the unit cell and (b) intermolecular contacts

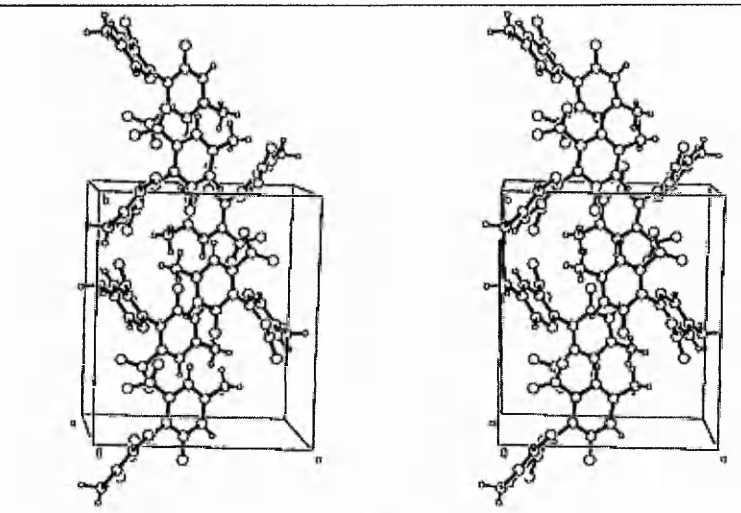

(a)

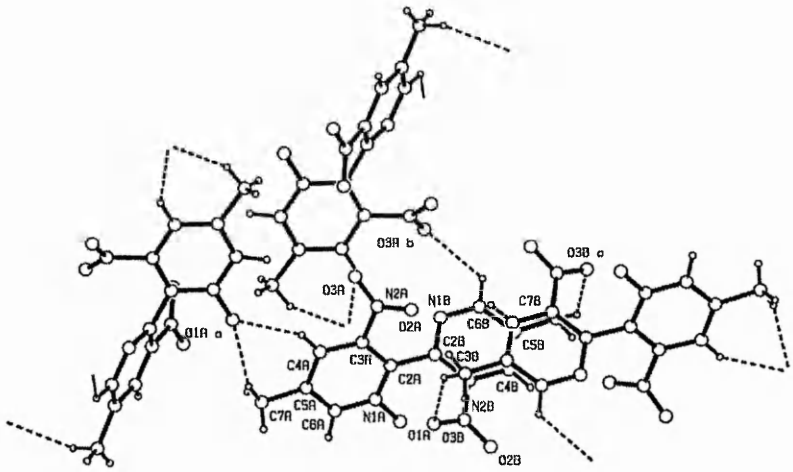

(b)

Figure 11 Crystal packing of **4** at 120 K (a) in the unit cell and (b) intermolecular

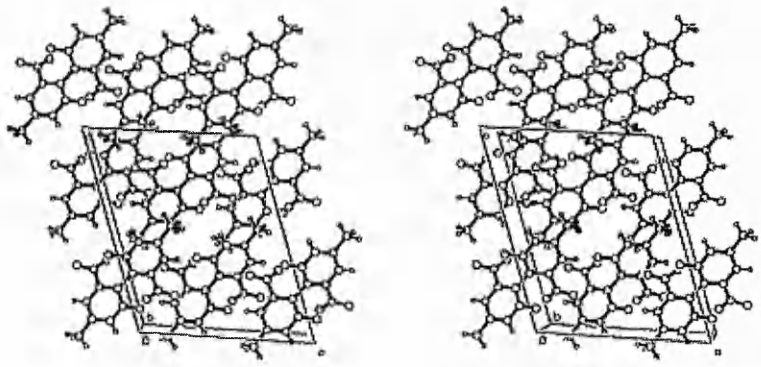

(a)

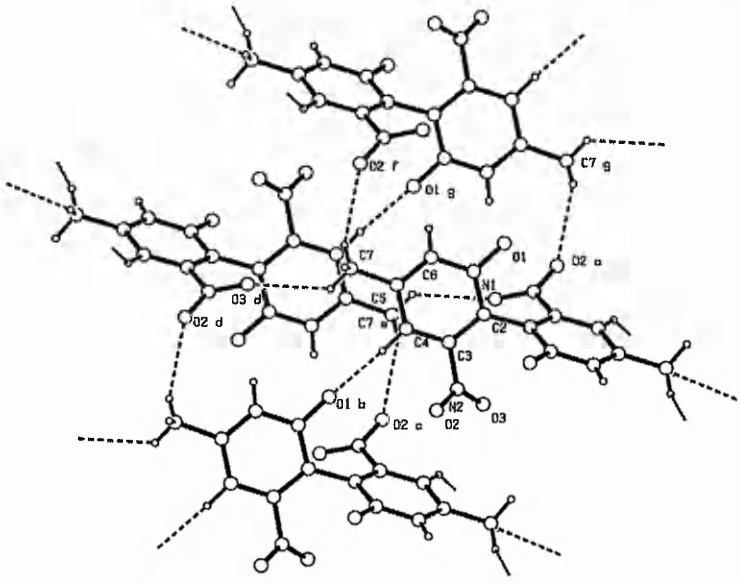

(b)

Figure 12 Crystal packing of **5** at 120 K (a) in the unit cell and (b) intermolecular

The crystal packing in compounds **2-5** is similar in such that there are an array of intermolecular hydrogen bonds between nitro oxygen atoms and aromatic hydrogen atoms in the range 2.35(2) – 2.51(2) Å, N-oxide oxygen atoms and aromatic hydrogen atoms in the range 2.28(4) – 2.53(2) Å and for compounds **4** and **5** between methyl hydrogen atoms and both nitro and N-oxide oxygen atoms in the range 2.39(4) – 2.50(4) Å.

5.4 Experimental

Preparation of 3,3′-Dinitro-2,2′-bipyridine **1**[3]

2-Chloro-3-nitropyridine **6** (2.0 g, 12.6 mmol) was reacted with freshly activated copper bronze (2.0 g) in dry DMF (40 ml) at 150°C under nitrogen. After 2 h. tlc (SiO_2, CH_2Cl_2) indicated that the starting material had been consumed. The resulting mixture was poured into water (40 ml), the solid filtered immediately and then washed with concentrated ammonia (2 x 20 ml). The remaining solid was then extracted into boiling dioxane (2 x 150 ml) stirring for about 20 mins. each time. After evaporating the combined extracts to dryness, the solid was recrystallised from ethanol to give 3,3′-dinitro-2,2′-bipyridine **1** (1.16 g, 73%), as a yellow solid, m.p. 205-206°C; ^{1}H NMR ($CDCl_3$) δ: 8.87 (2H, dd, J = 4.7, 1.7, 6-,6'-*H*) ; 8.58 (2H, dd, J = 8.4, 1.5, 4-,4'-*H*) ; 7.65 (2H, m, 5-,5'-*H*); ^{13}C NMR ($CDCl_3$) : 152.9 (6-,6'-*C*), 150.7 (2-,2'*C*), 144.0 (3-,3'-*C*), 133.1 (4-,4'-*C*), 124.6 (5-,5'-*C*); ν_{max}/cm^{-1}: 3084, 1590, 1561, 1534, 1440, 1417, 1366, 1048, 1038, 865, 855, 821, 790, 751, 621, 529.

Preparation of 3,3'-Dinitro-2,2'-bipyridine-1-oxide **2** and 3,3'-Dinitro-2,2'-bipyridine-1,1'-dioxide **3**

3-Chloroperbenzoic acid (5.98g, 58-84% purity, Aldrich) dissolved in chloroform (60 ml) was added to a solution of 3,3'-dinitro-2,2'-bipyridine **1** (2.0 g, 8.12 mmol) in chloroform (140 ml) at 0°C and stirred for 3 h., then stirred at 34°C overnight. Tlc ($CHCl_3$ with 5% CH_3OH) indicated formation of the monoxide as the main product. More peracid (1.70 g) in chloroform (25 ml) was added and the mixture stirred at

50°C overnight. The mixture was poured on to a basic alumina column and subjected to gradient elution (chloroform/methanol, methanol 0-10%) to give the monoxide **2** (0.77 g, 36%) and the dioxide **3** (1.23 g, 54%) as separate fractions.

3,3'-Dinitro-2,2'-bipyridine-1-oxide **2**

m.p. 184-188°C; ν_{max}/cm^{-1}: 1600, 1526, 1262, 1028, 864, 824, 815, 766, 738 cm^{-1}; ^1H NMR (DMSO-d_6) δ: 9.03 (1H, dd, J = 4.7, 1.2 Hz, 6'-*H*), 8.81 (1H, dd, J = 8.4, 1.2 Hz, 4'-*H*), 8.76 (1H, dd, J = 6.4, 0.7 Hz, 6-*H*), 8.28 (1H, dd, J = 8.6, 0.7 Hz, 4-*H*), 7.97-7.85 (2H, m, 5,5'-*H*); ^{13}C NMR (DMSO-d_6) δ: 154.3 (6'-*C*), 147.0 (Ar-C_1), 145.5 (Ar-C_1), 143.4 (6-*C*), 142.7 (Ar-C_1), 142.0 (Ar-C_1), 133.2 (4'-*C*), 126.9 (5- or 5'-*C*), 126.4 (5- or 5'-*C*), 122.2 (4-*C*); HRMS (EI): Found: 262.0338, $C_{10}H_6N_4O_5$ requires: 262.0338.

Crystal data for **2**: $C_{10}H_6N_4O_5$, M_r = 262.03, monoclinic, a = 9.873(2), b = 10.671(2), c = 10.577(7) Å, β = 104.583(30)°, V = 1078.47 $Å^3$, Z = 4, $P2_1/a$, D_c = 1.61 gcm^{-3}, μ (MoKα) = 0.13 mm^{-1}, 2430 unique reflections, 1820 with $F_o > 4\sigma(F_o)$, R = 0.046. Full data available on the crystallographic information file on the disk provided.

3,3'-Dinitro-2,2'-bipyridine-1,1'-dioxide **3**

m.p. 202-206°C; ν_{max}/cm^{-1} (nujol): 1555, 1536, 1419, 1278, 1258, 1020, 804, 726; ^1H NMR (DMSO-d_6) δ: 8.82 (2H, dd, J = 6.6, 0.7 Hz , 6-,6'-*H*), 8.32 (2H, dd, J = 8.5, 0.7 Hz, 4-,4'-*H*), 7.92 (2H, dd, J = 8.5, 6.6 Hz, 5-,5'-*H*); ^{13}C NMR (67.8 MHz, (DMSO-d_6) δ: 147.1 (2-,2'- or 3-,3'-*C*), 144.0 (6-,6'-*C*), 135.5 (2-,2'- or 3-,3'-*C*), 127.6 (5-,5'-*C*), 121.8 (4-,4'-*C*); HRMS (EI): Found: 278.0287, $C_{10}H_6N_4O_6$ requires: 278.0287.

Crystal data for **3**: $C_{10}H_6N_4O_6$, M_r = 278.03, triclinic, a = 6.1226 (3), b = 7.4847(4), c = 13.5200(8) Å, α = 102.8252(2) β = 90.226(2), γ = 111.154(3)°, V = 560.99 Å^3, Z = 2, P$\bar{1}$, D_c = 1.65 gcm^{-3}, μ (MoKα) = 0.14 mm^{-1}, 1916 unique reflections, 1279 with $F_o > 4\sigma(F_o)$, R = 0.057. Full data available on the crystallographic information file on the disk provided.

Preparation of 5-Methyl-3-nitro-pyridin-2-one **8**

2-Amino-5-picoline **7** (10.1 g, 93 mmol) was slowly added to conc. H_2SO_4 (48 ml). The mixture was cooled to 0°C before a mixture of conc. H_2SO_4 (7 ml) and conc. HNO_3 (7 ml) was added slowly. The mixture was allowed to warm to room temperature and stirred overnight. The mixture was then heated to 30 °C for 1 h., conc. HNO_3 (7 ml) was slowly added and the mixture stirred at this temperature for a further 1 h. The mixture was slowly added to boiling water (20 ml) and then this mixture was poured on to ice. The resulting precipitate was filtered and recrystallised from water to yield the product **8** as an orange solid (5.39 g, 37%), m.p. 248-250°C; ^{1}H NMR ($CDCl_3$ + DMDO-d_6) δ: 7.74 (1H, s, 6-*H*), 6.96 (1H, s, 4-*H*), 1.62 (3H, s, C*H*$_3$); ^{13}C NMR ($CDCl_3$ + DMDO-d_6) δ: 154.5 (2-*C*), 141.8 (3- or 4-*C*), 140.8 (3- or 4-*C*), 137.4 (5-*C*), 113.1 (6-*C*), 16.3 (*C*H$_3$).

Preparation of 2-Chloro-5-methyl-3-nitropyridine **9**

A mixture of 5-methyl-3-nitropyridin-2-one **8** (5.39 g, 35mmol) and $POCl_3$ (40 ml) was refluxed for 6 h. The excess $POCl_3$ was removed by vacuum distillation and the crude product poured on to ice. The resulting precipitate was collected by filltation to yield the product **9** as a pale brown solid (2.16 g, 36%), m.p. 50-52°C; ^{1}H NMR

($CDCl_3$) δ: 8.45 (1H, s, 6-*H*), 8.05 (1H, s, 4-*H*), 2.47 (3H, s, C*H*$_3$); ^{13}C NMR ($CDCl_3$) δ: 152.8 (6-*C*), 144.2 (2- or 3-*C*), 140.4 (2- or 3-*C*), 134.4 (4- or 5-*C*), 134.0 (4- or 5-*C*), 17.5 (*C*H_3).

Preparation of 5,5'-Dimethyl-3,3'-dinitro-2,2'-bipyridine **10**

2-Chloro-5-methyl-3-nitropyridine **9** (2.16 g, 12.5 mmol) was reacted with freshly activated copper bronze (2.0 g) in dry DMF (40 ml) at 120°C under nitrogen. After 6 h. the mixture was poured into water (150 ml), the solid filtered immediately and then washed with concentrated ammonia, water and CH_2Cl_2, to yield the product **10** as a brown solid (0.84 g, 24.5%), m.p. 194-196°C; ^{1}H NMR ($CDCl_3$ + DMSO-d_6) δ: 8.69 (2H, s, 6,6'-*H*), 8.41 (2H, s, 4,4'-*H*), 2.54 (6H, s, 2 x C*H*$_3$); ^{13}C NMR ($CDCl_3$ + DMSO-d_6) δ: 152.7 (6,6'-*C*), 146.9 (2,2'-*C*), 143.8 (3,3'-*C*), 135.0 (4,4'-*C*), 132.7 (5,5'-*C*), 17.3 (*C*H_3).

Preparation of 5,5'-Dimethyl-3,3'-dinitro-2,2'-bipyridine-1-oxide **4** and 5,5'-Dimethyl-3,3'-dinitro-2,2'-bipyridine-1,1'-dioxide **5**

3-Chloroperbenzoic acid (1.75 g, 10 mmol) was slowly added to a solution of 5,5'-dimethyl-3,3'-dinitro-2,2'-bipyridine **10** (0.84 g, 3 mmol) in $CHCl_3$ (30 ml) at 0°C. The mixture was allowed to warm to room temperature then heated to 50°C for 3 h. before being left to stir at room temperature for 48 h. The mixture was poured on to a basic alumina column and subjected to gradient elution ($CHCl_3$/CH_3OH, CH_3OH 0-10%) to give the monoxide **4** (0.09 g, 10%) and the dioxide **5** (0.16 g, 17%).

5,5'-Dimethyl-3,3'-dinitro-2,2'-bipyridine-1-oxide **4**

m.p. 211-214°C (melted to a dark brown liquid); ν_{max}/cm^{-1} (KBr): 3035, 2925, 1624, 1542, 1458, 1354, 1289, 1219, 1153, 1027, 863, 780; ^1H NMR (DMSO-d_6) δ: 8.82 (1H, s, 6'-*H*), 8.64 (1H, s, 4'-*H*), 8.60 (1H, s, 6-*H*), 8.13 (1H, s, 4-*H*), 2.51 (3H, s, C*H*$_3$), 2.43 (3H, s, C*H*$_3$); ^{13}C NMR (DMSO-d_6) δ: 154.3 (6'-*C*), 146.6, 145.3 (2 of 2-, 2'-, 3-, 3'-*C*), 142.7 (6-*C*), 139.8, 139.4 (2 of 2-, 2'-, 3-, 3'-*C*), 137.9 (5- or 5'-*C*), 137.1 (5- or 5'-*C*), 132.9 (4'-*C*), 122.9 (4-*C*), 17.6 (*C*H$_3$), 17.5 (*C*H$_3$). HRMS (ES): Found: 291.0739 $(M+H)^+$, $C_{12}H_{10}N_4O_5$ requires: 291.0729 $(M+H)^+$.

Crystal data for **4**: $C_{12}H_{10}N_4O_5$, M_r = 262.18, monoclinic, a = 8.1670(3), b = 13.4699(6), c = 11.3597(6) Å, β = 94.750(2)°, V = 1245.37 Å^3, Z = 4, $P2_1/a$, D_c = 1.55 gcm^{-3}, μ (MoKα) = 0.12 mm^{-1}, 2826 unique reflections, 1949 with $F_o > 4\sigma(F_o)$, R = 0.055. Full data available on the crystallographic information file on the disk provided.

5,5'-Dimethyl-3,3'-dinitro-2,2'-bipyridine-1,1'-dioxide **5**

m.p. decomposed at 211°C; ν_{max}/cm^{-1} (KBr): 3051, 1654, 1617, 1549, 1442, 1378, 1260, 1295, 1225, 1159, 1019, 911, 875, 782, 754; ^1H NMR (DMSO-d_6) δ: 8.72 (2H, s, 6-,6'-*H*), 8.23 (2H, s, 4-,4'-*H*), 2.45 (6H, s, 2 x C*H*$_3$); ^{13}C NMR (DMSO-d_6) δ: 147.3 (2-,2' or 3-,3'-*C*), 144.0 (6-,6'-*C*)*, 139.5 (5-,5'-*C*), 133.4 (2-,2'- or 3-,3'-*C*), 124.4 (4-,4'-*C*)*, 18.2 (2 x *C*H$_3$). HRMS (ES): Found: 307.0682 $(M+H)^+$, $C_{12}H_{10}N_4O_6$ requires: 307.0679 $(M+H)^+$. * Confirmed by C-H correlation.

Crystal data for **5**: $C_{12}H_{10}N_4O_6$, $M_r = 278.18$, monoclinic, $a = 12.044(4)$, $b = 7.544(3)$, $c = 15.093(5)$ Å, $\beta = 108.480(3)°$, $V = 1300.66$ Å^3, $Z = 4$, C2/c, $D_c = 1.56$ gcm^{-3}, μ (MoKα) = 0.13 mm^{-1}, 1465 unique reflections, 1275 with $F_o > 4\sigma(F_o)$, $R = 0.063$. Full data available on the crystallographic information file on the disk provided.

5.5 References

1. Rice, C.R., Wallis, J.D. and Povey, D.C., *Acta Cryst.*, 1992, **C48**, 1988.
2. Johnson, C.K. and Burnett, M.N., ORTEPIII, Report ORNL-6895, 1996, Oak Ridge National Laboratory, Tennessee, USA.
3. Kanoktaporn, S. and MacBride, J.A.H., *J. Chem. Soc., Perkin Trans. 1*, 1978, 1126.
4. Sheldrick, G.M., SHELXS-97, Program for the Solution of Crystal Structures, 1997, University of Göttingen, Germany.
5. Sheldrick, G.M., SHELXL-97, Program for Crystal Structure Refinement, 1997, University of Göttingen, Germany.
6. Allen, F.H. and Kennard, O., *Chem. Des. Autom. News*, 1993, **8**, 31.
7. a) Sutherland, H.H., Hogg, J.H.C. and Williams, D.J., *Acta Cryst.*, 1974, **B30**, 1562.

   b) Nafissi-V, M.M., Koharski, D.P., Puar, M.S. and McPhail, A.T., *J. Org. Chem.*, 1982, **47**, 3345.

   c) Zimmermann, T. and Pink, M., *Liebigs Ann. Chem.*, 1993, 1145.

   d) Sekine, A., Ohashi, Y., Yoshimura, K., Yagi, M. and Higuchi, J., *Acta Cryst.*, 1994, **C50**, 1101.

   e) Fallon, L. and Ammon, H.L., *J. Cryst. Mol. Struct.*, 1974, **4**, 63.

   f) Anulewicz, R., Pniewska, B. and Milart, P., *Acta Cryst.*, 1994, **C50**, 1516.
8. a) Popova, E.G., Chetkina, L.A., Bel'skii, V.K., Adrievskii, A.M., Poplavskii, A.N. and Dyumaev, K.M., *Zh. Strukt. Khim.*, 1987, **28**, 129.

   b) Popova, E.G., Chetkina, L.A., Bel'skii, V.K., Adrievskii, A.M., Poplavskii, A.N. and Dyumaev, K.M., *Zh. Strukt. Khim.*, 1988, **29**, 109.

c) Popova, E.G., Chetkina, L.A., Bel'skii, V.K., Adrievskii, A.M., Poplavskii, A.N. and Dyumaev, K.M., *Zh. Strukt. Khim.*, 1990, **31**, 189.

9. a) Popova, E.G., Chetkina, L.A., Bel'skii, V.K., Adrievskii, A.M., Poplavskii, A.N. and Dyumaev, K.M., *Zh. Strukt. Khim.*, 1985, **26**, 139.

b) Popova, E.G., Chetkina, L.A., Bel'skii, V.K., Adrievskii, A.M., Poplavskii, A.N. and Dyumaev, K.M., *Zh. Strukt. Khim.*, 1988, **29**, 109.

c) Popova, E.G., Chetkina, L.A. and Sobolev, A.N., *Zh. Strukt. Khim.*, 1991, **32**, 130.

d) Popova, E.G., Chetkina, L.A., Bel'skii, V.K., Adrievskii, A.M., Poplavskii, A.N., Dyumaev, K.M. and Sobolev, A.N., *Dokl. Akad. Nauk SSSR*, 1989, **304**, 127.

e) Popova, E.G., Chetkina, L.A., Bel'skii, V.K., Adrievskii, A.M., Poplavskii, A.N., Dyumaev, K.M. and Sobolev, A.N., *Zh. Strukt. Khim.*, 1988, **29**, 164.

f) Popova, E.G., Chetkina, L.A., Zavodnik, V.E., Andrievskii, A.M. and Poplavskii, A.N., *Zh. Strukt. Khim.*, 1991, **32**, 169.

10. Rice, C.G. and Wallis, J.D., *J. Chem. Soc., Chem. Commun.*, 1993, 572.
11. Bengaard, H., Larsen, S., Sorensen, H., Robinson, K. and Wallis, J.D., *Acta Cryst.*, 1999, **C55**, 106.
12. O'Leary, J., Bell, P.C., Wallis, J.D. and Schweizer, W.B., *J. Chem. Soc., Perkin Trans. 2*, 2001, 133.
13. Ford, A., Sinn, E. and Woodward, S., *J. Chem. Soc., Perkin Trans. 1*, 1997, 927.